From *Arabidopsis* Model to Green Revolution Cereal Crop Varieties: Studies of the Co-Regulation of Plant Growth and Nitrogen Metabolism

Zhe Ji

Department of Plant Sciences
St. Hugh's College
University of Oxford



Thesis Submitted for the Degree of Doctor of Philosophy

Trinity Term 2018

Abstract

From *Arabidopsis* Model to Green Revolution Cereal Crop Varieties: Studies of the Co-Regulation of Plant Growth and Nitrogen Metabolism

Zhe Ji, St. Hugh's College, University of Oxford

Thesis Submitted for the Degree of Doctor of Philosophy, Trinity Term 2018

Modern semi-dwarf "Green Revolution" varieties (GRVs) of wheat and rice dramatically increased global grain yields during the mid to late 20th Century. GRVs are dwarf because they accumulate growth-repressing DELLA proteins. GRVs are thus high yielding because they apportion more resource to grain filling than to stem elongation, and are less susceptible to the yield-reducing effect of "lodging". However, recent evidence suggests that GRVs have a low nitrogen-use efficiency (NUE) as a result of the negative pleiotropic effect of stabilised DELLAs. Therefore, the cultivation of GRVs requires environmentally unsustainable levels of inorganic fertiliser application.

The aim of this study is to uncover the underlying mechanism of DELLA-mediated inhibition of the metabolism of nitrate (the major form of nitrogen in most agricultural soils), using the *Arabidopsis* semi-dwarf GRV model mutant *ga insensitive* (*gai*). It was first established that *gai* is more resistant to chlorate, the toxic chemical analogue of nitrate, suggesting that like GRVs, *Arabidopsis gai* also exhibits compromised nitrate metabolism. Chimeric analyses and enzymatic assays discovered an inhibitory effect of DELLA proteins on shoot nitrate reductase activity. A similar effect of DELLAs was found to be conserved in rice, providing a potential explanation for the low NUE observed in GRV crop plants. Moreover, as DELLA-interacting proteins (DIPs), PHYTOCHROME-INTERACTING FACTOR3 (PIF3) was identified as a positive regulator of nitrate assimilation, potentially acting downstream of DELLAs.

Simultaneous forward screens for mutagenized *gai* isolated multiple mutants which genetically uncoupled *gai*-mediated inhibition of stem elongation and nitrate metabolism, with *usually multiple acids move in and out transporter32* (*umamit32*) identified as a potential novel mutation conferring enhanced chlorate resistance. Meanwhile, several tall *gai* mutants were selected and initially characterised, which provided new insights into the GA-DELLA signalling pathway and how it relates to the regulation of plant growth. The ultimate goal of this research is to apply the knowledge obtained from *Arabidopsis* to modern crops, in the hope of improving their NUE and thereby contributing to the development of the next generation of GRVs of crops.

Acknowledgments

First and foremost, I would like to express my deepest gratitude to Nick Harberd, for being the best supervisor I could ask for. Inspired by his tutorial during my undergraduate degree, I am extremely fortunate to be offered this opportunity to be his DPhil student. Without his insight, patience and support, I would never be able to complete my degree. I would also like to thank my second supervisor, Andrew Smith, for designing an exciting short rotation project for me, as well as his ongoing advice on my research.

I owe a great deal to the amazing people in the Harberd group. In particular, Eric Belfield for his guidance and creative ideas that encouraged me to work like a proper scientist; Chulmin Kim for his patient help with rice cultivation; Jay Biernaskie for the fascinating discussions on social evolution in plants; Josefina Rodriguez for our friendly competition of who is more hardworking; and Fiona Jamieson for her homemade cakes that are out of this world. I would also like to thank, as well as apologise to the technicians on our floor, Julie Bull, Lizzie Jamison and Robert Pinches for having to tolerate my messy work space. Additionally, I am tremendously grateful to the two Chinese academic visitors in our lab, Zhongjie Ding and Qi Meng, for not only providing instructions on various experimental techniques, but also keeping my Mandarin in check. I appreciate the two undergraduate students that I helped supervised during my degree, Ziqi Xu (Laura) and Joshua Thomas, for putting their trust in me and for causing a healthy amount of distraction from my own work. Finally, I would never forget the fun weekly cake club with the additional members of Hugh Dickinson, Kate Loven Rita Ross etc.

Oxford can be a stressful place to live in and I am blessed to have friends who brightened my days. A special thank you to my friends in the department, especially Shivani Malik, Khushboo Borah, Robert Sowden and Sabri Ali, who shared my frustration whenever my experiments didn't work. Having stayed in St. Hugh's College for seven years, I have become familiar with a lot of people who will hopefully stay life-long friends. I would like to particularly mention Jingjing Wan, who constantly distracted me from my work with social activities, but nevertheless taught me to be kind, generous and occasionally carefree. Similarly, I appreciate the short but invaluable company of Mengni, Yujie, Zhitong, Yunyi, Xiaoman, Tongran, Jun, etc. during their stay in Oxford.

In addition, I would like to thank Xiangdong Fu for the three-month internship opportunity in his lab at the Chinese Academy of Sciences in Beijing towards the end of my DPhil degree. Without the guidance from my mentor Shan Li, I would never be able to adapt to the dramatic culture shock in such a short period of time. Other people in the lab, including Xiuhua Gao and Yafeng Ye, also helped me tremendously during this internship. A special thank you to Shan, Jianqing, Ying, Hui, Jiangyi and Zhiyang, for frequently taking me to fancy restaurants after work.

Last but not least, I am forever indebted to my parents for their unconditional love and support, and to my grandma, who although has no idea why I am passionate about science, always has faith in me. To Ricky, thank you for always staying by my side.

List of Abbreviations

ABA	abscisic acid
APA	active phytochrome A-binding
APB	active phytochrome B-binding
At	*Arabidopsis thaliana*
bHLH	basic helix-loop-helix
bp	base pair
BR	brassinosteroid
bZIP	basic leucine zipper
cDNA	complement deoxyribonucleic acid
DIP	DELLA-interacting protein
DNA	deoxyribonucleic acid
DNase	deoxyribonuclease
EMS	ethyl methane sulfonate
FN	fast neutron
GA	gibberellic acid
GAI	GA INSENSITIVE
GAR	GAI REVERTANT
GID	GIBBERELLIN INSENSITIVE DWARF
GRV	Green Revolution variety
HATS	high-affinity transport system
INDEL	insertion/deletion
LATS	low-affinity transport system

mRNA	messenger ribonucleic acid
N	nitrogen
NIA	NITRATE REDUCTASE
NiR	nitrite reductase
NIR1	NITRITE REDUCTASE1
NR	nitrate reductase
NRT	NITRATE TRANSPORTER
NUE	nitrogen-use efficiency
Os	*Oryza sativa*
OX	overexpression
PAC	paclobutrazol
PCR	polymerase chain reaction
PIF	PHYTOCHROME-INTERACTING FACTOR
PIFq	PHYTOCHROME-INTERACTING FACTOR quartet
PIL	PHYTOCHROME-INTERACTING FACTOR-LIKE
Phy	phytochrome
RGA	REPRESSOR OF *ga1-3*
RGL	RGA-LIKE
Rht	Reduced height
RNA	ribonucleic acid
RNAi	ribonucleic acid interference
ROS	reactive oxygen species
RT-PCR	reverse transcription-polymerase chain reaction
RT-qPCR	quantitative reverse transcription-polymerase chain reaction

s.d.	standard deviation
SD1	SEMIDWARF-1
SLR	SLENDER1
SLY1	SLEEPY1
SNP/SNV	single nucleotide polymorphism/variant
SPY	SPINDLY
ssp.	subspecies
TOR	Target of Rapamycin
WGS	whole-genome sequencing
WT	wild type
UMAMIT	USUALLY MULTIPLE ACIDS MOVE IN AND OUT TRANSPORTER
UTR	untranslated region
Y2H	yeast two-hybrid
Zm	*Zea mays*

Table of Contents

Abstract *1*

Acknowledgments *2*

List of Abbreviations *4*

Table of Contents *7*

List of Figures *13*

List of Tables *18*

CHAPTER 1. Introduction *19*

1.1 The Need for a Second Green Revolution **19**

1.1.1 The first Green Revolution 19

1.1.2 Problems associated with modern GRVs 20

1.2 The GA-DELLA Signalling Pathway **21**

1.2.1 GA biosynthesis and deactivation 21

1.2.2 Regulation of DELLA activities 25

1.2.3 Transcriptional regulation by DELLAs 30

1.3 PIF Signalling Pathway **31**

1.3.1 PIF regulation by phytochromes 31

1.3.2 PIFs have both shared and distinct functions 35

1.3.3 Crosstalk between PIFs and hormonal pathways 38

1.4 Nitrate Metabolism and Signalling **42**

1.4.1 Nitrate uptake through nitrate transporters 42

1.4.2 Nitrate assimilation 46

1.4.3 Nitrate signalling 50

1.5 Project Aims **53**

1.6 Thesis Structure **55**

CHAPTER 2. Materials and Methods ***56***

2.1 General Materials and Methods **56**

2.1.1 Chemicals and primers 56

2.1.2 Sterilisation 56

2.1.3 Centrifugation 57

2.2 Plant Materials and Growth Conditions **57**

2.2.1 *Arabidopsis thaliana* 57

2.2.2 *Oryza sativa* 61

2.3 *Arabidopsis* Hypocotyl Graft **62**

2.4 Plant Phenotypic Studies **63**

2.4.1 Chlorate toxicity assay in *Arabidopsis* 63

2.4.2 Chlorate toxicity assay in *Oryza sativa* 64

2.4.3 Chlorophyll measurement 64

2.4.4 *Arabidopsis* hypocotyl length measurement 64

2.4.5 *Arabidopsis* height measurement 65

2.5 Protein Manipulation **65**

2.5.1 Protein extraction 65

2.5.2 Protein quantification 66

2.5.3 Nitrate reductase (NR) activity assay 66

2.5.4 Nitrite reductase (NiR) activity assay 67

2.6 RNA Manipulation **68**

2.6.1 RNA extraction 68

2.6.2 DNase treatment 68

2.6.3 cDNA synthesis 69

2.6.4 PCR and gel electrophoresis 69
2.6.5 Quantitative RT-PCR (RT-qPCR) 73
2.7 DNA Manipulation 75
2.7.1 *In silico* motif searches 75
2.7.2 DNA extraction for genotyping and sequencing 76
2.7.3 Sanger sequencing 76
2.7.4 DNA extraction for whole-genome sequencing (WGS) analysis 77
2.7.5 DNA precipitation 78
2.8 Mutant Screen 79
2.8.1 *Arabidopsis* seed mutagenesis 79
2.8.2 WGS analysis 80
2.9 Molecular Cloning 81
2.9.1 Bacterial growth conditions 81
2.9.2 Preparation of competent *E. coli* DH5α cells 82
2.9.3 Bacterial transformation 82
2.9.4 Plasmid recombination 83
2.10 Yeast Two-Hybrid Analysis 86
2.10.1 Yeast growth conditions 86
2.10.2 Preparation of competent yeast Y187 cells 86
2.10.3 Yeast transformation 87
2.10.4 Liquid culture β-galactosidase assay 88
CHAPTER 3. The Regulatory Relationship Between the GA-DELLA Signalling Pathway and Nitrate Metabolism 90
3.1 Introduction 90
3.2 Results 94
3.2.1 Mutants defective in low-affinity nitrate uptake and nitrate reduction are resistant to chlorate toxicity on soil 94

3.2.2 Mutants with stabilised DELLAs are resistant to chlorate toxicity 95

3.2.3 Mutant chlorate resistance cannot be explained by dwarfism *per se* 97

3.2.4 Using hypocotyl graft chimeras to determine root versus shoot contribution to mutant chlorate resistance 101

3.2.5 *gai*-conferred chlorate resistance is mainly shoot- rather than root-dependent 103

3.2.6 Mutants with stabilised DELLAs have reduced shoot nitrate reductase activity, whilst nitrite reductase activity is not detectably affected 107

3.2.7 The *gai* mutation upregulates the mRNA abundances of nitrate transporter genes and has no detectable effect on nitrate or nitrite reductase mRNA abundances 109

3.2.8 The rice *sd1* mutation confers chlorate resistance and reduced nitrate reductase activity 111

3.3 Discussion 113

3.3.1 General comments on chlorate toxicity assays and grafting experiments. 113

3.3.2 DELLAs negatively regulate shoot nitrate reductase activity 114

3.3.3 DELLAs positively regulate the transcript abundances of root nitrate transporter genes 118

3.3.4 Rice ssp. *indica sd1* mutant has a reduced nitrate reductase activity 119

3.3.5 Concluding remarks 120

CHAPTER 4. The Regulatory Relationship Between PIFs and Nitrate Metabolism 121

4.1 Introduction 121

4.2 Results 125

4.2.1 The *pifq* mutant is resistant to chlorate toxicity 125

4.2.2 *pifq*-conferred chlorate resistance is primarily due to shoot-dependent reduction in nitrate reductase activity 127

4.2.3 The *pifq* mutation down-regulates *NIA2* mRNA abundance but does not detectably affect that of other nitrate metabolism-related genes 129

4.2.4 Loss-of-function mutations of *PV42A* and *GRF7* do not confer detectably altered chlorate response compared to WT 132

4.2.5 *pif3* is majorly responsible for the *pifq*-conferred chlorate resistance and reduction in nitrate reductase activity. 134

4.2.6 Overexpression of *PIF3* in the *pif3* mutant complements *pif3*-mediated phenotypes 135
4.2.7 PIF4 does not play a significant role in regulating nitrate assimilation 138
4.2.8 PIF2 and PIF6 do not play a significant role in regulating nitrate assimilation 139
4.2.9 The *pif7* mutant exhibited an intermediate level of chlorate resistance between WT and the *pifq* mutant without detectably affecting nitrate reductase activity 140
4.2.10 The *pif8* mutant is resistant to chlorate without detectably affecting nitrate reductase activity 142

4.3 Discussion 145

4.3.1 PIFs potentially link the GA-DELLA signalling pathway with nitrate metabolism 145
4.3.2 PIFs regulate nitrate reductase activity at least partially through transcriptional regulation 146
4.3.3 PIF3, among the PIFq members, plays the predominant role in regulating nitrate reductase activity 149
4.3.4 PIF2 and PIF6 do not detectably participate in the regulation of nitrate metabolism 152
4.3.5 PIF7 and PIF8 promote nitrate metabolism with unknown mechanisms 153
4.3.6 Concluding remarks 155

CHAPTER 5. Identification of Novel Mutations Conferring Altered Chlorate Responses on gai Mutant Plants 157

5.1 Introduction 157

5.2 Results 160

5.2.1 Characterisation of chlorate hypersensitive mutants 160
5.2.2 Characterisation of chlorate resistant mutants 165
5.2.3 Identifying candidate causal mutations in chlorate resistant mutants 167
5.2.4 The *usually multiple acids move in and out transporters32* (*umamit32*) mutation might have conferred the chlorate resistance of FN2.7R 172

5.3 Discussion 173

5.3.1 General comments on mutagenesis and mutant screen 173
5.3.2 Mutations in the *NRT1.1* and *NIA2* genes were identified from the mutants selected for being chlorate resistant 176

5.3.3 *UMAMIT32* might be a novel gene involved in plant nitrogen metabolism 177

5.3.4 Concluding remarks 182

CHAPTER 6. Identification of Novel Mutations Conferring Increased Plant Height on gai Mutant Plants 183

6.1 Introduction 183

6.2 Results 187

6.2.1 Most tall *gai* mutants contain detectable mutations in *gai* 187

6.2.2 Intragenic *gai* nonsense and frame shift mutations generally result in complete suppression of *gai*-conferred inhibition of plant growth 189

6.2.3 Intragenic missense mutations increase *gai* plant height to various extents 191

6.2.4 Three *sly1* mutations suppress *gai*-conferred inhibition of stem growth and nitrate metabolism 193

6.2.5 Initial characterisation of tall mutants lacking detectable mutations in either of *gai* or *SLY1* 197

6.2.6 Initial characterisation of a tall *gai* mutant exhibiting a retained chlorate resistance phenotype 199

6.3 Discussion 201

6.3.1 General comments on the tall mutants with intragenic nonsense or frame shift mutations in *gai* 201

6.3.2 The tall mutants with missense mutations in *gai* represent a valuable genetic resource for the functional characterisation of DELLA subdomains 203

6.3.3 Novel mutant sly1 proteins identified in this study confer an enhanced interaction with gai 206

6.3.4 General comments on the tall mutants lacking detectable mutations in *gai* or *SLY1* 209

6.3.5 Concluding remarks 210

CHAPTER 7. General Discussion 212

7.1 Overview 212

7.2 DELLAs Negatively Regulate Plant Nitrate Assimilation 213

7.3 PIFs are Promising Targets for Enhancing Future Crop NUE 216

7.4 Future Work for the Novel Mutants Identified in This Study 222

Reference list 225

List of Figures

Figure 1.1 GRV of rice and wheat compared to their tall equivalents. 20

Figure 1.2 Schematic representation of GA biosynthesis and deactivation pathways. 23

Figure 1.3 Simplified schemes of the GA-DELLA signalling pathways in WT, GA-deficient mutant and GA-insensitive mutant plants. 24

Figure 1.4 The domain organisation of DELLA proteins. 26

Figure 1.5 Simplified scheme of PIF regulation by Phy. 35

Figure 1.6 Simplified diagram of the interactions between PIFs and various phytohormone signalling pathways resulting in the regulation of growth. 41

Figure 1.7 Nitrate transporters involved in nitrate uptake, efflux, translocation and redistribution. 43

Figure 1.8 Simplified diagram of nitrate assimilation within a cell. 48

Figure 2.1 The quadruple loss-of-function *pifq* mutant used in this study was confirmed to be homozygous by PCR prior to experiments. 58

Figure 3.1 Structures of WT, *Arabidopsis* gai and crop mutant DELLA proteins. 93

Figure 3.2 Chlorate responses of WT, *nrt1.1*, *nrt2.1 nrt2.2* and *nia2* mutant plants grown on soil. 95

Figure 3.3 Chlorate responses and leaf chlorophyll contents of WT and *gai* mutant plants. ..96

Figure 3.4 Chlorate responses of WT and *ga5* mutant plants. 97

Figure 3.5 Heights of WT and the five dwarf mutants included in this study. 99

Figure 3.6 Chlorate responses of WT and four dwarf mutants. 99

Figure 3.7 Chlorate responses of WT, *TOR-OX* and *TOR-RNAi* lines. 100
Figure 3.8 Chlorate responses of graft chimeras made by exchanging shoots and roots of WT and *nrt1.1* mutant plants. 102
Figure 3.9 Chlorate responses of graft chimeras made by exchanging shoots and roots of WT and *nia2* mutant plants. 103
Figure 3.10 Chlorate responses of graft chimeras made by exchanging shoots and roots of WT and *gai* mutant plants (*Ler* ecotype background). 104
Figure 3.11 Confirmation of the identities of the WT/*gai* and *gai*/WT graft chimeras. 105
Figure 3.12 Chlorate responses of graft chimeras made by exchanging the shoots and roots of WT and *gai* mutant plants (*Col-0* ecotype background). 106
Figure 3.13 Relative shoot nitrate reductase activities in WT, *gai*, *tt1*, *gai-t6 tt1* and *ga5*, and relative shoot nitrite reductase activities in WT and *gai*. 108
Figure 3.14 Abundances of mRNAs encoding major nitrate transporter, nitrate reductase and nitrite reductase activities visualised using RT-PCR. 110
Figure 3.15 Relative abundances of mRNAs encoding major nitrate transporters, and nitrate reductase and nitrite reductase activities as measured using RT-qPCR. 111
Figure 3.16 Chlorate responses of *indica* rice *SD1* and *sd1* mutant plants. 112
Figure 3.17 Relative shoot nitrate reductase activities in WT and *sd1 indica* rice. 113
Figure 3.18 Protein concentrations of *Arabidopsis* WT, *gai*, *ga5*, *tt1* and *gai-t6 tt1*, as well as rice *SD1* and *sd1*. 117

Figure 4.1 Hypocotyl etiolation phenotypes exhibited by WT versus *gai* and by WT versus *pifq*. 123
Figure 4.2 Phenotypes of dark-grown seedlings of various *pif* mutant combinations. 126

Figure 4.3 Chlorate responses and leaf chlorophyll contents of WT and *pifq* mutant plants. 127

Figure 4.4 Chlorate responses of graft chimeras made by exchanging shoots and roots of WT and *pifq* mutant plants. 128

Figure 4.5 Relative shoot nitrate and nitrite reductase activities in WT and *pifq*. 129

Figure 4.6 Positions of the putative PIF binding sites in the promoter regions of *NIA1* and *NIA2*. 130

Figure 4.7 Relative abundances of mRNAs encoding major nitrate transporters, and nitrate reductase and nitrite reductase activities as measured using RT-qPCR. 131

Figure 4.8 Abundances of mRNAs encoding nitrate reductase and nitrite reductase activities visualised using RT-PCR. 132

Figure 4.9 Chlorate responses of WT, *pv42a* and *grf7* mutant plants. 133

Figure 4.10 Chlorate responses of WT, *pifq* and the four single *pif* knock-out mutants. 134

Figure 4.11 Relative shoot nitrate reductase activities in WT, *pifq*, and the four *pif* single mutants. 135

Figure 4. 12 Relative *PIF3* mRNA abundances in WT, *pif3* and *PIF3OX*/*pif3*. 136

Figure 4.13 Chlorate responses of WT, *pif3* and *PIF3OX/pif3* mutant plants. 137

Figure 4.14 Relative shoot nitrate reductase activities in WT, *pif3* and *PIF3OX/pif3*. 137

Figure 4.15 Chlorate responses and relative shoot nitrate reductase activities of WT, *pif4* and *PIF4OX*/*pif4*. 139

Figure 4.16 Chlorate responses and relative shoot nitrate reductase activities of WT, *pif2* and *pif6*. 140

Figure 4.17 Chlorate responses and leaf chlorophyll contents of WT, *pif7* and *pifq* mutant plants. 141

Figure 4.18 Chlorate responses of graft chimeras made by exchanging shoots and roots of WT and *pif7* mutant plants, and relative nitrate reductase activities of WT and *pif7*. 142
Figure 4.19 Phenotypic characterisation of the *pif8* mutant. 143
Figure 4.20 Chlorate responses and relative shoot nitrate reductase activities of WT and *pif8*. 144

Figure 5.1 An example of a mutant *gai* plant identified to be hypersensitive to chlorate toxicity. 161
Figure 5.2 Chlorate responses of *gai*, E2.21S and E1.7S mutant plants.....162
Figure 5.3 Chlorate responses of *gai*, E2.21S and the F_2 generation of the backcross between *gai* and E2.21S. 163
Figure 5.4 Chlorate responses of *gai*, E1.7S and the F_2 generation of the backcross between *gai* and E1.7S. 164
Figure 5.5 Chlorate responses of *gai*, FN1.5S and FN2.5S mutant plants. 165
Figure 5.6 An example of a mutant *gai* plant identified to be resistant to chlorate toxicity..166
Figure 5.7 Chlorate responses of *gai*, E1.5R. E2.62R, FN2.11R and FN2.7R mutant plants. 166
Figure 5.8 The domain organisation of the NIA2 protein, and the mutation in the E2.62R mutant line. 168
Figure 5.9 Chlorate responses of the progenitor *gai* and M_4 plants of the E2.62R mutant line. 169
Figure 5.10 Schematic representation of the *NRT1.1* gene and the mutation in the FN2.11R mutant line. 170
Figure 5.11 Schematic representation of the *UMAMIT32* gene and the site of T-DNA insertion. 172

Figure 5.12 Chlorate responses of WT and *umamit32* mutant plants. 173

Figure 5.13 An example of a mutant line (FN4.2S) that exhibited early leaf chlorosis both with and without chlorate treatment. 175

Figure 6.1 Plant heights of WT, *gai* and *gai* plants with additional mutations that lead to a tall phenotype. 184

Figure 6.2 An example of a tall *gai* mutant stem identified within an EMS-mutagenized M_1 *gai* population. 188

Figure 6.3 Examples of M_4 generation tall *gai* mutants identified amongst mutagenized *gai* populations. 189

Figure 6.4 Secondary nonsense or deletion mutations in *gai* confer increased plant height. 190

Figure 6.5 Secondary missense mutations in *gai* confer increased plant height. 192

Figure 6.6 Domain organisation of the SLY1/GAR2 protein and positions of amino acid substitutions resulting in suppression of *gai* phenotype. 194

Figure 6.7 Growth phenotypes conferred by the *gar2* mutant alleles. 195

Figure 6.8 Strength of interaction between gai and WT SLY1 or mutant sly1 proteins as measured by quantitative yeast two-hybrid assays. 196

Figure 6.9 Chlorate responses of *gai*, WT, and the three *sly1*/*gar gai* mutant plants. 197

Figure 6.10 Heights of the 15 tall mutant *gai* lines lacking detectable mutations in *gai* or *SLY1*. 198

Figure 6.11 Growth phenotypes of E3.5 and E3.1 plants compared to progenitor *gai* and WT plants. 200

Figure 6.12 Chlorate responses of WT, *gai*, E3.5 and E3.1 mutant plants. 201

Figure 7.1 The working model of the regulation of nitrate metabolism by the GA-DELLA and PIF signalling pathways. 219

List of Tables

Table 2.1 *Arabidopsis* (*Landsberg erecta* ecotype) seeds used in this study. 59

Table 2.2 *Arabidopsis* (*Columbia* ecotype) seeds used in this study.....60

Table 2.3 General PCR thermal cycling programme.....70

Table 2.4 Primers used for semi-quantitative RT-PCR. 72

Table 2.5 Primers used for RT-qPCR. 74

Table 2.6 RT-qPCR thermal cycling programme. 75

Table 2.7 Primers used in Sanger sequencing. 77

Table 2.8 Antibiotics used in this study.....81

Table 2.9 Primers used in plasmid recombination.....83

Table 2.10 Vector plasmids used in this study. 84

Table 3.1 Three dwarf mutants selected in this study for chlorate toxicity assay and their WT gene functions. 98

Table 4.1 Motif search result for putative PIF binding sites.....130

Table 5.1 List of mutations located in the exon or UTR regions in the FN2.7R mutant line. 171

CHAPTER 1. Introduction

1.1 The Need for a Second Green Revolution

1.1.1 The first Green Revolution

The Green Revolution refers to a dramatic increase in agricultural production worldwide, which occurred during the mid-to-late 20th century (Trewavas, 2001, Hazell, 2009). The Green Revolution was multifactorial in nature, and was achieved via increased use of chemical fertilisers and agro-chemicals, better control of water irrigation systems, improved crop management techniques, and the development of high-yielding semi-dwarf crop "Green Revolution" varieties (GRVs, Figure 1.1, Peng et al., 1999a, Hazell, 2009). GRVs are dwarf because they have modified phytohormone gibberellic acid (GA)-DELLA signalling (see section 1.2 for details). This has been achieved through reduced levels of growth-promoting GAs, for example, the rice *semidwarf-1* (*sd1*) allele carries a loss-of-function mutation in *GA20ox2*, a GA biosynthesis gene. Alternatively, wheat GRVs rely on reduced GA response conferred by mutant growth-repressing DELLAs encoded by *Reduced height* (*Rht*), which lack part of the N-terminal region of the protein responsible for GA signal perception. Similar dwarfing mutations exist in other crop varieties, including barley *denso*/*semi-dwarf1* (*sdw1*) that is deficient in GA biosynthesis, and maize *dwarf-8* (*d8*) and Barley *slender1* (*sln1*) that are deficient in GA response, but they are not widely adopted as GRVs (Peng et al., 1999a, Monna et al., 2002, Sasaki et al., 2002, Spielmeyer et al., 2002, Chandler et al., 2002, Jia et al., 2009). In addition to these genetic approaches, chemical GA biosynthesis inhibitors (e.g., chlormequat) have also been employed to reduce crop height (Rademacher, 2016). As a

consequence, more energy can be diverted from stem elongation to grain filling, thus increasing yield, as well as reducing the "lodging" effect, where elongated stems collapse by wind and rain when they fail to support the heavy grains (Hedden, 2003). Both *Rht* wheat and *sd1* rice were recently shown to have a dampened responsivity to external nitrogen (N) supply, which further enhances their lodging resistance (Li et al., personal communication).

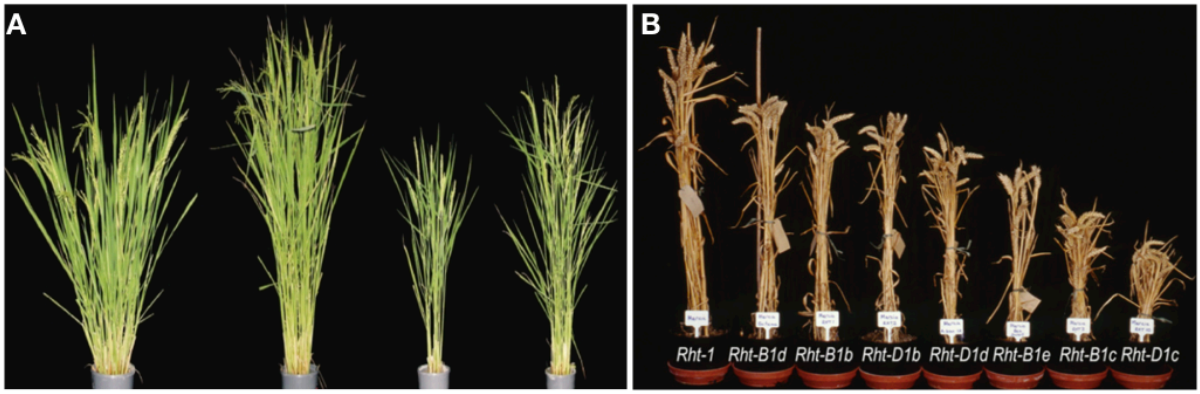


Figure 1.1 GRV of rice and wheat compared to their tall equivalents.
(A) Semi-dwarf rice *sd1* varieties and their equivalent wild type (WT). From left to right: dwarf *indica* cultivar, *indica* tall equivalent, dwarf *japonica* cultivar, *japonica* tall equivalent. Figure taken from (Hedden et al., 2013). (B) Semi-dwarf wheat *Rht* cultivars (*Mercia* variety) and their equivalent WT. *Rht-B1b* and *Rht-D1b* mutant alleles are adopted in the Green Revolution. Figure taken from the John Innes Centre archives (original photograph by Tony Worland).

1.1.2 Problems associated with modern GRVs

Unfortunately, two major problems are associated with these DELLA-stabilized GRVs. Firstly, they exhibit poor plant establishment due to enhanced seed dormancy, which is more or less compensated for by increased tillering and grains per spike (Uppal and Gooding, 2013). Second, in accordance with the aforementioned reduction in nitrogen responsivity, GRVs exhibit a low nitrogen-use efficiency (NUE, usually defined as grain yield per available nitrogen), likely due to an as yet unexplained reduction in N uptake and/or assimilation, which points to a previously unknown connection between the GA-DELLA signalling pathway and nitrogen metabolism

(Raun and Johnson, 1999, Gooding et al., 2012, Casebow et al., 2016). The latter downside of GRVs resulted in farmers using unsustainable levels of N fertilisers, leading to high production costs in terms of both energy and resources, and negative environmental and ecological impacts such as the eutrophication caused by fertiliser "run-offs" (LeGouis and Pluchard, 1996, Tilman et al., 2002). Agricultural expansion is not an available solution to combat this issue, as most suitable lands are already being used for farming (Khush, 2005). Therefore, in order to feed the predicted 50% increase in world population by 2050 without further compromising the ecosystem (Tilman et al., 2002, Godfray et al., 2010, Tilman et al., 2011), it is necessary to breed new crop varieties maintaining high yields but with a reduced dependency on high-level fertiliser application through biotechnological approaches, essentially initiating a second Green Revolution.

1.2 The GA-DELLA Signalling Pathway

1.2.1 GA biosynthesis and deactivation

GAs are a group of tetracyclic diterpenoid compounds that are present in bacteria, fungi and plants (Yamaguchi, 2008). In plants, bioactive GAs act as functional phytohormones and are essential growth regulators controlling a wide variety of developmental processes, ranging from seed germination, stem elongation, developmental stage transitions, to flowering (Harberd et al., 2009). GAs are biosynthesised from a common C_{20} precursor called geranylgeranynl diphosphate (GGDP) in a step-by-step fashion by three classes of enzymes: two plastid-localised terpene synthases (TPSs), *ent*-copalyl diphosphate synthase (CPS) and *ent*-kaurene synthase (KS) converts GGDP to *ent*-kaurene; sequential oxidation of *ent*-kaurene

to the intermediate product GA_{12} is catalysed by two cytochrome P450 monooxygenases (P450s), *ent*-kaurene oxidase (KO) and kaureoic acid oxidase (KAO), at plastid outer membrane and endoplasmic reticulum, respectively; bioactive GA_1, GA_3 and GA_4 are finally produced through oxidation by two 2-oxoglutarate-dependent dioxygenases (2-ODDs), GA 20-oxidase (GA20ox) and GA 3-oxidase (GA3ox) presumably in the cytosol (Figure 1.2, Yamaguchi, 2008). In the plant model organism *Arabidopsis thaliana*, each member of the TPSs and P450s are encoded by a single gene, which is why the loss-of-function mutations of these genes result in severe dwarfism (Koornneef and Vanderveen, 1980, Sakamoto et al., 2004). Contrarily, *Arabidopsis* GA20ox and GA3ox are encoded by multigene families consisting of five and four members respectively (Mitchum et al., 2006, Rieu et al., 2008). Therefore, single null mutants of these genes either have no visible phenotypic alterations, or cause subtle changes such as the semi-dwarf plant stature conferred by *ga20ox1* (Rieu et al., 2008), whereas overexpression of *GA20ox* induces exaggerated plant growth due to elevated GA concentration (Huang et al., 1998). The phenotype of mutants lacking genes encoding GA biosynthetic enzymes can be rescued through external application of bioactive GAs. In other words, these mutants are GA-sensitive (Yamaguchi, 2008).

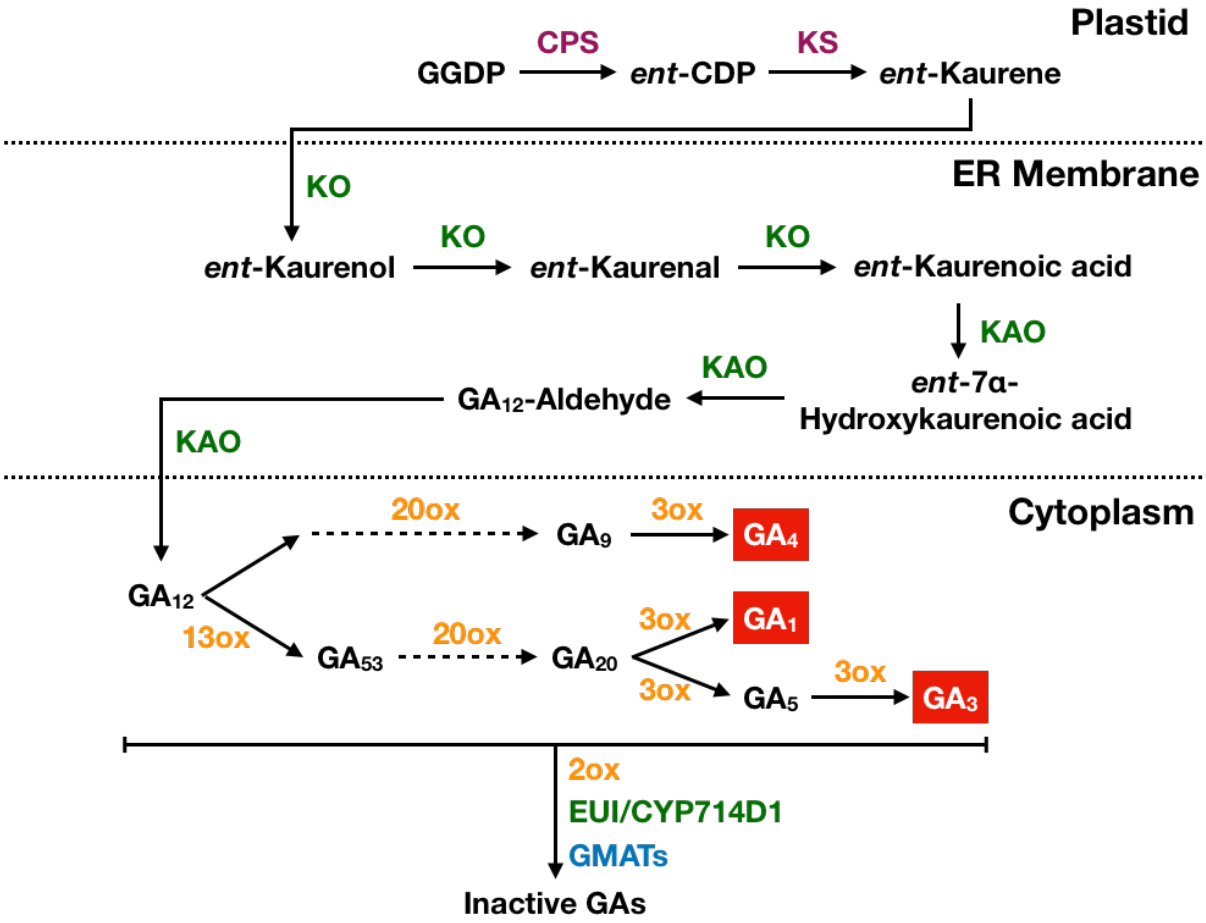


Figure 1.2 Schematic representation of GA biosynthesis and deactivation pathways. Bioactive GAs (GA_1, GA_3 and GA_4) are synthesised from GGDP through a series of reactions catalysed by three classes of enzymes at three subcellular locations. Both bioactive and precursor GAs are subject to deactivation by GA2ox, EUI/CYP714D1 and GMATs. Enzymes belonging to separate classes are labelled with different colours: TPSs in purple, P450s in green, 2-ODDs in orange, and methyl transferases in blue.

Green Revolution *sd1*rice carries a mutant form of one of its two *GA20ox* genes, *OsGA20ox2*, causing a reduction in levels of bioactive GAs (Figure 1.3, Sasaki et al., 2002, Ashikari et al., 2002). The original semi-dwarf *indica* Dee-geo-woo-gen cultivar contains a loss-of-function mutation in *GA20ox2* due to a 383-bp deletion introducing a premature stop codon, whereas semi-dwarf *japonica* subspecies harbour point mutations in this gene resulting in amino acid substitutions (Ashikari et al., 2002, Monna et al., 2002, Spielmeyer et al., 2002). The *japonica* mutant probably retains some enzymatic activity as *sd1* alleles in *japonica* in general have weaker phenotypic effect than those of *sd1* in *indica* cultivars (Hedden, 2003). The fact that

independent artificial selection for dwarfism in rice yielded mutations in *GA20ox2* rather than in other GA biosynthetic enzyme-encoding genes might be explained by its predominant expression in vegetative tissues, indicating its major role in determining plant height (Monna et al., 2002).

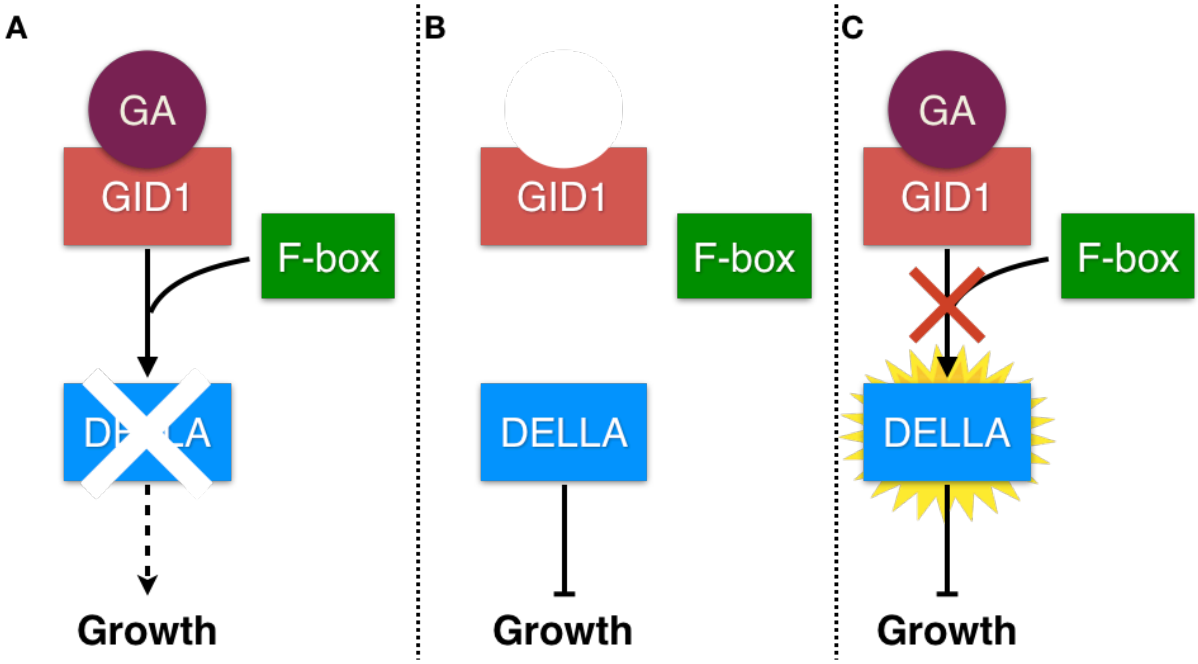


Figure 1.3 Simplified schemes of the GA-DELLA signalling pathways in WT, GA-deficient mutant and GA-insensitive mutant plants.
(A) In WT plants, GA binds to GID1, which induces DELLA ubiquitination by the SCF E3 ubiquitin ligase and subsequent degradation by the 26S proteasome. Growth repression by DELLAs is therefore relieved. (B) In GA-deficient mutants (e.g., rice *sd1* and barley *sdw1*), the pool of bioactive GAs is reduced because of mutations in GA biosynthetic enzymes, allowing DELLA proteins to accumulate and inhibit plant growth. (C) In GA-insensitive mutants (e.g., wheat *Rht*, maize *d-8* and barley *sln1*), mutations in DELLAs render them irresponsive to the GA signal. The stabilised DELLAs therefore constantly inhibit plant growth.

Homeostatic GA levels in plants are also maintained through GA deactivation (Figure 1.2). Both bioactive GAs and their precursors have long been known to be deactivated through 2β-hydroxylation by the 2-ODD GA 2-oxidases (GA2oxs, Thomas et al., 1999). Additional deactivation mechanisms of bioactive and/or precursor GAs have been discovered over the years, including oxidation by a new C_{20}-specific class III GA2ox; 16α,17-epoxidation by a

P450, ELONGATED UPPERMOST INTERNODE (EUI)/CYP714D1; and methylation of *Arabidopsis* seed GAs by gibberellin methyltransferases GMAT1 and GMAT2 (Schomburg et al., 2003, Lee and Zeevaart, 2005, Zhu et al., 2006, Varbanova et al., 2007). Expectedly, knocking out these genes leads to an accumulation of bioactive GAs (Zhu et al., 2006, Varbanova et al., 2007). In GA metabolism, both GA biosynthesis and deactivation processes are highly regulated in order to achieve a relatively stable pool of bioactive GAs in plants (Hedden and Phillips, 2000, Olszewski et al., 2002). Interestingly, transcript levels of the 2-ODDs involved in both pathways appear to be the major targets for such regulations (Yamaguchi, 2008).

1.2.2 Regulation of DELLA activities

GAs promote growth and development mainly through the degradation of the growth-repressive DELLA proteins (Peng et al., 1997, Peng et al., 1999a). Given their sessile nature, plants rely heavily on the GA-DELLA "relief of repression" mechanism for growth and survival. Under optimal growth conditions, plants produce bioactive GAs to promote growth. However, when facing adverse environments, DELLA proteins accumulate, which restrain growth whilst promoting survival through repressing stress-induced production of toxic reactive oxygen species (ROS, Achard et al., 2006, Achard et al., 2008a, Achard et al., 2008b).

DELLAs belong to the plant-specific GRAS (named after the first three members identified: GA INSENSITIVE [GAI], REPRESSOR OF *ga1-3* [RGA], and SCARECROW [SCR]) family transcription regulators and are highly conserved within the plant kingdom (Pysh et al., 1999). Like the other members of the GRAS family, the C termini of DELLAs contain two leucine heptad repeats (LHRI and LHRII), a nuclear localisation signal (NLS), followed by VHIID,

PFYRE and SAW subdomains (Pysh et al., 1999). They distinguish themselves from the other GRAS proteins by possessing a specific N-terminal sequence containing the conserved DELLA (which they are named after), LEQLE, TVHYNP, and a variable poly Ser/Thr/Val domain (Figure 1.4, Itoh et al., 2005a). In monocots, an additional methionine-rich MAMGM motif exists between the LEQLE and TVHYNP domains (Van De Velde et al., 2017). The DELLA and TVHYNP domains allow DELLA proteins to be recognised by and interact with the GA receptor GIBBERELLIN INSENSITIVE DWARF1 (GID1) when bound to GA (Ueguchi-Tanaka et al., 2005, Nakajima et al., 2006, Murase et al., 2008, Achard and Genschik, 2009). Protein crystallisation studies have revealed that bioactive GAs fit specifically into a central "pocket" structure in GID1, resulting in its N terminal helix forming a "lid" that encloses the pocket and binds with DELLAs (Murase et al., 2008, Shimada et al., 2008). The subsequent conformational change of DELLAs stimulates their C-terminal recognition and polyubiquitination by the $SCF^{SLEEPY1\ (SLY1)/GID2}$ E3 ubiquitin ligase (consisting of the Skp1, cdc53/cullin and F-box protein core components), followed by 26S proteasome-mediated degradation and relief of growth inhibition (Gagne et al., 2002, McGinnis et al., 2003, Sasaki et al., 2003, Dill et al., 2004, Fu et al., 2004).

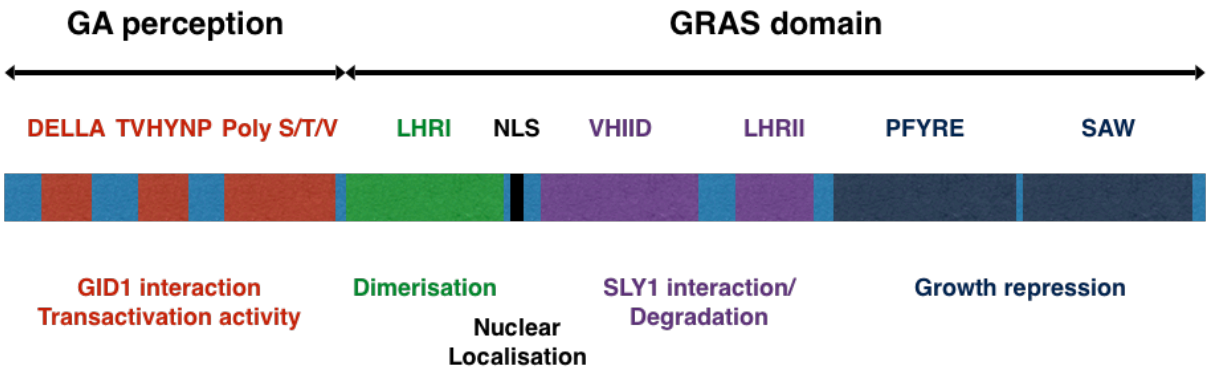


Figure 1.4 The domain organisation of DELLA proteins.
In general, domains at the N terminus of DELLAs are involved in GA signal perception, whereas those at the C terminus mediate transcriptional regulation by DELLAs. The domains are colour-coded with respect to their proposed functions. This diagram is not drawn to scale.

The *Arabidopsis* genome encodes five DELLA proteins: GAI, RGA, RGA-LIKE1 (RGL1), RGL2 and RGL3, among which GAI shares the highest amino acid similarity with crop DELLAs including wheat Rht-D1a and maize d8 (62% in both cases, Peng et al., 1999a, Gao et al., 2011). The *Arabidopsis gai* mutant was originally identified as conferring a GA-insensitive dwarf phenotype that is caused by a deficiency in GA signal transduction rather than GA biosynthesis (Koornneef et al., 1985, Talon et al., 1990a, Wilson et al., 1992, Peng and Harberd, 1993, Wilson and Somerville, 1995). In fact, *gai* mutant plants have an elevated bioactive GA concentration due to the perturbed negative feedback loop imposed by stabilised gai protein (Koornneef et al., 1985, Talon et al., 1990b). It was later discovered that *gai* mutant allele contains a 51 bp deletion within its N terminus that results in the production of truncated gai protein, leading to an altered GA response (Peng et al., 1997). Given the similarities in terms of both the nature and outcome of mutations shared by *gai* and Green Revolution mutant DELLA genes (see below), *Arabidopsis gai* is often employed as the experimental model for GRVs (Willige et al., 2007).

The wheat Green Revolution began with the production of the Norin-10 cultivar from crossing a semi-dwarf variety from Japan and a high-yielding variety from America (Hedden, 2003). Norin-10 possesses two dwarfing alleles located on two of the three wheat chromosomes, *Rht-B1b* and *Rht-D1b*, with similar effects on plant height reduction (Figure 1.1, Hedden, 2003). Both *Rht* alleles carry nonsense mutations at the DELLA domain of the genes, but translational reinitiation probably occurred at one of the methionine residues within the adjacent MAMGM domain, resulting in the production of stabilised N-terminally truncated DELLA proteins (Figure 1.3, Peng et al., 1999a). Similarly, maize *d-8* allele contains a deletion in the TVHYNP domain, which also leads to the production of GA-insensitive DELLAs (Figure 1.3, Peng et al.,

1999a). Dwarfism caused by these gain-of-function mutations cannot be reverted by external GA application (Hedden, 2003).

It is noteworthy that other regulatory mechanisms of DELLAs have been discovered in addition to the aforementioned canonical GA-GID1-DELLA pathway. Among the three *Arabidopsis* GA receptor GID1s (GID1a, GID1b and GID1c), GID1b has a uniquely high affinity with GAs and can interact with DELLAs even in the absence of GAs (Griffiths et al., 2007, Willige et al., 2007). Therefore, GID1b might act as an important mediator of GA-independent GA signalling under circumstances where GA concentration is particularly low. Additionally, DELLA activities can be inhibited by a degradation-independent interaction between GA-GID1 and DELLAs (Ariizumi et al., 2008, Ariizumi et al., 2011). Adding another layer of complexity, multiple pathways of post-translational modifications of DELLAs have been demonstrated. Stress-induced small ubiquitin-like modifier (SUMO) conjugation (SUMOylation) of DELLA proteins enables their interaction with the SUMO interaction motif (SIM) of GID1 in a GA-independent manner, thus allowing the accumulation of non-SUMOylated DELLAs to inhibit GA-induced activities (Conti et al., 2014). Phosphorylation of DELLAs has been observed and originally hypothesised to aid their recognition by the F-box proteins SLY1/GID2, thus promoting subsequent DELLA ubiquitination and degradation (Sasaki et al., 2003, Fu et al., 2004). However, more recent evidence indicates that phosphorylation not only stabilises DELLA proteins, but also represses GA biosynthetic gene expression, whereas dephosphorylation does the opposite, although details of the molecular mechanism is still lacking (Dai and Xue, 2010, Wang et al., 2014). In *Arabidopsis*, *SPINDLY* (*SPY*) has long been assumed to encode an O-linked N-acetylglucosamine (O-GlcNAc) transferase (OGT) based on sequence analysis (Jacobsen et al., 1996, Hartweck et al., 2002). Since loss-of-function *spy* can partially rescue the severe dwarfism exhibited by the GA-deficient *ga1* mutant, O-

GlcNAcylation was thought to promote DELLA activities (Silverstone et al., 2007). However, it was recently clarified that DELLA O-GlcNAcylation is mediated by the SPY paralog SECRET AGENT (SEC), which deactivates DELLAs, while SPY is actually a novel protein O-fucosyltransferase, and O-fucosylation activates DELLAs. Both DELLA activation and deactivation are achieved through differential allosteric changes induced by these two protein modifications (Zentella et al., 2016, Zentella et al., 2017). Moreover, since the sites of phosphorylation, O-GlcNAcylation and O-fucosylation are predicted to overlap at the same Ser/Thr residues on DELLA proteins, it is reasonable to speculate that these post-translational modifications of DELLAs compete with each other, allowing a more dynamic regulation of DELLA-mediated regulation of plant growth and development compared to DELLA degradation (Wang et al., 2014, Zentella et al., 2016, Zentella et al., 2017).

The five DELLA proteins in *Arabidopsis* display both overlapping and specific GA-responsive functions (Gao et al., 2011). For example, RGL2 plays the major role of inhibiting seed germination (Lee et al., 2002); RGL3 promotes plant survival under both biotic and abiotic stresses (Achard et al., 2008a, Wild et al., 2012); RGA, RGL1 and RGL2 act collectively to repress floral development (Cheng et al., 2004, Tyler et al., 2004); whilst GAI and RGA are the predominant growth repressors during plant vegetative growth as well as floral transition (Dill et al., 2001, King et al., 2001). Promoter swapping experiments suggest that the partially distinct functions of DELLAs are mainly achieved through differential gene expression patterns (Gallego-Bartolome et al., 2010). Intriguingly, recent phylogenetic analyses discovered a closely related clade of DELLA proteins that has been lost in Brassicaceae (Van De Velde et al., 2017). Members of this sister clade are termed the DGLLAs because instead of a DELLA domain, they contain a conserved DGLLA motif. Additional distinctions in protein structure between DGLLAs and DELLAs include the former containing a LERLE

(rather than LEQLE in DELLAs) and a conserved YNP (rather than a conserved TVHYNP in DELLAs) domain (Van De Velde et al., 2017). Furthermore, DGLLA proteins in the grass family (Poaceae) lack the N terminus containing the DGLLA, LERLE and YNP domains (Itoh et al., 2005b). Similar to N-terminally truncated DELLAs, these DGLLAs are not degraded in response to GA, but their expression correlates positively with GA concentration, suggesting that they are under repression by Poaceae DELLAs (Itoh et al., 2005b). A potential evolutionary significance for these DGLLA proteins is that they might confer a basal level of GA-insensitive growth repression even when DELLA abundance is low (Fukao and Bailey-Serres, 2008). Nevertheless, the molecular basis of DGLLA functioning, and why this clade is lost in Brassicaceae remain largely unknown.

1.2.3 Transcriptional regulation by DELLAs

Unlike the GA perception pathway, which has been rigorously investigated and relatively well-established, the exact mechanism of DELLA regulation of downstream targets remains elusive, partly due to the extensive crosstalk with other regulatory pathways. As strong transactivators without a DNA-binding motif, DELLAs modulate gene expression primarily through interacting with DELLA-interacting proteins (DIPs, Locascio et al., 2013). At least four main mechanisms of DELLA-mediated transcriptional regulation have been proposed. First, DELLAs sequester an ever-growing list of DNA-binding transcription factors from their target promoters, resulting in either induced or repressed downstream gene expressions involved in a wide range of biological activities. For example, DELLAs interact with PHYTOCHROME INTERACTING FACTORs (PIFs) to inhibit germination and hypocotyl elongation (also see section 1.3.3); with BRASSINAZOLE-RESISTANT 1 (BZR1) to regulate brassinosteroid (BR)-dependent hypocotyl elongation; with ETHYLENE INSENSITIVE 3 (EIN3) to modulate

ethylene-dependent apical hook development; with SQUAMOSA PROMOTER BINDING PROTEIN-LIKE 9 (SPL9) to repress floral transition; and with ALCATRAZ (ALC) to control fruit ripening (de Lucas et al., 2008, Feng et al., 2008, Arnaud et al., 2010, Gallego-Bartolome et al., 2011, An et al., 2012, Bai et al., 2012, Yu et al., 2012). Second, DELLAs interact with JASMONATE ZIM-DOMAIN (JAZ) proteins to relieve their repression of MYC2 activity, thereby activating downstream jasmonate (JA) signalling (Hou et al., 2010, Wild et al., 2012, Yang et al., 2012). Third, DELLAs and SCARECROW-LIKE 3 (SCL3) competitively interact with the INDETERMINATE DOMAIN (IDD) family proteins to respectively activate and inhibit downstream gene expression (including *SCL3* itself). In this case, DELLAs act as novel transcriptional coactivators through interacting with another transcription factor (Yoshida et al., 2014). Finally, DELLAs have been proposed to be able to interfere with chromatin remodelling proteins, based on the observed broad overlap between GA- and SWI/SNF- (a chromatin remodelling complex) regulated genes (Fukazawa et al., 2010, Archacki et al., 2013). In the next section, what is currently known about PIFs, one of the earliest known DIP family, will be reviewed.

1.3 PIF Signalling Pathway

1.3.1 PIF regulation by phytochromes

As the most well-known *Arabidopsis* DIPs, PIFs are basic helix-loop-helix (bHLH) transcription factors belonging to the bHLH subgroup 15 protein family (Bailey et al., 2003, Toledo-Ortiz et al., 2003). Eight members of this family (PIF1-PIF8) have been demonstrated to interact with the phytochrome (Phy) photoreceptors that are responsible for sensing red (R)

and far red (FR) light in plants, whereas the other seven members either do not interact with Phy or such an interaction is yet to be confirmed experimentally (Leivar and Quail, 2011). PIFs were first identified as positive regulators of plant skotomorphogenesis (characterised by an elongated hypocotyl, closed cotyledons, a sustained apical hook, negative hypocotyl gravitropism and inhibition of chlorophyll biosynthesis), as loss-of-function *pif* mutants exhibit the opposite photomorphogenic phenotypes in darkness, whereas overexpressing PIFs results in exaggerated skotomorphogenic phenotypes (Leivar et al., 2008). PIFs form protein dimers and bind to G-box (CACGTG) or PIF binding E-box (PBE-box, CACATG and CATGTG) motifs in the promoter regions of their target genes through their eponymous bHLH domains to repress photomorphogenesis in the dark (Hornitschek et al., 2012, Oh et al., 2012, Zhang et al., 2013).

Arabidopsis has five Phys (PhyA-PhyE) and they exist in two thermally stable forms: the inactive Pr form that absorbs R light, and the active Pfr form that absorbs FR light (Clack et al., 1994, Quail et al., 1995). In darkness or when shaded (where R:FR ratio is low), Pr predominantly localises in the cytosol, but upon red light exposure, the conformational change from Pr to Pfr activates their migration into the nucleus (Figure 1.5, Yamaguchi et al., 1999, Chen et al., 2004, Fankhauser and Chen, 2008). For PhyA that does not have an NLS, this process requires its association with other NLS-containing facilitators such as FAR RED ELONGATED HYPOCOTYL1 (FHY1) and FHY1 LIKE (FHL, Zhou et al., 2005, Genoud et al., 2008). On the other hand, the C terminus of PhyB, which plays the major role in plant developmental regulation in white light, contains a putative NLS that is believed to be unmasked during its conversion from Pr to Pfr, allowing its subsequent translocation into the nucleus (Johnson et al., 1994, Reed et al., 1994, Chen et al., 2005). Pfr has been shown to regulate mRNA translation in cytosol (Paik et al., 2012), but more importantly, it binds to the

conserved N-terminal active phytochrome B-binding (APB) and/or active phytochrome A-binding (APA) motifs in PIFs in the nucleus (Leivar and Quail, 2011). PIFs are subsequently rapidly phosphorylated at multiple sites, ubiquitinated and degraded by the 26S proteasome, resulting in downstream transcriptomic changes (Leivar and Monte, 2014). An exception to this module is PIF7, which does not appear to be degraded significantly upon phosphorylation (Leivar et al., 2008). Instead, phosphorylation deactivates PIF7 by repressing its binding to target genes under high R:FR ratio conditions (Li et al., 2012a). Both PhyA and PhyB are ubiquitinated by CONSTITUTIVELY PHOTOMORPHOGENIC1 (COP1) and then degraded in the nucleus (Saijo et al., 2008, Jang et al., 2010). Importantly, degradation of PhyB Pfr is dependent on its interaction with PIFs, thus forming a negative feedback loop thought to be important for attenuating prolonged light signalling (Ni et al., 2013).

Potential responsible kinases and E3 ubiquitin ligases mediating PIF degradation are only recently being identified, and for most of these candidates, the evidence remains somewhat controversial. To date, four categories of kinases have been proposed to phosphorylate PIFs: Phy itself functions as a Ser/Thr kinase targeting PIF3 and possibly other PIFs as well (Yeh and Lagarias, 1998, Shin et al., 2016); four members of the Photoregulatory Protein Kinases (PPK1-PPK4) phosphorylate PIF3 (Ni et al., 2017); Casein Kinase II (CK2) phosphorylates PIF1 (Bu et al., 2011); and BIN2 phosphorylates PIF3 and PIF4 (Bernardo-Garcia et al., 2014, Ling et al., 2017). All three classes of the *Arabidopsis* CULLIN (CUL) RING UBIQUITIN LIGASEs (CRLs), CUL1-, CUL3- and CUL4-based ubiquitin ligases, are involved in the ubiquitination of PIF3, PIF4 and PIF1, respectively. Specifically, PIF3 is recognised by two EIN3 BINDING F-BOX (EBF1/2) and three LIGHT-RESPONSE Bric-a-Brack/Tramtrack/Broad (LRB1/2/3) F-box proteins; PIF4 by two BLADE ON PETIOLE (BOP1/2) F-box proteins; and PIF1 by the COP1/SUPPRESSOR of *phyA-105* (SPA) complex

(Ni et al., 2014, Zhu et al., 2015, Dong et al., 2017, Zhang et al., 2017). Interestingly, while COP1 mediates light-induced PIF degradation, it stabilises PIF proteins in darkness (Xu et al., 2015). Further studies are essential to confirm the validity of the above-mentioned kinases and ubiquitin ligases, and will more than likely reveal additional candidates regulating PIF degradation as well as phosphatases that dephosphorylate and re-stabilise PIFs (Pham et al., 2018). Such light-induced, Pfr-mediated reduction in PIF abundance is conserved in the non-vascular liverwort *Marchantia*, emphasising the biological importance of this regulation (Lee and Choi, 2017). Similar to the GA-GID1-DELLA signalling pathway, degradation-independent Pfr-PIF interaction also prevents PIFs from binding to their target promoters (Li et al., 2012a, Park et al., 2012).

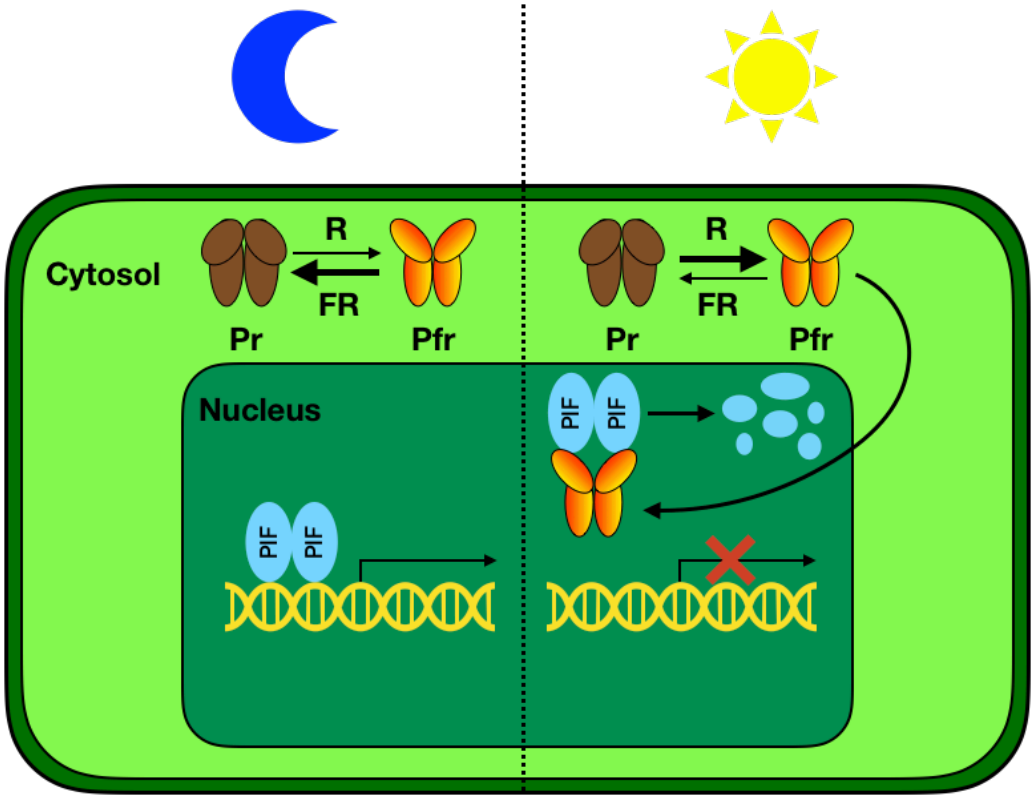


Figure 1.5 Simplified scheme of PIF regulation by Phy.
Left: in darkness (or shaded environments where R:FR ratio is low), Phy predominantly exists as the inactive Pr form, which does not interact with the nuclear transcription factors PIFs. PIFs in the nucleus therefore bind to promoters of their target genes and activate downstream gene expression. Right: when exposed to light (or when R:FR ratio is high), Pr converts to the active Pfr form and migrates to the nucleus. Pfr sequesters PIFs from their target promoters and trigger PIF degradation. PIF-regulated genes are therefore no longer activated.

1.3.2 PIFs have both shared and distinct functions

Although PIFs were originally identified as negative regulators of photomorphogenesis (Leivar et al., 2008, Shin et al., 2009), an ever-growing number of subsequent genetic, biochemical and physiological investigations have demonstrated a wide range of biological processes regulated by different PIFs, acting either independently or redundantly (Jeong and Choi, 2013). As an example, PIF1 plays a prominent role in inhibiting seed germination in the dark through repressing GA signalling while activating abscisic acid (ABA) signalling (Oh et al., 2006, Oh

et al., 2007, Kim et al., 2008, Oh et al., 2009). In the dark, PIF5 is involved in the maintenance of apical hook by upregulating ethylene biosynthesis (Khanna et al., 2007), whereas ethylene promotes hypocotyl elongation in the light in a PIF3-dependent manner (Zhong et al., 2012). PIF4 plays the unique role of enhancing hypocotyl elongation through upregulating various auxin biosynthetic genes, and floral transition through binding to the promoter of the *FLOWERING LOCUS T* (*FT*) gene under high ambient temperatures (Koini et al., 2009, Franklin et al., 2011, Kumar et al., 2012, Quint et al., 2016). PIF7 is the major modulator of plant shade avoidance responses through regulating auxin biosynthesis, although other PIFs probably also make small contributions to shade-induced hypocotyl and petiole elongation (Leivar et al., 2008, Lorrain et al., 2008, Li et al., 2012a).

On the other hand, certain biological processes are controlled by multiple PIFs. For example, PIF1 and PIF3 inhibit chlorophyll biosynthesis and chloroplast development in the dark, which prevents the accumulation of toxic protochlorophyllide (Moon et al., 2008, Stephenson et al., 2009). Meanwhile, under short-day conditions, *PIF4* and *PIF5* mRNA levels oscillate according to the circadian clock and increase towards the end of the night, which is at least partially determined by the evening complex, EARLY FLOWERING3 (ELF3)-ELF4-LUX ARRHYTHMO (LUX, Nusinow et al., 2011). This, together with Phy-regulated protein degradation, ensures that PIF4 and PIF5 protein abundances peak at dawn, thus coinciding with the rhythmic pattern of hypocotyl elongation in short-day grown seedlings (Nozue et al., 2007, Nusinow et al., 2011, Yamashino et al., 2013). Although the *PIF3* expression level does not seem to be obviously regulated by the circadian clock, the progressive accumulation of PIF3 protein through the night accelerates hypocotyl growth at dawn together with PIF4 and PIF5 (Soy et al., 2012). More recently, it was found that the central circadian clock component, TIMING OF CAB EXPRESSION1 (TOC1), also contributes to the diurnal oscillation of

hypocotyl elongation by interacting directly with both PIF3 and PIF4 to downregulate their activities at early dusk (Martin et al., 2016, Zhu et al., 2016). On the other hand, under long-day conditions and warm ambient temperatures, PIF4 and PIF7 repress photoperiod-dependent freezing tolerance responses by inhibiting *C-REPEAT BINDING FACTOR* (*CBF*) genes (Lee and Thomashow, 2012). In addition, *pif4* and *pif6* mutants exhibit reduced and increased stomatal density respectively, whereas repression of stomatal opening is weakened in *pif3* and *pif4* mutants, suggesting that PIF3, PIF4 and PIF6 differentially regulate light-dependent stomatal development and behaviour (Casson et al., 2009, Wang et al., 2010a). It is well-known that the so-called PIF quartet (PIFq), comprised of PIF1, PIF3, PIF4 and PIF5, acts redundantly to regulate seedling etiolated development in the dark, with PIF1 playing the major role (Leivar et al., 2008). As a result, single null mutants lacking one of these four PIFs have little or no effect on etiolation, but the quadruple loss-of-function mutant (*pifq*) displays dramatic photomorphogenic phenotypes in the dark (Leivar et al., 2009). Contrary to the other PIFs, PIF2 and PIF6 positively regulate photomorphogenesis, and are therefore speculated to be involved in fine-tuning PIF-mediated responses (Penfield et al., 2010, Luo et al., 2014). In fact, PIF2 is degraded by COP1 in the dark and stabilised by PhyB when exposed to the light. It even heterodimerises with PIFq members to prevent their binding to target promoters (Pham et al., 2018). Finally, the functional significance of PIF8 awaits to be characterised (Pham et al., 2018). This complex PIF signalling network is attributable to the differences in their intrinsic protein properties, gene expression patterns and interactions with other transcription regulators (Jeong and Choi, 2013).

1.3.3 Crosstalk between PIFs and hormonal pathways

Most of the above-mentioned PIF-regulated biological processes involve interacting with one or more phytohormone signalling pathways. For example, PIF1 is placed upstream of the GA-DELLA signalling pathway in controlling seed germination. PIF1 not only directly represses GA signalling by activating *GAI* and *RGA* gene expression (Oh et al., 2007), but also indirectly regulate GA level by promoting *DOF AFFECTING GERMINATION1* (*DOF1*) and *SOMNUS* (*SOM*) transcriptions, thus repressing GA biosynthetic genes *GA3ox1* and *GA3ox2*, and activating the GA catabolic gene *GA2ox2* (Kim et al., 2008, Gabriele et al., 2010). However, most other PIF activities are inhibited by DELLA proteins. For example, during photomorphogenesis, DELLAs exert a strong repression of PIF activities by sequestering them away from their target promoters (Feng et al., 2008, de Lucas et al., 2008, Gallego-Bartolome et al., 2010). Moreover, the interaction between DELLAs and PIFs also leads to PIF degradation, this more dramatic repression of PIF activities compared to PIF titration is light-independent (Li et al., 2016, Zheng et al., 2016).

The interaction between PIF1 and the ABA signalling pathway is perhaps the most straight-forward of all and is currently only known to occur in imbibed seeds. PIF1 inhibits seed germination by directly promoting *ABA-INSENSITIVE3* (*ABI3*) and *ABI5* expression, with both genes being positive regulators of ABA signalling (Oh et al., 2009, Park et al., 2011b). Additionally, PIF1 interacts with ABI3 to promote *SOM* transcription, thus enhancing seed dormancy (Park et al., 2011b). ABI5, a group A basic leucine zipper (bZIP) transcription factor, facilitates PIF1 binding to DNA and modulates its binding specificity (Kim et al., 2016). This property is probably shared by other group A bZIP proteins as well, but the biological significance of this regulatory mechanism is yet to be resolved.

In another hormonal interaction, BRs are involved in the promotion of hypocotyl elongation together with GA and PIFs (Tanaka et al., 2003). BR perception results in the activation of BZR1, a transcription factor that regulates BR responsive genes (Kim and Wang, 2010). BZR1 has been shown to interact with at least PIF1 and PIF4, with the BZR1-PIF4 complex being particularly important for the co-regulation of multiple downstream auxin-responsive and cell wall-related genes (Oh et al., 2012). The fact that DELLAs interact with both BZR1 and PIF4 to inhibit their transcriptional activities suggests that the DELLA-BZR1-PIF4 module is responsible for fine-tuning context-dependent seedling hypocotyl elongation (de Lucas and Prat, 2014). As described earlier, BIN2, a kinase responsible for phosphorylating BZR1 in response to BR, also phosphorylates PIF3 and PIF4 preceding their degradation (Bernardo-Garcia et al., 2014). Meanwhile, PIF4 and PIF5 induce the expression of two BR biosynthetic genes: *DWARF4* (*DWF4*) and *BR-6-OXIDASE2* (*BR6ox2*, Wei et al., 2017).

In the dark, overexpression of *PIF5* in *PIF5OX* plants results in the activation of 1-aminocyclopropane-1-carboxylic acid (ACC) SYNTHASE genes responsible for ethylene biosynthesis. The subsequent increase in ethylene level explains the characteristic ethylene overdose triple response phenotype exhibited by *PIF5OX* seedlings (Khanna et al., 2007). The resultant ethylene signal activates EIN3/EIN3-like (EIL) transcription factors, which inhibit hypocotyl elongation in the dark by regulating ETHYLENE-RESPONSE FACTOR1 (ERF1), whilst promoting hypocotyl elongation under light through upregulating PIF3 expression (Zhong et al., 2012). Again, DELLA proteins might interfere with this process because DELLAs can bind to both EIN3 and PIF3 to inhibit their activities (An et al., 2012).

PIF3 and PIF4 play important roles in plant growth-defence trade-offs through integrating JA signalling. Under optimal plant growth conditions and therefore low JA levels, one of the JA

negative mediator, JAZ9, binds to DELLAs competitively with PIF3. Free from DELLA repression, PIF3 then induces plant growth at the expense of lowered defence response (Yang et al., 2012). Enhanced JA signalling in response to pathogen attack results in JAZ9 degradation, which indirectly facilitates DELLA-PIF3 interaction and therefore inhibits growth (Yang et al., 2012). Integrating light and BR signals, one of the BZR1-PIF4 targets is *PACLOBUTRAZOL RESISTANCE* (*PRE*) genes, which indirectly reduces plant defence responses in favour of growth (Lozano-Duran and Zipfel, 2015).

Finally, for auxin, unlike the other phytohormones, almost all PIF-auxin crosstalk reported to date occurs unidirectionally, i.e., with PIFs being upstream of the auxin signalling pathway (de Lucas and Prat, 2014). Indeed, the activation of cell division and elongation in response to PIF signalling is achieved through enhanced auxin biosynthesis, responses and/or transport. First, vegetative shade or high ambient temperatures induce PIF-mediated promotion of several auxin biosynthetic genes including *TRYPTOPHAN AMINOTRANSFERASE OF ARABISOPSIS1* (*TAA1*), *CYP79B2*, and members of the *YUCCA* gene family (Franklin et al., 2011, Li et al., 2012a, Sun et al., 2012). Second, PIF4 and PIF5 increase auxin sensitivity and response through upregulation of *AUXIN SIGNALLING F-BOX1* (*AFB1*), *INDOLE-3-ACETIC ACID INDUCIBLE19* (*IAA19*), *IAA29*, and members of the *SMALL AUXIN REGULATED RNA* (*SAUR*) genes (Hornitschek et al., 2012, Hersch et al., 2014, Sun et al., 2016). Similar to BZR1, AUXIN RESPONSE FACTOR6 (ARF6) also form a regulatory complex with PIF4 and co-regulate genes involved in auxin and light signalling (Oh et al., 2014). Lastly, apical hook maintenance in the dark require PIF5-induced indirect phosphorylation of PIN FORMED (PIN) proteins that mediate auxin efflux and therefore accurate auxin distribution in the hook structure (Willige et al., 2012). Overall, PIFs are increasingly being recognised as constituting a signalling hub that integrate external (e.g., light and temperature) and internal (e.g., circadian

clock and phytohormone) signals for optimal plant growth and developmental regulation (Figure 1.6, Leivar and Monte, 2014).

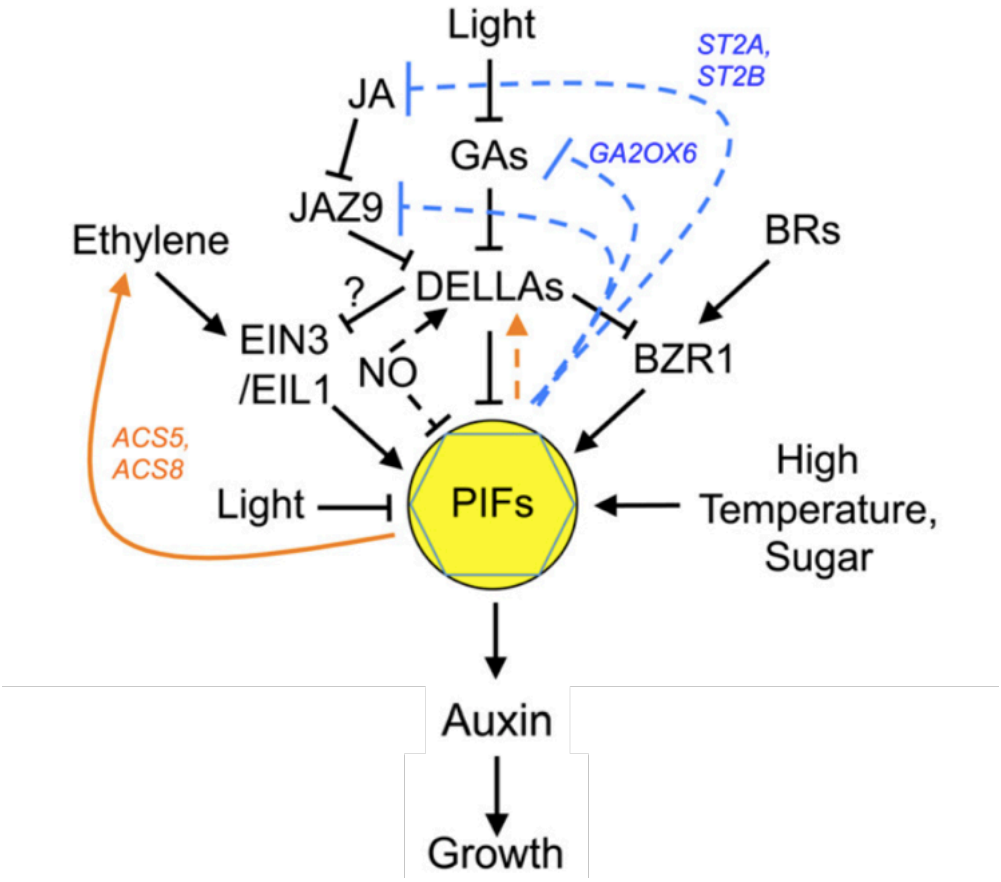


Figure 1.6 Simplified diagram of the interactions between PIFs and various phytohormone signalling pathways resulting in the regulation of growth.
PIFs act as a signalling hub integrating external and internal signals to regulate growth mainly through modulating the auxin signalling pathway. Solid lines indicate experimentally confirmed interactions with PIFs whereas dotted lines and the question mark indicate potential connections that require further investigation. Orange and blue lines represent PIF-mediated promotion and repression of gene expression, respectively. Figure adapted from (Leivar et al., 2014).

1.4 Nitrate Metabolism and Signalling

1.4.1 Nitrate uptake through nitrate transporters

Due to its involvement in the biosynthesis of proteins, nucleic acids, and other essential cellular components such as chlorophyll and phytohormones, nitrogen is one of the most-needed plant mineral nutrients, and therefore often limits growth (Crawford, 1995). In order to reduce nitrogen fertiliser application and increase plant NUE, it is essential to understand the molecular basis of nitrogen uptake, allocation, storage and assimilation. Plants extract nitrogen from the soil in a variety of forms ranging from inorganic (e.g., nitrate and ammonium) to organic (e.g., urea and amino acids), depending on soil types and species-specific preferences (Williams and Miller, 2001). For example, whist ammonium (NH_4^+) is present in abundance in anaerobic environments such as flooded rice paddy fields, nitrate (NO_3^-) predominates in most agricultural soils as the major source of available nitrogen to plants (Crawford and Forde, 2002). In higher plants, four gene families have been shown to be involved in nitrate influx, efflux, and redistribution within the plant: NITRATE TRANSPORTER1/PEPTIDE TRANSPORTER FAMILY (NRT1/NPF), NRT2, CHLORIDE CHANNEL FAMILY (CLC) transporters, and SLOW ANION CHANNEL-ASSOCIATED HOMOLOG (SLAC/SLAH, Dechorgnat et al., 2010, Wang et al., 2012). While the CLCs and SLAC/SLAH are mainly responsible for transporting nitrate across tonoplast and guard cell membranes, respectively, only members of the NRT1/NPF and NRT2 families have been shown to be involved in nitrate uptake from the soil (Figure 1.7, Wang et al., 2012, Krapp et al., 2014).

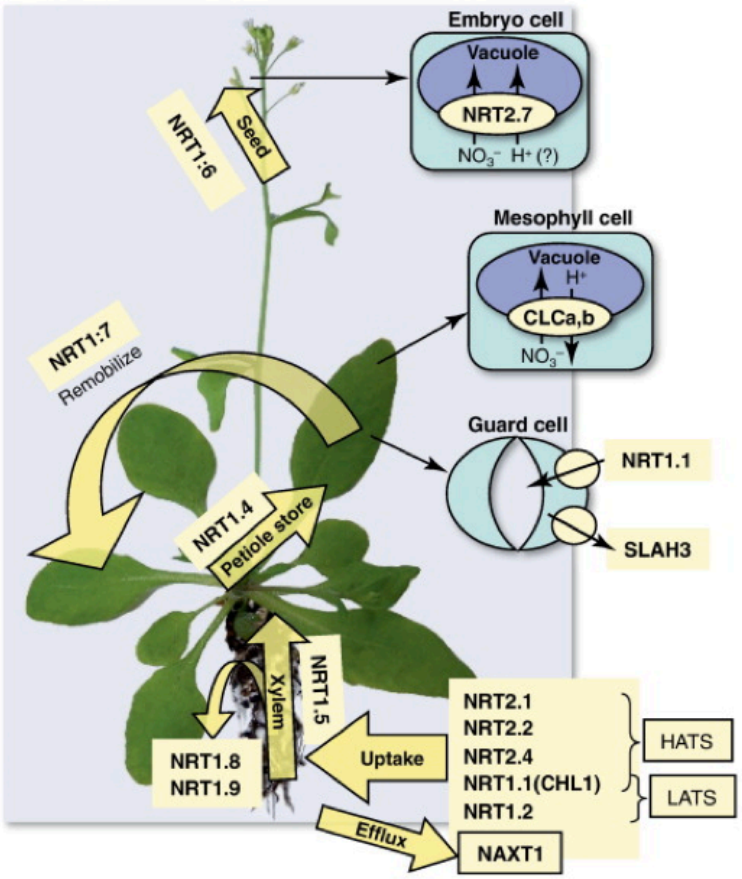


Figure 1.7 Nitrate transporters involved in nitrate uptake, efflux, translocation and redistribution.
Soil nitrate is taken up by the plant through nitrate transporters belonging to the NRT1/NPF and NRT2 families. Nitrate translocation and redistribution is mainly mediated by NRT1/NPF transporters. CLC and NRT2.7 transporters are responsible for nitrate transport across the tonoplast, whereas SLAC/SLAH and NRT1.1/NPF6.3 transport nitrate across guard cell membranes. NAXT1/NPF2.7 regulates nitrate efflux in the root. Figure taken from (Wang et al., 2012).

Nitrate has a highly heterogeneous soil distribution, both spatially and temporally, which poses a great challenge for efficient uptake by sessile plants. Therefore, it is not surprising that plants have evolved complex nitrate transport and assimilation systems to maximise nitrate utilisation (Crawford and Glass, 1998). Two kinetically distinct nitrate transport systems mediated by $2H^+/1NO_3^-$ symporters exist in plants: the low-affinity transport system (LATS, $K_M \approx$ mM) and the high-affinity transport system (HATS, $K_M \approx \mu$M), both of which can be further divided into an inducible (i) and a constitutive (c) component (Crawford and Glass, 1998, Zhuo et al., 1999,

Filleur et al., 2001). Sequence comparisons, mutant analyses, heterologous expression in oocytes, and physiological influx correlation studies in *Arabidopsis* have identified members of the NRT1/NPF and NRT2 families as being respectively responsible for LATS and HATS (Huang et al., 1999, Forde, 2000, Okamoto et al., 2003, Orsel et al., 2004).

The *Arabidopsis* genome encodes 53 NPF family proteins belonging to the large peptide transporter (PTR) family (Leran et al., 2014). PTRs are likely to exist in all organisms, and with their 12 transmembrane domains they function as transporters for a variety of substrates (Daniel, 2004, Meredith and Price, 2006). In *Arabidopsis*, substrate identities of 32 NPF transporters have been investigated, of which 17 are confirmed to transport nitrate (Corratge-Faillie and Lacombe, 2017). The founding member of the nitrate-transporting NPF family is NRT1.1/NPF6.3/CHL1, which was originally identified as an inducible low affinity nitrate transporter (Tsay et al., 1993). *NRT1.1* is expressed extensively in root tissue and is responsible for nitrate uptake from the soil (Crawford, 1995, Munos et al., 2004). Later, NRT1.1 was found to be a bidirectional nitrate transporter that is present in aerial tissues as well, and is involved in long distance translocation of nitrate (Boursiac et al., 2013, Leran et al., 2013). Moreover, NRT1.1 is frequently referred to as a dual-affinity nitrate transporter because it is involved in both LATS and HATS activities (Wang et al., 1998, Liu et al., 1999). The switch between NRT1.1 high and low affinity uptake depends on the phosphorylation state of the Thr101 residue, as catalysed by the CALCINEURIN-LIKE PROTEIN (CBL)-INTERACTING PROTEIN KINASE 23 (CIPK23)-CBL9 or CIPK23-CBL1 complex (Ho et al., 2009, Leran et al., 2015). Phosphorylated NRT1.1 is a high-affinity carrier, whereas non-phosphorylated NRT1.1, de-phosphorylated by the protein phosphatases PP2C and ABI2, is a low-affinity carrier (Liu and Tsay, 2003, Leran et al., 2015). It was suggested that the Thr101 phosphorylation triggered by low external nitrate level leads to a conformational disruption of

NRT1.1 N terminal bundle helices, which increases the flexibility of the transporter, and thus results in a higher transport rate of nitrate (Parker and Newstead, 2014). Nevertheless, doubts have previously been cast on the extent of the contribution of NRT1.1 to HATS (Glass and Kotur, 2013). NRT1.2/NPF4.6, on the other hand, exclusively regulates the cLATS (Liu et al., 1999). Both NRT1.1 and NRT1.2 were first identified through screening mutant *Arabidopsis* plants for resistance to chlorate, a toxic nitrate analogue that causes chlorosis in leaves when taken up by nitrate transporters and reduced to chlorite by nitrate reductase (Tsay et al., 1993, Wang and Crawford, 1996).

Other members of the NPF family regulate nitrate long distance translocation from root to shoot or from source to sink (e.g., NPF2.9, NPF2.13, NPF7.2 and NPF7.3), nitrate redistribution (e.g., NPF1.1 and NPF1.3), nitrate embryo accumulation (e.g., NPF5.5) and nitrate efflux (NPF2.7/NAXT1, Guan, 2017). A unique feature of plant NPF proteins is that they generally have low substrate specificities. In fact, some of the aforementioned nitrate transporting NPFs have been shown to also transport downstream nitrate metabolites (nitrite and amino acids), chloride, glucosinolates, and almost all plant hormones (Corratge-Faillie and Lacombe, 2017). The multi-substrate feature of NPFs might indicate their novel roles as integrators of the external nutrient and internal physiological signals (Corratge-Faillie and Lacombe, 2017).

To date, four members of the NRT2 family, NRT2.1, NRT2.2, NRT2.4 and NRT2.5, have been reported to mediate the HATS, of which NRT2.5 regulates the cHATS while the other three regulate the iHATS (Orsel et al., 2002, Kiba et al., 2012, Lezhneva et al., 2014, Kiba and Krapp, 2016). NRT2.1 and NRT2.2 appear to be the major regulators of the HATS, as NRT2.4 only contributes to the HATS significantly under extremely low external nitrate concentrations

(Kiba et al., 2012, Lezhneva et al., 2014). An additional layer of NRT2 regulation involves a strict requirement for them to interact with a partner protein NRT3.1/NAR2.1, resulting in a hetero-oligomer that not only increases NRT2 nitrate uptake capacity, but also promotes NRT2 trafficking to the plasma membrane as well as its stability (Orsel et al., 2006, Li et al., 2007, Wirth et al., 2007, Kotur et al., 2012). Additionally, NRT2.4 and NRT2.5 also regulate nitrate translocation from source to sink in the shoot, whereas another NRT2 member, NRT2.7, transports nitrate into seeds (Chopin et al., 2007, Kiba et al., 2012, Lezhneva et al., 2014).

1.4.2 Nitrate assimilation

Following uptake, most nitrate is translocated to shoot tissue for assimilation, because photosynthesis provides the high-level reducing energy required for nitrate reduction (Krapp et al., 2011). Nitrate reduction by nitrate reductase (NR) occurs in the cytosol, and is the major rate-limiting step in the nitrate assimilation pathway (Figure 1.8, Campbell, 2001). The end product of nitrate reduction, nitrite (NO_2^-), is cytotoxic and mutagenic (Bartsch et al., 1992, Sugimura, 2000). NO_2^- can also be converted to nitrous acid, which is especially toxic to the photosynthetic apparatus; and NO, which can lead to unwanted protein modifications when it reacts with active oxygen species (Sinclair, 1987, Morot-Gaudry-Talarmain et al., 2002). Therefore, NR is under extensive regulation both transcriptionally at the mRNA level and post-transcriptionally at the protein level. *Arabidopsis* mutant screens for resistance to chlorate toxicity has revealed two homologous NR genes, *NIA1* and *NIA2*, which are respectively responsible for 10 and 90% of the total plant NR activity (Cheng et al., 1988, Wilkinson and Crawford, 1991, Wilkinson and Crawford, 1993). Both *NIA1* and *NIA2* expression is promoted by the presence of nitrate as a signalling molecule (see below), and inhibited by products of nitrate metabolism (especially glutamate, Hoff et al., 1994, Crawford, 1995). The latter

feedback repression of *NR* transcription is mediated by three zinc-finger DNA binding transcription factors, LATERAL ORGAN BOUNDARIES DOMAIN37 (LBD37), LBD38, and LBD39, which possibly also downregulate nitrate transporter gene expression in response to nitrate provision (Rubin et al., 2009). Contrarily, light and/or sugar positively regulate *NR* expression, in a process potentially contributing to the maintenance of plant carbohydrate and amino acid balance, although the molecular mechanism of this is largely unknown (Crawford, 1995). Mutant studies suggest two photomorphogenesis-promoting proteins belonging to the bZIP transcription factors, LONG HYPOCOTYL5 (HY5) and HOMOLOG OF HY5 (HYH), as potential candidates for light activation of *NIA2*, whereas the negative regulator of photomorphogenesis PIF4 inhibits *NIA2* gene expression (Jonassen et al., 2008, Jonassen et al., 2009). Interestingly, HY5 was also recently identified as a shoot-to-root mobile signal promoting root growth and nitrate uptake through the activation of *NRT2.1* expression, thus contributing to the maintenance of the light-dependent balance between carbon and nitrogen metabolites (Chen et al., 2016). Multiple studies have confirmed that NR gene expression, protein abundance and enzyme activity oscillate according to the circadian clock, with NR mRNA level peaking pre-dawn (Deng et al., 1991, Lillo, 1991, Pilgrim et al., 1993, Tucker et al., 2004, Cookson et al., 2005). The molecular basis of NR diurnal regulation remains unresolved, although it has been suggested that the circadian pattern is merely due to fluctuations in nitrate and/or glutamine contents throughout the day (Hoff et al., 1994, Crawford, 1995). Alternatively, it was discovered that CIRCADIAN CLOCK-ASSOCIATED1 (CCA1) binds to the promoter regions of both *NIA1* and *NIA2* genes in vitro, and loss-of-function *cca1-1* mutant display disrupted *NIA1* and *NIA2* expression patterns (Teng et al., 2017). Finally, environmental stresses such as low temperature and drought, and phytohormones including cytokinin and ABA, possibly also affect NR at the transcript level,

although little is known about the underlying mechanisms of these regulations (Hoff et al., 1994, Foyer et al., 1998, Jones et al., 1998, Sakakibara, 2003).

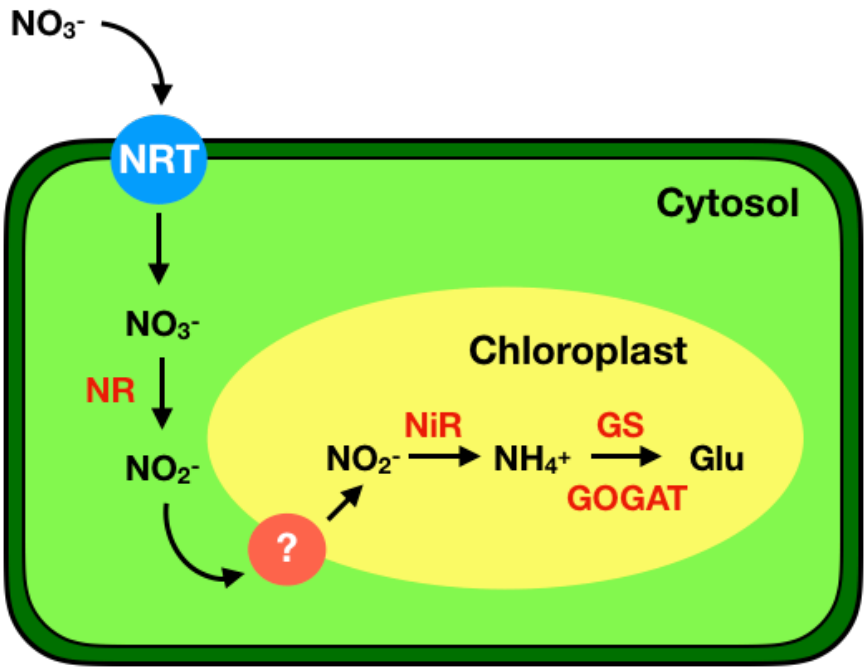


Figure 1.8 Simplified diagram of nitrate assimilation within a cell.
Nitrate enters the cell through nitrate transporters and is reduced to nitrite by cytosolic nitrate reductase (NR). An unknown nitrite transporter sequesters cytotoxic nitrite into the chloroplast, where it is reduced further to ammonium by nitrite reductase (NiR). Finally, ammonium is incorporated into amino acid through the GS/GOGAT pathway.

NR has long been known to be regulated post-translationally, which is speculated to be essential for flexible adjustment of NR activity to prevent accumulation of toxic NO_2^- in the cell (Lillo et al., 2004). Active NR is formed by homodimerization of two subunits, each containing three prosthetic groups, molybdenum cofactor (Moco), heme b_{557} and FAD, and two flexible hinge regions in between (Campbell and Kinghorn, 1990). This structural arrangement facilitates electron transfer from the electron donor NAD(P)H to nitrate through the three protein domains (Campbell, 2001). In *Arabidopsis*, NR deactivation starts with phosphorylation of Ser534 in the hinge I domain connecting Moco and heme b_{557} groups (Campbell and Kinghorn, 1990). NR phosphorylation is mediated by yet to be identified

enzymes, which has been proposed to involve a variety of kinases belonging to the calcium-dependent protein kinase (CPK) and the calcium-independent SNF1 resembling kinase (SnRK1) families responsible for inactivating NR under specific circumstances (Bachmann et al., 1996, Douglas et al., 1998, Sugden et al., 1999, Ikeda et al., 2000, Lillo et al., 2004). However, NR is only inactivated after the binding of 14-3-3 protein members to the phosphorylated NR in the presence of cations (Mg^{2+} and/or Ca^{2+}) and polyamines (Provan et al., 2000, Kaiser and Huber, 2001). 14-3-3 proteins preferentially bind to the phosphorylated Ser with a high affinity, but complete inactivation of NR requires an additional low affinity binding of 14-3-3 to the N terminal acidic motif of NR (Chi et al., 2015). The resultant NR conformational change blocks the electron transfer pathway within the enzyme and therefore renders it inactive (Lambeck et al., 2012). NR phosphorylation was first thought to promote NR degradation at the hinge regions, but more recent studies suggest that NR is degraded at a relatively constant rate regardless of its phosphorylation state (Lillo et al., 2004). NR re-activation involves dephosphorylation by the protein phosphatase 2A (PP2A), whose C2 catalytic subunit appears to be particularly important for NR activation (MacKintosh and Meek, 2001, Creighton et al., 2017). On the other hand, phosphorylation of another serine residue (Ser627) located within the hinge II domain by *Arabidopsis* MITOGEN-ACTIVATED PROTEIN KINASE6 (MPK6) in response to hydrogen peroxide (H_2O_2) has been shown to promote nitrate reductase activity, thus regulating lateral root development (Wang et al., 2010b). Interestingly, NR also plays an important role in maintaining plant NO homeostasis through its ability to transfer electrons to NO-FORMING NITRITE REDUCTASE (NOFNiR), which synthesises NO from NO_2^-, as well as to the TRUNCATED HAEMOGLOBIN (THB1), which regenerates NO_3^- from NO (Chamizo-Ampudia et al., 2017).

NO_2^- produced by NR is immediately translocated to the chloroplast by an unknown transport system, where it is reduced to ammonium by plastid nitrite reductase (Dose et al., 1997, Fernandez and Galvan, 2007, Sanz-Luque et al., 2015). It is generally believed that plant nitrite reductase has a much higher activity compared to that of nitrate reductase, possibly due to the need to avoid the accumulation of cytotoxic NO_2^- (Pilgrim et al., 1993, Du et al., 2008). Ammonium is then incorporated into the amino acid pool via the action of the glutamine synthase/glutamine oxoglutarate aminotransferase or glutamate synthase (GS/GOGAT) pathway (Figure 1.8, Williams and Miller, 2001).

1.4.3 Nitrate signalling

In addition to its role as a fundamental nutrient, nitrate has long been known to function as a signal molecule controlling a wide spectrum of plant metabolic and developmental processes (Crawford, 1995, Gojon et al., 2011). Most significantly, it has been estimated that up to 10% of the transcriptome is responsive to the nitrate signal, including genes involved in the nitrate metabolic pathway (e.g., nitrate transporters, nitrate and nitrite reductases) as well as genes required for carbon metabolism and chemical energy provision (Wang et al., 2009b, Krouk et al., 2010a). However, the molecular identity of genes regulating this primary nitrate response has only recently been investigated, and despite extensive research, a reliable nitrate-responsive promoter element is yet to be identified (Krapp et al., 2014). The dual affinity nitrate transporter NRT1.1 has been proposed to act as a major upstream nitrate sensor, based on the observation that multiple primary nitrate responses are damped in the *nrt1.1* null mutant (Gojon et al., 2011). As an example, *NRT2.1* gene expression is closely regulated by NRT1.1 in response to the nitrate signal. Short-term exposure to nitrate induces rapid *NRT2.1* expression that is regulated by NRT1.1 (Ho et al., 2009, Bouguyon et al., 2015). On the other hand, long-

term high nitrogen supply down-regulates *NRT2.1* expression by the combined effect of two different signalling pathways: systemic feedback repression from nitrogen metabolite products (Crawford and Glass, 1998, Gojon et al., 2011), and local inhibition through NRT1.1-dependent nitrate signalling (Munos et al., 2004, Krouk et al., 2006). Similar to nitrate uptake, the primary response mediated by NRT1.1 also displays a two-phase pattern depending on the phosphorylation state of the Thr101 residue: phosphorylated and unphosphorylated NRT1.1 mediate low and high primary response, respectively (Ho et al., 2009). Therefore, proteins that regulate NRT1.1 activity, including CIPK8, CIPK23, CBL1/9, PP2C and ABI2, are indirectly implicated in nitrate sensing (Noguero and Lacombe, 2016). Moreover, the isolation of the *chl1-9* mutant with a single amino acid substitution at Pro492 of NRT1.1, which exhibits defective nitrate uptake in both high- and low-affinity ranges but shows a normal biphasic primary nitrate response with respect to *NRT2.1* gene expression, strengthens the hypothesis that the nitrate transport activity of NRT1.1 can be genetically separated from its sensing function (Ho et al., 2009, Bouguyon et al., 2015). Apart from gene expression regulation, there is accumulating evidence indicating that nitrate signalling through NRT1.1 also regulates longer-term responses, such as root architecture (Zhang and Forde, 1998). Specifically, localised nitrate distribution stimulates lateral root proliferation and growth through the putative MADS-box transcription factor ARABIDOPSIS NITRATE REGULATED1 (ANR1, Zhang and Forde, 1998, Remans et al., 2006a). This regulation is dependent on the NRT1.1-mediated nitrate sensing, but the resultant phenotype relies on the ability of NRT1.1 to transport auxin in order to promote root growth (Krouk et al., 2010b). Other nitrate-regulated long-term responses include resistance to ammonium toxicity, shot/root ratio, organogenesis, flowering, ABA-independent stomata opening, and seed dormancy (Guo et al., 2001, Guo et al., 2003, Wang et al., 2009b, Hachiya and Noguchi, 2011, Krapp et al., 2014).

In addition, recent studies have suggested that the high-affinity uptake complex NRT2.1-NAR2.1 also functions in nitrate signalling through exerting context-dependent dual effects on lateral root development as well as the promotion of pathogen defence (Little et al., 2005, Remans et al., 2006b, Camañes et al., 2012). Therefore, NRT1.1 and NRT2.1 are the first nitrate, or even nutrient transceptors (transporters that also act as sensors) discovered in plants. However, as compared to the nitrate transport system, it remains the case that relatively little is currently known about the mechanism of nitrate signalling, especially with regard to the connection between nitrate signal perception and subsequent changes in gene expression (Krapp, 2015).

Recent forward genetic screens and systems approaches have identified a suite of transcription factors involved in nitrate sensing that act upstream of the nitrate transceptors mentioned above (Vidal et al., 2015). Two of the nine members of the *Arabidopsis* family of NODULE INCEPTION (NIN)-LIKE PROTEINs (NLPs), NLP6 and NLP7, have been extensively studied recently and are recognised as crucial regulators of the nitrate-induced activation of genes involved in nitrate uptake and assimilation (Castaings et al., 2009, Wang et al., 2009b, Konishi and Yanagisawa, 2013, Yu et al., 2016). *NLP6* and *NLP7* expression is not affected by nitrate, but nitrate interacts with the N termini of the NLP6 and NLP7 transcription factors and promotes their nuclear retention by an unknown post-translational mechanism (Konishi and Yanagisawa, 2013, Marchive et al., 2013), which subsequently leads to the activation of nitrate transporter genes (*NRT1.1*, *NRT2.1* and *NRT2.2*), nitrate reductase genes (*NIA1* and *NIA2*), and the nitrite reductase gene (*NIR1*, Vidal et al., 2015). It is tempting to speculate that other NLP members are potentially involved in nitrate signalling as well (Vidal et al., 2015). Similarly, TEOSINTE BRANCHED/CYCLOIDEA/PROLIFERATING CELL FACTOR20 (TCP20) upregulates the transcription levels of *NRT1.1*, *NRT2.1* and *NIA1* in response to the

nitrate signal (Guan et al., 2014). Notably, given that TCP20 also directly promotes *PROLIFERATING CELL NUCLEAR ANTIGEN2* (*PCNA2*), *CYCB1;1* (which controls G2/M cell cycle transition) and several ribosomal proteins in the root apical meristem, TCP20 probably integrates local nitrate signals and directly modulates root architecture (Guan et al., 2014, Li et al., 2005, Strzalka and Ziemienowicz, 2011). A recent novel approach combining time-course transcriptome analysis of nitrate response and mathematical modelling identified SPL9 as a bottleneck of the early nitrate signalling response, controlling the expression of at least *NRT1.1*, *NIA2* and *NIR* (Krouk et al., 2010c). An SPL9 overaccumulation mutation in turn disrupts root architecture by repressing lateral root initiation, proliferation and growth (Krouk et al., 2010c).

1.5 Project Aims

Our understanding of plant nitrogen metabolism and signalling has been advancing rapidly over the last two decades. Previous attempts at increasing plant NUE have been made through simply overexpressing nitrogen transporters or nitrogen assimilation enzymes, but have seldom succeeded. Some recent positive examples include the overexpression of *OsAMT1;1*, *OsNPF6.3*, *OsNPF7.3*, and *OsNRT2.3* in rice; although in some cases, undesirable pleiotropic effects such as delayed flowering are associated with an increase in yield (Fang et al., 2013, Ranathunge et al., 2014, Fan et al., 2016, Wang et al., 2018). The low success rate may be explained by the extensive regulatory network controlling nitrogen metabolism and its crosstalk with other pathways (Krapp, 2015). This emphasises the importance of a deeper understanding of nitrogen metabolism in a much broader context.

This research project takes as one start point the recent discovery that semi-dwarf "Green Revolution" crop varieties have a relatively low NUE, an effect potentially attributable to the stabilised growth repressive DELLA proteins (Gooding et al., 2012). The signalling pathway for GA perception and subsequent protein destruction of DELLAs is well-established, and the understanding of the various mechanisms via which DELLAs regulate downstream gene expression is progressing (Harberd et al., 2009, Locascio et al., 2013). However, the relationship between the GA-DELLA signalling and nitrogen metabolic pathways has hitherto been sparsely investigated. This study utilises the *Arabidopsis* gain-of-function mutant *gai* as the experimental model for modern GRVs, and aims to clarify how, as master growth regulators in plants, DELLAs regulate nitrate uptake and/or assimilation. Such an understanding would provide a molecular explanation for the compromised nitrate metabolism caused by DELLA accumulation. PIFs, as the most important DIPs, are increasingly being recognised as crucial integrators of external and internal signals, and have previously been shown to modulate *Arabidopsis* NR activity (Jonassen et al., 2009, Li et al., 2016). Therefore, this study also addresses the roles played by PIFs in nitrate metabolism regulation. Finally, an *Arabidopsis* mutant screen on chlorate (the toxic analogue of nitrate) using the *gai* mutant background as the starting point attempts to genetically uncouple DELLA-mediated inhibition of plant growth and nitrate metabolism, i.e., to isolate *gai* mutants maintaining a dwarf stature but having improved nitrate metabolism (and therefore increased sensitivity to chlorate), or *gai* mutants maintaining a deficient nitrate metabolism (therefore maintaining resistance to chlorate) but reverting to a tall statue. Identified genes responsible for these phenotypic changes might provide strategic targets for future biotechnological breeding of desirable crops.

In conclusion, this project is important in terms of unravelling fundamental understanding of how plant nitrogen metabolism is coordinated with the regulation of growth and development.

This advanced knowledge might in turn pave the way for the development of future crops having improved NUE whilst maintaining the yield benefits conferred by stabilised DELLAs. Such high-yielding crop varieties with a reduced yield-dependency on high fertiliser input levels is an ultimate goal for achieving future global food security with minimal environmental degradation.

1.6 Thesis Structure

In Chapter 3, the underlying mechanism of DELLA inhibition of nitrate metabolism is investigated in the *Arabidopsis* semi-dwarf GRV model *gai*. Chapter 4 describes the contribution of PIFs to regulation of nitrate metabolism, and thereby proposes a hypothetical model of PIFs (specifically PIF3) transducing the GA-DELLA signal to regulate downstream nitrate assimilation. Chapter 5 and Chapter 6 outline chlorate-response mutant screens of a mutagenized *gai* population, with Chapter 5 focusing on the identification of *gai* mutants that are still dwarf but have altered chlorate responses, and Chapter 6 focusing on the isolation of tall *gai* mutants in the hope of breaking the correlation between *gai*-mediated inhibition of growth and inhibition of nitrate metabolism. Finally, in Chapter 7, knowledge obtained in this study from the model organism *Arabidopsis* is compiled, and the potential for relevant application in crop plants is discussed.

CHAPTER 2. Materials and Methods

2.1 General Materials and Methods

2.1.1 Chemicals and primers

All chemicals described in this study were purchased from Sigma-Aldrich (www.sigmaaldrich.com), Fisher Scientific (www.fisher.co.uk), Duchefa Biochemie (https://www.duchefa-biochemie.com), or Clontech (www.clontech.com) unless otherwise specified. Chemical solutions were prepared with de-ionised water (dH_2O). Synthetic primers used for polymerase chain reactions (PCRs) and Sanger sequencings were purchased from Sigma-Aldrich. Primers were dissolved and diluted with sterilised dH_2O that was purified with MilliQ (Millipore, www.millipore.com) cartilages.

2.1.2 Sterilisation

Most sterilisation was performed by autoclaving at 121 °C under 100 kPa of pressure for 20 minutes. Yeast media were sterilised at the same temperature and under the same pressure, but for 15 minutes. Chemicals that are heat-unstable were sterilised using 0.2 μm syringe filters (VWR, www.uk.vwr.com/store).

2.1.3 Centrifugation

If not otherwise specified, centrifugation was carried out at room temperature using a benchtop MiniSpin^{TM} plus centrifuge machine (Eppendorf, catalogue number: 5453000011). The maximum speed of 14,100 rpm can be reached within 13 seconds.

2.2 Plant Materials and Growth Conditions

2.2.1 *Arabidopsis thaliana*

Arabidopsis seeds used in this study are listed in Table 2.1 (*Landsberg erecta* ecotype) and Table 2.2 (*Columbia* ecotype). T-DNA knock-out mutant lines obtained from the European Arabidopsis Stock Centre (NASC, UK, www.arabidopsis.info) belong to either SALK, SAIL, or GABI-Kat collection, details of which can be found on the NASC website. All seed stocks were genotyped and confirmed to be homozygous by PCR (see section 2.6.4) prior to experiments (for an example of the genotyping of the *pifq* [*pif1 pif3 pif4 pif5*] mutant, see Figure 2.1).

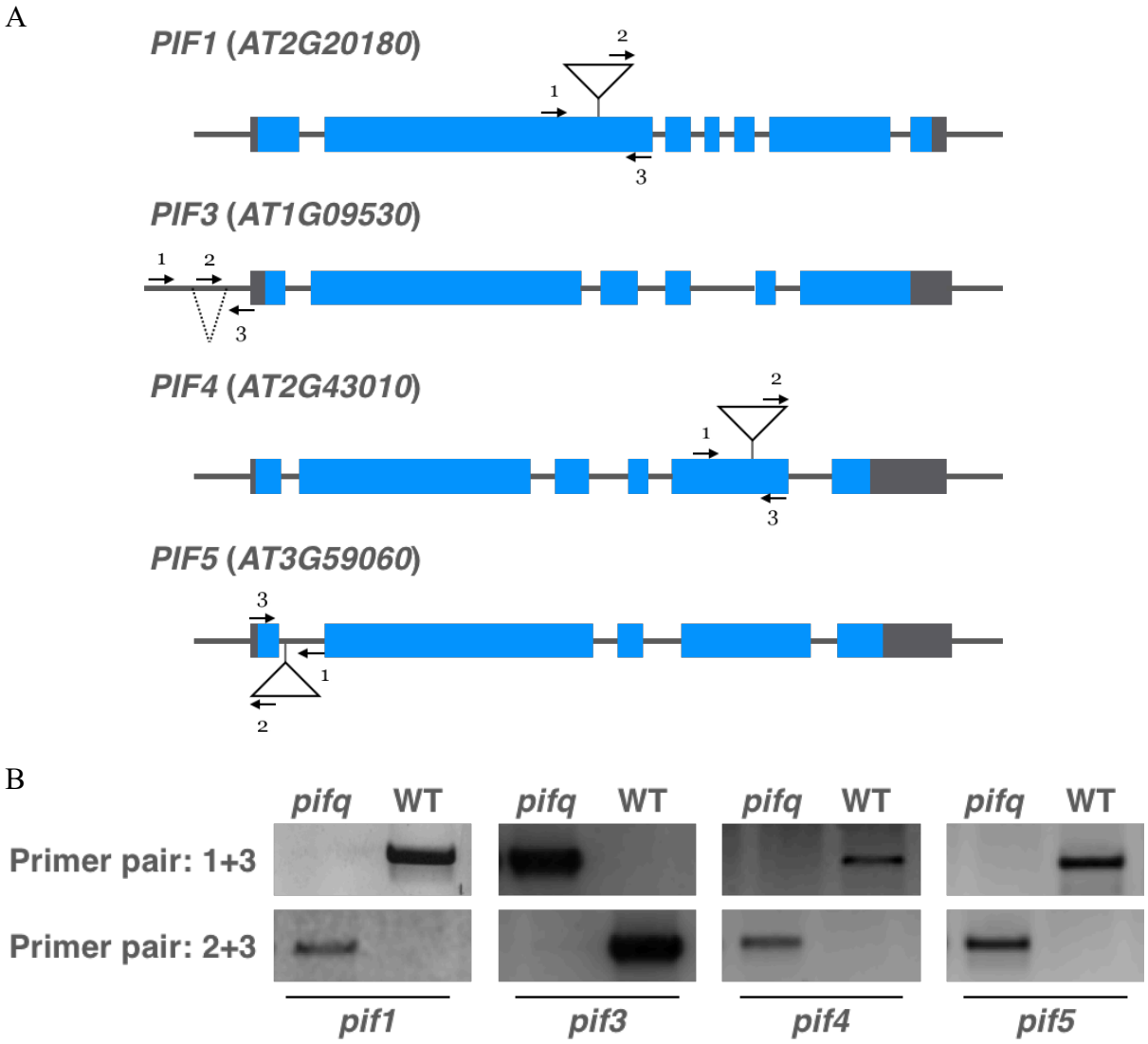


Figure 2.1 The quadruple loss-of-function *pifq* mutant used in this study was confirmed to be homozygous by PCR prior to experiments.
(A) Schematic representation of the gene structures of the four *PIFq* members (*PIF1*, *PIF3*, *PIF4* and *PIF5*) and the mutation sites in the *pifq* quadruple loss-of-function mutant. 5' and 3' untranslated regions (UTRs) are represented by grey boxes. Exons are represented by blue boxes. Lines connecting exons represent introns whereas lines outside of 5' and 3' UTRs are promoter or intergenic regions. The inverted triangles indicate the sites of T-DNA insertion (in the cases of *pif1*, *pif4* and *pif5*) whilst the dotted lines indicate the site of deletion (in the case of *pif3*). Primers used for genotyping are represented as arrows with designated numbers. This diagram is not drawn to scale. (B) DNA materials from WT and the *pifq* mutant plant were extracted for PCR with the primer pairs indicated on the left-hand-side of the gel pictures. Four independent pairs of PCR reactions (labelled below the gel pictures) were carried out to confirm that all four mutations are homozygous in the *pifq* mutant. It can be concluded in this case that the *pifq* mutant is homozygous for all four loss-of-function mutations.

Table 2.1 *Arabidopsis* (*Landsberg erecta* ecotype) seeds used in this study.

Seed Genotype	Stock ID	Ecotype	Source
WT	\	*Ler*	Lab
gai	\	*Ler*	Lab
tt1	\	*Ler*	Lab
gai-t6 tt1	\	*Ler*	Lab
cp3-1	N48	*Ler*	NASC
dw1-1	N50	*Ler*	NASC
ga5	N62	*Ler*	NASC
min-1	N74	*Ler*	NASC
***pif8* (*une10*)**	N25591	*Ler*	NASC

Table 2.2 *Arabidopsis* (*Columbia* ecotype) seeds used in this study.

Seed Genotype	Stock ID	Ecotype	Source
WT	\	*Col-0*	Lab
***nrt1.1* (*nrt1.1-1*)**	N597431	*Col-0*	NASC
***nrt2.1 nrt2.2* (*nrt2.1-1*)**	N535429	*Col-0*	NASC
***nia2* (*nia2-5*/*chl3-5*)**	N2355	*Col-0*	NASC
TOR-OX	\	*Col-0*	Lab
TOR-RNAi	\	*Col-0*	Lab
gai	\	*Col-0*	Chinese Academy of Sciences
***pif1* (*pif1-1*)**	N66041	*Col-0*	NASC
pif2	N525598	*Col-0*	NASC
***pif3* (*pif3-3*)**	N66042	*Col-0*	NASC
***pif4* (*pif4-2*)**	N66043	*Col-0*	NASC
***pif5* (*pif5-3*)**	N66044	*Col-0*	NASC
***pifq* (*pif1-1 pif3-7 pif4-2 pif5-3*)**	N66049	*Col-0*	NASC
pif6	N590239	*Col-0*	NASC
pif7	N68809	*Col-0*	NASC
PIF3OX*/*pif3	\	*Col-0*	University of California Berkeley
PIF4OX*/*pif4	\	*Col-0*	University of California Berkeley
pv42a	N840253	*Col-0*	NASC
grf7	N584141	*Col-0*	NASC

Arabidopsis seeds were sterilised with 75% ethanol for 10 minutes before being sown on half-strength MS (2.15 g/l Murashige & Skoog) salt media (pH 5.8) containing 0.5% sucrose and 0.6% agarose. Seeds were subsequently stratified at 4 °C in the dark for 2–5 days. For mutant lines that are difficult to germinate, seeds were submerged in 10 μM GA_3 solution and stratified under the same conditions. Before being sown on plates, these seeds were washed with dH_2O for at least four times to minimise residue GA_3 and then sterilised. Plates were then transferred to controlled growth conditions (22–24 °C under 16-h light/8-h dark photoperiod [irradiance 120 μmol of photons/m^2 per second]) in tissue culture rooms (TCRs) and mounted vertically.

After 10 days, if necessary, seedlings were transplanted to sieved soil (ICL Levington Advanced F2 compost, http://www.gro-welldirect.co.uk/, particle size < 2 cm). They were then placed in controlled environment rooms (CERs) with the same environmental conditions as above.

2.2.2 *Oryza sativa*

Seeds of *Oryza sativa* subspecies (ssp). *inidca* (Nanjing-6 [NJ6] variety) were kindly provided by Prof. Xiangdong Fu (Chinese Academy of Sciences, Beijing, China). Seeds were peeled before being submerged in 70% ethanol for 30 seconds in a sterilised 15 mL falcon tube. Ethanol was then replaced by 15 mL of 10% Sodium Hypochlorite (NaClO), and the seeds were shaken on a benchtop Rotatest shaker (Luckham, catalogue number: R100) for 30 minutes. The seeds were rinsed three times with dH_2O, and then placed on top of two layers of water-soaked 8.5 mm Whatman filter paper in a sterilised petri dish. The plates were sealed and incubated at 37 °C in the dark for 3–7 days to synchronise germination.

Following germination, rice seedlings were transferred to 1.5 L hydroponic devices containing 1 L of ½ MS liquid media supplemented with vitamins in Sanyo #MLR 351 plant growth incubators set at 22 °C under 16-h light/8-h dark photoperiod (irradiance 200 μmol of photons/m^2 per second). Nutrient solution was replaced every 5 days initially, and then every 3 days.

2.3 *Arabidopsis* Hypocotyl Graft

Grafting with *Arabidopsis* seedlings was performed as described before (Melnyk, 2017). *Arabidopsis* seeds were sown on ½ MS media and stratified as described above. Plates were then moved into Sanyo #MLR 351 plant growth incubators set at 22 °C under 8-h light/16-h dark photoperiod (irradiance 100 μmol of photons/m^2 per second), and the seedlings were allowed to grow vertically for 7 days. Two days prior to grafting, the temperature was raised to 27 °C to promote hypocotyl elongation.

Grafting was performed in a sterilised environment (in a laminar flow hood) under a stereomicroscope. 6–8 seedlings to be grafted were transferred onto a 2.5×4 cm strip of Hybond N membrane (GE Healthcare, catalogue number: RPN203N) placed on top of two layers of water-soaked 8.5 mm Whatman filter paper in a petri dish. With a sterile stainless-steel scalpel (Swann-Morton, catalogue number: 0501), one cotyledon was removed from each seedling, and a clean horizontal cut was made on the hypocotyl at a position close to the shoot meristem, which minimises the chance of adventitious root development (Melnyk, 2017). After exchanging the shoot with another seedling using a pair of forceps, graft chimeras were assembled by carefully attaching the scion and rootstock tissues. Once grafting was performed

for all of the seedlings, the plates were sealed with parafilm and returned to the growth incubators. Grafted seedlings were grown at 27 °C for 5 days to induce auxin production that facilitates graft recovery (Turnbull et al., 2002), before decreasing the temperature back to 22 °C and grown for 3 more days.

Successfully grafted seedlings without developing adventitious roots were transferred to soil and grown in CERs at 22–24 °C under 16-h light/8-h dark photoperiod (irradiance 120 μmol of photons/m^2 per second). Inspection for adventitious root formation was performed with a magnifying glass for at least 7 days after transplanting, and graft chimeras that have grown adventitious roots were discarded.

2.4 Plant Phenotypic Studies

2.4.1 Chlorate toxicity assay in *Arabidopsis*

Four-week old *Arabidopsis* plants grown on soil were treated with Potassium Chlorate ($KClO_3$) in a similar fashion as previously described (Park et al., 2011a). Preliminary experiments indicate that the optimal chlorate concentration is 1.0 mM for *Ler* and 1.5 mM for *Col-0 Arabidopsis*. Soil was soaked in 1 L of chlorate solution by bottom feeding for 1 hour to reach maximum soil capacity, before the extra solution was discarded. Chlorate treatment was repeated every 5 days for three times, or until a clear phenotype could be observed. Generally, leaf chlorosis became apparent for WT leaves shortly after the onset of the second chlorate treatment.

2.4.2 Chlorate toxicity assay in *Oryza sativa*

Four-week old rice plants grown hydroponically were treated with 0.1, 0.5, 1.0, 1.5 and 2.0 mM $KClO_3$. The appropriate concentrations of chlorate were added directly to the nutrient solution, which was renewed every 3 days until leaf chlorosis became apparent.

2.4.3 Chlorophyll measurement

Leaf chlorophyll concentration was measured using a SPAD-502 meter (Konica-Minolta, Japan) as described before (Ling et al., 2011). For each plant, the average of 3 independent SPAD readings recorded from 3 different fully-expanded rosette leaves (a total of 9 readings) was calculated. 10–12 samples were taken for each genotype under both control and chlorate-treated conditions. Absolute chlorophyll concentration in nmol/mg fresh weight was calculated using the previously derived equation:

$$y = 0.0007x^2 + 0.0230x + 0.0544$$

where: **y** is the absolute chlorophyll concentration and $\boldsymbol{x}$ is the SPAD meter reading (Ling et al., 2011). Two-way Analysis of Variance (ANOVA) statistical analyses were performed for the decrease in chlorophyll content after chlorate treatment between genotypes as an indication of chlorate sensitivity.

2.4.4 *Arabidopsis* hypocotyl length measurement

For the measurement of hypocotyl length of dark-grown seedlings, stratified seeds were transferred to TCR and exposed to light briefly for 6 hours to induce germination. The plates were then wrapped in aluminium foil before being returned to TCR where the seedlings were

grown vertically. After 7 days, seedling hypocotyl length was measured with a ruler to the closest 1 mm. At least 15 individual seedlings were measured for each genotype.

2.4.5 *Arabidopsis* height measurement

Plant height measurements were performed for six-week old *Arabidopsis* plants. Plant shoot was cut at the base of the rosette, and then its longitudinal length was measured with a ruler to the closest 1 mm. At least 10 individual plants were measured for each genotype.

2.5 Protein Manipulation

2.5.1 Protein extraction

Plant tissue (0.5 g *Arabidopsis* rosette leaf or rice whole shoot) was harvested 3 hours after the start of the light photoperiod, and ground to fine powder in liquid nitrogen with pestle and mortar. 5 mL/g of extraction buffer containing 50 mM Potassium Phosphate (KH_2PO_4, pH 7.6), 1 mM Ethylenediaminetetraacetic Acid (EDTA), 5 mM 1,4-Dithiothreitol (DTT), 0.5% Triton and 1x HALT™ Protease Inhibitor Cocktail (ThermoFisher, catalogue number: 78430) was then added and the sample was homogenised further until thawed. 2 mL of the crude protein extract was transferred to an Eppendorf tube, followed by two rounds of centrifugation at 13,500 rpm for 15 minutes. 1 mL of the supernatant was transferred to a new tube and preserved on ice.

2.5.2 Protein quantification

Protein extracted from *Arabidopsis* leaf and rice shoot was diluted five and six folds respectively with dH_2O. Diluted protein sample was quantified with the Bio-Rad *DC* colorimetric protein assay kit (Bio-Rad, catalogue number: 500-0116) following the manufacturer's instructions. Prior to protein quantification, both Solution A and Solution B were brought to room temperature. 20 µL per 1 mL of Solution S was added to Solution A to make Solution A'. 100 µL of protein extract was mixed with 500 µL of Solution A' and 4 mL of Solution B by vigorous vortexing. The reaction solution was incubated at room temperature for 15–30 minutes (final colour stable for up to 60 minutes), before 1 mL was transferred to a cuvette. The absorbance at 750 nm (OD_{750}) was measured using the Evolution 260 BIO UV-Visible Spectrophotometer (Thermo Scientific, catalogue number: 912A0888), from which the protein concentration can be derived. Protein standard curve was made with serial dilutions of bovine serum albumin (BSA) provided with the kit.

2.5.3 Nitrate reductase (NR) activity assay

NR activity was measured with a modified protocol as described before (Park et al., 2011a). 200 µL of protein extract from above was added to 800 µL of reaction buffer and incubated at 30 °C in the dark for 10 minutes. For total NR activity, the reaction buffer consisted of 50 mM KH_2PO_4 pH 7.6, 5 mM EDTA, 10 mM Potassium Nitrate (KNO_3) and 0.2 mM Nicotinamide Adenine Dinucleotide Hydride (NADH). The reaction was stopped by adding 1 mL of 0.5 mM zinc acetate ($Zn[OAc]_2$), followed by centrifugation at 12,000 rpm for 5 minutes. 500 µL of the supernatant was transferred to a new tube, before adding 1 mL of colour development reagent made by mixing equal volumes of 1% sulfanilic acid in 3 M hydrochloric acid (HCl)

and 0.1% *N*-(1-naphthyl)-ethylenediamine dihydrochloride. After incubation at room temperature for 30 minutes in the dark, the absorbance of the reaction mixture at 540 nm (OD_{540}) was measured using the Evolution 260 BIO UV-Visible Spectrophotometer, from which the nitrite concentration can be determined. NR activity was finally calculated as the concentration of nitrite produced per minute (nmol NO_2^- min^{-1}) normalised against sample protein concentration (mg ml^{-1}). Nitrite standard curve was made with serial dilutions of Sodium Nitrite ($NaNO_2$).

2.5.4 Nitrite reductase (NiR) activity assay

NiR activity was measured with a modified protocol as described before (Takahashi et al., 2001). 45 µL of protein extract from above was added to 195 µL of assay solution (50 mM KH_2PO_4 pH7.5, 1 mM $NaNO_2$, 1 mM methyl viologen). The reaction was started with the addition of 60 µL of 57.4 mM Sodium Dithionite ($Na_2S_2O_4$) in 290 mM Sodium Bicarbonate ($NaHCO_3$). After a 10-minute incubation at 30 °C in the dark, 20 µL of the reaction mixture was transferred to a new tube and diluted 25-fold with dH_2O. The solution was vortexed vigorously until colourless, before being added 1 mL of colour development reagent (1:1 volume of 1% sulfanilic acid in 3 M HCl and 0.1% *N*-[1-naphthyl]-ethylenediamine dihydrochloride). After incubation at room temperature for 30 minutes in the dark, the absorbance of the reaction mixture at 540 nm (OD_{540}) was measured as described above. NiR activity was calculated as the decrease in nitrite concentration per minute (nmol NO_2^- min^{-1}) normalised against sample protein concentration (mg ml^{-1}). Nitrite standard curve was made with serial dilutions of $NaNO_2$.

2.6 RNA Manipulation

2.6.1 RNA extraction

Arabidopsis leaf and root samples were collected 3 hours after the start of the light photoperiod. Approximately 200–250 mg of four-week old *Arabidopsis* rosette leaf was ground in liquid nitrogen with pestle and mortar, whereas 100–150 mg of ten-day old *Arabidopsis* seedling root was homogenised with the Tissuelyser II (Qiagen, catalogue number: 85300) following the manufacturer's instructions. 1 mL of TRIzol™ Reagent (ThermoFisher, catalogue number: 15596026) was added to each sample, mixed and incubated at room temperature for 5 minutes, before centrifuging at 12,000 *g* for 10 minutes at 4 °C. The supernatant was vigorously mixed with 200 µL of chloroform. After a brief incubation at room temperature for 2–3 minutes, the sample was centrifuged at 12,000 *g* for 15 minutes at 4 °C. The clear layer of the supernatant was transferred to a new tube, before being added 500 µL of isopropanol to precipitate the RNA at room temperature for 10 minutes. The sample was spun again at 12,000 *g* for 10 minutes at 4 °C and washed with 75% ethanol. After centrifugation at 7,500 *g* for 5 minutes at 4 °C, the ethanol was discarded, and the RNA pellet was air-dried for 5–10 minutes, before being dissolved in 30–50 µL of dH_2O at 55–60 °C. The extracted RNA was stored at -80 °C.

2.6.2 DNase treatment

RNA concentration was quantified with the Nanodrop™ ND-1000 Spectrophotometer (Thermo Scientific), and then diluted to 200 µg/mL. Genomic DNA was removed using the DNA-*free*™ DNA removal kit (ThermoFisher, catalogue number: AM1906) following the

manufacturer's instructions. Briefly, 0.1 volume of DNase I buffer and 1 µL of rDNase I were added to 45 µL of diluted RNA. After incubation at 37 °C for 25 minutes, 0.1 volume of DNase Inactivation Reagent was added and mixed occasionally for 2 minutes at room temperature. The reaction mixture was centrifuged at 10,000 *g* for 90 seconds, before the supernatant was transferred to a new tube. The DNase-treated RNA was stored at -80 °C.

2.6.3 cDNA synthesis

cDNA was synthesised from DNase-treated RNA with the SuperScript™ IV Reverse Transcriptase (ThermoFisher, catalogue number: 18090010) following the manufacturer's instructions. 1 µL of 50 µM Oligo(dT)$_{20}$ primer (ThermoFisher, catalogue number: 1818-020) and 1 µL of 10 mM dNTPs (ThermoFisher, catalogue number: 18427-013) were added to 11 µL of template RNA (equivalent to approximately 2–5 µg of RNA). The mixture was heated at 65 °C for 5 minutes, before being cooled on ice for 2 minutes. 4 µL of 5x SSIV buffer, 1 µL of 100 mM DTT, 1 µL of 200 U/µL SuperScript™ IV Reverse Transcriptase and 1 µL of RNaseOUT™ RNase Recombinant Inhibitor (ThermoFisher, catalogue number: 10777-019) were added to the solution, which was followed by a 10-minute incubation at 53 °C. Finally, the reaction was stopped by a10-minute incubation at 80 °C. The cDNA was stored on ice for short-term use, or at -20 °C for long time preservation.

2.6.4 PCR and gel electrophoresis

Primers used for genotyping *Arabidopsis* mutant lines from NASC were recommended by the SALK institute (http://signal.salk.edu/). Other primers were designed with Primer3Web (http://primer3.ut.ee/, Koressaar and Remm, 2007, Untergasser et al., 2012) and primer

specificities to target genes were confirmed with Primer-BLAST prior to purchase (www.ncbi.nlm.nih.gov/tools/primer-blast/).

PCR reactions were assembled on ice with the following components: 1x MyTaq™ Reaction Buffer Red (containing 5 mM dNTPs and 15 mM $MgCl_2$, Bioline, Catalogue number: BIO-37112), 0.1 µM of each primer, 0.025 unit/µL of homemade Taq enzyme, and 0.05–0.5 µg of template DNA. PCR was carried out using the DNA Engine Tetra™ 2 Peltier Thermocycler (Bio-Rad, catalogue number: PLC-0240G) with the program shown in Table 2.3.

Table 2.3 General PCR thermal cycling programme.

Step	Temperature	Duration	Cycle
Initial Denaturation	94 °C	2 minutes	\
Denaturation	94 °C	1 minutes	22 – 35 cycles
Annealing	Tm - 3 °C*	30 seconds	
Extension	72 °C	1 minute/kb + 1 minute**	
Final Extension	72 °C	5 minutes	\

*: the annealing temperature was determined as 3 °C lower than the lower Tm of each primer set.
**: the extension time was determined as 1 minute per kb of expected PCR product plus 1 extra minute.

Primers used for semi-quantitative RT-PCR are listed in Table 2.4. For RT-PCR, the optimal cycle number (< 30) was determined for each reaction, which corresponded to the linear range of PCR amplification kinetics. Minor adjustment of the amount of cDNA template for each genotype was achieved according to the band intensities of the internal reference gene *eIF4E1*, which encodes the eukaryotic translation initiation factor 4E (Rodriguez et al., 1998). Relative

transcript abundance of a particular gene was calculated by dividing the band intensity of that gene by that of *eIF4E1*.

Table 2.4 Primers used for semi-quantitative RT-PCR.

Primer Name	Sequence (5'–3')
RT_NIA1_F	AAACTCATCTGGAACCTCATG
RT_NIA1_R	GAGGCACCATGAACTGAGAC
RT_NIA2_F	GGGTTACGCATATTCCGGAG
RT_NIA2_R	GCTTCTTGACCTCGGACATC
RT_NIR1_F	GGCTTATCGACGAACTTGGTG
RT_NIR1_R	ACATCCTGTCCAATGCATCC
RT_NRT1.1_F	CGGCGTGGAGGAATAGGAAG
RT_NRT1.1_R	TCACGAGAACCGAGCTGAAG
RT_NRT1.2_F	TCGGCAAATGACGTCACCAA
RT_NRT1.2_R	GAGCAGCACTTAACCGAAGC
RT_NRT2.1_F	AGAAAGCGGGAGAAGTTGCC
RT_NRT2.1_R	TGAGCCTCTGTACCTTTCACTG
RT_NAR2.1_F	CACTAAACCCAGCCGAGAAG
RT_NAR2.1_R	TGCTTTGCTCTATCTTGGCC
RT_NRT2.4_F	GGACATGGGTTTTCGTGCTG
RT_NRT2.4_R	TCCATGTCAGCCCTTGTTCC
RT_NRT2.5_F	GCCCATCGTGTTCTCGTTGA
RT_NRT2.5_R	AATCCACCAAGCCCACAACC
RT_eIF4E1_F	AAACAATGGCGGTAGAAGACACTC
RT_eIF4E1_R	AAGATTTGAGAGGTTTCAAGCGGTGTAAG

PCR products were run across 1.5–2% agarose gels containing 5 μL/mL Ethidium Bromide in 1x TAE buffer (40 mM Tris-acetate, 1 mM EDTA, pH 8.3) by electrophoresis (electrophoresis apparatus by Bio-Rad). DNA band was visualised using the BioSpectrum^{TM} MultiSpectral Imgaing System (UVP) with the AC Chemi HR410 camera, and when necessary, band intensity quantified with the VisionWorksLS software.

2.6.5 Quantitative RT-PCR (RT-qPCR)

Primers used for RT-qPCR were published before (Table 2.5, Huang et al., 2015). The differences in the annealing temperatures for each primer pair were smaller than 1 °C, and the product sizes lied within the 100–200 bp range.

Table 2.5 Primers used for RT-qPCR.

Primer Name	Sequence (5'–3')
Q_NIA1_F	AACGCAGGTACAGATTGC
Q_NIA1_R	GGAAGAGTCGTAGCCAGT
Q_NIA2_F	GGCGGCCTCTGTAGATAA
Q_NIA2_R	AACGGGAGGTTTGTAAGA
Q_NIR1_F	AGCGATTCCTCTTGATGC
Q_NIR1_R	GTTCGTCGATAAGCCACA
Q_NRT1.1_F	TCTAAGACCGCTTCAACGGATCG
Q_NRT1.1_R	ACTGTTGGACCATGAGCGTGTG
Q_NRT2.1_F	TGCCTCCTTCCACAGATCCAG
Q_NRT2.1_R	TGGCGTTCTCGGCAAACCGG
Q_NRT2.2_F	GTTACCTTAATCCACTTTCCTC
Q_NRT2.2_R	TCTGCTGCTCCTCCTTACTA
Q_PIF3_F	CTGAAAGGAGACGGCGTGATAG
Q_PIF3_R	CAGATAGTAACCAGACGCCATTGAC
Q_ACTIN_F	TGACAGAGAAGAACAAGGA
Q_ACTIN_R	AAGAGCGGAAGAAGATGA

PCR reactions were assembled on ice with the following components: 1x qPCRBIO SyGreen Mix Hi-Rox (PCR Biosystems, catalogue number: PB20.12), 400 nM of each primer, and 100 ng of template cDNA. For each sample, three technical replicates were included to detect systematic errors. PCR was carried out using the Applied Biosystem StepOnePlus™ Real-

Time PCR System (Thermo Scientific, catalogue number: 4376600) with the program shown in Table 2.6. RT-qPCR result was analysed using the StepOnePlus™ software V2.3.

Table 2.6 RT-qPCR thermal cycling programme.

Step	Temperature	Duration	Cycle
Polymerase Activation	95 °C	2 minutes	\
Denaturation	95 °C	5 seconds	40 cycles
Anneal/Extension	60–65°C	20–30 seconds	

Prior to experiments, primer efficiency test was performed for each primer pair using 4x 2-fold dilution series of 300 ng of template cDNA, and confirmed that they have an amplification efficiency of 90–110%. The melting curve for each reaction was analysed to ensure that the primer pair was specific to the gene of interest, and that the product did not form any secondary structure. Four biological replicates were included in each analysis, and the relative gene transcript level was calculated by normalising against the mRNA abundance of the internal reference gene *Actin* (specifically, $2^{-\Delta C_T}$, where ΔC_T is the difference in C_T values of the gene of interest and *Actin*).

2.7 DNA Manipulation

2.7.1 *In silico* motif searches

Arabidopsis Col-0 genomic DNA sequences of *NIA1* and *NIA2* were obtained from the Arabidopsis Information Resource (TAIR, www.arabidopsis.org). Previously identified

putative binding site sequences of PIFs were searched for in the promoter regions of these genes. Sequences up to 5,000 base pairs before the ATG start codon for each gene was searched for.

2.7.2 DNA extraction for genotyping and sequencing

For general PCR, *Arabidopsis* DNA was extracted with a simple method reported before (Edwards et al., 1991). A small amount of leaf or root tissue (about 20 mg) was ground in 400 µL of extraction buffer (200 mM Tris-HCl pH 7.5, 250 mM Sodium Chloride (NaCl), 25 mM EDTA, 0.5% Sodium Docecyl Sulfate [SDS]) at room temperature, followed by centrifugation at 14,000 rpm for 1 minute. The supernatant was mixed with an equal volume of isopropanol in a new tube, and incubated at room temperature for 2 minutes with occasional mixing. After centrifugation at 14,000 rpm for 5 minutes, the supernatant was removed, and the DNA pellet was washed with 400 µL of 75% ethanol. The ethanol was then discarded after centrifugation at 14,000 rpm for 2 minutes, and the pellet air-dried for 5–10 minutes. The DNA was finally dissolved in 100 µL of TE buffer, and the solution was centrifuged at 14,000 rpm for 2 minutes. The supernatant was transferred to a new tube and stored at -20 °C.

2.7.3 Sanger sequencing

Primers used for amplifying target genes and for sequencing are shown in Table 2.7. PCR products and plasmid DNA for Sanger sequencing were diluted to 10 ng/µL and 100 ng/µL respectively. Sequencing primers were diluted to 3.2 pmol/µL. Sanger sequencing service was provided by SourceBioscience (www.sourcebioscience.com), and sequencing results were compiled and analysed using CodonCode Aligner 8.0.1 (https://codoncode.com/aligner/).

Table 2.7 Primers used in Sanger sequencing.

Primer Name	Sequence (5'–3')	Purpose
GAI_1_F	CCCTCTGATCCATGATTCATCG	Gene amplification
GAI_1_R	CTAAATGAGCCAGCTTACACC	Gene amplification
GAI_2_F	ATGAGTCAAGGTCTTCAATGGC	Gene amplification
GAI_2_R	AACTGAAAACGACTTAGCATTG	Gene amplification
GAI_S1	GGACATCGAGCCCCATCAC	Sequencing
GAI_S2	AAGCAAATCGGATTCTTAGCC	Sequencing
GAI_S3	CGCTTATGCAGGCTCTTG	Sequencing
GAI_S4	CGACGTTGTTTGACTCGTTG	Sequencing
GAI_S5	TTGATCTGTTGAACCGGTTATG	Sequencing
GAI_SR1	TGAGCCAGCTTACACCCAAC	Sequencing
GAI_SR2	GCATTGTTAAAATAATCTGGTCCAC	Sequencing
SLY1_F	ACAGCTATGGAGTATATGAGGG	Gene amplification
SLY1_R	TAGCTTGACGTTGATTCCGG	Gene amplification
SLY_S1	TTTATCTTCGTTTTGTCGTCTTC	Sequencing
SLY_S2	GTCGACGCAAAGACCTTAGC	Sequencing
SLY_S3	TTAGAGTTTGGTTTTGGAGTTTG	Sequencing
SLY_S4	TGCTAGGTTCGGTAAGGACG	Sequencing

2.7.4 DNA extraction for whole-genome sequencing (WGS) analysis

Approximately 0.8–1.6 g of *Arabidopsis* leaf was harvested from a mixture of 5–10 plants. DNA was extracted using the Plant/Fungi DNA Isolation Kit (Norgen, catalogue number:

26200) following the manufacturer's instructions. In brief, plant sample was ground into powder in liquid nitrogen with pestle and mortar. 500 µL of Lysis Buffer L and 1 µL of RNase A were added to the sample, followed by a 10-minute incubation at 65 °C with occasional mixing. 100 µL of Binding Buffer I was added to the mixture, before a 5-minute incubation on ice. The lysate was then centrifuged in a Filter Column at 20,000 *g* for 2 minutes. The supernatant was transferred to a new tube and mixed with an equal volume of 70% ethanol. The mixture was centrifuged in a Spin Column at 10,000 *g* for 1 minute. The flow-through was discarded and the column was washed once with 500 µL of Solution WN and then twice with 500 µL of Wash Solution A by three sequential centrifugations each at 10,000 *g* for 1 minute. The column was dried by spinning at 20,000 *g* for 2 minutes. Finally, DNA was eluted by adding 100 µL of Elution Buffer B and centrifuging at 20,000 *g* for 2 minutes. The DNA was stored at -20 °C.

2.7.5 DNA precipitation

DNA was precipitated by adding 0.1 volume of 3 M Sodium Acetate (NaOAc, pH 5.2) and 2.5 volume of 100% ethanol. The solution was mixed and incubated on dry ice for 1 hour, before centrifugation at 14,000 rpm at 4 °C for 15 minutes. The supernatant was removed, and the DNA pellet was resuspended in 500 µL of 70% ethanol. The DNA was stored at -20 °C.

2.8 Mutant Screen

2.8.1 *Arabidopsis* seed mutagenesis

Approximately 50,000 *Arabidopsis gai* progenitor seeds were mutagenized with Ethyl Methane Sulfonate (EMS). 0.1% of Tween-20 was used to wash the seeds for 15 minutes before being replaced by either 0.2% or 0.4% of EMS solution. The seeds were mixed on a benchtop shaker for 15 hours (for 0.2% EMS treatment) or 8 hours (for 0.4% EMS treatment), followed by rigorous washing with dH_2O for 10 times. The seeds were soaked in dH_2O for another hour to allow residue EMS to diffuse out of the seeds, which were then left to dry overnight on a filter paper.

Approximately 50,000 *Arabidopsis gai* progenitor seeds were mutagenized by 60 Gray (Gy) of fast neutron (FN) radiation at the KFKI Atomic Energy Research Institute (Budapest, Hungary).

Mutagenized seeds (M_1 seeds) were separated into batches of around 2,000 seeds, each mixed with 10 g of sand, and then sown evenly on soil. They were stratified at 4 °C in the dark for 5 days, and grown in CERs at 22º–24 °C under 16-h light/8-h dark photoperiod (irradiance 120 μmol of photons/m^2 per second). The M_1 plants were allowed to self, and the resultant M_2 seeds were collected in batches before being sown on soil for genetic screens.

Four-week old M_2 plants were treated with 0.5 mM of chlorate (a lower concentration of chlorate was used to aid the identification of chlorate hypersensitive mutants) in the same way

as described above. From the fifth day onwards, plants displaying early leaf chlorosis were rescued by being transplanted to normal soil and allowed to set seeds. Chlorate resistant mutants were identified after prolonged chlorate treatment. Throughout the screen, mutants that were visually taller than the *gai* progenitor were also transplanted to normal soil for seed collection. Heritability and segregation of the mutant phenotypes were tested for the subsequent M_3 generation plants. Leaf materials from homozygous populations of identified mutants were collected for DNA extraction and whole-genome sequence (WGS) analysis.

2.8.2 WGS analysis

Around 7–15 µg of DNA materials extracted from three chlorate resistant *gai* mutants and the progenitor *gai* were sent for WGS at the Beijing Genomic Institute (BGI), Beijing, using the 150 bp paired-end Illumina technology according to the manufacturer's instructions.

The methodologies for detecting mutations were described previously (Belfield et al., 2012, Jiang et al., 2014, Belfield et al., 2018). Briefly, with Stampy, the sequencing results were aligned to the TAIR10 reference genome (Lunter and Goodson, 2011), before unmapped reads were aligned five times using iterative read-mapping and realignment/*De novo* assembly based variant-calling (IMR/DENOM, Gan et al., 2011). The lists of single nucleotide variants (SNVs), insertions and deletions (INDELs) were subsequently produced (in the form of BAM files) by IMR/DENOM as a result of incorporating sequence reads that are of high quality (with a Phred quality score of ≥ 20) and uniquely mapped. Sequence variants against TAIR10 reference that were present in the *gai* progenitor or shared by more than one mutant were removed in Excel using the VLOOKUP function. The remaining variants in the lists were inspected manually using Integrative Genomics Viewer (IGV), and false positives were further filtered out

(Robinson et al., 2011, Robinson et al., 2017). Only variants with a relatively high-quality score (Phred score ≥ 60 for SNVs and phred score of 1 for INDELs) were visually scanned to eliminate false reports. The resultant putative candidate mutants were compiled for each sample.

2.9 Molecular Cloning

2.9.1 Bacterial growth conditions

Escherichia coli (*E. coli*) DH5α strain was used in this study for plasmid manipulation. *E. coli* was grown either in liquid Luria-Bertani (LB) medium (10 g tryptone, 5 g yeast and 5 g NaCl per litre, pH 7.0) at 37 °C with shaking at 250 rpm, or on solid LB medium (supplemented with 15 g agar per litre) in a static incubator at 37 °C for 12–16 hours. For selection of successfully transformed bacteria, appropriate antibiotics were added to the media at the concentrations shown in Table 2.8.

Table 2.8 Antibiotics used in this study.

Antibiotic	**Concentration (µg/ml)**
Kanamycin	50
Ampicillin	100

2.9.2 Preparation of competent *E. coli* DH5α cells

Stock *E. coli* stored in glycerol at -80 °C was streaked onto a LB plate and incubated at 37 °C overnight. A single colony was selected and transferred to 3 mL of liquid LB medium for incubation at 37 °C overnight with shaking at 250 rpm until the exponential phase of bacterial growth was reached. 1 mL of the culture was transferred to 100 ml of fresh LB medium and incubated further for at least 2 hours until the optical density (OD_{600}) is within 0.4–0.5. The culture was then transferred into 50 mL falcon tubes and placed on ice for 15 minutes, before centrifuging at 4,000 *g* for 10 minutes at 4 °C. After discarding the supernatant, 30 mL of pre-cooled 0.1 M Calcium Chloride ($CaCl_2$) was added to resuspend the bacteria, which was then incubated on ice for 15–30 minutes. The solution was centrifuged at 4,000 *g* for 10 minutes at 4 °C, and the supernatant was replaced by 2 mL of 0.1 M $CaCl_2$. For long-term storage, 2 mL of 30% glycerol was added to the bacterial culture, which was divided into 100 µL aliquots and preserved at -80 °C.

2.9.3 Bacterial transformation

10 µL of the ligation product (see below) was mixed gently with 100 µL of competent DH5α cells. The mixture was incubated on ice for 30 minutes, before heat-shock at 42 °C for 90 seconds. After 2 minutes of cooling on ice, 1 mL of liquid LB medium (without antibiotics) was added to the bacterial culture, which was incubated at 37 °C for 45 minutes with shaking at 150 rpm. The transformed bacterial culture was then centrifuged at 3,500 rpm for 5 minutes. Most of the supernatant was discarded while the rest (at least 100 µL) was used to resuspend

the bacteria, and was spread on LB plate supplemented with appropriate antibiotics using a sterile spreader. The transformed bacteria were incubated at 37 °C overnight.

2.9.4 Plasmid recombination

DNA fragments were amplified from cDNA by standard PCR using the primers listed in Table 2.9, before being run on an agarose gel and excised for purification using the QIAquick gel extraction kit (Qiagen, catalogue number: 28704) following the manufacturer's instructions. The gel slice was weighed and dissolved in 3 gel volumes of Buffer QG at 50 °C for 10 minutes. 1 gel volume of isopropanol was added to the sample, followed by transferring the mixture into a QIAquick spin column for a 1-minute centrifugation at 10,000 *g*. The flowthrough was discarded and the column was spun again at 10,000 *g* for 1 minute after adding 0.5 ml of Buffer QG. Subsequently, the column was washed with 0.75 mL of Buffer PE followed by centrifugation at 10,000 *g* for 1 minute, and dried by centrifuging at 17,900 *g* for another minute. DNA bound to the spin column was eluted by adding 50 µL of Buffer EB, incubating at room temperature for 1–5 minutes, and centrifuging at 10,000 *g* for 1 minute.

Table 2.9 Primers used in plasmid recombination.

Primer Name	Sequence (5'–3')
Y2H_GAI_F	GCATATGAAACCAACCATGAAGAGAGATCAT
Y2H_GAI_R	GGAATTCTGCCTATCCAATTTACCCTCC
Y2H_SLY1_F	CCATATGATGAAGCGCAGTACTACCGA
Y2H_SLY1_R	GGAATTCTTGCCAGCATTGAACATCAC

DNA fragments were first cloned using the pGEM-T™ Easy Vector System (Promega, A1360) following the manufacturer's instructions. The ligation reaction was set up by mixing 1x Rapid Ligation Buffer, 50 ng of pGEM-T Easy Vector (Table 2.10), appropriate amount of PCR product (to reach an insert:vector molar ratio of 3:1), 3 Weiss units of T4 DNA ligase and dH_2O in a 10 µL reaction system, and incubated overnight at 4 °C. Bacterial transformation was then performed with the entire ligation reaction, before being plated on LB plates supplemented with ampicillin, 0.5 mM isopropyl β-D-1thiogalactopyranoside (IPTG) and 80 µg/mL 5-bromo-4-chloro-3-indolyl-β-D-galactoside (X-Gal) for blue/white selection for recombinants. After incubation at 37 °C overnight, white colonies were transferred with a pipette tip and resuspended in 10 µL of dH2O, 2 µL of which was then proceeded to PCR (colony PCR) to confirm the presence of the target DNA fragment. Once confirmed, the rest of the bacterial suspension (8 µL) was added to 10 mL of liquid LB medium for overnight incubation at 37 °C with shaking at 250 rpm.

Table 2.10 Vector plasmids used in this study.

Vector	**Antibiotic Selection**	**Restriction Enzymes**	**Genes Cloned**	**Source**
pGEM™-T Easy	Ampicillin	\	*gai*, *SLY1* & *sly1*	Promega
pGADT7 AD	Ampicillin	NdeI & EcoRI	*gai*	Clontech
pGBKT7	Kanamycin	NdeI & SalI	*SLY1* & *sly1*	Clontech

Plasmid isolation was performed with the Wizard™ *Plus* SV Minipreps DNA Purification System (Promega, catalogue number: A1340) following the manufacturer's instructions. 5 mL of the overnight bacterial culture was centrifuged at 10,000 *g* for 5 minutes. The supernatant

was discarded, and the pellet was resuspended in 250 µL of Cell Resuspension Solution. The cell suspension was cleared by adding 250 µL of Cell Lysis Solution followed by a 5-minute incubation. Another 5-minute incubation was carried out after adding 10 µL of Alkaline Protease Solution. After adding 350 µL of Neutralisation Solution, the bacterial lysate was centrifuged at 14,000 *g* for 10 minutes at room temperature. The supernatant was transferred to a Spin Column and centrifuged at 14,000 *g* for 1 minutes. The Spin Column was then washed twice with 750 µL of Column Wash Solution followed by a 1-minute spin at 14,000 *g*, and a 2-minute spin at 14,000 *g* after adding 250 µL of Column Wash Solution. Finally, the plasmid DNA was eluted by adding 100 µL of dH_2O and centrifuging at 14,000 *g* for 1 minute. Sanger sequencing was performed for the plasmid DNA to confirm that no amplification mistakes were present, before the plasmid DNA was stored at -20 °C.

Both destination plasmids (Table 2.10) and DNA inserts were digested with appropriate Invitrogen™ Anza™ restriction enzymes. Specifically, 20 µL reaction volume consisting of 1x Anza Red Buffer, 0.1–1 µg DNA and 1 µL (20 U) of each restriction enzyme and dH_2O was incubated at 37 °C for 15 minutes. The entire reaction solution was then run on an agarose gel before DNA purification as described above. A 20 µL reaction system consisting of a 5:1 molar ratio of insert and vector DNA, 1x T4 ligase buffer, T4 DNA ligase (New England Biolabs, catalogue number: M0202) and dH_2O was incubated at 16 °C overnight, followed by heat inactivation at 65 °C for 10 minutes. The reaction mixture was subsequently transformed into competent cells as described above, before plasmid isolation. The plasmid DNA was Sanger sequenced again to ensure correct sequence of the insert, before being preserved at -20 °C.

2.10 Yeast Two-Hybrid Analysis

2.10.1 Yeast growth conditions

The *Saccharomyces cerevisiae* yeast strain Y187 (genotype: *MATα, ura3-52, his3-200, ade 2-101, trp 1-901, leu 2-3, 112, gal4Δ, met⁻, gal80Δ, URA3:GAL1$_{UAS}$-GAL1$_{TATA}$-lacZ, MEL1*) was kindly provided by Dr. Shao Jian Zheng (Zhejiang University, Hangzhou, China; Harper et al., 1993). Untransformed yeast stains were grown either in liquid rich medium (YPDA) at 30 °C with shaking at 250 rpm for 16–18 hours to reach stationary phase, or on solid YPDA medium in a static incubator at 30 °C for 3–5 days until the colonies were about 2–3 mm in diameter. Transformed yeast cultures were grown on minimal media single dropout (SDO) SD/-Trp, SD/-Leu, or minimal media double dropout (DDO) SD/-Leu/-Trp liquid or solid meda for selecting transformants. For short-term storage, untransformed and transformed yeast strains were stored in YPDA and appropriate selection media respectively at 4 °C for up to 2 months. For long-term storage, yeast strains were stored in appropriate liquid media with 25% glycerol at -80 °C.

2.10.2 Preparation of competent yeast Y187 cells

A 1–3 weeks old fresh yeast colony grown on solid YPDA medium was inoculated into 3 mL of liquid YPDA medium and incubated at 30 °C with shaking at 250 rpm overnight. 5 µL of the overnight culture was transferred to 50 mL of YPDA and incubated for a further 16–20 hours until the OD_{600} was within 0.15–0.3. The yeast culture was centrifuged at 700 *g* for 5 minutes at room temperature, before the supernatant was discarded and the pellet was resuspended in 100 mL of fresh YPDA medium. After further incubation (3–5 hours) until the

OD_{600} reached 0.4–0.5, the culture was centrifuged at 700 *g* for 5 minutes and the supernatant was replaced by 30 mL of dH_2O. The cells were centrifuged again at 700 *g* for 5 minutes and the supernatant discarded. 1.5 mL of 1.1x TE/0.1M Lithium Acetate (TE/LiAc) was added to resuspend the cells, which was followed by a high-speed centrifugation for 15 seconds. The supernatant was replaced by 600 µL of 1.1x TE/LiAc, and the cells were ready for transformation with plasmid DNA.

2.10.3 Yeast transformation

50 µg of Sheared Salmon Sperm DNA (ThermoFisher, catalogue number: AM9680) was denatured by repetitive (at least twice) heating at 95–100 °C for 5 minutes and then cooled rapidly on ice, before being added to a sterile tube with 100 ng of plasmid DNA, 50 µL of competent cells and 500 µL of PEG/LiAc (40% polyethylene glycol 3350, 1x TE buffer and 0.1 M LiAc). The mixture was incubated at 30 °C for 30 minutes, before being added 20 µL of dimethyl sulfoxide (DMSO) and heat-shock at 42 °C for 15 minutes. Yeast cells were collected by a high-speed centrifugation for 15 seconds, and the supernatant was replaced by 1 mL of YPDA medium. The yeast culture was incubated at 30 °C with shaking for 90 minutes before centrifugation at a high speed for 15 seconds. The supernatant was discarded, and 0.9 % NaCl was added to resuspend the yeast cells. 100 µL of 1x, 1/10x and 1/100x transformed yeast culture was spread onto appropriate SD selection media (for example, for co-transformation of pGBKT7 and pGADT7, SD/-Leu/-Trp medium was used). The plates were incubated at 30 °C for 3–5 days until the colonies were approximately 2–3 mm in diameter.

2.10.4 Liquid culture β-galactosidase assay

Chlorophenol red-β-D-galactopyranoside (CPRG, Sigma-Aldrich, catalogue number: 59767) was chosen as the substrate for the β-galactosidase assay in this study because of its fast reaction rate and therefore high sensitivity (Schneider et al., 1996). A co-transformed yeast colony was inoculated into 5 mL of SD/-Leu/-Trp medium and incubated overnight at 30 °C with shaking at 250 rpm. The overnight culture was vigorously vortexed for 45 seconds to disperse cell clumps, before 2 mL of the culture was transferred to 8 mL of YPDA medium. This fresh culture was incubated at 30 °C with shaking at 250 rpm for 3–5 hours until the OD_{600} was within 0.5–0.8. The exact OD_{600} value was recorded, before 1.5 mL of the culture was transferred to an Eppendorf tube and centrifuged at 14,000 rpm for 30 seconds. The supernatant was discarded, and 1 mL of Buffer 1 (2.38 g 4-[2-hydroxyethyl]-1-piperazineethanesulfonic acid [HEPES], 0.9 g NaCl, 0.065 g L-Aspartate, 1 g BSA and 50 µL Tween-20 in 100 mL solution, pH adjusted to 7.25–7.30, filter sterilised) was added to resuspend the cells. The culture was centrifuged at 14,000 rpm for 30 seconds, before the supernatant was discarded and replaced by 300 µL of Buffer 1 (giving a concentration factor of 5). 0.1 mL of the cell suspension was transferred to a new tube, and the yeast cells were broken open by repetitively (at least 3 times) freezing the culture in liquid nitrogen and then thaw it immediately in a 37 °C water bath. 0.7 mL of Buffer 2 (2.23 mM CPRG in Buffer 1, filter sterilised) was then added, and the mixture was vortexed before starting the timer. The reaction was stopped when the colour of the sample turned orange/red by adding 0.5 mL of 3 mM Zinc Chloride ($ZnCl_2$), and the stop time was recorded. Cell debris was removed by centrifuging the reaction mixture at 14,000 rpm for 1 minute and transferring the supernatant to a cuvette. The spectrophotometer was zeroed at OD_{578} with the buffer blank (0.3 mL dH_2O and 0.7 mL Buffer 2), and the OD_{578}

for each sample was recorded. The OD_{578} value should lie within 0.25–1.8 for it to be within the linear range of the assay. Finally, β-galactosidase unit was calculated using the following equation:

$$y = 1{,}000 \times OD_{578}/(t \times V \times OD_{600})$$

where **y** is the β-galactosidase unit; **t** is the elapsed time (in minute) of incubation; **V** is 0.1 x concentration factor (in this case **V**=0.5).

CHAPTER 3. The Regulatory Relationship Between the GA-DELLA Signalling Pathway and Nitrate Metabolism

3.1 Introduction

Artificial selection for plant dwarfing traits led to a dramatic increase in global crop yield during the mid-to-late 20th century "Green Revolution" (Hedden, 2003). The subsequent extensive genetic studies reveal that the genes responsible for crop dwarfism are involved in the plant phytohormone GA-DELLA signalling pathway. Specifically, Green Revolution rice varieties are deficient in GA biosynthesis due to loss-of-function mutations in their GA biosynthetic gene *GA20ox2* (Monna et al., 2002, Sasaki et al., 2002, Spielmeyer et al., 2002); whereas modern semi-dwarf varieties of wheat have disrupted GA signalling due to stabilised DELLA proteins that are irresponsive to the GA signal (Peng et al., 1997, Peng et al., 1999a, Chandler et al., 2002, Gubler et al., 2002). Whilst the yield benefit conferred by dwarfism is indisputable, modern Green Revolution crops suffer from a low nitrogen-use efficiency (NUE), and thus require unsustainably high levels of fertiliser application that is not only economically expensive, but also environmentally damaging (Raun and Johnson, 1999, Gooding et al., 2012, Casebow et al., 2016). For example, a negative correlation between plant NUE and the severity of the dwarfing alleles (*Rhts*) was discovered in wheat, although the mechanism for this was unresolved (Gooding et al., 2012). Therefore, it is reasonable to speculate that, as a major modulator of multiple plant growth and developmental processes, the GA-DELLA signalling pathway also regulates plant nitrogen metabolism.

As the predominant source of nitrogen available for plant absorption in most agricultural soils, nitrate metabolism has been the subject of extensive investigations. Nitrate is taken up by the plants through root nitrate transporters belonging to the NRT1/NPF and NRT2 family proteins, followed by its long-distance translocation to shoot tissue for assimilation (Wang et al., 2012, Krapp et al., 2014). Nitrate assimilation is a linear process involving two major reduction steps, nitrate reduction to nitrite, and nitrite reduction to ammonium, which then enters the amino acid pool (Crawford, 1995, Lillo et al., 2004, Du et al., 2008). Both nitrate transporters and enzymes involved in nitrate assimilation are embedded in a complex regulatory network involving external signals (e.g., nutrient, light) and internal signals (e.g., phytohormones, Vidal et al., 2015, Guan, 2017). However, a regulatory relationship between the GA-DELLA signalling pathway and nitrate metabolism has been little explored, with previous investigations yielding ambiguous conclusions. For example, two DELLA genes, *RGA* and *GAI*, have been discovered from a screen for *Arabidopsis* cDNA that rescue the growth of a mutant yeast strain deficient in nitrogen metabolism, raising the possibility of the involvement of DELLA proteins in plant nitrogen metabolism (Truong et al., 1997, Bouton et al., 2002). However, the authors could not explain this complementation as they failed to identify any impact on nitrate-related gene expression or enzymatic activities by the GA-DELLA signalling pathway (Bouton et al., 2002). Meanwhile, light-mediated activation of nitrate reductase activity in *Arabidopsis* seedlings has been shown to be repressed by GA and promoted by the GA biosynthetic inhibitor paclobutrazol (PAC, Zhang et al., 2011). The same study reports an increased nitrate reductase activity in the severely GA deficient *ga1-3* mutant seedlings, which lack a GA biosynthetic enzyme involved in an early step of bioactive GA production, compared to WT (Koornneef and Vanderveen, 1980, Zeevaart and Talon, 1992, Zhang et al., 2011). These results seem contradictory to the low NUE conferred by DELLA stabilisation in modern semi-

dwarf crops. Therefore, further studies are essential to clarify the role played by the GA-DELLA signalling pathway in regulating nitrate metabolism.

As a mutant orthologue of wheat, maize and barley DELLA genes, the *Arabidopsis gai* allele encodes a protein lacking 17 amino acids of the N-terminal DELLA domain (Figure 3.1, Peng et al., 1999a). As a result, *gai* mutant plants are also irresponsive to the GA signal and are therefore dwarfed, enabling them to be utilised as experimental models for modern Green Revolution crops (Koornneef et al., 1985, Peng et al., 1997). The *Ds* transposon insertion in the C terminus of the *gai-t6* allele disrupts the *gai* open reading frame, thus leading to a loss-of-function mutation that confers a height similar to that of WT (Peng et al., 1997). In addition, *Arabidopsis GA20ox1* (*GA5*) is the functional orthologue gene of the rice *SD1* and barley *Denso*/*Sdw1* genes, all of which encode the GA20ox biosynthetic enzyme involved in the final steps of GA biosynthesis (Rieu et al., 2008, Jia et al., 2009). Because of functional redundancy with the other four paralogue *GA20ox* genes, *Arabidopsis ga5* mutant plants exhibit a semi-dwarf phenotype that is milder than both *ga1-3* and *gai* (Rieu et al., 2008).

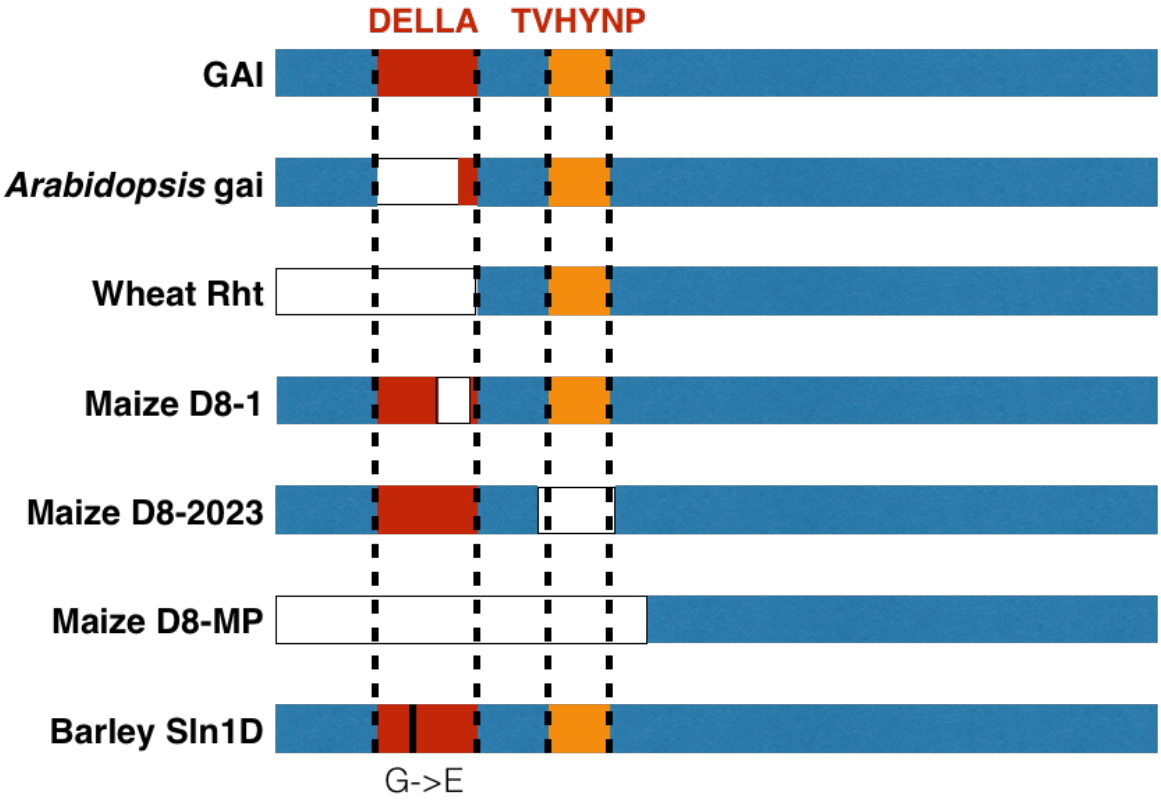


Figure 3.1 Structures of WT, *Arabidopsis* gai and crop mutant DELLA proteins.
Modern semi-dwarf crops including wheat, maize and barley contain mutations affecting the N termini of their respective encoded DELLA proteins, within the conserved DELLA (red boxes) and/or TVHYNP (orange boxes) domains, causing them to confer GA insensitivity. A similar mutation is shared by the *Arabidopsis gai* mutant, making it a suitable experimental model for Green Revolution crops. White boxes represent deletions. This diagram is not drawn to scale. Data from Peng et al.,2009, Chandler et al., 2002, Gubler et al., 2002, Willige et al., 2007.

As mentioned in Chapter 1, chlorate is commonly used as a toxic chemical analogue for studying plant nitrate metabolism, and has been employed as selective agent in the identification of several nitrate transporter and nitrate reductase genes (Wilkinson and Crawford, 1991, Tsay et al., 1993, Wilkinson and Crawford, 1993, Wang and Crawford, 1996). In this chapter, *Arabidopsis gai* and *ga5* mutants were shown to be relatively resistant to chlorate toxicity. The underlying mechanism of *gai*-mediated chlorate resistance was investigated through seedling hypocotyl grafting as a novel approach. A negative regulatory effect on nitrate reductase activity by DELLAs was discovered, and this regulatory pattern was shown to hold true for rice ssp. *indica*. Conclusions drawn from Chapter 3 therefore provide

an initial explanation for the relatively low NUE exhibited by modern semi-dwarf crop varieties.

3.2 Results

3.2.1 Mutants defective in low-affinity nitrate uptake and nitrate reduction are resistant to chlorate toxicity on soil

The *Arabidopsis nrt1.1* and *nia2* mutants are known to be resistant to chlorate toxicity when grown on a vermiculite/perlite mixture supplemented with nutrient solution, which is the condition under which these mutants were originally discovered (Wilkinson and Crawford, 1991, Tsay et al., 1993). However, in order to mimic the natural growth environment of modern crop varieties, it was decided that the chlorate treatments should be performed on plants growing on nutrient-rich soil. It was therefore necessary to include the *nrt1.1* and *nia2* mutants as positive controls to confirm the validity of our soil-based experimental system. The *nrt2.1 nrt2.2* double mutant, which lacks the two major high affinity nitrate transporters, was also included to investigate which nitrate transport system, high affinity (as conferred primarily by NRT2.1 and NRT2.2) or low affinity (as conferred primarily by NRT1.1), predominates in nitrate uptake from soil. On control soil without chlorate, all three mutants displayed no detectable phenotypic difference with respect to WT plants (Figure 3.2). When treated with chlorate, as expected, both *nrt1.1* and *nia2* exhibited strong resistance compared to WT, based on the differential extents of leaf chlorosis, with *nrt1.1* mutant plants being slightly more resistant than *nia2* (Figure 3.2). However, there was no detectable difference in the chlorate responses of WT and *nrt2.1 nrt2.2* mutant plants (Figure 3.2), indicating that the high affinity

nitrate transport system plays only a minor role in nitrate/chlorate uptake from nutrient-rich soil. Therefore, the soil-based chlorate toxicity assay has the capacity to identify mutants that are defective in low affinity nitrate uptake and/or nitrate reduction, but not mutants defective in high affinity nitrate uptake.

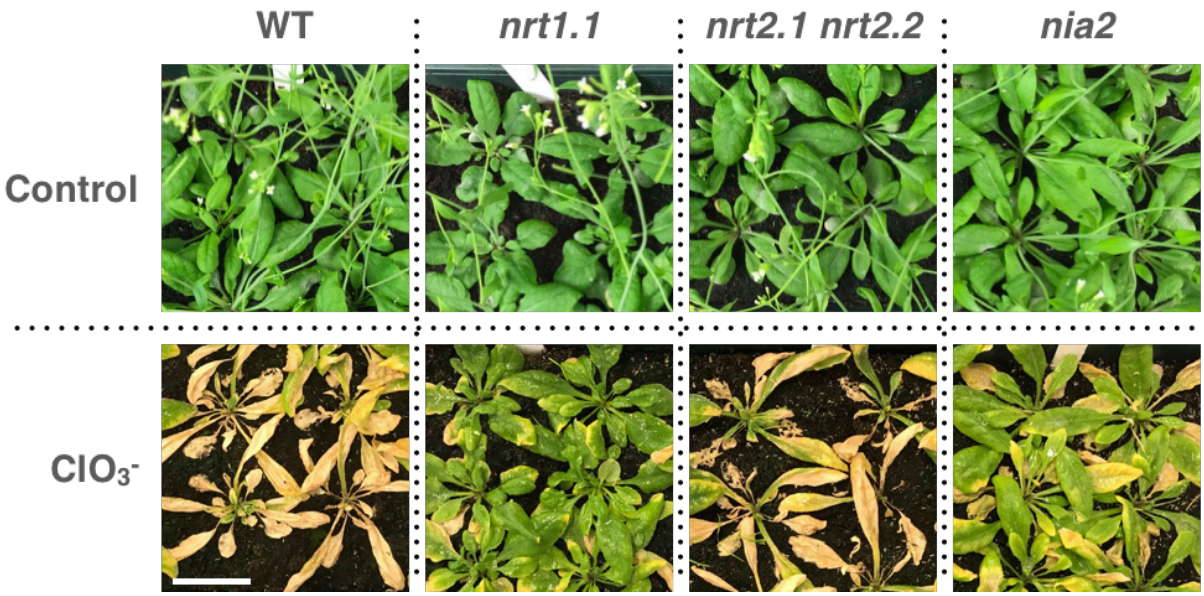


Figure 3.2 Chlorate responses of WT, *nrt1.1*, *nrt2.1 nrt2.2* and *nia2* mutant plants grown on soil.
The *Arabidopsis nrt1.1*, *nrt2.1 nrt2.2* and *nia2* mutant plants are respectively deficient for the NRT1.1 low affinity nitrate transporter, the NRT2.1 and NRT2.2 high affinity nitrate transporters and nitrate reductase activity, and are phenotypically similar compared to WT when grown on control soil without chlorate. However, the *nrt1.1* and *nia2* mutants are clearly more resistant to chlorate than both WT and the *nrt2.1 nrt2.2* mutant, with *nrt1.1* being slightly more resistant than *nia2*. All plants were germinated on agarose before being transplanted to soil and grown at 22–24 °C under 16-h light/8-h dark photoperiod (irradiance 120 µmol of photons/m^2 per second). Four-week old plants were watered with 1.5 mM chlorate to soil saturation, which was repeated every five days (for full details see section 2.4.1). Photos of the plants were taken two weeks after the first chlorate treatment. For plants growing on chlorate (lower panel), inflorescence stems were removed to facilitate the observation of plant chlorate responses. Scale bar = 3 cm.

3.2.2 Mutants with stabilised DELLAs are resistant to chlorate toxicity

To determine if, as the experimental model for Green Revolution crops, *Arabidopsis gai* also has a compromised nitrate metabolism, *gai* mutant plants were treated with chlorate in the same

way as described above. Figure 3.3A indicates that *gai* mutants are visibly more resistant to chlorate than WT plants. Since the major symptom of chlorate toxicity is leaf chlorosis, to obtain a quantitative measure of *gai*-mediated chlorate resistance, leaf chlorophyll contents of plants grown with or without chlorate were measured for both WT and *gai*. A much smaller decrease in chlorophyll level upon chlorate treatment was seen with *gai* than with WT (Figure 3.3B). *gai* mutant plants have dark green leaves regardless of chlorate treatment due to the positive regulation of DELLAs on plant chlorophyll biosynthesis (Peng and Harberd, 1997a, Peng and Harberd, 1997b, Cheminant et al., 2011), which gave rise to a consistently higher leaf chlorophyll content of *gai* than WT (Figure 3.3B).

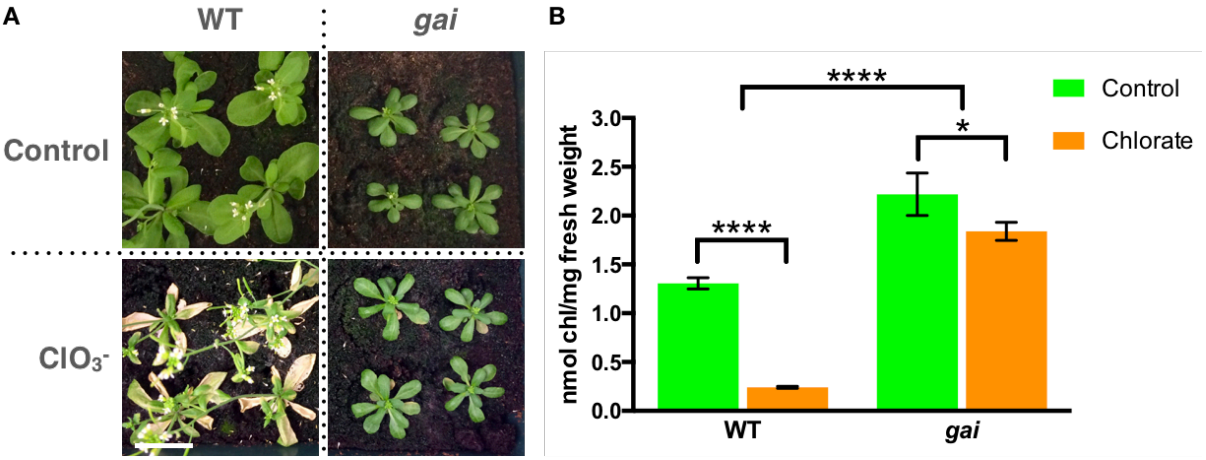


Figure 3.3 Chlorate responses and leaf chlorophyll contents of WT and *gai* mutant plants. (A) *Arabidopsis gai* mutant plants are more resistant to chlorate toxicity than WT plants. All plants were germinated on agarose before being transplanted to soil and grown at 22–24 °C under 16-h light/8-h dark photoperiod (irradiance 120 µmol of photons/m^2 per second). Four-week old plants were watered with 1.0 mM chlorate to soil saturation, which was repeated every five days (for full details see section 2.4.1). Photos of the plants were taken two weeks after the first chlorate treatment. Scale bar = 3 cm. (B) Leaf chlorophyll measurement confirms the strong chlorate resistance conferred by the *gai* mutation. Chlorophyll measurements were taken from fully-expanded rosette leaves two weeks after the first chlorate treatment (for full details see section 2.4.3). Data are means ± s.d. (n [number of biological replicates] = 12). Statistical analysis was performed with two-way ANOVA, and statistical significance (P value) was depicted by the number of asterisks, where * means $P \leq 0.05$, and **** means $P \leq 0.0001$.

Similarly, the *ga5* mutation, which also confers stabilised DELLA proteins due to deficient bioactive GA biosynthesis (Rieu et al., 2008), confers a chlorate resistance phenotype (Figure 3.4). Taken together (Figure 3.3 and Figure 3.4), these observations suggest that DELLA accumulation, regardless of the mechanism, renders the plant resistant to chlorate, potentially due to compromised nitrate/chlorate metabolism.

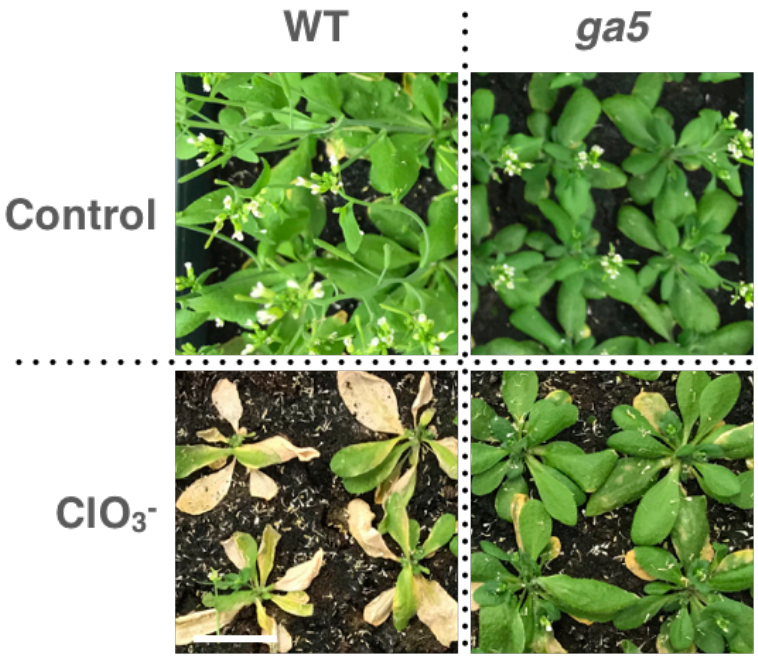


Figure 3.4 Chlorate responses of WT and *ga5* mutant plants.
Arabidopsis ga5 mutant plants are more resistant to chlorate toxicity than WT plants. All plants were germinated on agarose before being transplanted to soil and grown at 22–24 °C under 16-h light/8-h dark photoperiod (irradiance 120 µmol of photons/m^2 per second). Four-week old plants were watered with 1.0 mM chlorate to soil saturation, which was repeated every five days (for full details see section 2.4.1). Photos of the plants were taken two weeks after the first chlorate treatment. For plants growing on chlorate (lower panel), inflorescence stems were removed to facilitate the observation of plant chlorate responses. Scale bar = 3 cm.

3.2.3 Mutant chlorate resistance cannot be explained by dwarfism *per se*

DELLA accumulation confers growth inhibition and hence decreased plant size and stature (Koornneef et al., 1985). A potential explanation for the chlorate resistance phenotype of the *gai* and *ga5* mutants is that, because of their reduced sizes, they require less nitrate for growth

and thus do not absorb as much nitrate/chlorate as WT plants do. If this hypothesis is true, a negative correlation between plant height and chlorate resistance would be expected. To investigate this possibility, three mutants (*miniature-1* [*min-1*], *dwarf1-1* [*dw1-1*] and *compacta3-1* [*cp3-1*]) that are known to be dwarf but whose dwarfism is not directly associated with perturbation of the GA-DELLA signalling pathway (Table 3.1 and Figure 3.5) were treated with chlorate. Figure 3.6 shows that these three mutants are not detectably more resistant to chlorate than WT despite having a dwarf phenotype. Notably, the *cp3-1* mutant, with a height similar to that of *ga5*, and the *dw1-1* mutant, which is significantly shorter than *ga5* and slightly taller than *gai* (Figure 3.5), are both as sensitive to chlorate as WT (Figure 3.6).

Table 3.1 Three dwarf mutants selected in this study for chlorate toxicity assay and their WT gene functions.

Mutant	WT Gene Function	Reference
***min-1* (*Ler*)**	Unknown	\
***cp3-1* (*Ler*)**	Inhibit phytochrome A signalling in seedlings	(Quinn et al., 2002)
***dw1-1* (*Ler*)**	Biosynthesis of active brassinosteroids (BRs)	(Youn et al., 2018)

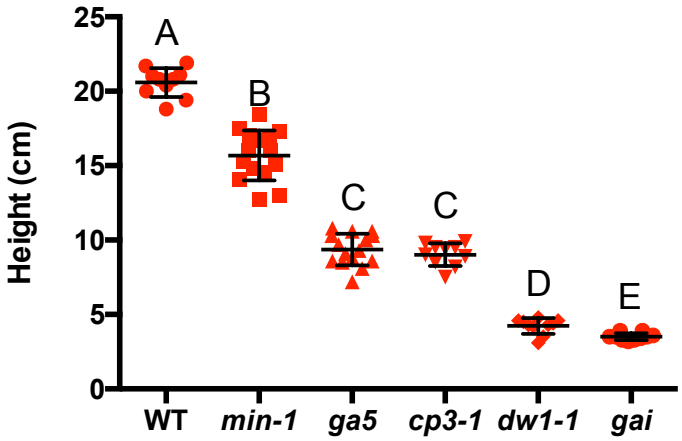


Figure 3.5 Heights of WT and the five dwarf mutants included in this study.
All plants were germinated on agarose before being transplanted to soil and grown at 22–24 °C under 16-h light/8-h dark photoperiod (irradiance 120 µmol of photons/m^2 per second). The lengths of the inflorescence stems of six-week old plants were recorded as a measurement of plant heights. The heights of *ga5* and *gai* are included for comparison. Data are means ± s.d. ($n \geq 10$). Statistical analyses were performed with pairwise student's t-tests. Same letters depict no statistically significant difference ($P \geq 0.05$) whereas different uppercase letters depict a P value ≤ 0.01.

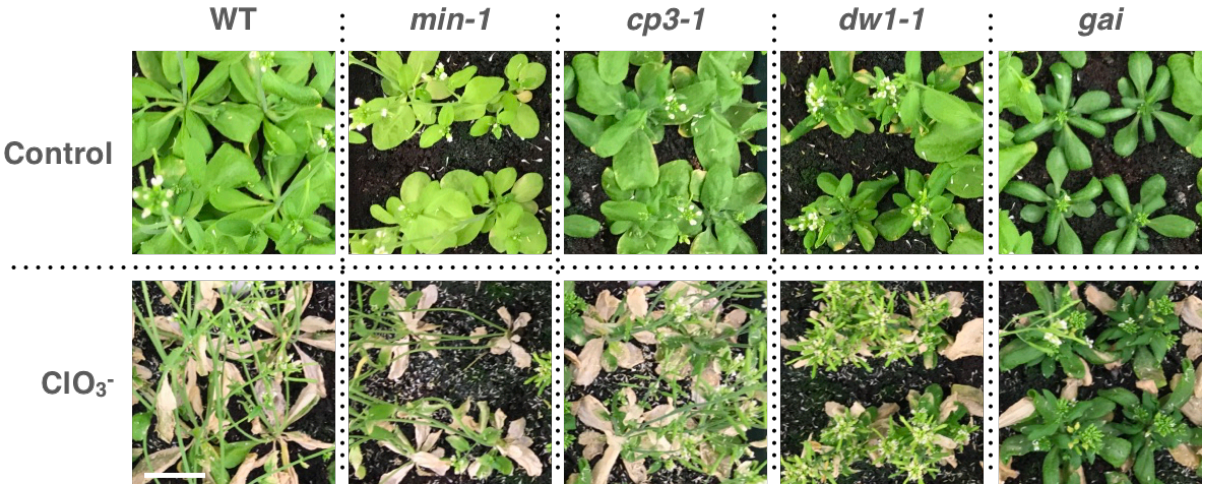


Figure 3.6 Chlorate responses of WT and four dwarf mutants.
The chlorate responses of three selected dwarfed mutants (*min-1*, *cp3-1* and *dw1-1*) are not detectably different to that of WT. The chlorate response of *gai* is included for comparison. All plants were germinated on agarose before being transplanted to soil and grown at 22–24 °C under 16-h light/8-h dark photoperiod (irradiance 120 µmol of photons/m^2 per second). Four-week old plants were watered with 1.0 mM chlorate to soil saturation, which was repeated every five days (for full details see section 2.4.1). Photos of the plants were taken two weeks after the first chlorate treatment. Scale bar = 3 cm.

In further experiments, the effect of plant Target of Rapamycin (TOR) protein kinases was investigated. TOR kinases act as positive growth and developmental regulators which are

activated by an array of nutrient signals, the best understood of these being the glucose and sucrose derived from photosynthesis (Xiong and Sheen, 2015). Accordingly, TOR overexpression (*TOR-OX*) and RNAi knockdown (*TOR-RNAi*) lines respectively exhibit promoted and inhibited growth phenotypes. Thus, *TOR-OX* plants are of a larger whereas *TOR-RNAi* plants are of a smaller size than WT (Figure 3.7). Interestingly, the chlorate toxicity assay reveals an unexpected positive correlation between plant size and chlorate resistance for these lines (Figure 3.7), the opposite of the negative correlation proposed above, and initially suggesting that *Arabidopsis* TOR kinases might negatively regulate nitrate metabolism, a possibility meriting further future explanation.

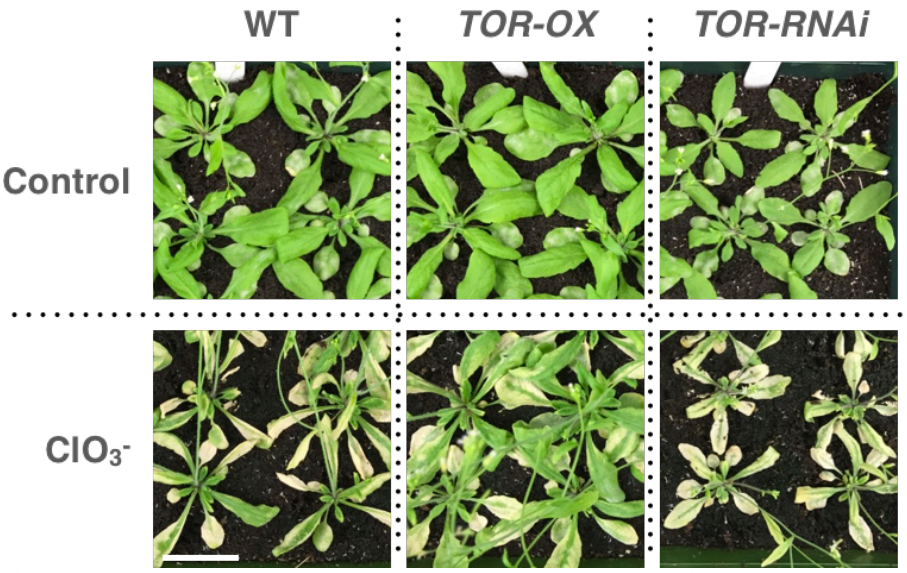


Figure 3.7 Chlorate responses of WT, *TOR-OX* and *TOR-RNAi* lines.
Compared to WT plants, the *TOR-OX* and *TOR-RNAi* lines exhibited respectively larger and smaller rosette sizes. *TOR-OX* plants are more resistant than WT to chlorate whilst *TOR-RNAi* plants are more sensitive. All plants were germinated on agarose before being transplanted to soil and grown at 22–24 °C under 16-h light/8-h dark photoperiod (irradiance 120 µmol of photons/m^2 per second). Four-week old plants were watered with 1.5 mM chlorate to soil saturation, which was repeated every five days (for full details see section 2.4.1). Photos of the plants were taken two weeks after the first chlorate treatment. Scale bar = 3 cm.

Overall, these various observations disprove the hypothesis that the chlorate resistances conferred by *gai* and *ga5* are an automatic consequence of the fact that these mutations confer

dwarfism. It is therefore worth further investigating the underlying mechanism of *gai*-mediated chlorate resistance.

3.2.4 Using hypocotyl graft chimeras to determine root versus shoot contribution to mutant chlorate resistance

As discussed above, chlorate resistance can be explained by a root-dependent deficiency in nitrate/chlorate uptake, or a shoot-dependent deficiency in nitrate/chlorate reduction, or both. Based on this spatial separation, grafting provides a potentially useful method for understanding the mechanisms of modified chlorate responses exhibited by mutants. To provide positive controls, grafting experiments with the *nrt1.1* and *nia2* mutants were initially performed, thus confirming the validity of this approach.

Control graft chimeras, i.e., WT shoot on WT root (WT/WT) and mutant shoot on mutant root (*mutant*/*mutant*) grafted plants, shown in Figure 3.8 and Figure 3.9, demonstrate that the grafting procedure itself does not affect plant chlorate responses. After exchanging the root and shoot tissues between WT and the mutants, graft chimeras with a *nrt1.1* rootstock or a *nia2* scion exhibited strong chlorate resistance, whereas reciprocal *nrt1.1* (shoot)/WT (root) and WT (shoot)/*nia2* (root) graft chimeras are as sensitive to chlorate toxicity as WT/WT controls (Figure 3.8 and Figure 3.9).

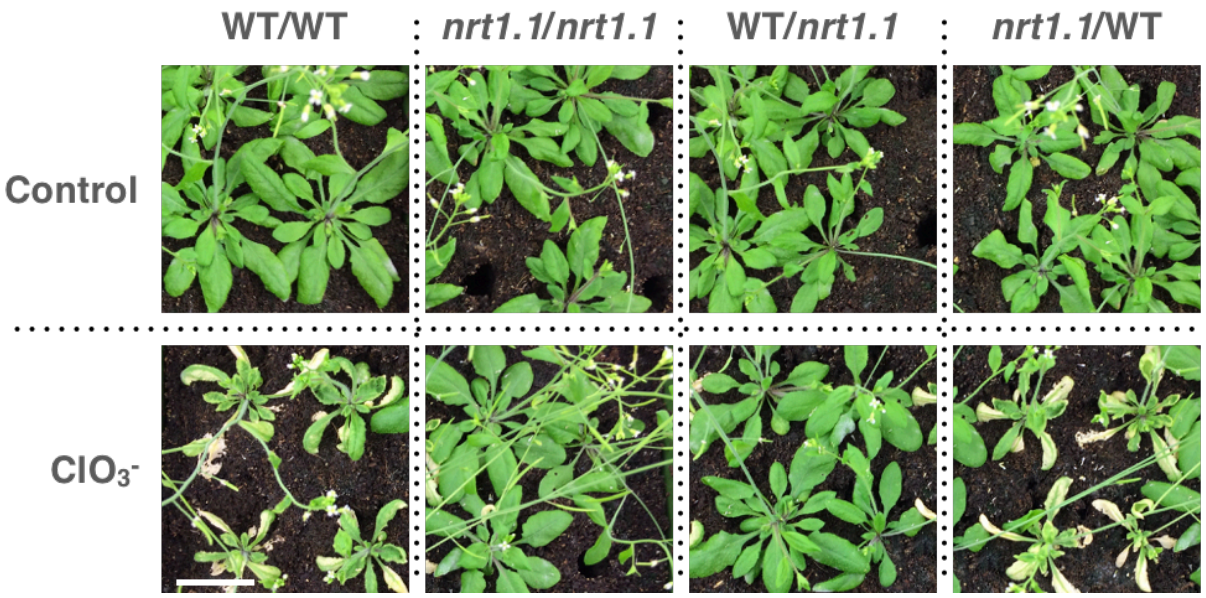


Figure 3.8 Chlorate responses of graft chimeras made by exchanging shoots and roots of WT and *nrt1.1* mutant plants.

Control grafts, WT/WT and *nrt1.1*/*nrt1.1*, remained respectively sensitive and resistant to chlorate. The *nrt1.1* mutant root of the WT/*nrt1.1* graft rescued the WT shoot sensitivity to chlorate, suggesting that *nrt1.1*-mediated chlorate resistance is root- rather than shoot-dependent. All graft chimeras were constructed at seedling stage, transplanted to soil after recovery, and grown at 22–24 °C under 16-h light/8-h dark photoperiod (irradiance 120 µmol of photons/m^2 per second, for full details see section 2.3). Four-week old plants were watered with 1.5 mM chlorate to soil saturation, which was repeated every five days (for full details see section 2.4.1). Photos of the plants were taken two weeks after the first chlorate treatment. The graft chimeras are labelled as shoot genotype/root genotype. Scale bar = 3 cm.

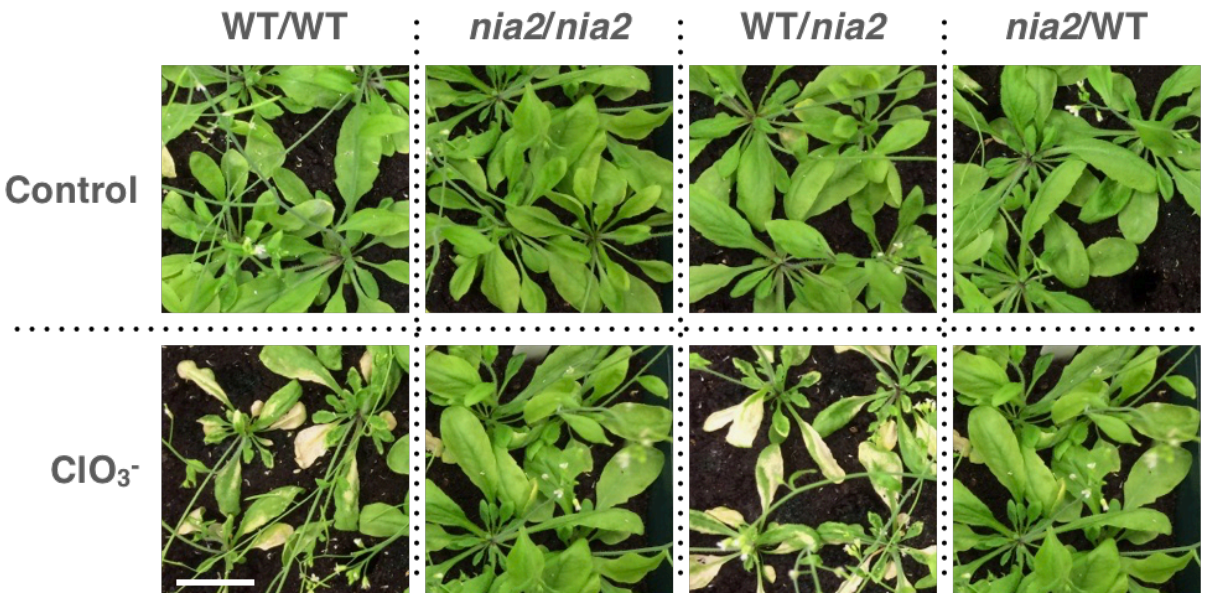


Figure 3.9 Chlorate responses of graft chimeras made by exchanging shoots and roots of WT and *nia2* mutant plants.
Control grafts, WT/WT and *nia2*/*nia2*, remained respectively sensitive and resistant to chlorate. The *nia2* mutant shoot of the *nia2*/WT graft confers resistance to chlorate, suggesting that *nia2*-mediated chlorate resistance is shoot- rather than root-dependent. All graft chimeras were constructed at seedling stage, transplanted to soil after recovery, and grown at 22–24 °C under 16-h light/8-h dark photoperiod (irradiance 120 µmol of photons/m^2 per second, for full details see section 2.3). Four-week old plants were watered with 1.5 mM chlorate to soil saturation, which was repeated every five days (for full details see section 2.4.1). Photos of the plants were taken two weeks after the first chlorate treatment. The graft chimeras are labelled as shoot genotype/root genotype. Scale bar = 3 cm.

These two control experiments prove that grafting is a legitimate way to study the mechanisms of modified chlorate responses in mutants. More importantly, although nitrate reduction is generally believed to occur predominantly in the shoot when soil nitrate concentration is high (Andrews, 1986), the grafting experiment involving *nia2* here provides a definitive proof that this is indeed the case under our experimental conditions.

3.2.5 *gai*-conferred chlorate resistance is mainly shoot- rather than root-dependent

Next, grafting was performed to determine whether *gai*-conferred chlorate resistance is shoot-dependent, root-dependent, or both. Similar to the above-mentioned grafting experiments for

plants in the *Col*-0 ecotype background, the grafting procedure itself did not affect the expected chlorate responses of the control graft chimeras in the *Ler* background. Specifically, WT/WT and *gai*/*gai* remained respectively sensitive and resistant to chlorate. Only graft chimeras with a *gai* mutant shoot exhibited resistance to chlorate (Figure 3.10), suggesting a clear shoot-dependency of the chlorate resistance conferred by the *gai* mutation.

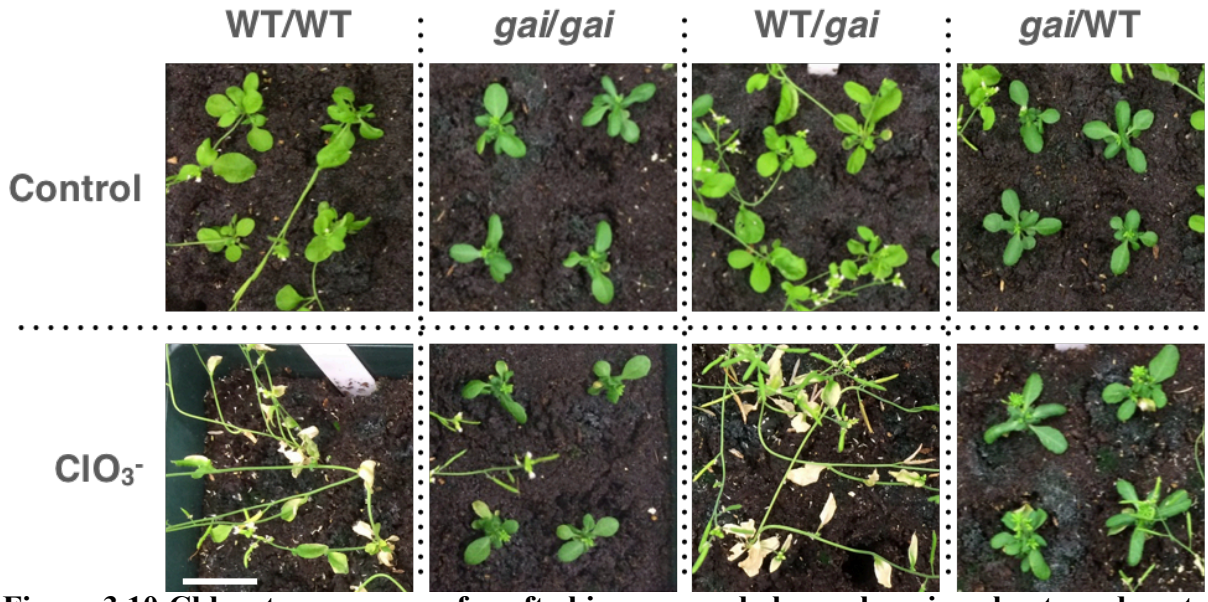


Figure 3.10 Chlorate responses of graft chimeras made by exchanging shoots and roots of WT and *gai* mutant plants (*Ler* ecotype background).
Control grafts, WT/WT and *gai*/*gai*, remained respectively sensitive and resistant to chlorate. The graft chimeras with a *gai* mutant shoot exhibited resistance to chlorate, whereas those with a *gai* mutant root are sensitive to chlorate, suggesting a shoot-dependency of *gai*-mediated chlorate resistance. It is worth noting that graft chimeras made from *Ler* plants appeared to be under stress (see main text). All graft chimeras were constructed at seedling stage, transplanted to soil after recovery, and grown at 22–24 °C under 16-h light/8-h dark photoperiod (irradiance 120 µmol of photons/m^2 per second, for full details see section 2.3). Four-week old plants were watered with 1.0 mM chlorate to soil saturation, which was repeated every five days (for full details see section 2.4.1). Photos of the plants were taken two weeks after the first chlorate treatment. The graft chimeras are labelled as shoot genotype/root genotype. Scale bar = 3 cm.

Surprisingly, grafting with *Ler* ecotype plants had a much lower success rate compared to that with *Col-0* ecotype (data not shown), due to the higher incidence of developing adventitious roots on scion rather than callus tissue at the scion/stock interface. Therefore, although continuous inspection for the outgrowth of adventitious roots from the scions was performed

after grafting, it was important to ensure that the shoot and root tissues of the resultant graft chimeras were of the correct genotypes. Five WT/*gai* and *gai*/WT chimeras were randomly selected, whose shoot and root DNA was extracted for PCR amplification of the 5' fragment of the *GAI*/*gai* gene, which contains the 51 bp that is deleted in *gai* (Peng et al., 1997). The difference between WT and *gai* tissue can therefore be easily distinguished based on the difference in size of the PCR products. The result shown in Figure 3.11 confirms that these selected graft chimeras had the expected shoot and root compositions and that grafting was thus successful.

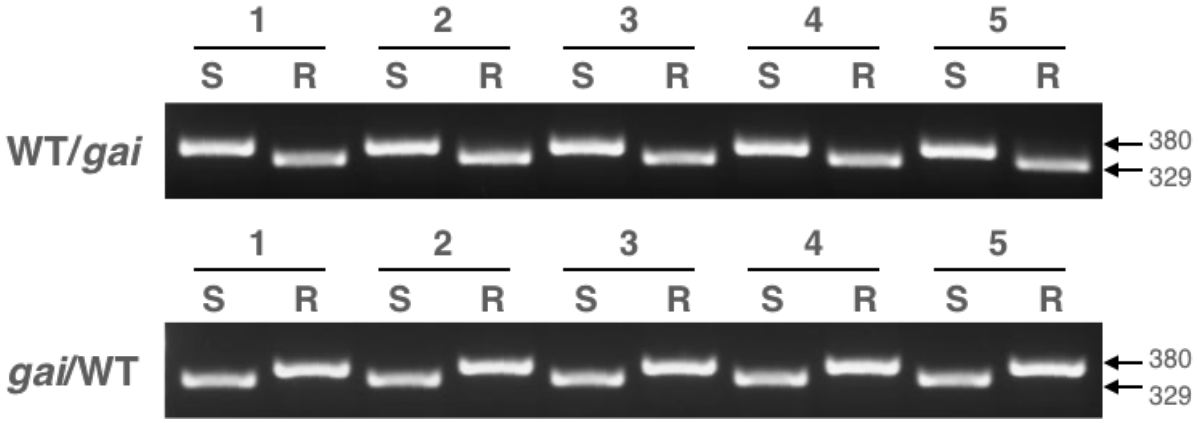


Figure 3.11 Confirmation of the identities of the WT/*gai* and *gai*/WT graft chimeras.
Five WT/*gai* and *gai*/WT graft chimeras were selected randomly. DNA from their shoot and root tissues were extracted, from which PCR was performed to amplify the 5' fragment of their *GAI*/*gai* genes. These graft chimeras were confirmed to have the correct scion and rootstock partners. The intended identities of the chimeras are indicated on the left-hand side of the gel pictures, and the band sizes of the PCR products (380 bp for *GAI* and 329 bp for *gai*) are labelled next to the gel pictures on the right. R, root; S, shoot. The graft chimeras are labelled as shoot genotype/root genotype. DNA band was visualised using the BioSpectrum™ MultiSpectral Imgaing System (UVP) with the AC Chemi HR410 camera.

In addition, the resultant graft chimeras appeared stressed, which was evident from their small rosette leaves, elongated and slender stems, and advanced flowering (Figure 3.10). A potential explanation for this phenomenon is that *Ler* plants harbour a loss-of-function mutation in the growth and developmental regulator *ERECTA* (*ER*) gene in their genetic background (van

Zanten et al., 2009, Qu et al., 2017). Therefore, a similar grafting experiment was performed using WT and *gai* mutant plants in the *Col-0* ecotype background, the observations from which strengthened the conclusion that *gai*-mediated chlorate resistance is largely shoot- rather than root-dependent (Figure 3.12).

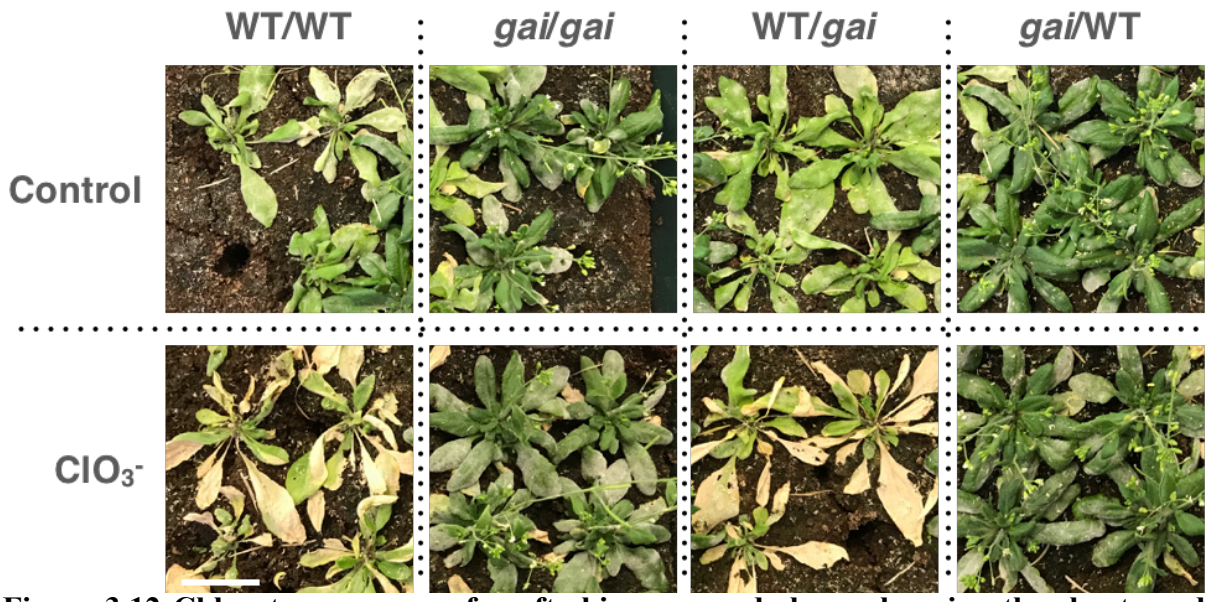


Figure 3.12 Chlorate responses of graft chimeras made by exchanging the shoots and roots of WT and *gai* mutant plants (*Col-0* ecotype background).
Control grafts, WT/WT and *gai*/*gai*, remained respectively sensitive and resistant to chlorate. The graft chimeras with a *gai* mutant shoot remained resistant to chlorate, whereas those with a *gai* mutant root are sensitive to chlorate, suggesting a shoot-dependency of *gai*-mediated chlorate resistance. All graft chimeras were constructed at seedling stage, transplanted to soil after recovery, and grown at 22–24 °C under 16-h light/8-h dark photoperiod (irradiance 120 µmol of photons/m^2 per second, for full details see section 2.3). Four-week old plants were watered with 1.5 mM chlorate to soil saturation, which was repeated every five days (for full details see section 2.4.1). Photos of the plants were taken two weeks after the first chlorate treatment. Inflorescence stems were removed from WT plants to facilitate the observation of plant chlorate responses. The graft chimeras are labelled as shoot genotype/root genotype. Scale bar = 3 cm.

3.2.6 Mutants with stabilised DELLAs have reduced shoot nitrate reductase activity, whilst nitrite reductase activity is not detectably affected

The shoot-dependency of *gai*-mediated chlorate resistance raised the possibility that stabilised DELLAs (including gai) result in compromised nitrate assimilation in the shoot. Indeed, it was discovered that the *gai* mutant shoot has an approximately 20–25% lower nitrate reductase activity than that of WT (Figure 3.13A), but a similar nitrite reductase activity to that of WT (Figure 3.13B). In contrast, the *gai-t6 tt1* double mutant, which carries a *gai* loss-of-function mutation and a background marker mutation *transparent testa1* (*tt1*; Peng et al., 1997), had a higher nitrate reductase activity than both WT and the *tt1* single mutant (Figure 3.13C). *TT1* encodes a nuclear protein, whose only known function is to regulate seed pigmentation (Sagasser et al., 2002, Appelhagen et al., 2011). Hence, the *tt1* loss-of-function mutation leads to yellow instead of brown seed coats and is unlikely to affect plant nitrate metabolism. Moreover, the GA deficient mutant *ga5* displayed a reduction in nitrate reductase activity similar to that of *gai* (Figure 3.13D). These observations led to the conclusion that stabilised DELLAs have a negative impact on shoot nitrate reductase activity, thus contributing to the shoot-dependent chlorate resistance exhibited by *gai* and *ga5* (as shown above).

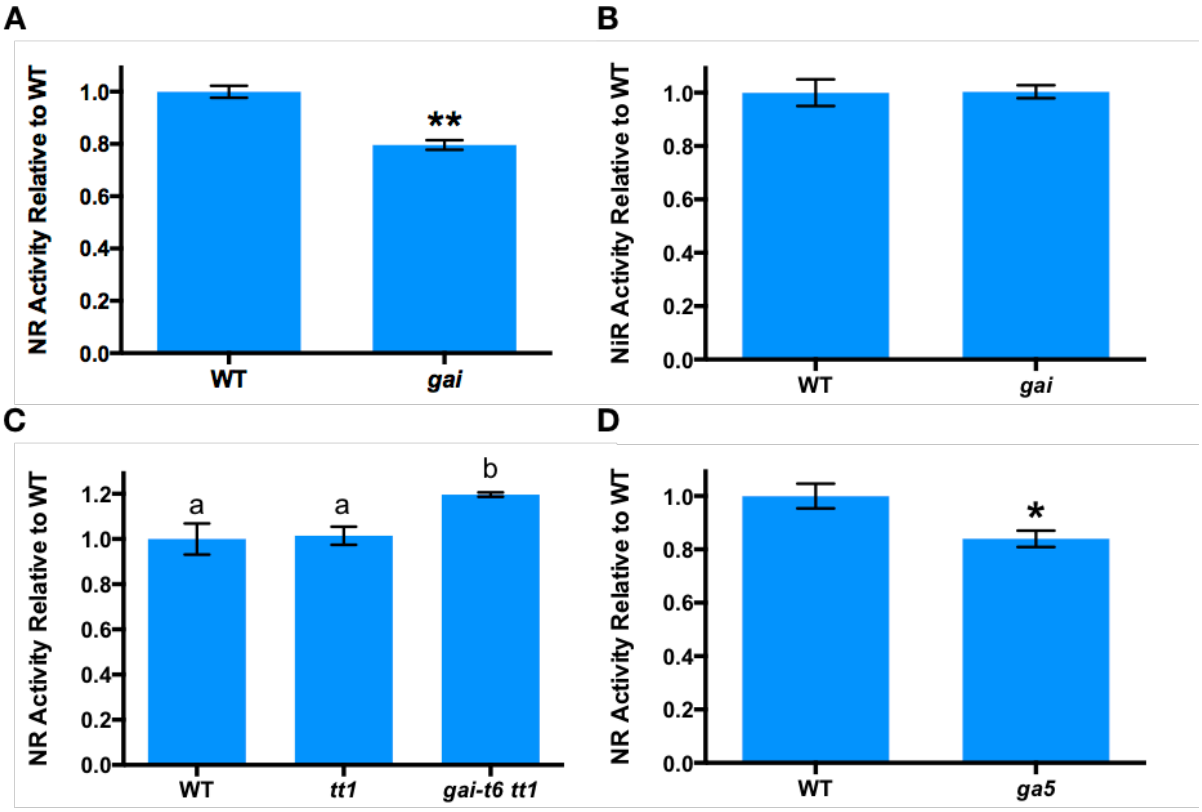


Figure 3.13 Relative shoot nitrate reductase activities in WT, *gai*, *tt1*, *gai-t6 tt1* and *ga5*, and relative shoot nitrite reductase activities in WT and *gai*.
(A) The nitrate reductase activity in *gai* mutant shoots is significantly lower than that of WT. Data are means ± s.d. (n = 4) and statistical analysis was performed with student's t-test. ** means $P \leq 0.01$. The value of 1 corresponds to 9.80 nmol NO_2^- min^{-1} per unit protein (mg ml^{-1}). (B) No significant difference ($P \geq 0.05$) in shoot nitrite reductase activity was detected between WT and *gai*. Data are means ± s.d. (n = 4), and statistical analysis was performed with student's t-test. The value of 1 corresponds to 1.31 nmol NO_2^- min^{-1} per unit protein (mg ml^{-1}). (C) The nitrate reductase activity in *gai-t6 tt1* mutant shoots is significantly higher than that of both WT and *tt1*. Data are means ± s.d. (n = 3), and statistical analysis was performed with pairwise student's t-tests. Same letters depict no statistically significant difference ($P \geq 0.05$) whereas different lowercase letters depict a P value ≤ 0.05. The value of 1 corresponds to 9.95 nmol NO_2^- min^{-1} per unit protein (mg ml^{-1}). (D) The nitrate reductase activity in *ga5* mutant shoots is significantly lower than that of WT. Data are means ± s.d. (n = 4), and statistical analysis was performed with student's t-test. * means $P \leq 0.05$. The value of 1 corresponds to 9.61 nmol NO_2^- min^{-1} per unit protein (mg ml^{-1}). Rosette leaves of four-week old plants were harvested three hours after the onset of the light photoperiod (16-h light/8-h dark) for nitrate reductase activity assay (for full details see section 2.5).

3.2.7 The *gai* mutation upregulates the mRNA abundances of nitrate transporter genes and has no detectable effect on nitrate or nitrite reductase mRNA abundances

Following on from the results of the grafting and nitrate reductase activity assays, the effect of the *gai* mutation on the transcript abundances of several nitrate metabolism-related genes was investigated. First, semi-quantitative RT-PCR found no apparent difference between WT and *gai* in the root abundances of mRNAs from the dual affinity nitrate transporter *NRT1.1*, the constitutive low affinity nitrate transporter *NRT1.2*, or the major high affinity nitrate transporter *NRT2.1* gene (Figure 3.14). However, mRNA from *NAR2.1*, which encodes the NRT2 partner protein (Orsel et al., 2006, Li et al., 2007, Wirth et al., 2007, Kotur et al., 2012), appeared to be expressed at a slightly higher level in *gai* than in WT (Figure 3.14). The levels of mRNAs encoding the other major high affinity nitrate transporters, from the *NRT2.2*, *NRT2.4* and *NRT2.5* genes, were too low in both genotypes to be detected by RT-PCR (data not shown). Next, despite *gai* having a reduced shoot nitrate reductase activity, no difference in the abundances of mRNAs from the two nitrate reductase genes (*NIA1* and *NIA2*) or from the nitrite reductase gene (*NIR1*) was observed (Figure 3.14).

Subsequently, the more sensitive quantitative RT-PCR (RT-qPCR) technique was employed to extend the above findings. RT-qPCR detected small yet significant increases in *NRT1.1*, *NRT2.1* and *NRT2.2* mRNA abundances in the *gai* mutant, but similar abundances of mRNAs encoding nitrate and nitrite reductase activities in WT and *gai* (Figure 3.15). Overall, the *gai* mutation appears to cause mild increases in the abundances of mRNAs encoding nitrate transporters, but has no impact on the abundances of mRNAs encoding nitrate and nitrite reductase activities.

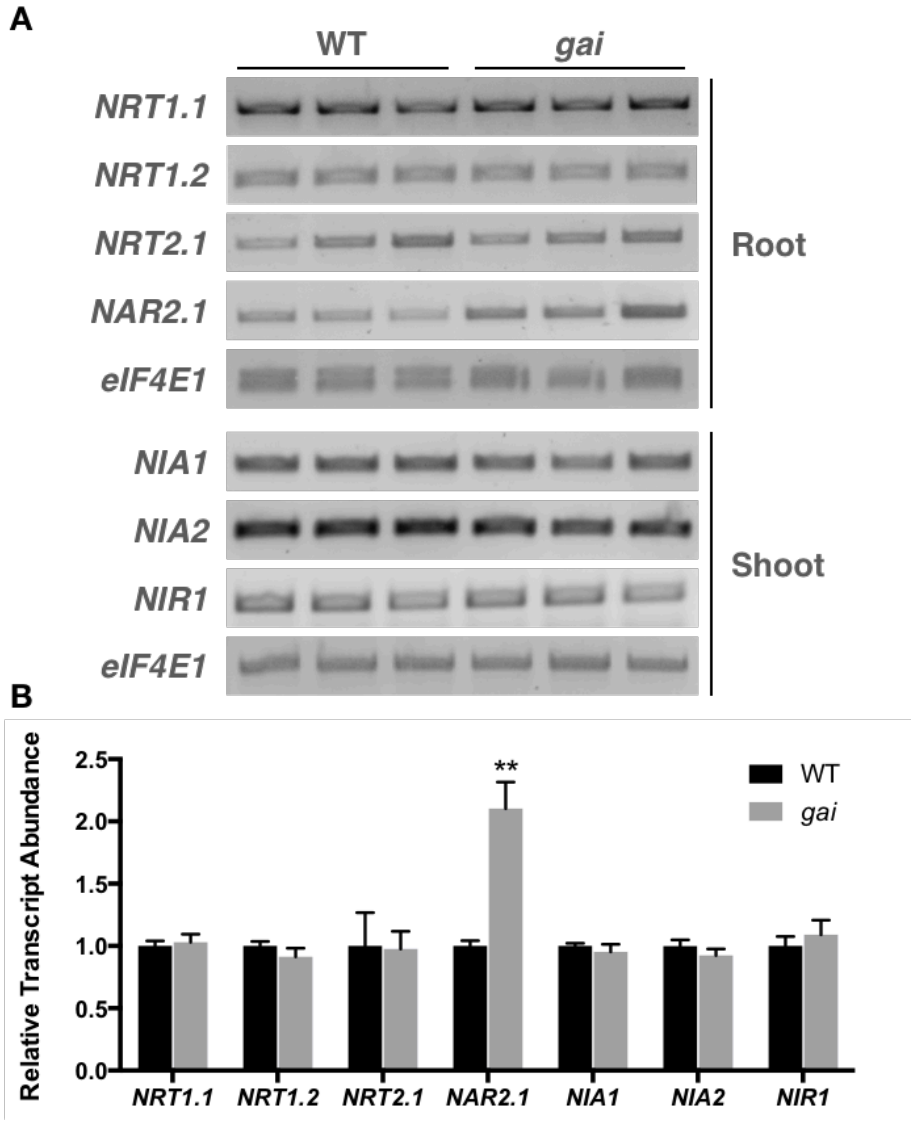


Figure 3.14 Abundances of mRNAs encoding major nitrate transporter, nitrate reductase and nitrite reductase activities visualised using RT-PCR.

(A) mRNA abundances visualised using RT-PCR. DNA band was visualised using the BioSpectrum™ MultiSpectral Imgaing System (UVP) with the AC Chemi HR410 camera. (B) Quantification of transcript levels expressed as the relative band intensities (quantified with the VisionWorksLS software) normalised to that of the control gene *eIF4E1*. Statistical analyses were performed with pairwise student's t-tests. ** means $P \leq 0.01$. Semi-quantitative RT-PCR did not detect any obvious difference in the mRNA levels of the indicated genes except for *NAR2.1*, which was found to have a significantly higher mRNA abundance in *gai* versus WT. The transcript levels of *NRT2.2*, *NRT2.4* and *NRT2.5* were too low to be detected in both genotypes (no visible band even after 30 cycles of PCR) and therefore are not shown here. *eIF4E1* gene was included as the internal control. Three biological replicates were included in this study. Ten-day old seedling roots and four-week old adult plant rosette leaves were collected three hours after the onset of the light photoperiod (16-h light/8-h dark) for RT-PCR analysis (for full details see section 2.6).

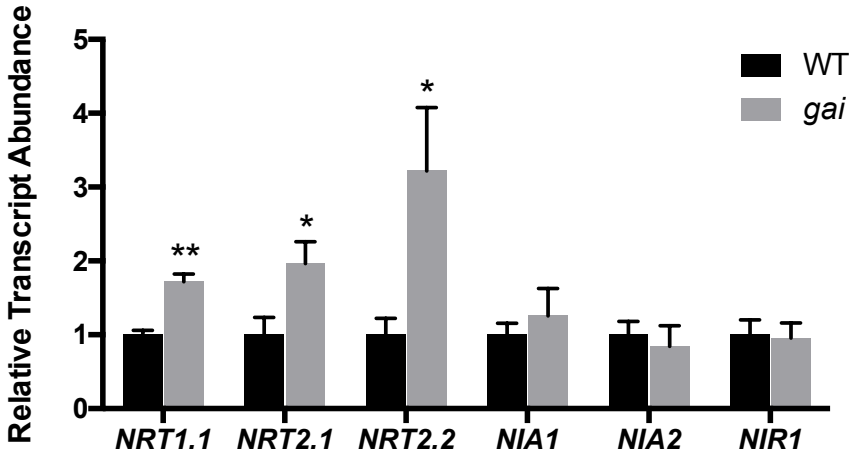


Figure 3.15 Relative abundances of mRNAs encoding major nitrate transporters, and nitrate reductase and nitrite reductase activities as measured using RT-qPCR.
Quantitative RT-qPCR showed small but significant increases in the abundances of mRNAs encoding NRT1.1, NRT2.1 and NRT2.2 in *gai* versus WT. No difference in the abundances of *NIA1*, *NIA2* or *NIR1* mRNAs was detected ($P \geq 0.05$). mRNA abundances were normalised to that of the internal control gene *Actin*. Data are means $\pm$ s.d. (n = 4 biological replicates of 3 technical replicates). Statistical analyses were performed with pairwise student's t-tests. * means $P \leq 0.05$ and ** means $P \leq 0.01$. Ten-day old seedling roots and four-week old adult plant rosette leaves were collected three hours after the onset of the light photoperiod (16-h light/8-h dark) for RT-qPCR analysis (for full details see section 2.6).

3.2.8 The rice *sd1* mutation confers chlorate resistance and reduced nitrate reductase activity

As shown above, *Arabidopsis ga5* mutant plants are relatively resistant to chlorate, and this phenomenon is at least partially attributable to their having reduced levels of nitrate reductase activity compared to WT. Since rice *SD1* gene is a functional orthologue of *Arabidopsis GA5* (Rieu et al., 2008), it would be interesting to see if parallel effects could be observed in the rice *sd1* mutant. *Indica* rice (*SD1* and *sd1* mutant) plants were treated with various concentrations of chlorate within the range of 0–2 mM (see section 2.4.2 for details), and *sd1* mutants were found to survive better than WT following treatment with 2 mM chlorate (Figure 3.16).

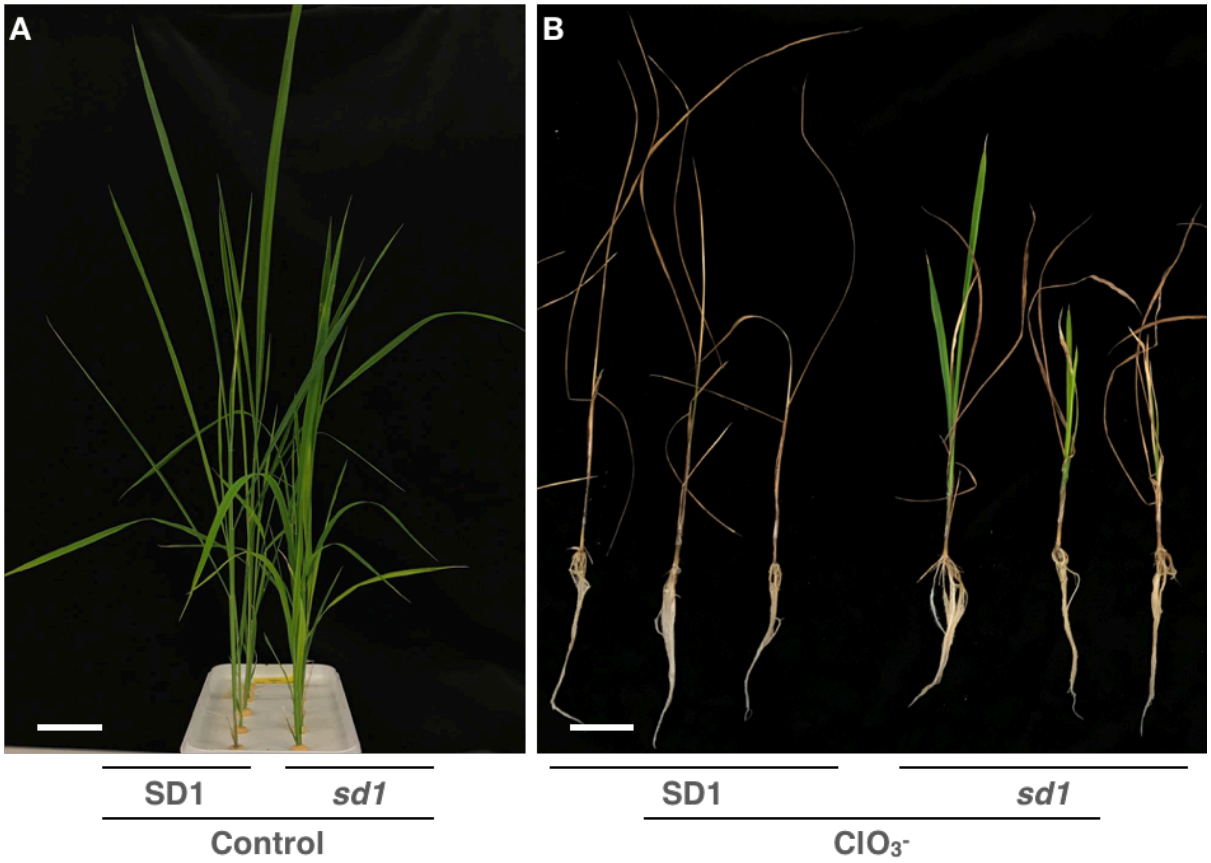


Figure 3.16 Chlorate responses of *indica* rice *SD1* and *sd1* mutant plants.
(A) Four-week old *Indica* rice (*SD1* and *sd1* mutant) growing in nutrient solution without chlorate. Scale bar = 5 cm. (B) *Indica* rice *sd1* mutant plants exhibited a higher resistance to chlorate toxicity than WT at a concentration of 2 mM. Rice seeds were germinated on wet filter paper before being transplanted to hydroponic growth conditions and grown at 22–24 °C under 16-h light/8-h dark photoperiod (irradiance 120 μmol of photons/m^2 per second). Nutrient solution was renewed every five days initially, and then every three days. For chlorate treatment, four-week old rice plants were grown in nutrient solution supplemented with 2 mM of chlorate, which was renewed every three days (for full detail see sections 2.2.2 and 2.4.2). Photos of the plants were taken two weeks after the first chlorate treatment. Scale bar = 5 cm.

In accordance with the results from the chlorate toxicity assay, the *sd1* mutation significantly reduced *indica* rice shoot nitrate reductase activity (Figure 3.17). Therefore, the stabilised DELLA (SLENDER1 [SLR1]) conferred by the *sd1* mutation in *indica* rice negatively regulates nitrate reductase activity and results in chlorate resistance, in a manner similar to that of the *Arabidopsis gai* and *ga5* mutants.

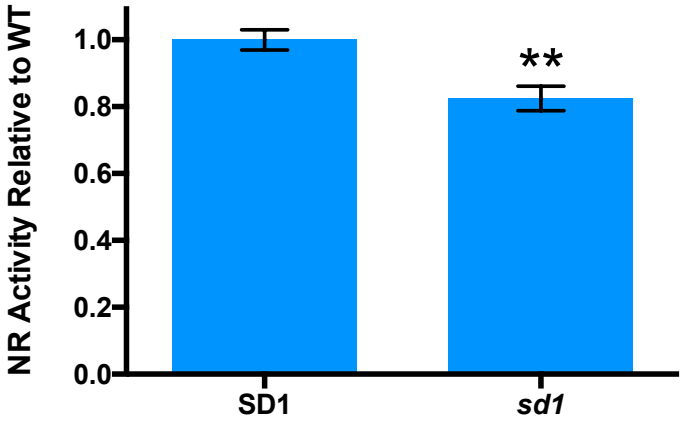


Figure 3.17 Relative shoot nitrate reductase activities in WT and *sd1 indica* rice.
The nitrate reductase activity in rice *sd1* mutant shoots is significantly lower than that in WT. Data are means ± s.d. (n = 5) and statistical analysis was performed with student's t-test. ** means $P \leq 0.01$. The value of 1 corresponds to 6.12 nmol NO_2^- min^{-1} per unit protein (mg ml^{-1}). Whole shoots of four-week old plants grown hydroponically were harvested three hours after the onset of the light photoperiod (16-h light/8-h dark) for nitrate reductase activity assay (for full details see section 2.5).

3.3 Discussion

3.3.1 General comments on chlorate toxicity assays and grafting experiments.

Unlike most previously reported chlorate treatments for *Arabidopsis* plants, which were performed on vermiculite/perlite systems, chlorate was directly added to nutrient-rich soil in this study to maximise the similarity to the agricultural environment. Although chlorate is chemically similar to nitrate, higher plant nitrate transporters and nitrate reductases both have a higher affinity for nitrate than for chlorate (Solomons and Vennesla, 1972, Nakagawa and Yamashita, 1986, Wang et al., 1988, Lin and Cheng, 1997). Therefore, in order to overcome nitrate competition, high concentrations of chlorate (≥1.0 mM) were applied to the soil. At these high concentrations, most of the chlorate is suspected to be absorbed by the plants through the low affinity ($K_M \approx$ mM) rather than high affinity ($K_M \approx$ µM) nitrate transport system. As a result, whilst *nrt1.1* (lacking low affinity nitrate transport) and *nia2* (lacking nitrate reductase

activity) mutant plants were resistant to chlorate, *nrt2.1 nrt2.2* (lacking high affinity nitrate transport) mutant plants were not in our experimental conditions.

Additionally, it has been shown previously that nitrate reduction occurs in the root under low nitrate conditions, but progressively shifts to the shoot with increased external nitrate concentrations (Andrews, 1986). Given the high nitrate concentration in the soil used in this study, nitrate reduction is expected to take place predominantly in the shoot. The grafting experiment with WT and the *nia2* mutant confirms this hypothesis, with *nia2* (shoot)/WT (root) but not WT (shoot)/*nia2* (root) graft chimeras being resistant to chlorate. Overall, this observation, together with the result obtained from the grafting of WT and the *nrt1.1* mutant, justify the use of grafting as a tool to distinguish chlorate resistance due to shoot-dependent deficiency in nitrate reduction and/or root-dependent deficiency in nitrate uptake.

3.3.2 DELLAs negatively regulate shoot nitrate reductase activity

The *Arabidopsis gai* and *ga5* mutants both exhibited a relatively strong chlorate resistance phenotype. However, the inhibitory effect of DELLA accumulation on growth alone is not sufficient to govern the plants chlorate resistance. Multiple different mutations that lead to dwarf statures and/or small rosette sizes without necessarily directly affecting the GA-DELLA signalling pathway were shown to confer sensitivity to chlorate toxicity at least as great as that of WT plants, raising the possibility that stabilised DELLAs somehow result directly in compromised nitrate metabolism.

Previous studies have reported root-to-shoot long-distance transport of DELLA mRNAs after grafting in certain plant species, for example, tomato, cucumber and tobacco, leading to GA-

insensitive phenotypes in the scions (Haywood et al., 2005, Xu et al., 2013). However, in this study, no obvious change in shoot morphology was observed following grafting of a WT scion onto a *gai* rootstock, or vice versa, suggesting that DELLA mRNA movement plays a minor effect, if any, on the phenotype of grafted *Arabidopsis* plants. It is possible that the more pronounced DELLA mRNA movement previously reported is due to the use of transgenic rootstocks that either overexpress DELLA genes (in the case of tomato and cucumber, Haywood et al., 2005), or express companion cell-specific DELLAs, which facilitates their transport into the phloem (in the case of tobacco, Xu et al., 2013).

Graft chimeras having a *gai* mutant scion and a WT rootstock remained chlorate resistant, which is potentially attributable to the reduction in nitrate reductase activity in *gai* shoot tissue. Furthermore, nitrate reductase activity was found to be similarly repressed in the *ga5* mutant but increased in the loss-of-function *gai-t6* mutant. The relatively minor increase in nitrate reductase activity conferred by the *gai-t6* mutation versus that seen in WT is probably due to the fact that the GA concentration is in general close to saturation in WT *Arabidopsis* plants (Rieu et al., 2008). Taken together, these results imply a negative regulatory relationship between DELLAs and nitrate reductase activity. It would be interesting to include more dramatic mutants, such as the severely GA deficient mutant *ga1-3* and the five DELLA knockout mutant *global* (*gai-t6 rga-t2 rgl1-1 rgl2-1 rgl3-4*) in future studies to see if more pronounced alterations in chlorate responses and/or nitrate reductase activities can be observed. One of the five *Arabidopsis* DELLAs, *GAI*, has been focused on in this study, but the other DELLAs might also contribute to the regulation of nitrate metabolism to different extents, which should be investigated further.

Whilst this study indicates that DELLA accumulation inhibits nitrate reductase activity, previous studies have either suggested that there is no impact on nitrate reductase activity of the GA-DELLA signalling pathway (Bouton et al., 2002), or suggested the opposite regulatory effect, i.e., GA inhibits while DELLAs promote nitrate reductase activity (Zhang et al., 2011). One obvious explanation for these apparent discrepancies is differences in plant developmental stages and growth conditions. Whilst both previous studies measured nitrate reductase activity of one-week or two-week old seedlings grown on plates, nitrate reductase activity assays were performed on four-week old adult plants grown on soil in this study. Furthermore, it is preferable, when calculating nitrate reductase activity, to normalise against protein content rather than against plant fresh weight (as in the previous studies). This is especially important in the case of mutants defective in GA-DELLA signalling because GA promotes both cell division through promoting cell cycling, and cell expansion through modulating microtubule reorganisation as well as activating cell wall loosening enzymes (Ogawa et al., 2003, Achard et al., 2009, Sambade et al., 2012). As a result, cell density and therefore protein concentration are both expected to be higher in DELLA-accumulating plants and vice versa (Cowling and Harberd, 1999). Indeed, as shown in Figure 3.18, protein concentration per fresh weight was found to be significantly higher in the *gai* and *ga5* mutants than in WT (Figure 3.18A&B), and lower in the *gai-t6 tt1* mutant than in *tt1* (Figure 3.18C). Similarly, in rice, protein extracted from the *sd1* mutants had a higher concentration than from WT (Figure 3.18D). Therefore, normalising nitrate reductase activity against plant fresh weight rather than against protein content will inevitably lead to an overestimation of nitrate reductase activity in DELLA-stabilising mutants and an underestimation in DELLA-deficient mutants. This is especially relevant in the case of the *ga1-3* mutant investigated in Zhang et al., 2011, which is expected to have a considerably higher protein concentration than WT.

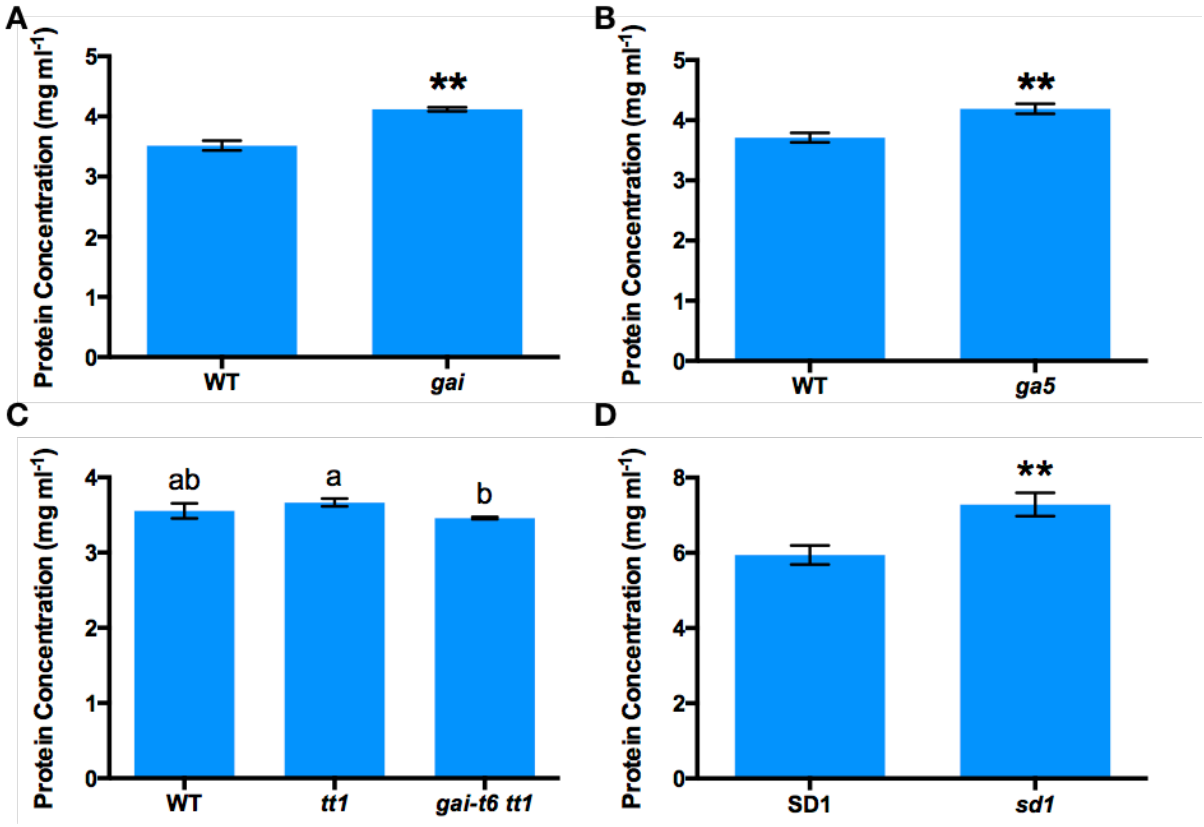


Figure 3.18 Protein concentrations of *Arabidopsis* WT, *gai*, *ga5*, *tt1* and *gai-t6 tt1*, as well as rice *SD1* and *sd1*.

(A) The protein concentration in *gai* mutant shoots is significantly higher than that of WT. Data are means ± s.d. (n = 4), and statistical analysis was performed with student's t-test. ** means $P \leq 0.01$. (B) The protein concentration in *ga5* mutant shoots is significantly higher than that of WT. Data are means ± s.d. (n = 4), and statistical analysis was performed with student's t-test. ** means $P \leq 0.01$. (C) The protein concentration in *gai-t6 tt1* mutant shoots is significantly lower than that of *tt1* but not WT. Data are means ± s.d. (n = 3), and statistical analysis was performed with pairwise student's t-tests. Same letters depict no statistically significant difference ($P \geq 0.05$) whereas different lowercase letters depict a P value ≤ 0.05. (D) The protein concentration in rice *sd1* mutant shoots is significantly higher than that of *SD1*. Data are means ± s.d. (n = 5), and statistical analysis was performed with student's t-test. ** means $P \leq 0.01$. Both *Arabidopsis* and rice plants were grown at 22–24 °C under 16-h light/8-h dark photoperiod (irradiance 120 μmol of photons/m^2 per second). Four-week old *Arabidopsis* rosette leaves and four-week old rice shoots were collected three hours after the onset of the light photoperiod.

As nuclear transactivators, DELLAs function mainly by modifying downstream gene expression through interaction with transcription factors (Locascio et al., 2013). However, despite the inhibition of nitrate reductase activity by DELLAs, the abundances of nitrate reductase-encoding mRNAs were not detectably affected in the *gai* mutant, an observation

which agrees with previous findings (Bouton et al., 2002, Zhang et al., 2011). Therefore, DELLAs might inactivate nitrate reductase indirectly through upregulation of genes encoding protein kinases, 14-3-3 inhibitors, or protein proteases that modulate nitrate reductase activity post-translationally (Lillo et al., 2004). In future experiments, the effect of DELLAs on nitrate reductase protein abundance could be investigated through performing Western blot analysis, whilst transcriptome comparison of *gai* or *ga5* against WT might facilitate the identification of DELLA-regulated genes encoding candidate kinases and/or 14-3-3 proteins potentially involved in the inhibition of nitrate reductase activity.

3.3.3 DELLAs positively regulate the transcript abundances of root nitrate transporter genes

The abundances of mRNAs from several nitrate transporter genes, specifically *NRT1.1*, *NRT2.1*, *NRT2.2* and *NAR2.1*, were found to be increased moderately in the *gai* mutant compared to WT. The effect of any resultant increase in nitrate uptake in *gai* is apparently outweighed by the effect of the reduction in shoot nitrate reductase activity, as *gai* confers strong resistance to chlorate. It is also possible that the GA-DELLA signalling pathway regulates other nitrate transporters that are not investigated here. Recently, NPF3.1, a nitrate/nitrite transporter located in the root endodermis, was identified as a GA transporter and reported as being responsible for relaying the GA signal in low-nitrate conditions (Sugiura et al., 2007, Leran et al., 2014, David et al., 2016). In turn, *NPF1.3* relative transcript abundance is inhibited by external application of GA while promoted by the antagonistic phytohormone ABA, although it is yet to be confirmed whether nitrate/nitrite uptake is accordingly affected by these hormones (Tal et al., 2016). Future physiological studies such as N^{15} stable isotope uptake analysis and tissue nitrate content measurement should be performed to establish

whether *gai*-mediated upregulation of nitrate transporter-encoding mRNA abundances translates to an actual increase in plant nitrate uptake. If the positive regulatory effect of DELLAs on nitrate uptake is broadly conserved in crop plants, attempts might be made to enhance root DELLA accumulation through the use of root-specific promoters, thus improving crop nitrate uptake and NUE. Alternatively, increased mRNA abundances of nitrate transporters in *gai* relative to WT might be a secondary effect triggered by the decrease in nitrate reductase activity in *gai* mutant shoot. After all, a reduction in the abundance of nitrogen metabolite products has long been known to exert a systemic feedback upregulation on nitrate transporters at the transcript level (Crawford and Glass, 1998, Gojon et al., 2011). This hypothesis can be tested by examining the abundance of mRNAs encoding nitrate transporters in the root of WT/*gai* compared to that of *gai*/*gai* graft chimeras, with the feedback loop in theory perturbed in the former construct.

3.3.4 Rice ssp. *indica sd1* mutant has a reduced nitrate reductase activity

WT and *sd1* rice plants were investigated to see if conclusions drawn from the GRV experimental model *Arabidopsis* mutants are transferable to crop species. Rice *sd1* is a mutant orthologue allele of *Arabidopsis GA5*, thus conferring DELLA accumulation and a semi-dwarf stature (Monna et al., 2002, Sasaki et al., 2002, Spielmeyer et al., 2002). Indeed, the *sd1* mutation rendered *indica* rice plants resistant to chlorate toxicity, a resistance which is potentially explained by a compromised nitrate reductase activity, similar to that seen in the *Arabidopsis ga5* mutant.

Future studies should include other semi-dwarf to dwarf crop varieties with modified GA-DELLA signalling pathways, such as wheat, maize and barley, to see if the negative regulatory

relationship between DELLAs and nitrate reductase activity is more broadly conserved in the plant kingdom. Unlike the growth conditions for most agricultural crops, rice is commonly grown under anaerobic conditions (e.g., paddy fields), where ammonium concentration is high (Crawford and Forde, 2002). Therefore, the potential effect of stabilised DELLAs on ammonium metabolism in rice (and also other crop species) should be clarified as it might also contribute to the low nitrogen use efficiency exhibited by modern crops.

3.3.5 Concluding remarks

In Chapter 3, *Arabidopsis gai* and *ga5*, as the experimental models for modern Green Revolution crops, were discovered to have compromised nitrate metabolism based on their observed strong resistance to the toxic nitrate chemical analogue chlorate. Grafting experiments and nitrate reductase activity assays suggest that DELLAs inhibit whereas GA (or the absence of DELLAs) promotes shoot nitrate reductase activity. mRNA abundance analyses indicate that DELLA-mediated repression of nitrate reductase probably occurs at the post-translational level, and reveal unexpected positive regulatory roles played by DELLAs on the abundances of mRNAs encoding nitrate transporters. Encouragingly, a reduced nitrate reductase activity was also found in *indica* rice *sd1*, which is actually grown in agriculture, compared to WT. Therefore, this chapter provides an initial answer to the long-standing question of why modern Green Revolution crop cultivars have a low NUE, although future studies are required to test this hypothesis in other crop species.

CHAPTER 4. The Regulatory Relationship Between PIFs and Nitrate Metabolism

4.1 Introduction

In the previous chapter, a negative regulatory effect of DELLAs on plant shoot nitrate reductase activity was established, which could potentially be opposed by GA through DELLA degradation. DELLAs are a group of transcription regulators that mainly function by modifying downstream gene expression (Ogawa et al., 2000, Daviere and Achard, 2013). In this case, it is speculated that DELLAs control the expression of genes encoding post-translational regulators of nitrate reductase, given that the mRNA abundances of the two nitrate reductase genes were not found to be not detectably affected by DELLAs. However, rather than binding to DNA directly, DELLAs interact with DNA-binding transcription factors to modulate gene expression (Locascio et al., 2013). Amongst the most well-studied DELLA-interacting transcription factors are the phytochrome interacting factors (PIFs), especially PIF3 and PIF4, which integrate GA-DELLA and light signals to regulate seedling hypocotyl elongation (de Lucas et al., 2008, Feng et al., 2008).

Of the eight PIF proteins identified in *Arabidopsis* so far (PIF1–PIF8), members of the PIF quartet (PIFq), PIF1, PIF3, PIF4 and PIF5 collectively play a major role in activating seedling etiolation in the dark (Leivar et al., 2008). Light and GA antagonistically regulate skotomorphogenesis through PIFs: whereas light triggers the phosphorylation and degradation of PIFs, GA promotes PIF activities by inducing DELLA degradation (vonArnim and Deng,

1996, Alabadi et al., 2004). The first leucine heptad repeat (LHRI) domain of DELLA proteins interacts with the DNA-binding bHLH domains of PIF3 and PIF4, therefore titrating PIFs from their target promoters and thus preventing PIF-activated gene transcription (de Lucas et al., 2008, Feng et al., 2008). DELLAs have also been shown to interact with PIF1, PIF5 and PIF6, presumably supressing their activities through sequestration as well (Gallego-Bartolome et al., 2010, Li et al., 2016). Moreover, it has been recently shown that DELLAs also induce degradation of PIFq members through the 26S proteasome, which is light-independent since it occurs independent of the phytochrome signalling pathway (Li et al., 2016, Zheng et al., 2016). This new regulatory mechanism of DELLAs has been shown to be applicable to other DELLA-interacting proteins as well, for example, BZR1 and EIN3 (Li et al., 2012c, Li et al., 2016). As a result of DELLA-mediated inhibition of PIF activities, in agreement with previous work (Leivar et al., 2009, Li et al., 2016), both the gain-of-function mutation of DELLAs (e.g., *gai*) and the quadruple loss-of-function mutation *pifq* (*pif1 pif3 pif4 pif5*) conferred photomorphogenic phenotypes (exemplified by the abrogation of hypocotyl elongation) when grown in darkness (Figure 4.1).

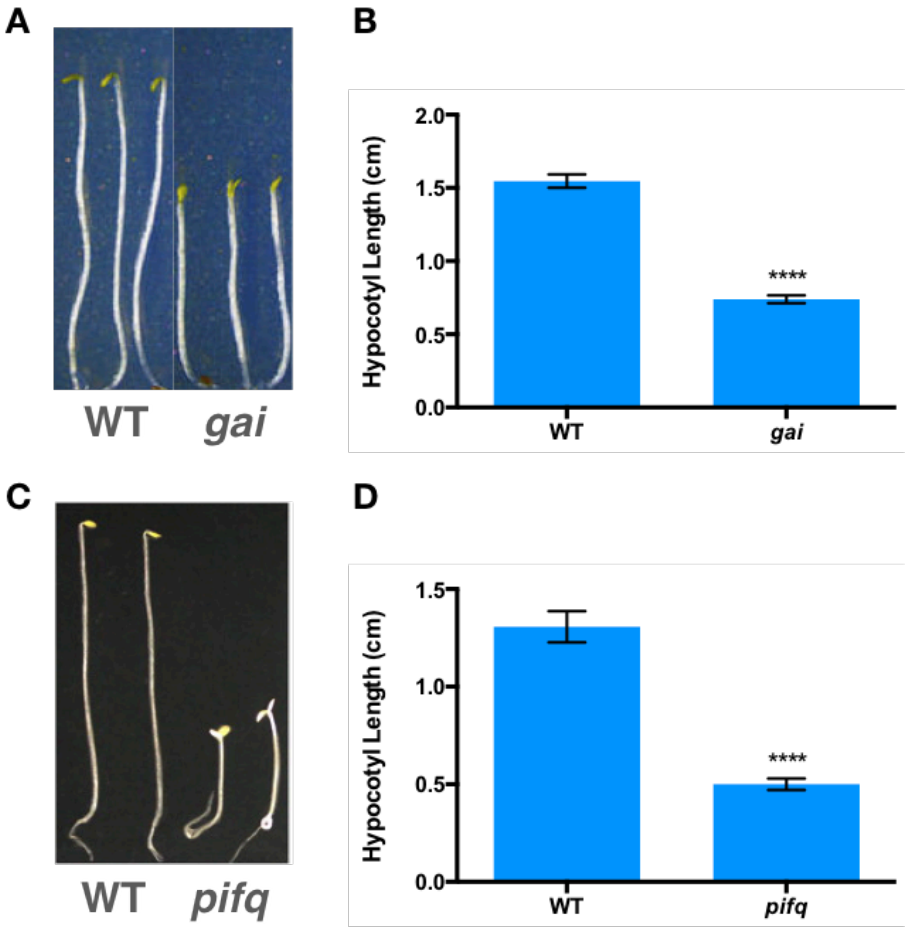


Figure 4.1 Hypocotyl etiolation phenotypes exhibited by WT versus *gai* and by WT versus *pifq*.
(A) Phenotypes of 4-day old WT and *gai* seedlings grown in the dark (adapted from Li et al., 2016). (B) Dark-grown 7-day old *gai* seedlings exhibited a much shorter hypocotyl compared to WT. Data are means ± s.d. (n = 15) and statistical analysis was performed with student's t-test. **** means $P \leq 0.0001$. (C) Phenotypes of 4-day old WT and *pifq* seedlings grown in the dark (adapted from Leivar et al., 2009). (D) Dark-grown 7-day old *pifq* seedlings exhibited a much shorter hypocotyl compared to WT. Data are means ± s.d. (n = 15) and statistical analysis was performed with student's t-test. **** means $P \leq 0.0001$. Stratified seeds were exposed to light for six hours to induce germination. Hypocotyl lengths of 7-day old seedlings grown at 22–24 °C in darkness were measured (for full details see section 2.4.4).

In recent years, accumulating evidence has shown that in addition to the regulation of skotomorphogenesis, PIFs function as signalling hubs upstream of a variety of developmental processes ranging from seed germination, shade avoidance, temperature responses, and stomatal development to ovule fertilisation (e.g., Pagnussat et al., 2005, Casson et al., 2009, Franklin et al., 2011, Lee and Thomashow, 2012, Leivar et al., 2012a, Leivar et al., 2012b).

However, the regulatory link between PIFs and nitrate metabolism has not been extensively explored. Jonassen et al., 2009 concluded that the *Arabidopsis* positive regulators of photomorphogenesis HY5 and HYH upregulate *NIA2* transcript abundance as well as nitrate reductase activity. On the other hand, among the three *pif* loss-of-function mutants investigated (*pif1*, *pif3* and *pif4*), the *pif4* mutant was found to exhibit a decreased *NRT1.1* transcript level, an increased *NIA2* transcript level, and an increased nitrate reductase activity, especially under red light, suggesting that PIF4 promotes nitrate uptake whilst inhibiting nitrate reductase activity (Jonassen et al., 2009). This observation is consistent with a previous microarray analysis showing that *NIA2* transcript abundance is enhanced in the *Arabidopsis pifq* mutant compared to WT (Shin et al., 2009). However, these conclusions are somewhat paradoxical given the results from the previous chapter of this thesis, as they imply that DELLAs and PIF4 simultaneously upregulate nitrate reductase activity.

In order to clarify the regulatory roles played by PIFs on nitrate metabolism, a similar set of approaches were taken for PIFs as outlined for DELLAs in Chapter 3. In this chapter, the *Arabidopsis pifq* mutant was first shown to be resistant to chlorate toxicity, which, similar to that found in *gai*, is attributable to a shoot-dependent repression of nitrate reductase activity. However, unlike *gai*, the *pifq* mutation results in a detectable decrease in the abundance of mRNA from the *NIA2* gene, which presumably contributes in turn to the reduced nitrate reductase activity. Studies with the single *pif* knock-out mutants indicate that the effect of *pifq* on nitrate assimilation can be achieved by the *pif3* loss-of-function mutation alone, implying that PIF3 plays a predominant role in the regulation of nitrate reductase activity. Interestingly, loss-of-function mutations of *PIF7* and *PIF8*, which do not belong to the *PIFq* family, displayed chlorate resistance as well, although the underlying mechanism remain unresolved in this study. Overall, these parallel discoveries of *gai* and *pif* mutants raised the hypothesis

that DELLAs inhibit nitrate reductase activity through antagonising PIF activities, especially that of PIF3.

4.2 Results

4.2.1 The *pifq* mutant is resistant to chlorate toxicity

PIFs often redundantly regulate downstream biological processes, a famous example being the redundant regulation of skotomorphogenesis by all PIFq members (Figure 4.2). Accordingly, the quadruple loss-of-function mutant, *pifq*, was first chosen to be investigated for its chlorate response, so as to reduce the risk of potential PIF functional redundancy from masking any mutant phenotype.

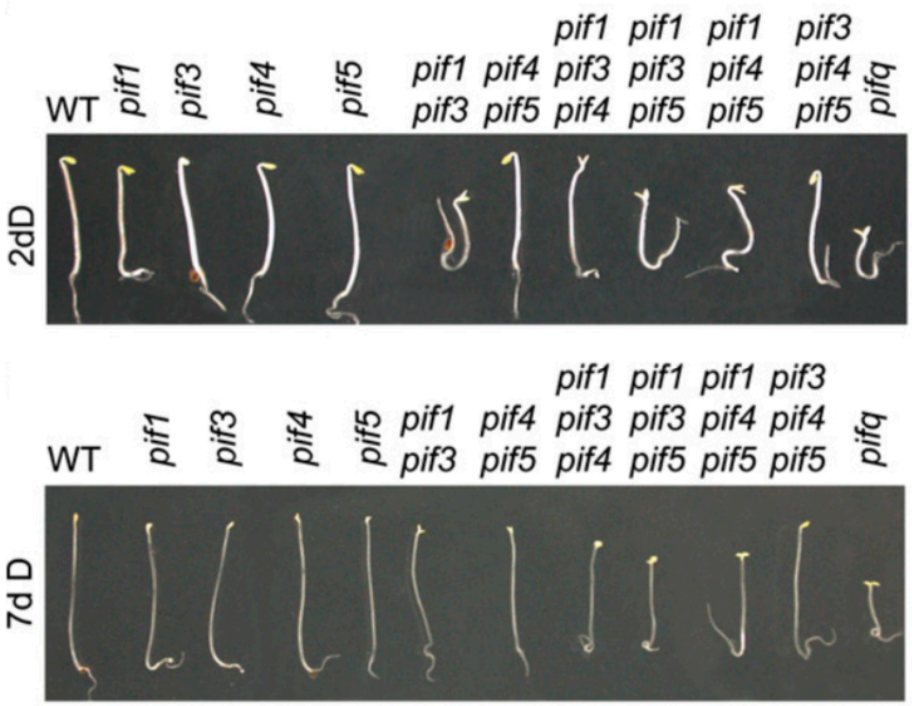


Figure 4.2 Phenotypes of dark-grown seedlings of various *pif* mutant combinations. Seedlings of WT and various *pif* mutants growing in the dark for 2 days (upper panel) and 7 days (lower panel). Single loss-of-function *pif* mutations result in similar phenotypes as WT, whereas the accumulation of *pif* mutations (especially *pifq*) exhibited exaggerated mutant phenotypes, suggesting redundant roles played by the PIFq members in regulating skotomorphogenesis. Figure adapted from (Leivar et al., 2012b).

Adult *pifq* mutant plants are phenotypically similar to WT when grown on control soil without chlorate apart from having slightly more compact rosettes (Figure 4.3A). However, *pifq* exhibited a strong resistance to chlorate toxicity compared to WT (Figure 4.3A). This phenotypic difference on chlorate can be quantitatively demonstrated as a smaller decrease in leaf chlorophyll content between *pifq* mutant plants treated with and without chlorate, compared to that of WT (Figure 4.3B).

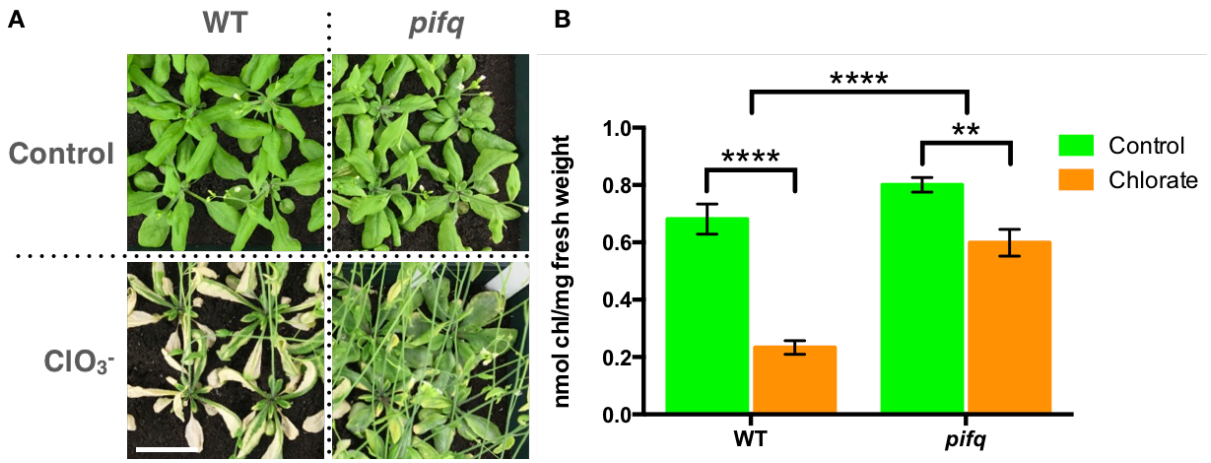


Figure 4.3 Chlorate responses and leaf chlorophyll contents of WT and *pifq* mutant plants. (A) *Arabidopsis pifq* mutant plants are more resistant to chlorate toxicity than WT plants. All plants were germinated on agarose before being transplanted to soil and grown at 22–24 °C under 16-h light/8-h dark photoperiod (irradiance 120 µmol of photons/m^2 per second). Four-week old plants were watered with 1.5 mM chlorate to soil saturation, which was repeated every five days (for full details see section 2.4.1). Photos of the plants were taken two weeks after the first chlorate treatment. Scale bar = 3 cm. (B) Leaf chlorophyll measurement confirms the strong chlorate resistance conferred by the *pifq* mutation. Chlorophyll measurements were taken from fully-expanded rosette leaves two weeks after the first chlorate treatment (for full details see section 2.4.3). Data are means ± s.d. (n = 10). Statistical analysis was performed with two-way ANOVA, ** means $P \leq 0.01$, and **** means $P \leq 0.0001$.

4.2.2 *pifq*-conferred chlorate resistance is primarily due to shoot-dependent reduction in nitrate reductase activity

Seedling hypocotyl graft experiments with WT and *pifq* mutant plants reveal the underlying mechanism of *pifq*-conferred chlorate resistance. As shown in Figure 4.4, only graft chimeras with *pifq* mutant shoots displayed resistance to chlorate, suggesting a clear shoot-dependency of chlorate resistance conferred by the *pifq* mutation. On the contrary, the WT (shoot)/*pifq* (root) grafted plants appeared to be as sensitive to chlorate as the WT (shoot)/WT (root) grafted plants.

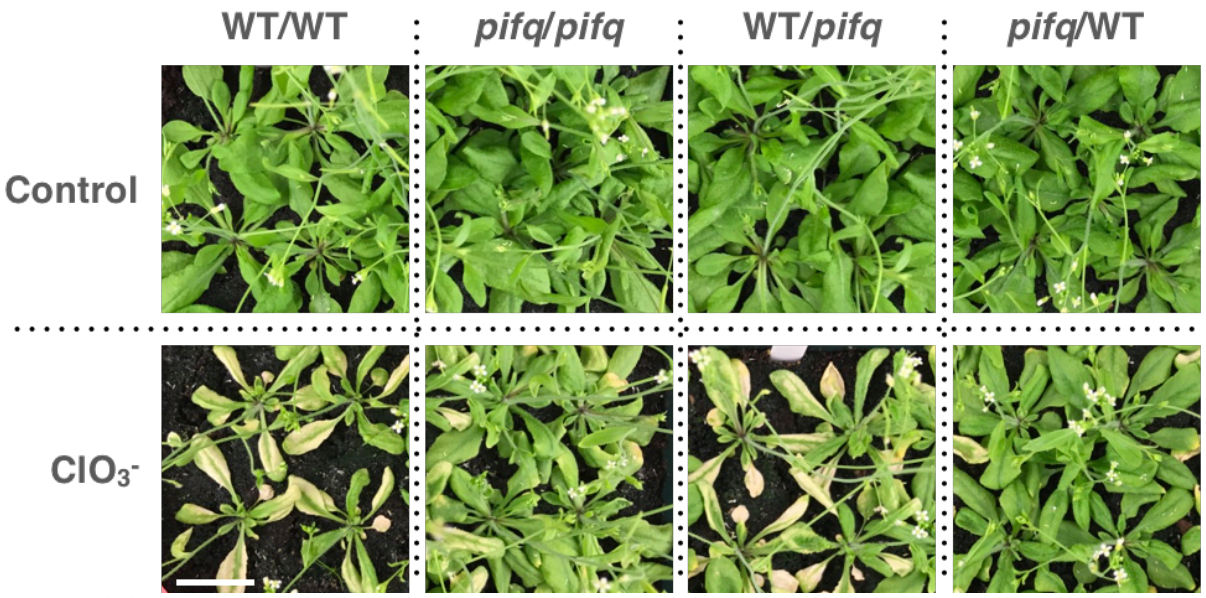


Figure 4.4 Chlorate responses of graft chimeras made by exchanging shoots and roots of WT and *pifq* mutant plants.
Control grafts, WT/WT and *pifq*/*pifq*, remained respectively sensitive and resistant to chlorate. The graft chimeras with a *pifq* mutant shoot exhibited resistance to chlorate, whereas those with a *pifq* mutant root are sensitive to chlorate, suggesting a shoot-dependency of *pifq*-mediated chlorate resistance. All graft chimeras were constructed at seedling stage, transplanted to soil after recovery, and grown at 22–24 °C under 16-h light/8-h dark photoperiod (irradiance 120 μmol of photons/m^2 per second, for full details see section 2.3). Four-week old plants were watered with 1.5 mM chlorate to soil saturation, which was repeated every five days (for full details see section 2.4.1). Photos of the plants were taken two weeks after the first chlorate treatment. The graft chimeras are labelled as shoot genotype/root genotype. Scale bar = 3 cm.

The shoot-dependency of *pifq*-mediated chlorate resistance raised the possibility that the *pifq* mutation confers compromised shoot nitrate assimilation. Accordingly, it was discovered that *pifq* mutant shoots have a dramatically decreased nitrate reductase activity (approximately 80–90%) compared to that of WT (Figure 4.5A), but a similar nitrite reductase activity to that of WT (Figure 4.5B). In conclusion, similar to the case for *gai*, the chlorate resistance exhibited by *pifq* mutant plants can at least primarily be explained by a conferred reduction in shoot nitrate reductase activity.

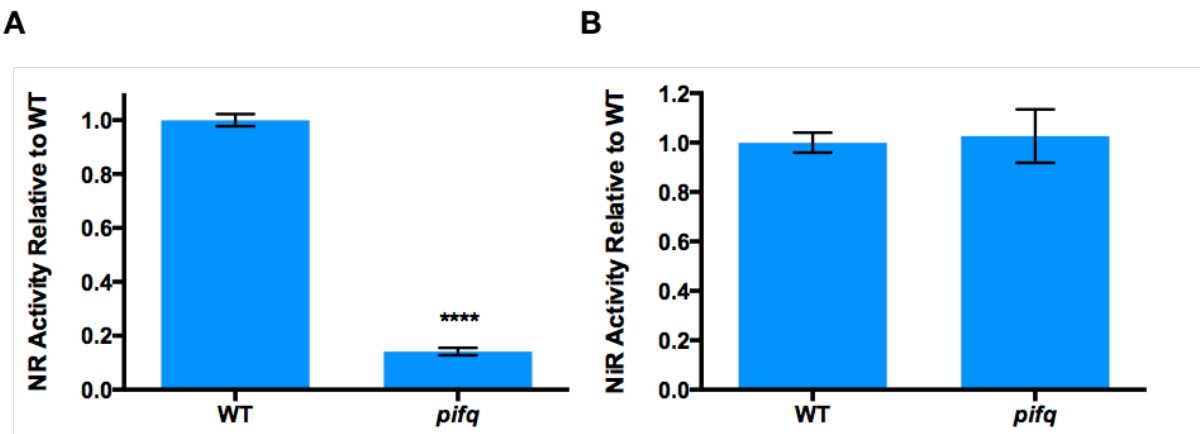


Figure 4.5 Relative shoot nitrate and nitrite reductase activities in WT and *pifq*.
(A) The nitrate reductase activity in *pifq* mutant shoots is significantly lower than that of WT. Data are means ± s.d. (n = 4) and statistical analysis was performed with student's t-test. **** means $P \leq 0.0001$. The value of 1 corresponds to 10.09 nmol NO_2^- min^{-1} per unit protein (mg ml^{-1}). (B) No significant difference ($P \geq 0.05$) in shoot nitrite reductase activity was detected between WT and *pifq*. Data are means ± s.d. (n = 4), and statistical analysis was performed with student's t-test. The value of 1 corresponds to 1.50 nmol NO_2^- min^{-1} per unit protein (mg ml^{-1}). Rosette leaves of four-week old plants were harvested three hours after the onset of the light photoperiod (16-h light/8-h dark) for nitrate reductase activity assay (for full details see section 2.5).

4.2.3 The *pifq* mutation down-regulates *NIA2* mRNA abundance but does not detectably affect that of other nitrate metabolism-related genes

PIFs are nuclear transcription factors that directly bind to the promoter regions of their target genes at the G-box (CACGTG) or PIF binding E-box (PBE-box, CACATG and CATGTG) motifs (Hornitschek et al., 2012, Oh et al., 2012, Zhang et al., 2013). Therefore, it is reasonable to speculate that PIFs positively regulate nitrate reductase activity by promoting the expression of the nitrate reductase genes, *NIA1* and *NIA2*. To test this hypothesis, an *in silico* motif search was first performed for putative PIF binding sites within the region of DNA ≤ 5,000 bp 5' of the start codons of *NIA1* and *NIA2* to account for possible long-distance binding sites. The promoter regions were chosen to be scanned because the majority of PIF3 binding sites (89%) are reported to be present in intergenic regions rather than coding sequences, introns or UTRs (Zhang et al., 2013). As shown in Table 4.1 and Figure 4.6, potential PIF bindings sites are

present in both *NIA1* and *NIA2* promoter regions, with the *NIA1* promoter harbouring two G-box and five PBE-box motifs, and the *NIA2* promoter harbouring a G-box and a PBE-box motif.

Table 4.1 Motif search result for putative PIF binding sites.

PIF Putative Binding Sites	Location Relative to the ATG Start Codon of the Gene	
	NIA1	***NIA2***
G-Box (CACGTG)	-1,500; -2,846	-3,069
PBE-Box 1 (CACATG)	-2,026; -2,327; -2,387	-4,245
PBE-Box 2 (CATGTG)	-838; -3,621	\

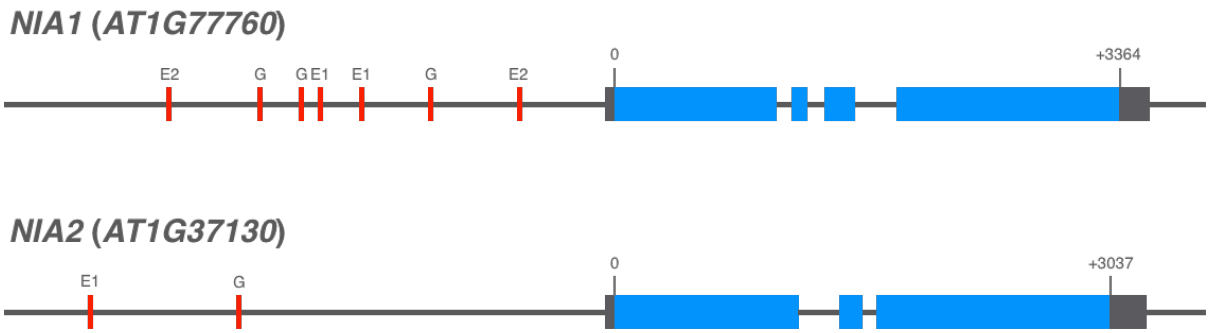


Figure 4.6 Positions of the putative PIF binding sites in the promoter regions of *NIA1* and *NIA2*.
Schematic representation of the gene structures of *NIA1* and *NIA2* and the positions of the putative PIF binding sites within the 5,000 bp 5' promoter region. 5' and 3' untranslated regions (UTRs) are represented by grey boxes. Exons are represented by blue boxes. Lines connecting exons represent introns whereas lines outside of 5' and 3' UTRs are promoter or intergenic regions. Numbers indicate the positions of the start codons and stop codons. G, G-box motifs (CACGTG); E1, PBE-box 1 motifs (CACATG); E2, PBE-box 2 motifs (CATGTG). This diagram is not drawn to scale.

RT-qPCR was performed for three major nitrate transporter genes (*NRT1.1*, *NRT2.1* and *NRT2.2*), the nitrate reductase genes (*NIA1* and *NIA2*) and the nitrite reductase gene (*NIR1*) for WT and *pifq* mutant plants. The only significant difference in transcript abundance was detected for *NIA2*, which encodes the major nitrate reductase protein in shoots (Wilkinson and

Crawford, 1991), with *pifq* having a reduced mRNA abundance compared to WT (Figure 4.7). Semi-quantitative RT-PCR performed for *NIA1*, *NIA2* and *NIR1* genes confirms that the *pifq* mutation clearly reduced *NIA2* mRNA abundance, without affecting that of the other two genes (Figure 4.8). Therefore, PIFs might promote *NIA2* gene expression and as a result, promote nitrate reductase activity.

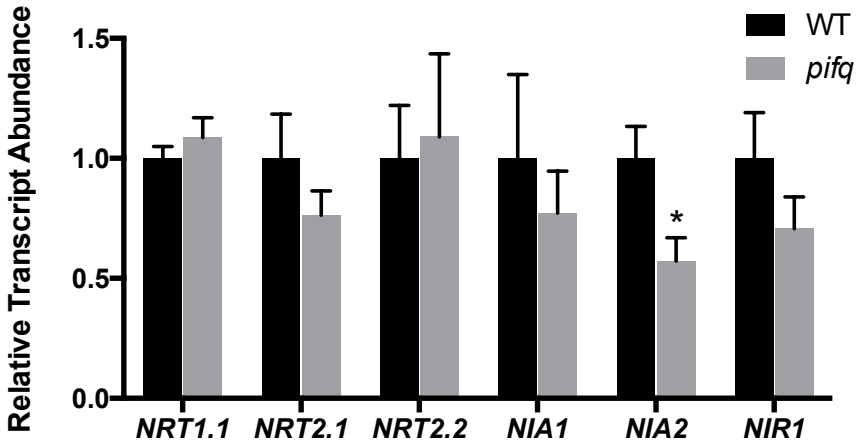


Figure 4.7 Relative abundances of mRNAs encoding major nitrate transporters, and nitrate reductase and nitrite reductase activities as measured using RT-qPCR.
Quantitative RT-qPCR showed a significant decrease in the expression level of *NIA2* in *pifq* versus WT. No difference in the abundances of *NRT1.1*, *NRT2.1*, *NRT2.2*, *NIA1*, or *NIR1* mRNAs was detected ($P \geq 0.05$). mRNA abundances were normalised to that of the internal control gene *Actin*. Data are means $\pm$ s.d. ($n = 4$ biological replicates of 3 technical replicates). Statistical analyses were performed with pairwise student's t-tests. * means $P \leq 0.05$. Ten-day old seedling roots and four-week old adult plant rosette leaves were collected three hours after the onset of the light photoperiod (16-h light/8-h dark) for RT-qPCR analysis (for full details see section 2.6).

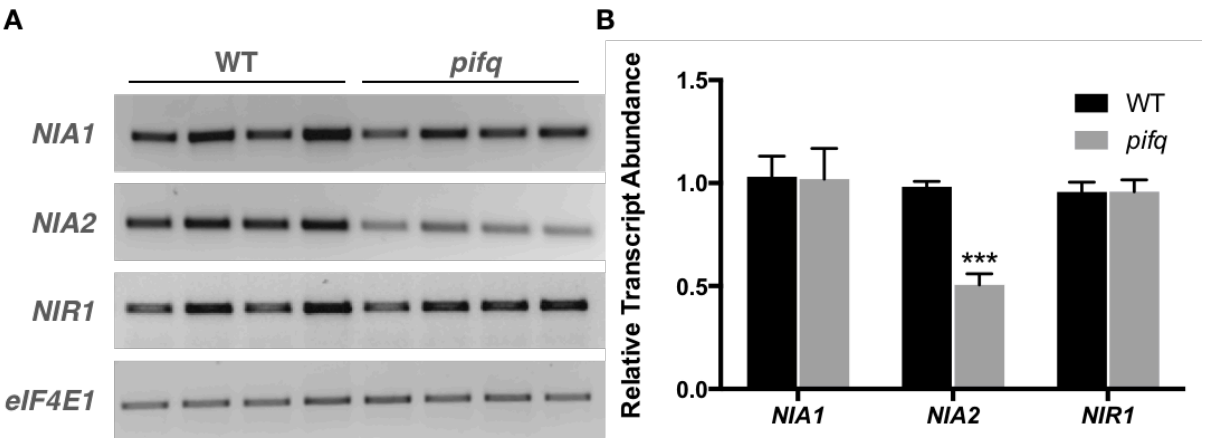


Figure 4.8 Abundances of mRNAs encoding nitrate reductase and nitrite reductase activities visualised using RT-PCR.
(A) mRNA abundances visualised using RT-PCR. DNA band was visualised using the BioSpectrum™ MultiSpectral Imgaing System (UVP) with the AC Chemi HR410 camera. (B) Quantification of transcript levels expressed as the relative band intensities (quantified with the VisionWorksLS software) normalised to that of the control gene *eIF4E1*. Statistical analyses were performed with pairwise student's t-tests. *** means $P \leq 0.001$. Semi-quantitative RT-PCR did not detect any obvious difference in the mRNA levels of *NIA1* or *NIR1*. On the other hand, mRNA abundance of *NIA2* was found to be significantly lower in *pifq* versus WT. *eIF4E1* gene was included as the internal control. Four biological replicates were included in this study. Rosette leaves of four-week old plants were harvested three hours after the onset of the light photoperiod (16-h light/8-h dark) for RT-PCR analysis (for full details see section 2.6).

4.2.4 Loss-of-function mutations of *PV42A* and *GRF7* do not confer detectably altered chlorate response compared to WT

In the original *nia2*/*chl3-5* mutant identified from the chlorate mutant screen, a complete deletion of the *NIA2* gene was found to result in a residue nitrate reductase activity of only 10% compared to WT (Wilkinson and Crawford, 1991). In this study, it was concluded that the *pifq* mutation leads to a similar degree of decrease (80–90%) in nitrate reductase activity as *nia2*, but only moderately affects the mRNA abundance of *NIA2* (~50% decrease in *pifq*). Therefore, it is speculated that PIFs might additively regulate the transcription of genes responsible for post-translational modifications of nitrate reductase. Making use of an available transcriptome analysis on GENEVESTIGATOR (Hruz et al., 2008) for *pifq* versus WT seedlings growing in

continuous white light (Leivar et al., 2009), two promising genes out of 234 were identified whose mRNA abundances are upregulated in *pifq*, *PV42A*, which encodes the SNF1-related protein kinase (SnRK1) regulatory subunit gamma-like PV42a, and *GENERAL REGULATORY FACTOR7* (*GRF7*), which encodes the 14-3-3 protein isoform nu (ν). Members of the SnRK1 family have been proposed to phosphorylate nitrate reductase and therefore inhibiting its activity (Sugden et al., 1999, Ikeda et al., 2000), and the *GRF7*-encoded 14-3-3 isoform ν has actually been shown to bind to and inhibit the activity of phosphorylated NR *in vitro* (Lambeck et al., 2010). Therefore, chlorate toxicity assay was performed for the knock-out mutants of these genes (*pv42a* and *grf7*) to determine if the repression of nitrate reductase activity conferred by *pifq* is contributed by the increased abundances of mRNAs encoding either or both of these two proteins. Unfortunately, neither of these mutants are detectably more sensitive to chlorate toxicity than WT, as would be expected if nitrate reductase activity is increased in these mutants (Figure 4.9).

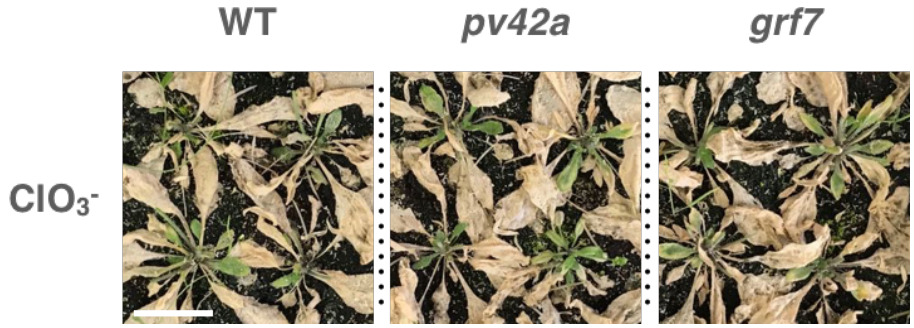


Figure 4.9 Chlorate responses of WT, *pv42a* and *grf7* mutant plants.
WT, *pv42a* and *grf7* mutant plants exhibited similar phenotypes upon chlorate treatment. All plants were germinated on agarose before being transplanted to soil and grown at 22–24 °C under 16-h light/8-h dark photoperiod (irradiance 120 μmol of photons/m^2 per second). Four-week old plants were watered with 1.5 mM chlorate to soil saturation, which was repeated every five days (for full details see section 2.4.1). Photos of the plants were taken three weeks after the first chlorate treatment. Scale bar = 3 cm.

4.2.5 *pif3* is majorly responsible for the *pifq*-conferred chlorate resistance and reduction in nitrate reductase activity.

Based on the observations described above, it would be interesting to determine whether the four members of the PIFq family redundantly regulate nitrate reductase activity, or if a subset of the family predominates in this regulation. To answer this question, single *pif* knock-out mutants were treated with chlorate. It was found that *pif3* was the only single *pif* knock-out mutant exhibiting a similar degree of chlorate resistance to *pifq*, with the chlorate responses of the other *pif* mutants being not detectably different from that of WT (Figure 4.10). Therefore, the *pifq*-conferred resistance to chlorate toxicity is mainly attributable to the *pif3* loss-of-function mutation.

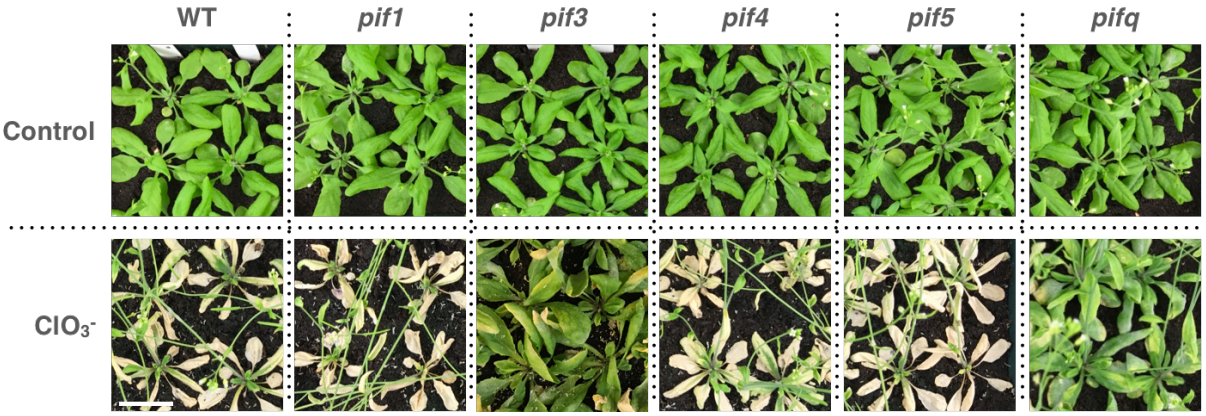


Figure 4.10 Chlorate responses of WT, *pifq* and the four single *pif* knock-out mutants. *Arabidopsis pif1*, *pif4* and *pif5* mutant plants were as sensitive to chlorate toxicity as WT, whilst *pif3* and *pifq* exhibited similarly strong chlorate resistance phenotypes, suggesting that the *pif3* mutation in *pifq* is largely responsible for the *pifq*-mediated chlorate resistance. All plants were germinated on agarose before being transplanted to soil and grown at 22–24 °C under 16-h light/8-h dark photoperiod (irradiance 120 µmol of photons/m^2 per second). Four-week old plants were watered with 1.5 mM chlorate to soil saturation, which was repeated every five days (for full details see section 2.4.1). Photos of the plants were taken two weeks after the first chlorate treatment. Scale bar = 3 cm.

The next experiments sought to determine if the reduction in shoot nitrate reductase activity conferred by *pifq* is also largely due to the *pif3* mutation. The results clearly indicate that the *pif3* mutation alone can reduce nitrate reductase activity to a level similar to that of *pifq*, whilst the other single *pif* mutations do not significantly affect nitrate reductase activity (Figure 4.11). Overall, these results suggest that among the PIFq members, PIF3 plays the predominant, and possibly unique, role in positively regulating nitrate reductase activity.

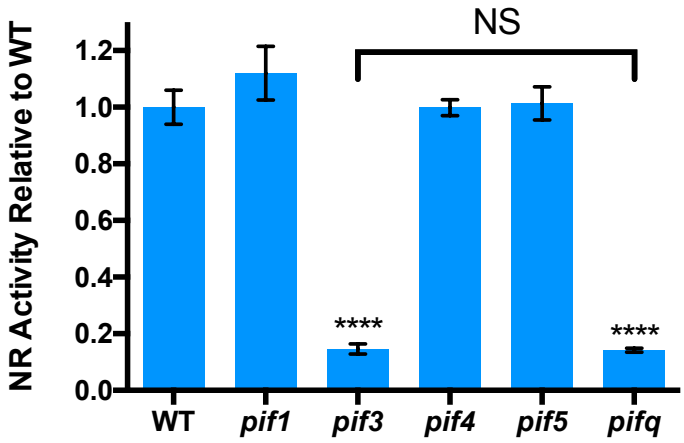


Figure 4.11 Relative shoot nitrate reductase activities in WT, *pifq*, and the four *pif* single mutants.
The nitrate reductase activities in shoots of both *pif3* and *pifq* are significantly lower than that of WT. No significant difference ($P \geq 0.05$) in shoot nitrate reductase activity was found among WT, *pif1*, *pif4* and *pif5* mutants, as well as between *pif3* and *pifq* mutants. Data are means ± s.d. (n = 3) and statistical analysis was performed with pairwise student's t-test. **** means $P \leq 0.0001$. NS, not significant ($P \geq 0.05$). The value of 1 corresponds to 10.55 nmol NO_2^- min^{-1} per unit protein (mg ml^{-1}). Rosette leaves of four-week old plants were harvested three hours after the onset of the light photoperiod (16-h light/8-h dark) for nitrate reductase activity assay (for full details see section 2.5).

4.2.6 Overexpression of *PIF3* in the *pif3* mutant complements *pif3*-mediated phenotypes

In order to further confirm the role played by PIF3 in regulating nitrate reductase activity, a line overexpressing *PIF3* in the *pif3* mutant background (*PIF3OX*/*pif3*; as described in Ni et

al., 2013) was acquired. RT-qPCR verifies that *PIF3* is indeed overexpressed in *PIF3OX*/*pif3*, and shows that *PIF3* mRNA abundance is approximately twice as high as in WT (Figure 4.12).

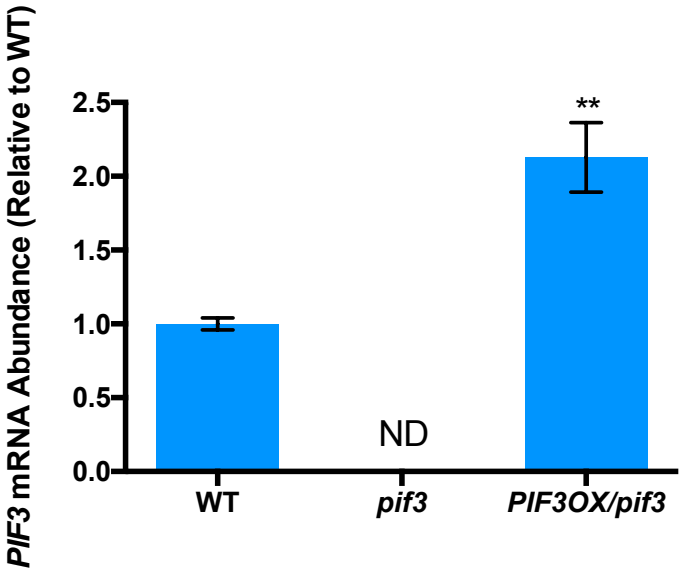


Figure 4. 12 Relative *PIF3* mRNA abundances in WT, *pif3* and *PIF3OX*/*pif3*.
Quantitative RT-qPCR confirms that *PIF3* is not expressed in the *pif3* loss-of-function mutant, and is overexpressed in *PIF3OX*/*pif3* to a level twice as high as that in WT. mRNA abundances were normalised to that of the internal control gene *Actin*. Data are means ± s.d. (n = 4 biological replicates of 3 technical replicates). Statistical analysis was performed with pairwise student's t-tests. ** means $P \leq 0.01$. ND, not detectable. Rosette leaves of four-week old plants were harvested three hours after the onset of the light photoperiod (16-h light/8-h dark) for RT-qPCR analysis (for full details see section 2.6).

A chlorate toxicity assay performed on WT, *pif3* and *PIF3OX*/*pif3* plants indicates that overexpression of *PIF3* in the *pif3* mutant background complements *pif3*-mediated chlorate resistance (Figure 4.13). Furthermore, *PIF3OX*/*pif3* mutant plants are slightly more sensitive to chlorate toxicity than WT (Figure 4.13). In addition, *PIF3* overexpression restores *pif3* nitrate reductase activity to a level similar to that of WT (Figure 4.14). Taken together, these results strengthened the conclusion that PIF3 is a positive regulator of nitrate reductase activity.

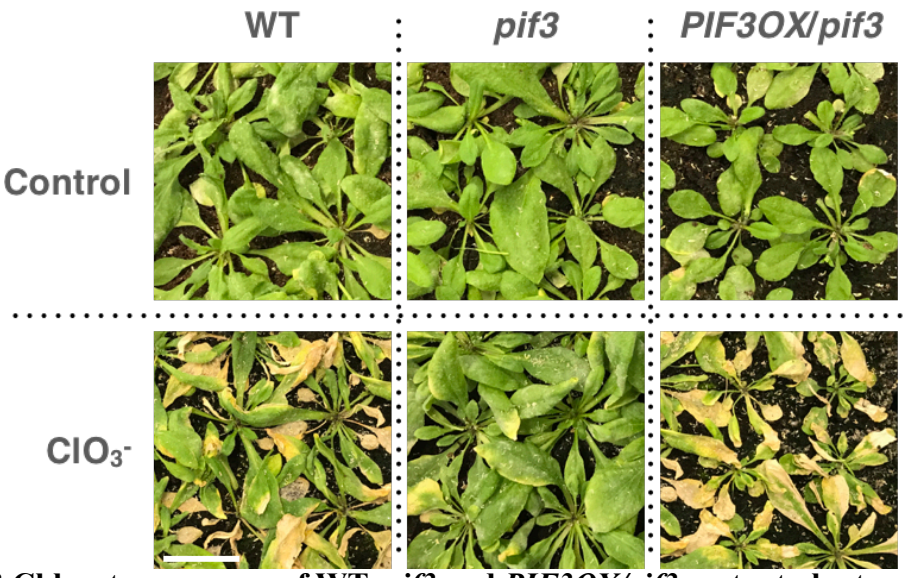


Figure 4.13 Chlorate responses of WT, *pif3* and *PIF3OX/pif3* mutant plants.
The overexpression of *PIF3* complements the *pif3*-mediated chlorate resistance phenotype. *PIF3OX*/*pif3* plants appear even slightly more sensitive to chlorate toxicity than WT. All plants were germinated on agarose before being transplanted to soil and grown at 22–24 °C under 16-h light/8-h dark photoperiod (irradiance 120 µmol of photons/m^2 per second). Four-week old plants were watered with 1.5 mM chlorate to soil saturation, which was repeated every five days (for full details see section 2.4.1). Photos of the plants were taken two weeks after the first chlorate treatment. Inflorescence stems were removed to facilitate the observation of chlorate responses. Scale bar = 3 cm.

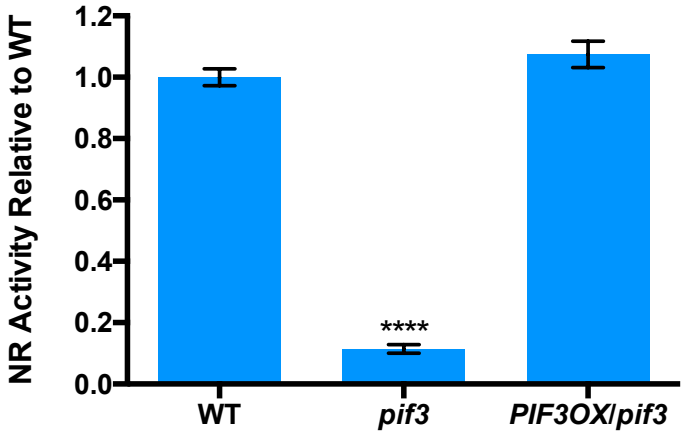


Figure 4.14 Relative shoot nitrate reductase activities in WT, *pif3* and *PIF3OX/pif3*.
The overexpression of *PIF3* complements the *pif3*-mediated reduction in nitrate reductase activity. The difference between the nitrate reductase activities of WT and *PIF3OX/pif3* is not statistically significant ($P \geq 0.05$). Data are means ± s.d. (n = 3) and statistical analysis was performed with pairwise student's t-test. **** means $P \leq 0.0001$. The value of 1 corresponds to 10.27 nmol NO_2^- min^{-1} per unit protein (mg ml^{-1}). Rosette leaves of four-week old plants were harvested three hours after the onset of the light photoperiod (16-h light/8-h dark) for nitrate reductase activity assay (for full details see section 2.5).

4.2.7 PIF4 does not play a significant role in regulating nitrate assimilation

Since PIF4 has previously been proposed as a negative regulator of nitrate reductase activity (Jonassen et al., 2009), chlorate responses and nitrate reductase activities of WT, *pif4*, and a line overexpressing *PIF4* in the *pif4* mutant background *(PIF4OX/pif4*; as described in Pfeiffer et al., 2014) were investigated further. Consistent with our previous observations, the *pif4* mutation did not result in any detectable difference in chlorate response or nitrate reductase activity versus WT plants (Figure 4.15). Similarly, the *PIF4* overexpression line exhibited a similar phenotype in response to chlorate as seen in WT and *pif4*, and has an apparently unchanged nitrate reductase activity (Figure 4.15). Therefore, it is concluded that PIF4 does not regulate nitrate assimilation, at least under the current experimental conditions.

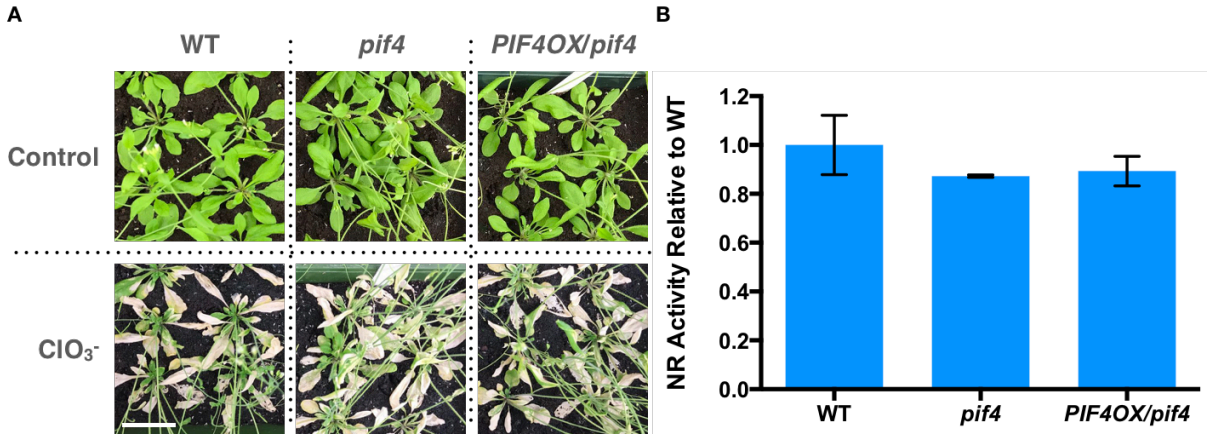


Figure 4.15 Chlorate responses and relative shoot nitrate reductase activities of WT, *pif4* and *PIF4OX*/*pif4*.

(A) WT, *pif4* and *PIF4OX*/*pif4* mutant plants exhibited similar phenotypes upon chlorate treatment. All plants were germinated on agarose before being transplanted to soil and grown at 22–24 °C under 16-h light/8-h dark photoperiod (irradiance 120 µmol of photons/m^2 per second). Four-week old plants were watered with 1.5 mM chlorate to soil saturation, which was repeated every five days (for full details see section 2.4.1). Photos of the plants were taken two weeks after the first chlorate treatment. Scale bar = 3 cm. (B) No significant difference ($P \geq 0.05$) was found in shoot nitrate reductase activity among WT, *pif4* and *PIF4OX*/*pif4* plants. Data are means ± s.d. (n = 3) and statistical analysis was performed with pairwise student's t-tests. The value of 1 corresponds to 10.04 nmol NO_2^- min^{-1} per unit protein (mg ml^{-1}). Rosette leaves of four-week old plants were harvested three hours after the onset of the light photoperiod (16-h light/8-h dark) for nitrate reductase activity assay (for full details see section 2.5).

4.2.8 PIF2 and PIF6 do not play a significant role in regulating nitrate assimilation

Next, we investigated whether the other four PIF members (PIF2, PIF6, PIF7 and PIF8) that are not part of the PIFq family regulate nitrate metabolism. Contrary to most other PIFs, PIF2 and PIF6 are positive regulators of plant photomorphogenesis (Penfield et al., 2010, Luo et al., 2014). However, PIF2 and PIF6 both seem not to be involved in the regulation of nitrate metabolism, since both *pif2* and *pif6* mutants displayed similar levels of chlorate sensitivity and nitrate reductase activity as WT plants (Figure 4.16).

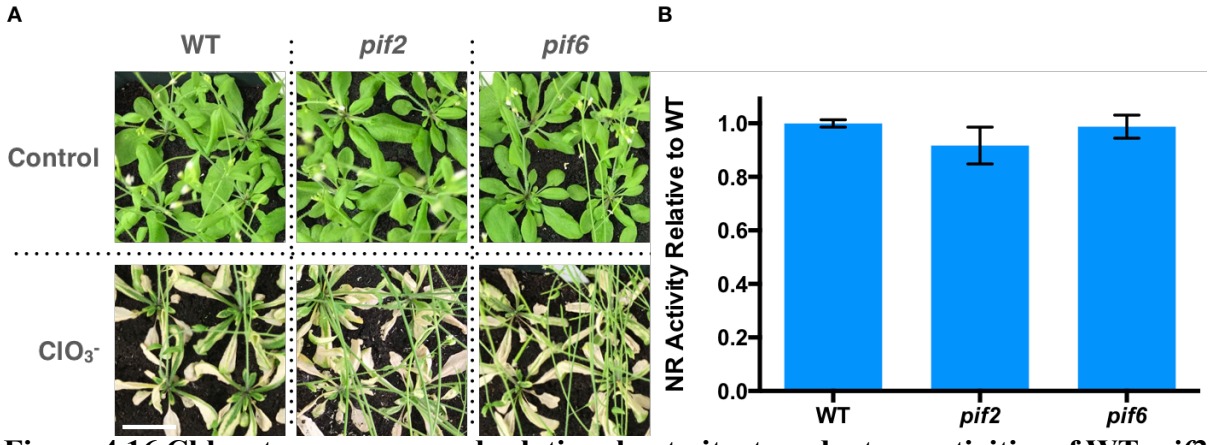


Figure 4.16 Chlorate responses and relative shoot nitrate reductase activities of WT, *pif2* and *pif6*.

(A) WT, *pif2* and *pif6* mutant plants exhibited similar phenotypes upon chlorate treatment. All plants were germinated on agarose before being transplanted to soil and grown at 22–24 °C under 16-h light/8-h dark photoperiod (irradiance 120 µmol of photons/m^2 per second). Four-week old plants were watered with 1.5 mM chlorate to soil saturation, which was repeated every five days (for full details see section 2.4.1). Photos of the plants were taken two weeks after the first chlorate treatment. Scale bar = 3 cm. (B) No significant difference ($P \geq 0.05$) was found in shoot nitrate reductase activity among WT, *pif4* and *PIF4OX*/*pif4* plants. Data are means ± s.d. (n = 3) and statistical analysis was performed with pairwise student's t-tests. The value of 1 corresponds to 10.59 nmol NO_2^- min^{-1} per unit protein (mg ml^{-1}). Rosette leaves of four-week old plants were harvested three hours after the onset of the light photoperiod (16-h light/8-h dark) for nitrate reductase activity assay (for full details see section 2.5).

4.2.9 The *pif7* mutant exhibited an intermediate level of chlorate resistance between WT and the *pifq* mutant without detectably affecting nitrate reductase activity

Intriguingly, the *pif7* loss-of-function mutant was identified as being moderately more resistant to chlorate toxicity than WT. When grown together with WT and *pifq* mutant plants, *pif7* mutant plants displayed an intermediate level of chlorate resistance that is consistently milder than that of *pifq*, but clearly greater than that of WT (Figure 4.17A). Accordingly, leaf chlorophyll measurements indicate that the extent of decrease in chlorophyll content upon chlorate treatment in *pif7* was smaller than WT but greater than *pifq* (Figure 4.17B).

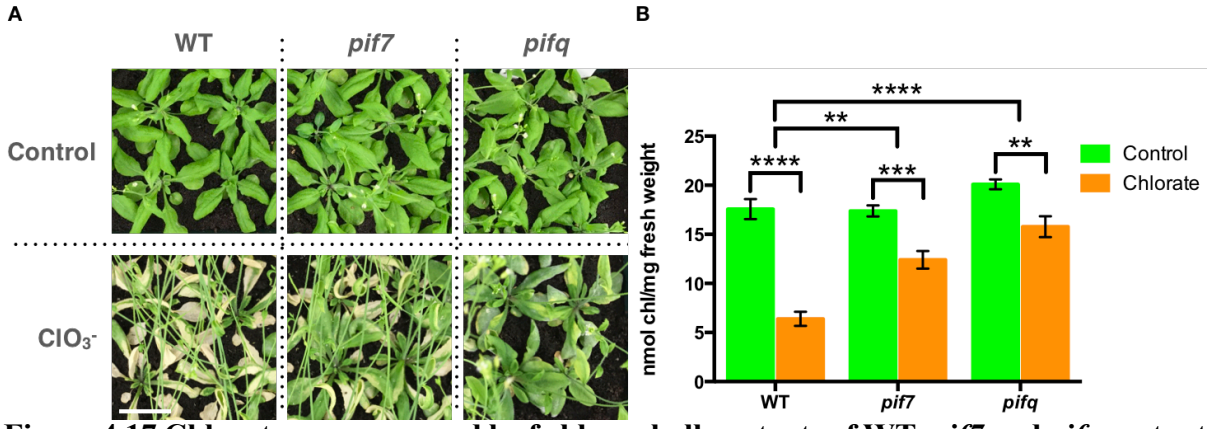


Figure 4.17 Chlorate responses and leaf chlorophyll contents of WT, *pif7* and *pifq* mutant plants.

(A) *Arabidopsis pif7* mutant plants are more resistant to chlorate toxicity than WT plants, but less resistant than *pifq* mutant plants. All plants were germinated on agarose before being transplanted to soil and grown at 22–24 °C under 16-h light/8-h dark photoperiod (irradiance 120 µmol of photons/m^2 per second). Four-week old plants were watered with 1.5 mM chlorate to soil saturation, which was repeated every five days (for full details see section 2.4.1). Photos of the plants were taken two weeks after the first chlorate treatment. Scale bar = 3 cm. (B) Leaf chlorophyll measurement confirms the intermediate level of chlorate resistance conferred by the *pif7* mutation. Chlorophyll measurements were taken from fully-expanded rosette leaves two weeks after the first chlorate treatment (for full details see section 2.4.3). Data are means ± s.d. (n = 10). Statistical analysis was performed with two-way ANOVA. ** means $P \leq 0.01$, *** means $P \leq 0.001$, and **** means $P \leq 0.0001$.

Following the previously established workflow, grafting was then performed to determine if *pif7*-conferred chlorate resistance is dependent on shoot, root or both. As shown in Figure 4.18A, the graft chimeras with either *pif7* shoot or *pif7* root seemed to be mildly more resistant to chlorate than the WT/WT chimeras, with the *pif7*/WT exhibiting a greater resistance than WT/*pif7*. Therefore, chlorate resistance conferred by the *pif7* mutation appears to be largely shoot-dependent, but to a lesser extent dependent on the root as well. However, a difference in shoot nitrate reductase activity between WT and *pif7* was not detected (Figure 4.18B), suggesting that the *pif7* mutation might cause chlorate resistance through another unknown mechanism.

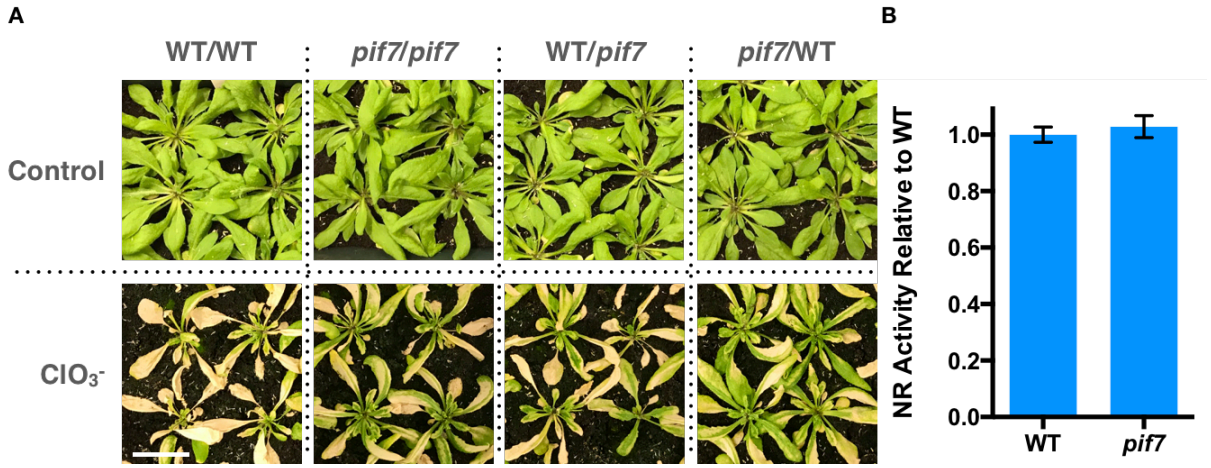


Figure 4.18 Chlorate responses of graft chimeras made by exchanging shoots and roots of WT and *pif7* mutant plants, and relative nitrate reductase activities of WT and *pif7*. (A) Control grafts, WT/WT and *pif7*/*pif7*, remained respectively sensitive and relatively resistant to chlorate. The graft chimeras with *pif7* mutant shoot remained resistant to chlorate, and those with *pif7* mutant root are also moderately chlorate resistant, suggesting that *pif7*-mediated chlorate resistance is dependent on both shoot and root tissues. All graft chimeras were constructed at seedling stage, transplanted to soil after recovery, and grown at 22–24 °C under 16-h light/8-h dark photoperiod (irradiance 120 µmol of photons/m^2 per second, for full details see section 2.3). Four-week old plants were watered with 1.5 mM chlorate to soil saturation, which was repeated every five days (for full details see section 2.4.1). Photos of the plants were taken two weeks after the first chlorate treatment. Inflorescence stems were removed to facilitate the observation of chlorate responses. Scale bar = 3 cm. (B) No significant difference ($P \geq 0.05$) was found in shoot nitrate reductase activity between WT and *pif7*. Data are means ± s.d. (n = 3) and statistical analysis was performed with student's t-test. The value of 1 corresponds to 10.55 nmol NO_2^- min^{-1} per unit protein (mg ml^{-1}). Rosette leaves of four-week old plants were harvested three hours after the onset of the light photoperiod (16-h light/8-h dark) for nitrate reductase activity assay (for full details see section 2.5).

4.2.10 The *pif8* mutant is resistant to chlorate without detectably affecting nitrate reductase activity

Finally, the involvement of PIF8, the least characterised PIF member in *Arabidopsis*, in the regulation of nitrate metabolism was investigated. Whereas all other *pif* mutants described above have been published previously, the *pif8* mutant used in this study has not been described in previous literatures to our knowledge. The *pif8* mutant line selected is in the *Ler* ecotype background with a 670 bp insertion at the start of the second exon (Figure 4.19A), which presumably would lead to a loss-of-function *pif8* mutation. This *pif8* mutant is the only *pif*

mutant in this study that exhibited a clear phenotypic difference with respect to plant growth and development under our experimental conditions. Specifically, *pif8* mutant plants exhibited bigger rosette sizes and sturdier inflorescence stems than WT, and were late flowering yet only slightly shorter than WT at adult stage (Figure 4.19B&C and Figure 4.20A).

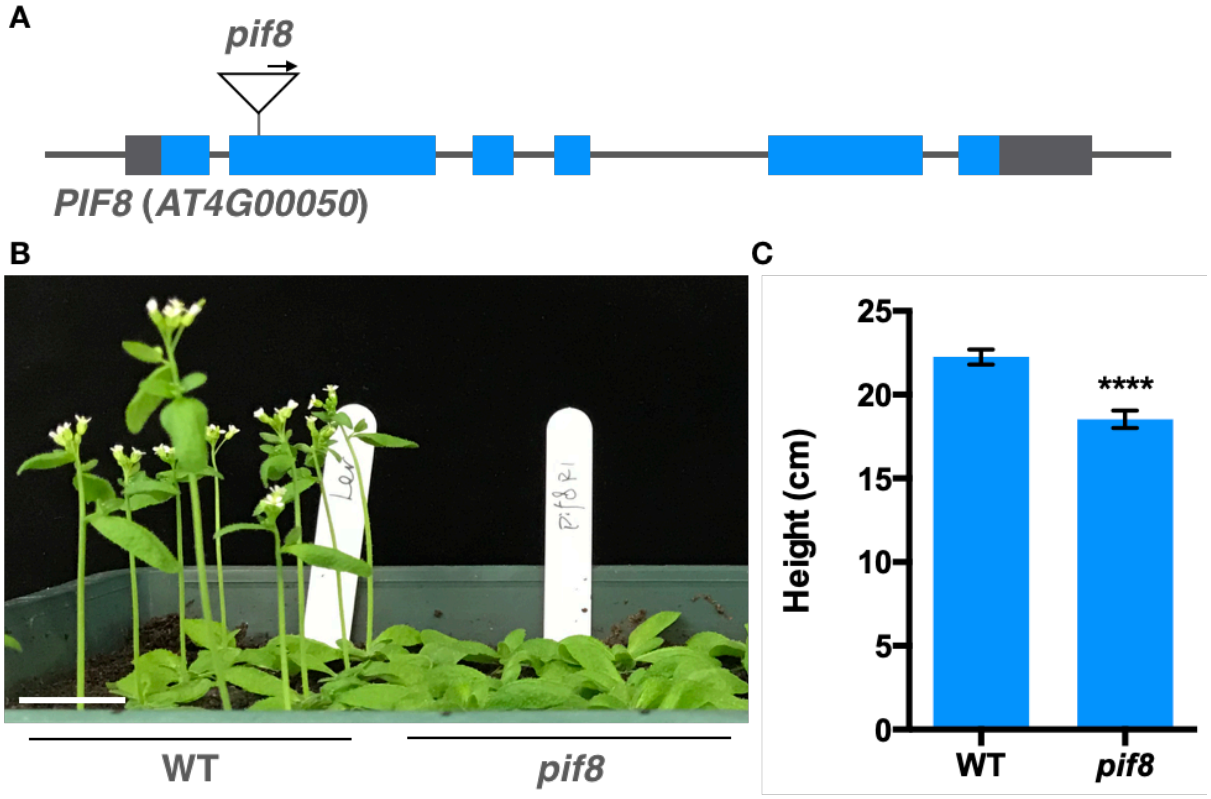


Figure 4.19 Phenotypic characterisation of the *pif8* mutant.
(A) Gene structure of *PIF8* and the position of the 670 bp insertion (indicated by the inverted triangle) in the *pif8* mutant used in this study. 5' and 3' untranslated regions (UTRs) are represented by grey boxes. Exons are represented by blue boxes. Lines connecting exons represent introns whereas lines outside of 5' and 3' UTRs are promoter or intergenic regions. (B) *pif8* mutant plants flowered at a later stage compared to WT (in *Ler* background). WT and *pif8* plants were germinated on agarose before being transplanted to normal F2 soil without chlorate and grown at 22–24 °C under 16-h light/8-h dark photoperiod (irradiance 120 µmol of photons/m^2 per second). Photo of the plants was taken when the plants were three-week old. Scale bar = 3 cm. (C) At adult stage (six-week old), *pif8* mutant plants are slightly but significantly shorter than WT. The lengths of the inflorescence stems of six-week old plants were recorded as a measurement of plant heights. Data are means ± s.d. (n = 15). Statistical analyses were performed with student's t-test. **** means $P \leq 0.0001$.

When treated with chlorate, *pif8* mutant plants exhibited a strong resistance to chlorate toxicity compared to WT (Figure 4.20A), suggesting that the *pif8* mutation somehow leads to compromised nitrate metabolism. However, *pif8*-mediated chlorate resistance was not due to reduced nitrate reductase activity like *pifq* or *pif3*, since no significant difference in nitrate reductase activity was detected between WT and *pif8* (Figure 4.20B). Therefore, similar to the case of PIF7, PIF8 is likely to be responsible for positively regulating nitrate metabolism, although the underlying mechanism of this regulation is not resolved at this stage.

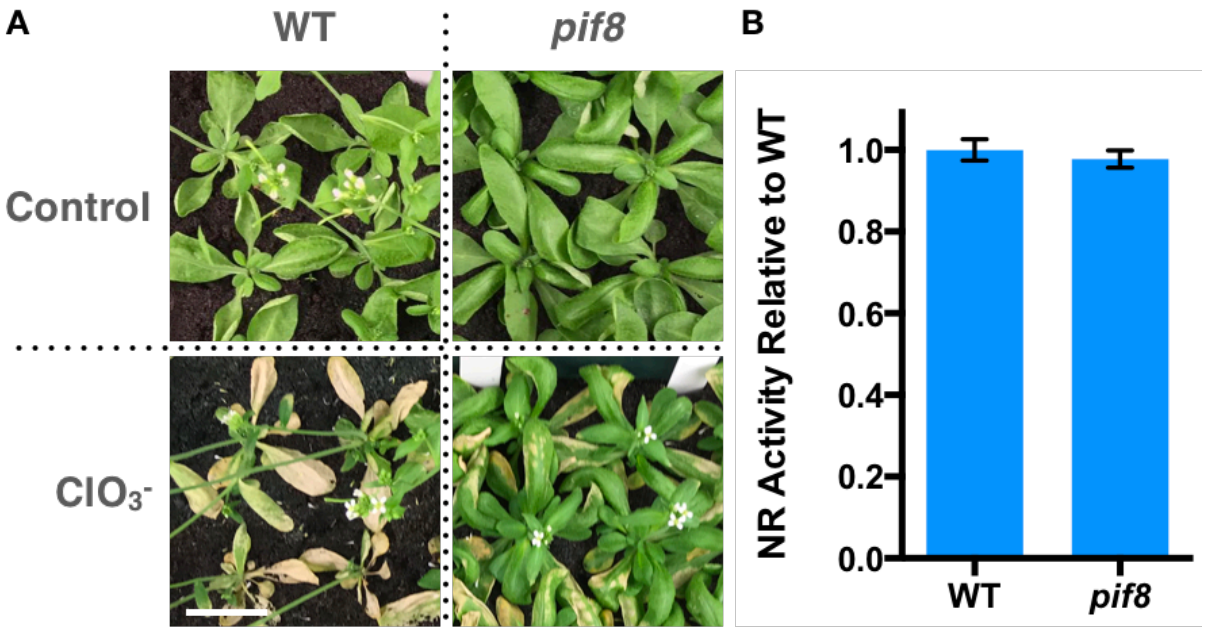


Figure 4.20 Chlorate responses and relative shoot nitrate reductase activities of WT and *pif8*.
(A) *Arabidopsis pif8* mutant plants are more resistant to chlorate toxicity compared to WT. Note also that *pif8* mutant plants have bigger rosette sizes than WT. All plants were germinated on agarose before being transplanted to soil and grown at 22–24 °C under 16-h light/8-h dark photoperiod (irradiance 120 µmol of photons/m^2 per second). Four-week old plants were watered with 1.0 mM chlorate to soil saturation, which was repeated every five days (for full details see section 2.4.1). Photos of the plants were taken two weeks after the first chlorate treatment. Scale bar = 3 cm. (B) No significant difference ($P \geq 0.05$) was found in shoot nitrate reductase activity between WT and *pif8*. Data are means ± s.d. (n = 4) and statistical analysis was performed with pairwise student's t-tests. The value of 1 corresponds to 9.17 nmol NO_2^- min^{-1} per unit protein (mg ml^{-1}). Rosette leaves of four-week old plants were harvested three hours after the onset of the light photoperiod (16-h light/8-h dark) for nitrate reductase activity assay (for full details see section 2.5).

4.3 Discussion

4.3.1 PIFs potentially link the GA-DELLA signalling pathway with nitrate metabolism

Light, in a similar fashion as nitrate, is not only metabolically important as it provides the energy for the most essential process in plants, photosynthesis; but also acts as a crucial signal dictating plant growth and development (Jiao et al., 2007). Red and far-red light signals are perceived by phytochromes (Phys) and transduced by a group of transcription factors called PIFs, resulting in an extensive transcriptome reprogramming (Castillon et al., 2007, Bae and Choi, 2008, Leivar and Quail, 2011). PIFs positively regulate plant skotomorphogenesis, a process regarded as critical for the evolution of land plants as it allows rapid growth of subterranean seedlings to reach light (Zhang et al., 2013). Therefore, it is not surprising that the Phy-PIF signalling pathway is widely conserved among land plants (Lee and Choi, 2017). In addition, an increasing amount of evidence indicates that PIFs are responsible for integrating light signal with other internal and external signalling pathways to modulate a wide variety of biological processes, essentially forming a complicated regulatory network (Leivar and Monte, 2014). The coordination of GA-DELLA and PIF signalling is among one of the most well-established example of crosstalk between phytohormones and PIFs, where DELLAs have been shown to antagonise PIF activities through the additive effect of PIF sequestration and degradation (Li et al., 2016).

In Chapter 3, it was found that DELLAs negatively regulate plant nitrate metabolism through inhibiting shoot nitrate reductase activity. This regulation can be reverted by DELLA degradation as the *gai-t6* loss-of-function mutation results in an increased nitrate reductase

activity. In an attempt to identify the missing link between DELLAs and nitrate metabolism, PIFs were chosen to be investigated to see if they act upstream of nitrate reductase activity, not only because they are known to interact with DELLAs, but also because PIF4 has previously been suggested to repress nitrate reductase activity through transcriptional regulation (Jonassen et al., 2009).

The quadruple loss-of-function mutant, *pifq*, was studied initially because PIFq members have been known to redundantly regulate biological processes such as skotomorphogenesis (Leivar et al., 2008, Shin et al., 2009). Unexpectedly, a strong chlorate resistance phenotype was exhibited by the *pifq* mutant plants. The chlorate resistance conferred by *pifq* is clearly shoot- rather than root-dependent, which is consistent with the fact that all four PIFq members are expressed at a higher level in vegetative shoot tissue than in root (Jeong and Choi, 2013). Subsequently, the *pifq* mutant was found to have a dramatically reduced nitrate reductase activity. Therefore, at least one PIF member of the PIFq quartet is involved in positively regulating nitrate metabolism. The striking similarities between the conclusions drawn from *gai* and *pifq* experiments led to the hypothesis that DELLAs negatively regulate nitrate metabolism through opposing PIF-mediated activation of nitrate reductase activity.

4.3.2 PIFs regulate nitrate reductase activity at least partially through transcriptional regulation

PIFs are transcription factors that activate or repress gene expression by binding to target promoters (Hornitschek et al., 2012, Oh et al., 2012, Zhang et al., 2013). RT-PCR and RT-qPCR experiments performed in this study suggest that the mRNA abundances of the three major nitrate transporter genes (*NRT1.1*, *NRT2.1* and *NRT2.2*) and of the nitrite reductase gene

NIR1 are not affected in *pifq*. Although putative PIF binding sites (G-box and PBE-box) were identified in the promoter regions of both *NIA1* and *NIA2*, only *NIA2* mRNA abundance was found to be reduced significantly in the *pifq* mutant. The downregulation of *NIA2* transcript level can potentially explain the reduced nitrate reductase activity, but contradicts a previous transcriptome analysis suggesting a doubling in *NIA2* transcript abundance in *pifq* compared to WT (Shin et al., 2009). This discrepancy is possibly due to the fact that Shin et al., 2009 performed the transcriptome analysis using WT and *pifq* seedlings growing in the dark, whereas adult plants growing under long-day photoperiod light regime were used in this study. Nevertheless, whether or not PIFs actually recognise these motifs and thereby affect mRNA abundance should be further investigated with, for example, chromatin immunoprecipitation (ChIP) analysis and/or electrophoretic mobility shift assay (EMSA) technique.

Given the relatively small reduction in *NIA2* mRNA abundance versus the dramatic decrease in nitrate reductase activity of *pifq* compared to WT, possibility of the upregulated transcript abundances of *PV42A* or *GRF7* in the *pifq* mutant (Leivar et al., 2009) contributing to the post-translational inhibition of nitrate reductase activity was explored. The *PV42A* gene was chosen because a subset of the SnRK1 family proteins have been shown to phosphorylate nitrate reductase preceding its full inhibition, although the only known function of *Arabidopsis PV42A* is to regulate male gametogenesis and pollen tube guidance (Sugden et al., 1999, Ikeda et al., 2000, Fang et al., 2011). On the other hand, the *GRF7*-encoded 14-3-3 isoform ν was found to suppress the activity of phosphorylated NR *in vitro* with a high inhibition strength (I_{max} = 85%) despite an intermediate binding affinity (K_i = 230 nM), amongst the eight *Arabidopsis* 14-3-3 isoforms investigated (Lambeck et al., 2010).

However, the loss-of-function mutants of either of these two genes are not detectably more sensitive to chlorate toxicity than WT plants. Therefore, *pifq*-mediated chlorate resistance might not be attributable to the upregulation of *PV42A* and/or *GRF7* gene expression. On the other hand, the regulation of *Arabidopsis* reproductive development is redundantly regulated by PV42A and its homologous protein PV42B (Fang et al., 2011), and the 14-3-3 proteins are generally considered to be present in saturation in eukaryotes (with the total abundance constituting up to 1% of the proteome; Boston et al., 1982, Pawson and Scott, 1997, Swatek et al., 2011, Chi et al., 2015). Hence, the loss-of-function mutation of *pv42a* or *grf7* alone might not produce an observable phenotype upon chlorate treatment. Future studies are necessary to clarify the functional connection between the upregulation of these two genes in *pifq* and its compromised nitrate metabolism.

Alternatively, various transcriptome analyses have confirmed that PIFs are high hierarchical regulators whose major targets are other transcription factors involved in diverse signalling pathways (Shin et al., 2009, Leivar et al., 2009, Leivar et al., 2012b, Hornitschek et al., 2012, Zhang et al., 2013). Therefore, PIFs might exert an indirect effect on nitrate reductase activity regulation through the integration with another signalling pathway. Last but not least, it is perhaps more appropriate in this case to perform a transcriptome analysis for *pifq* versus WT plants at the adult developmental stage, as it corresponds to the age of the plants in our experimental settings and might reveal more relevant candidate genes that are differentially regulated in the *pifq* mutant.

4.3.3 PIF3, among the PIFq members, plays the predominant role in regulating nitrate reductase activity

Since PIFs have both shared and distinct functions, *pifq*-mediated repression of shoot nitrate reductase activity and the consequent chlorate resistance may be due to the additive effect of the loss-of-function of the four PIFq members. However, chlorate toxicity assay indicates that only *pif3* mutant plants exhibited a chlorate resistance phenotype similar to that of *pifq*, whereas the other three single *pif* mutants are as sensitive to chlorate as WT. Additionally, the *pif3* mutation alone is capable of decreasing shoot nitrate reductase activity to a level similar to that of *pifq*. These observations imply that, similarly to PIF1 predominantly regulating seed germination and PIF4 predominantly regulating plant thermomorphogenesis etc. (Jeong and Choi, 2013), PIF3 is the member of the PIFq family that predominantly regulates nitrate metabolism. At this point, the apparent discrepancy between this study and the one conducted by Jonassen et al., 2009 with regard to the *pif4* loss-of-function mutant needs to be addressed. Jonassen et al., 2009 discovered a 50% increase in nitrate reductase activity in the *pif4* mutant compared to WT at the seedling stage under red light. In addition, the nitrate reductase activity of *pif4* rosette leaves that have been grown in darkness for 72 hours followed by red light exposure for 4 hours is also higher than WT rosette leaves under the same treatment (Jonassen et al., 2009). In our study, however, no difference in nitrate reductase activity between *pif4* and WT was detected, nor did we observe an increased sensitivity to chlorate exhibited by *pif4* mutant plants as expected from an increased nitrate reductase activity. It is plausible that these discrepancies are due to the developmental stages of the plants and the growth conditions used in the two studies, since Jonassen et al., 2009 in turn did not detect any difference in nitrate reductase activity between WT and the *pif3* mutant.

The PIF3 overexpression line in the *pif3* mutant background (*PIF3OX*/*pif3*), whose *PIF3* transcript abundance is twice as high as that of WT, resulted in a more sensitive chlorate response than both *pif3* and WT. This result strengthens the conclusion that PIF3 upregulates nitrate metabolism. Curiously, although the nitrate reductase activity of *PIF3OX*/*pif3* is unsurprisingly much higher than that of *pif3*, it is not significantly higher than that of WT, as would be expected from an increased PIF3 mRNA abundance. One plausible explanation for this observation is that the enzymatic activity of nitrate reductase is close to saturation at the time point when plant tissue was collected for nitrate reductase activity assay (shortly after the start of the photoperiod), and therefore the overexpression of *PIF3* is unable to increase the enzymatic activity any further. Meanwhile, the cumulative effect of PIF3 on nitrate reductase activity can be more accurately and clearly conveyed by the chlorate toxicity assay (Reed et al., 1992). It would be interesting to next investigate whether the abundances of mRNAs from the nitrate reductase genes are similarly affected in *pif3* as in *pifq*, and whether this regulation is opposed by *PIF3* overexpression.

Caution is necessary in interpreting the observations of PIF overexpression analyses for two main reasons. Firstly, ectopic expression of a particular PIF member might lead to a phenotype that is not regulated by the endogenous protein because of its restricted expression pattern. Secondly, PIFs, as bHLH transcription factors, function by homo- or heterodimerising with other bHLH proteins. The overexpression of PIFs, therefore, could potentially lead to an excess interaction with, and subsequently the sequestration of other bHLH proteins, resulting in a dominant negative effect. As an example, both of these complications have been proposed to explain the observation that the overexpression of PIF5 triggers ethylene overdose phenotypes whereas the *pif5* loss-of-function mutation caused no ethylene-related phenotypes (Khanna et al., 2007, Jeong and Choi, 2013, Paik et al., 2017). This study demonstrates that the

overexpression of *PIF4* did not affect either chlorate response of the plants or nitrate reductase activity. Further preliminary experiments with transgenic *Arabidopsis* lines overexpressing the other two *PIFq* members, *PIF1* and *PIF5*, from two independent sources (Khanna et al., 2007, Pfeiffer et al., 2014, Xie et al., 2017), also showed no effect on chlorate response or nitrate reductase activity (data not shown). Therefore, the above-described phenotypes resulted from *PIF3* overexpression are likely to be reflective of a genuine function of promoting nitrate reductase activity.

This study does not provide a definitive explanation as to what it is that enables PIF3 to be the unique PIFq protein regulating nitrate metabolism. The expression patterns of the PIFq members are largely overlapping in the shoot tissue. In fact, *PIF3* was found to have the lowest total transcript level among the *PIFq* members in most organs (Jeong and Choi, 2013). Therefore, the unique role played by PIF3 in nitrate metabolism cannot be explained by a differential expression pattern. Previous integrated ChIP-seq and RNA-seq analyses of WT, *pif3*, *pif1 pif4 pif5* and *pifq* dark grown seedlings indicate that 26% of PIF3-regulated genes are not targeted by the other three PIFs, although the nitrate reductase genes are not in this list of genes specifically regulated by PIF3 (Zhang et al., 2013). Furthermore, even when one or more PIFq proteins target the same gene, their quantitative contributions to its transcriptional regulation often vary enormously (Zhang et al., 2013). Adding another layer of complexity, a recent *in vivo* ChIP-chip microarray analysis for PIF1 DNA binding sites demonstrates that as much as 41% of PIF1-binding sites lack a canonical G-box motif (Kim et al., 2016). They found that PIF1 also binds to ACGT-containing GCE motifs in association with ABI5, a group A bZIP transcription factor (Kim et al., 2016). Similarly, it is possible that PIF3 also binds to specific binding elements of genes responsible for the promotion of nitrate metabolism through unique interactions with other transcription factors (Pham et al., 2018).

4.3.4 PIF2 and PIF6 do not detectably participate in the regulation of nitrate metabolism

Among all of the eight *Arabidopsis* PIF proteins, PIF2 and PIF6 are the only so-called "fruit PIFs" because of their higher transcript abundances in the flower and fruit organs compared to the root and the other shoot organs (Jeong and Choi, 2013). Moreover, PIF2 and PIF6 independently play an antagonistic role against the other PIFs with regard to the regulation of photomorphogenesis. PIF2 (recently renamed from PIL1), unlike most other PIF proteins, is degraded by COP1 and stabilised by interacting with PhyB, and consequently promotes rather than inhibits photomorphogenesis (Luo et al., 2014). *PIF2* gene expression is under positive regulation by PIFq members (Hornitschek et al., 2009, Zhang et al., 2013). The PIF2 protein, on the other hand, heterodimerises with an atypical bHLH transcription factor LONG HYPOCOTYL IN FAR-RED1 (HFR1) and additively represses the activities of members of the PIFq family, possibly through physical interactions (Luo et al., 2014).

There are two naturally-occurring splice variants of *PIF6* designated *PIF6-α* and *PIF6-β*, with the former encoding the full-length protein and the latter encoding a truncated PIF6 protein that retains the PhyB-interacting (APB) domain but lacks the DNA-binding bHLH domain (Penfield et al., 2010). Overexpression of *PIF6-β* but not *PIF6-α* promotes seed germination, whereas overexpression of either splice variants mildly activates photomorphogenesis (Penfield et al., 2010).

The chlorate toxicity and nitrate reductase activity assays performed in this study for the *pif2* and *pif6* loss-of-function mutants suggest that neither PIFs are involved in the regulation of nitrate metabolism. However, the possibility that their roles are masked by functional

redundancy shared by other factors cannot be ruled out. For example, PIF2 has been shown to interact with and therefore counter PIF3 (and other PIFq members) activity additively with HFR1, and the *pif2 hfr1* double mutant exhibits a more exaggerated mutant phenotype than either *pif2* or *hfr1* single mutant in terms of hypocotyl elongation (Luo et al., 2014). Therefore, it is worth including this double mutant in future studies as well as mutant lines overexpressing *PIF2* or *PIF6* genes to clarify their functional connections with nitrate metabolism.

4.3.5 PIF7 and PIF8 promote nitrate metabolism with unknown mechanisms

In response to red light, photoactivated PhyB migrates to the nucleus and interacts with PIF7. However, unlike PIFq proteins, which are degraded in response to this interaction, PIF7 is consequently converted into an inactivated form by phosphorylation (Leivar et al., 2008). PIF7 was shown to contribute moderately with PIF4 and PIF5 to promoting hypocotyl elongation under prolonged red-light treatment, whilst acting as the predominant regulator of shade avoidance responses with PIF3, PIF4 and PIF5 through activation of auxin biosynthesis (Leivar et al., 2008, Li et al., 2012a). Additionally, along with PIF4, PIF7 also regulates photoperiod-dependent plant freezing tolerance by repressing *CBF* gene expression (Lee and Thomashow, 2012).

PIF8 is the only *Arabidopsis* PIF protein whose function is largely uncharacterised. The *pif8* mutant, known as *UNFERTILISED EMBRYO SAC10* (*une10*) at the time, was originally identified for having unfertilised ovules without affecting pollen tube attraction (Pagnussat et al., 2005). On the other hand, *PIF8* mRNA abundance was shown to be up-regulated by prolonged low R/FR treatment in a HY5-dependent manner, suggesting its potential involvement in shade avoidance responses (Devlin et al., 2003, Tepperman et al., 2004, Ciolfi

et al., 2013). The *pif8* mutant used in our study exhibited a few phenotypic differences in growth and development compared to WT. To be specific, *pif8* mutant plants were found to have a prolonged vegetative developmental stage, which led to a bigger rosette than WT and an accumulation of leaves before bolting. At adult stage, *pif8* mutant plants had sturdier inflorescent stems and were slightly shorter than WT. These phenotypic differences suggest a possible role played by PIF8 in plant growth and developmental regulation, which deserves further investigation.

Unexpectedly, *pif7* and *pif8* mutants respectively displayed a moderate and strong relative chlorate resistance phenotype, indicating that their nitrate metabolism is somehow compromised. Grafting experiments with WT and *pif7* shoot and root tissues lead to the conclusion that *pif7*-mediated chlorate resistance is largely dependent on the shoot but also, to a lesser extent, on the root as well. This is consistent with the expression pattern of *PIF7*, which, like all other PIF members, is higher in shoot than in root. Additionally, compared to that of the other PIFs, *PIF7* has the highest mRNA abundance in root (Jeong and Choi, 2013). Given the fact that the transcript level of *PIF8* is relatively high in all aboveground tissues but low in the root (Jeong and Choi, 2013), it is expected that the chlorate resistance conferred by the *pif8* mutation is predominantly shoot-dependent, although this hypothesis has to be confirmed by grafting experiments in the future. In striking contrast to the *pif3* mutant, the *pif7* and *pif8* mutations render the plants chlorate resistant without affecting their nitrate reductase activities, indicating that PIF7 and PIF8 upregulate nitrate metabolism through a different underlying mechanism that is yet to be uncovered.

4.3.6 Concluding remarks

In Chapter 4, in an attempt to identify the molecular link between the GA-DELLA signalling pathway and nitrate metabolism through reverse genetics, it was discovered that the quadruple loss-of-function mutant *pifq*, which lacks four DELLA-interacting PIF transcription factors, has a compromised nitrate metabolism similar to the DELLA-stabilising mutants *gai* and *ga5*. Chlorate toxicity assays, grafting experiments and nitrate reductase activity measurements yielded strikingly similar results for *pifq* and *gai*, suggesting that GA-DELLA signalling and PIFs potentially regulate nitrate assimilation through the same pathway. However, in contrast to *gai*, the *pifq* mutation results in a reduced transcript abundance of *NIA2*, the major nitrate reductase gene, although the extent of decrease in *NIA2* mRNA abundance is surprisingly mild considering the dramatic decrease in the enzymatic activity.

Among the PIFq members, PIF3 was identified as the dominant regulator of nitrate metabolism, as the *pif3* mutation alone confers chlorate response indistinguishable from that of *pifq* and can reduce nitrate reductase activity to similar levels to that of *pifq*. The overexpression of *PIF3* complements the mutant phenotypes (both chlorate response and nitrate reductase activity) exhibited by *pif3*, whilst overexpressing the other *PIFs* does not affect plant nitrate assimilation significantly, suggesting a very specific role played by PIF3 in promoting nitrate reductase activity. In addition, PIF3 is also one of the earliest PIF proteins that were robustly proved to interact with DELLAs (Feng et al., 2008). Therefore, PIF3 might act as the bridge that connects DELLAs with downstream nitrate reductase activity, and more importantly, a signalling hub that integrates the internal phytohormone GA and the external light signalling pathway to finetune downstream nitrate metabolism. This hypothesis can be tested by constructing the *gai*

pif3 double mutant to see whether adding the *gai* mutation can decrease nitrate reductase activity to a level even lower than that of *pif3*.

However, the functional significance of PIF3, which is a negative light regulator, upregulating nitrate assimilation is not clear, as it seems contradictory to the general principle of light positively modulating nitrogen metabolism in order to maintain C-N balance. One potential explanation is that PIF3 might contribute to the diurnal oscillation of nitrate reductase activity, in a similar fashion as how PIF3 functions in regulating hypocotyl elongation in accordance with the circadian clock (Soy et al., 2012). Specifically, PIF3 protein abundance peaks at the end of the night, which coincides with the peak in nitrate reductase mRNA level (Lillo et al., 2001). Accordingly, the nitrate reductase activity reaches its maximum shortly after, preparing the plant for optimal nitrate metabolism at the start of the photoperiod (Lillo et al., 2004). It would therefore be interesting to confirm whether *pif3* mutation leads to a perturbation of the diurnal oscillation of the mRNA abundances of nitrate reductase genes as well as enzymatic activity.

Finally, it was shown in this study that PIF7 and PIF8 also positively regulate plant nitrate metabolism because mutations lacking either of these genes confer resistance to chlorate toxicity. However, PIF7 and PIF8 do not affect nitrate reductase activity, suggesting that they regulate nitrate metabolism through a distinct mechanism from the DELLA-PIF3 pathway. Accordingly, the experimental evidence for a protein-protein interaction between DELLAs and either PIF7 or PIF8 is still lacking. Further studies are required to elucidate the molecular mechanism of PIF7- and PIF8-mediated promotion of nitrate metabolism.

CHAPTER 5. Identification of Novel Mutations Conferring Altered Chlorate Responses on *gai* Mutant Plants

5.1 Introduction

Forward genetic screens are powerful tools for the identification of genes responsible for particular mutant phenotypes, including altered growth morphologies and physiological responses, and hence determining the WT functions of the genes affected (Rice, 2014). The forward genetic approach therefore relies on the production of a randomly mutagenized population by high-energy physical mutagens (e.g., fast neutrons [FN], X-rays, ultraviolet [UV] light and γ radiation), chemical mutagens (e.g., ethyl methane sulfonate [EMS], diethyl sulfonate [DES] and methyl methanesulfonate [MMS]) or insertions (e.g., transposon or T-DNA; Addo-Quaye et al., 2018). These mutagenesis methods result in different types of mutations at various densities, therefore have their own advantages and disadvantages (Waugh et al., 2006).

EMS, as an alkylating agent, preferentially modifies the guanine (G) nucleotide and results in the formation of O^6-ethylguanine, which pairs with thymine (T) instead of cytosine (C; Rubin, 1990). Failed DNA repair then leads to a G/C to A/T base pair substitution, which accounts for 98–99% of EMS-induced mutations (Greene et al., 2003). Alternatively, EMS is also known to induce 7-ethylguanine hydrolysis, which causes G/C to C/G or G/C to T/A transversions, or 3-ethyladenine pairing errors, which cause A/T to G/C transitions, at much lower frequencies (1–2%; Krieg, 1963). Rarely (< 1%), EMS can produce insertions/deletions (INDELs) of

various sizes (Henry et al., 2014, Addo-Quaye et al., 2018). EMS-induced mutations are distributed relatively evenly throughout the *Arabidopsis* genome without apparent hotspots, although local biases have been discovered depending on the identities and the methylation states of neighbouring nucleotides, which are probably due to their effects on the efficiency of DNA repair (Vidal et al., 1995, Marsischky and Kolodner, 1999, Greene et al., 2003, Henry et al., 2014). Overall, EMS has the advantage of generating random mutations that lead to not only full knock-out mutations, but also weaker loss-of-function or even gain-of-function mutations (Kim et al., 2006).

On the other hand, it was originally thought that FN ionising irradiation induces large deletions (predominantly within the range of 2–4 kb) and insertions, as well as gross chromosomal aberrations, all of which almost inevitably lead to complete loss-of-function mutations (Sun et al., 1992, Bruggemann et al., 1996, Li et al., 2001, Shikazono et al., 2005). However, more recently, an analysis of the genome-wide effects of FN irradiation in *Arabidopsis* has revealed a wider range of mutations caused by FN (Belfield et al., 2012). Specifically, it was discovered that the most prevalent type of FN-induced mutation is single base substitutions (59%), with C/G to A/T transitions being the most common consequence, although this bias is much less significant than that caused by EMS mutagenesis (Greene et al., 2003, Belfield et al., 2012). Therefore, in theory, FN should also be capable of inducing partial loss-of-function or gain-of-function mutations similar to EMS (Belfield et al., 2012). In addition, with regard to the INDELs produced by FN mutagenesis, the majority of deletions (97%) were found to be smaller than 56 bp, whereas all insertions were by single base pairs (Belfield et al., 2012). Finally, similar to EMS, FN generates mutations at random sites throughout the genome without apparent local preferences (Belfield et al., 2012).

As discussed in previous chapters, several major nitrate transporter genes and both of the nitrate reductase genes were originally identified from mutagenized *Arabidopsis* populations (generated by EMS, γ radiation or insertional mutagens) because loss-of-function or reduced function mutations confer resistance to chlorate toxicity (Wilkinson and Crawford, 1991, Wilkinson and Crawford, 1993, Tsay et al., 1993, Wang and Crawford, 1996). Early selection for chlorate-hypersensitive *Arabidopsis* seedlings resulted in the isolation of two mutants, designated C1 and C4, which exhibited an increased nitrate/chlorate uptake and nitrate/chlorate reduction efficiency respectively, although the genes responsible for these phenotypes were never identified (Wang et al., 1986, Wang et al., 1988). In the present study, a similar mutant screen on chlorate was performed, but with the starting material being *Arabidopsis gai*, which has been shown to display compromised nitrate metabolism and therefore strong resistance to chlorate toxicity (see Chapter 3). The primary goal of this study was to isolate mutant *gai* plants maintaining a dwarf stature, but which are chlorate sensitive, suggestive of improved nitrate metabolism. Such mutants might provide a model for improving the nitrogen-use efficiency (NUE) of Green Revolution crop varieties, whilst retaining the yield-enhancing dwarfism. Additionally, mutant *gai* plants with increased resistance to chlorate compared to the progenitor *gai* population were also selected for further characterisation.

Approximately 50,000 *Arabidopsis gai* progenitor seeds (M_1) were mutagenized with either 0.2% or 0.4% EMS, for 15 or eight hours. Both treatments were known to result in a saturating mutagenesis (1000–1500 mutations per *Arabidopsis* genome), allowing a theoretical 95% chance of inducing a mutation at any G/C site in the genome (Greene et al., 2003, Martin et al., 2009). In addition, another batch of 50,000 *gai* M_1 seeds were mutagenized with 60 Gy of FN irradiation, which has been shown to induce ~ 8 to 32 mutations per *Arabidopsis* genome (Belfield et al., 2012). Around 100,000 EMS-mutagenized and 70,000 FN-mutagenized M_2

seeds were screened on chlorate for mutants exhibiting an altered chlorate response. A relatively low concentration of chlorate (0.5 mM) was used in order to maximise the window for the identification of mutants hypersensitive to chlorate (see section 2.8.1). In this chapter, four potentially chlorate sensitive and four potentially chlorate resistant mutant *gai* plant lines are described in detail. Furthermore, the USUALLY MULTIPLE ACIDS MOVE IN AND OUT TRANSPORTER32 (UMAMIT32) gene, whose function remains unknown, is highlighted for potentially playing a novel role in regulating plant nitrate metabolism.

5.2 Results

5.2.1 Characterisation of chlorate hypersensitive mutants

Mutants that are hypersensitive to chlorate displayed early leaf chlorosis shortly after chlorate treatment in contrast to neighbouring plants (Figure 5.1). These mutants were subsequently transplanted to normal soil without chlorate for seed collection. As expected, the most chlorate sensitive mutants often died even after rescuing, or failed to produce viable seeds for further characterisation. Surviving mutants were allowed to self, and heritability and homozygosity of the phenotype (chlorate hypersensitivity) were tested in subsequent generations. Once confirmed, they were backcrossed with progenitor *gai* plants to "clean-up" irrelevant mutations from the background.



Figure 5.1 An example of a mutant *gai* plant identified to be hypersensitive to chlorate toxicity.
Mutagenized M_2 *gai* plants were germinated directly on soil and grown at 22–24 °C under 16-h light/8-h dark photoperiod (irradiance 120 µmol of photons/m^2 per second). Four-week old plants were watered with 0.5 mM chlorate to soil saturation, which was repeated every five days (for full details see section 2.8.1). Mutants displaying early leaf chlorosis (such as the one highlighted in this Figure) were rescued by transplanting to normal soil and allowed to set seeds. Photo of the plants was taken one week after the first chlorate treatment. Scale bar = 3 cm.

Two independent chlorate hypersensitive mutant lines were isolated from the EMS-mutagenized M_2 population, E2.21S and E1.7S (Figure 5.2). Leaves of both mutant lines went through necrosis much earlier than progenitor *gai* plants following chlorate treatment, with the E2.21S line showing a more severe phenotype than the E1.7S line. In addition, both mutants were smaller in size compared to *gai* specifically when grown on chlorate (Figure 5.2).

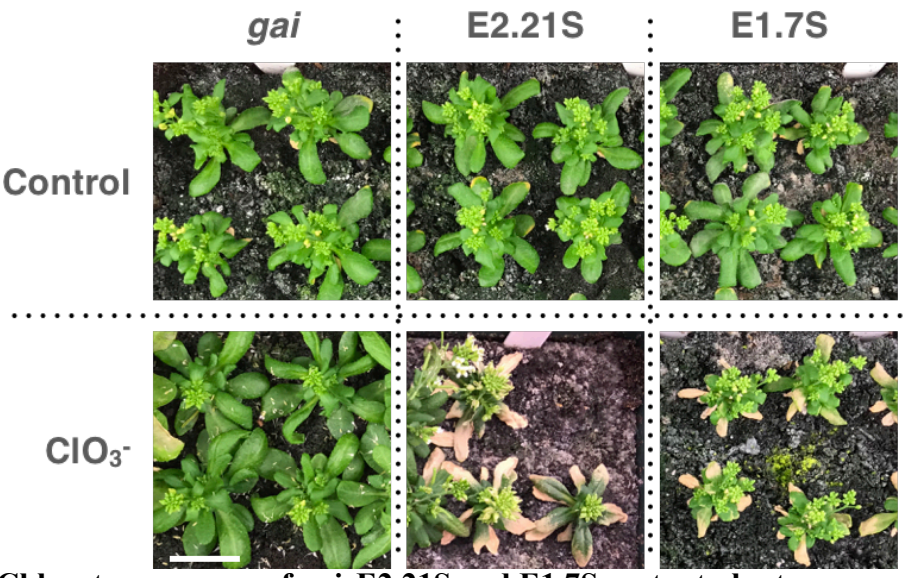


Figure 5.2 Chlorate responses of *gai*, E2.21S and E1.7S mutant plants.
Both E2.21S and E1.7S mutant lines exhibited a smaller plant size and an earlier onset of leaf chlorosis following chlorate treatment compared to progenitor *gai* plants. M_4 generation plants of the mutant lines were shown in this Figure. All plants were germinated on agarose before being transplanted to soil and grown at 22–24 °C under 16-h light/8-h dark photoperiod (irradiance 120 µmol of photons/m^2 per second). Four-week old plants were watered with 0.5 mM chlorate to soil saturation, which was repeated every five days (for full details see section 2.4.1). Photos of the plants were taken one week after the first chlorate treatment. Scale bar = 3 cm.

Thereafter, both E2.21S and E1.7S were backcrossed as pollen donors with *gai* plants. The F_2 generation plants from these backcrosses were treated with chlorate to confirm segregation of the mutant phenotype. However, for E2.21S, the F_2 plants displayed a wide variety of mutant phenotypes in terms of morphology (rosette size, leaf shape, leaf colour, etc.) in addition to chlorate hypersensitivity (Figure 5.3). This phenomenon is suggestive of an unusually high mutation density in the genome. Therefore, in spite of its strong chlorate hypersensitivity originally selected for, characterisation of the E2.21S mutant line was discontinued in this study.



Figure 5.3 Chlorate responses of *gai*, E2.21S and the F_2 generation of the backcross between *gai* and E2.21S.
Backcross between *gai* and E2.21S resulted in the segregation of various mutant phenotypes in addition to chlorate hypersensitivity. All plants were germinated on agarose before being transplanted to soil and grown at 22–24 °C under 16-h light/8-h dark photoperiod (irradiance 120 µmol of photons/m^2 per second). Four-week old plants were watered with 0.5 mM chlorate to soil saturation, which was repeated every five days (for full details see section 2.4.1). Photos of the plants were taken two weeks after the first chlorate treatment. BC1F2, F_2 generation of the first backcross. Scale bar = 3 cm.

In contrast, the F_2 generation plants produced by crossing *gai* with E1.7S were more clearly segregating at a ratio of four in 20 for decreased plant size and chlorate hypersensitivity after chlorate treatment (Figure 5.4), indicating that the responsible mutation is recessive. Hence, the E1.7S mutant line was regarded as a promising candidate for further analysis in the hope of identifying the mutant gene causal of the observed hypersensitivity to chlorate.



Figure 5.4 Chlorate responses of *gai*, E1.7S and the F_2 generation of the backcross between *gai* and E1.7S.
Backcross between *gai* and E1.7S resulted in the segregation of chlorate hypersensitivity linked to a decreased rosette size (two plants potentially homozygous for this mutation are highlighted in the Figure). All plants were germinated on agarose before being transplanted to soil and grown at 22–24 °C under 16-h light/8-h dark photoperiod (irradiance 120 µmol of photons/m^2 per second). Four-week old plants were watered with 0.5 mM chlorate to soil saturation, which was repeated every five days (for full details see section 2.4.1). Photos of the plants were taken two weeks after the first chlorate treatment. BC1F2, F_2 generation of the first backcross. Scale bar = 3 cm.

From the FN-mutagenized M_2 population, two additional independent chlorate hypersensitive mutant lines were identified, and chlorate hypersensitivity was confirmed to be heritable in subsequent generations (Figure 5.5). Both mutant lines exhibited leaf chlorosis earlier than *gai*, but had similar sizes and were at a similar developmental stage to the *gai* control. At the time of writing, both mutants have been backcrossed to *gai* and allowed to self (BC1F1 generation). In the F_2 generation, DNA from individuals displaying early chlorate sensitivity will be collected for whole-genome sequencing analysis and subsequent gene identification.

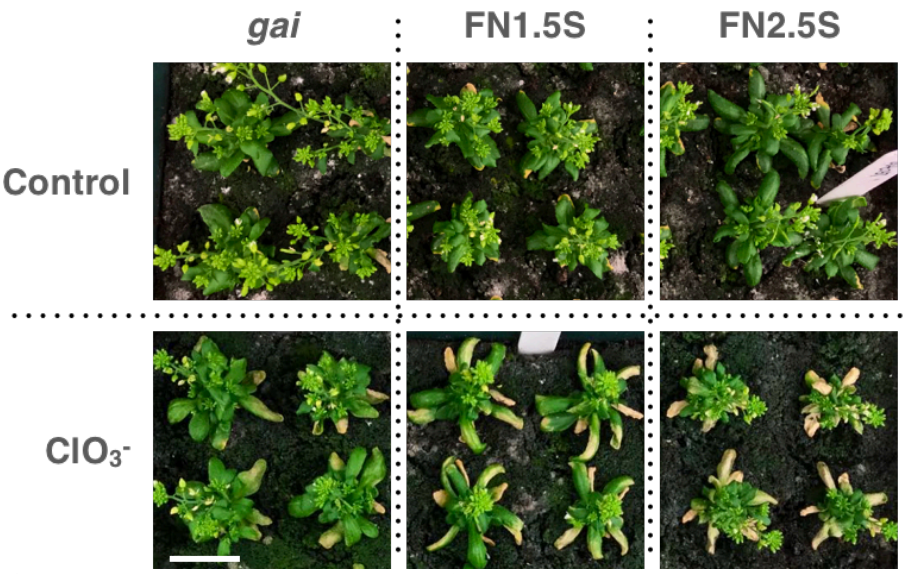


Figure 5.5 Chlorate responses of *gai*, FN1.5S and FN2.5S mutant plants.
Both FN1.5S and FN2.5S mutant lines exhibited an earlier onset of leaf chlorosis upon chlorate treatment compared to the progenitor *gai*. M_4 generation plants of the mutant lines were shown in this Figure. All plants were germinated on agarose before being transplanted to soil and grown at 22–24 °C under 16-h light/8-h dark photoperiod (irradiance 120 µmol of photons/m^2 per second). Four-week old plants were watered with 0.5 mM chlorate to soil saturation, which was repeated every five days (for full details see section 2.4.1). Photos of the plants were taken one week after the first chlorate treatment. Scale bar = 3 cm.

5.2.2 Characterisation of chlorate resistant mutants

Although being more resistant to chlorate than WT, *Arabidopsis gai* mutant plants also exhibit symptoms of chlorate toxicity over time, and severe leaf chlorosis in all rosette leaves can be observed before the end of the fourth week after the first chlorate treatment. Eight independent mutants were selected as being even more resistant to chlorate toxicity than the progenitor *gai* (Figure 5.6). Initial characterisation was carried out for four of these mutants, two identified from the EMS-mutagenized M_2 population (E1.5R and E2.62R) and two from the FN-mutagenized M_2 population (FN2.11R and FN2.7R; Figure 5.7).



Figure 5.6 An example of a mutant *gai* plant identified to be resistant to chlorate toxicity. Mutagenized M_2 *gai* plants were germinated directly on soil and grown at 22–24 °C under 16-h light/8-h dark photoperiod (irradiance 120 µmol of photons/m^2 per second). Four-week old plants were watered with 0.5 mM chlorate to soil saturation, which was repeated every five days (for full details see section 2.8.1). Mutant plants whose leaves remain healthy even after extended chlorate treatment (such as the one highlighted in this Figure) were selected and allowed to set seeds. Photo of the plants was taken four weeks after the first chlorate treatment. Scale bar = 3 cm.



Figure 5.7 Chlorate responses of *gai*, E1.5R. E2.62R, FN2.11R and FN2.7R mutant plants. Four mutant lines (E1.5R, E2.62R, FN2.11R and FN2.7R) were isolated for being more resistant to chlorate toxicity than the progenitor *gai*. In addition, the E1.5R mutant plants exhibited a severe late-flowering phenotype, whereas the FN2.7R mutant plants exhibited a slower growth rate and paler leaves than *gai*. M_4 generation plants of the mutant lines were shown in this Figure. All plants were germinated on agarose before being transplanted to soil and grown at 22–24 °C under 16-h light/8-h dark photoperiod (irradiance 120 µmol of photons/m^2 per second). Four-week old plants were watered with 0.5 mM chlorate to soil saturation, which was repeated every five days (for full details see section 2.4.1). Photos of the plants were taken four weeks after the first chlorate treatment. Scale bar = 3 cm.

5.2.3 Identifying candidate causal mutations in chlorate resistant mutants

Next, attempts were made to identify the mutations responsible for the increased chlorate resistance exhibited by the four mutant lines (E1.5R, E2.62R, FN2.11R and FN2.7R) mentioned above. Using whole-genome sequencing data obtained from a mixture of *gai* mutant plants, the progenitor *gai* reference sequence was created following previously described methods (Belfield et al., 2012, Jiang et al., 2014, Belfield et al., 2018; see section 2.8.2). Next, DNA sequence data from a mixture of M_4 plants of each of these four mutant lines were aligned with the *gai* progenitor reference sequence to obtain a list of SNPs and INDELs potentially responsible for their mutant phenotypes.

In addition to exhibiting a chlorate resistance phenotype (Figure 5.7), plants of the E1.5R mutant line were found to have an extended generation time (approximately 16–20 weeks), almost twice as long as that of *gai* due to severely delayed flowering (data not shown). As expected for EMS-induced mutants, a large number of homozygous mutations were discovered for E1.5R (420 mutations with a Phred quality score of 100–200, see section 2.8.2), suggesting that the identification of the gene responsible for chlorate resistance will likely require at least one backcross with the progenitor *gai*. Genes already known to confer chlorate resistance when mutated, including *NRT1.1*, *NIA2* and *PIFs* (see Chapter 4), were inspected manually and confirmed to have nucleotide sequences identical to that of the progenitor reference genome, suggesting that a previously unknown gene may have been affected. Nevertheless, considering the unusually long generation time and the relatively mild chlorate resistance phenotype exhibited by this mutant line (Figure 5.7), it was decided that the priority should be given to the other mutant lines for the time being.

The E2.62R mutant line exhibited one of the strongest chlorate resistance phenotypes amongst the chlorate resistant mutants selected (Figure 5.7). Similar to that of E1.5R, the mutation density of E2.62R was found to be relatively high (data not shown), which is characteristic of EMS-induced mutants. However, a heterozygous G/C to A/T mutation (64% C and 36% T) was identified at the 3' end of the *Arabidopsis NIA2* gene, which when knocked-out is known to confer strong chlorate resistance (Wilkinson and Crawford, 1991). The identified mutation is expected to result in an amino acid substitution of proline (P) to serine (S) within the NADH binding domain of the nitrate reductase protein (Figure 5.8). Assuming that this mutation in *NIA2* was responsible for the chlorate resistance phenotype exhibited by E2.62R, the fact that the ten M_4 population plants were uniformly chlorate resistant relative to the progenitor *gai*, in other words, lacking an obvious 1:3 segregation of resistant to non-resistant chlorate responses as expected for a recessive mutation (Figure 5.9), would suggest that the *NIA2* gene is potentially haploinsufficient. On the other hand, the fact that individuals as sensitive to chlorate as the progenitor *gai* was not seen is probably due to the insufficient number of M_4 plants tested for chlorate response (Figure 5.9).



Figure 5.8 The domain organisation of the NIA2 protein, and the mutation in the E2.62R mutant line.
Schematic representation of the domain organisation of the NIA2 protein. The domains are colour coded and labelled: Moco (dark blue), Moco-molybdopterin domain; Dimer (yellow), dimerization domain; Hinge (blue), hinge I and hinge II domains; Heme (red), heme b_{557} domain; FAD (green), FAD prosthetic group and NADH (purple), NADH-binding domain. The amino acid substitution (P800 to S) in E2.62R is labelled at the corresponding site on the protein. This diagram is not drawn to scale.



Figure 5.9 Chlorate responses of the progenitor *gai* and M_4 plants of the E2.62R mutant line.
Ten progenitor *gai* plants and ten plants of the E2.62R mutant line were treated with chlorate together. Among the ten E2.62R mutant plants, an apparent 1:3 segregation of resistant to non-resistant individuals was not seen despite the segregating mutation in their *NIA2* genes. All plants were germinated on agarose before being transplanted to soil and grown at 22–24 °C under 16-h light/8-h dark photoperiod (irradiance 120 µmol of photons/m^2 per second). Four-week old plants were watered with 0.5 mM chlorate to soil saturation, which was repeated every five days (for full details see section 2.4.1). Photos of the plants were taken four weeks after the first chlorate treatment. Scale bar = 3 cm.

Two mutant lines were selected from the FN-mutagenized M_2 population for being more resistant to chlorate than the progenitor *gai*. The FN2.11R mutant line exhibited the strongest chlorate resistance amongst all mutants isolated (Figure 5.7). Whole-genome sequencing data indicate that this mutant line contains 12 homozygous SNPs and 13 homozygous INDELs (data not shown). A 22 bp deletion was identified in the last exon of the *NRT1.1* gene, resulting in a frame shift that is more than likely to cause a loss-of-function mutation that confers chlorate resistance (Figure 5.10).



Figure 5.10 Schematic representation of the *NRT1.1* gene and the mutation in the FN2.11R mutant line.
The FN2.11R mutant line contains a 22 bp deletion in the last exon of the *NRT1.1* gene. 5' and 3' untranslated regions (UTRs) are represented by grey boxes. Exons are represented by blue boxes. Lines connecting exons represent introns whereas lines outside of 5' and 3' UTRs are promoter and intergenic regions. Dotted lines indicate the position of the 22 bp deletion in FN2.11R. This diagram is not drawn to scale.

Finally, plants of the FN2.7R mutant lines exhibited a relatively strong chlorate resistance, as well as having a smaller size and paler leaves than progenitor *gai* mutant plants (Figure 5.7). Whole-genome sequencing analysis reveals 26 homozygous mutations in FN2.7R, of which 13 are SNPs and 13 are INDELs. Among these mutations, 11 are located in gene sequences (protein coding sequence as well as 5' and 3' UTRs) and therefore potentially altering gene functions, unless the consequence of the mutation is synonymous amino acid substitution (Table 5.1). None of these mutations affect genes known to be directly involved in the regulation of nitrate metabolism (e.g., *NRT1.1*, *NIA2* and *PIFs*). Interestingly, one of the genes affected, *LOW PSII ACCUMULATION1* (*LPA1*), encodes a chloroplast protein that is essential for efficient photosystem II (PSII) assembly (Peng et al., 2018). It has been reported that *lpa1* loss-of-function mutant plants have pale green leaves and are approximately 75% smaller in size compared to WT plants (Peng et al., 2018), which are phenotypes shared by the FN2.7R mutant plants. Unfortunately, the FN2.7R mutant line was eventually lost due to poor seed quality, possibly attributable to the mutation in its *CRUCIFERIN 2/ CRUCIFERIN B* (*CRU2/CRB*) gene, which is expressed mainly in *Arabidopsis* seeds and encodes a seed storage protein responsible for the regulation of seed maturation (Pang et al., 1988, Fujiwara et al., 2002). Nevertheless, attempts have been made to identify the mutation responsible for the

mutant chlorate resistance phenotype based on the list of genes identified to be affected in FN2.7R (Table 5.1).

Table 5.1 List of mutations located in the exon or UTR regions in the FN2.7R mutant line.

Gene Accession	Gene Name	Position	Consequence of Mutation
AT5G04630	CYTOCHROME P450, FAMILY 77, SUBFAMILY A, POLYPEPTIDE 9 (CYP77A9)	Exon	Point-nonsense mutation
AT3G30340	USUALLY MULTIPLE ACIDS MOVE IN AND OUT TRANSPORTERS 32 (UMAMIT32)	Exon	Amino acid substitution (S to R)
AT1G16130	WALL ASSOCIATED KINASE-LIKE 2 (WAKL2)	Exon	Amino acid substitution (R to G)
AT3G53270	Small nuclear RNA activating complex (SNAPc), subunit SNAP43 protein	Exon	Amino acid substitution (H to N)
AT3G42850	ARABINOKINASE 2 (ARA2)	Exon	Synonymous mutation
AT3G53270	Small nuclear RNA activating complex (SNAPc), subunit SNAP43 protein	Exon	Amino acid substitution (H to N)
AT1G76430	PHOSPHATE TRANSPORTER 1;9 (PHT1;9)	Exon	23 bp deletion
AT1G02910	LOW PSII ACCUMULATION1 (LPA1)	Exon	1 bp deletion
AT1G03880	CRUCIFERIN 2 (CRU2) / CRUCIFERIN B (CRB)	Exon	1 bp deletion
AT1G66830	Leucine-rich repeat protein kinase family protein	UTR	1 bp deletion
AT5G22400	Rho GTPase activating protein with PAK-box/P21-Rho-binding domain-containing protein	UTR	1 bp deletion

5.2.4 The *usually multiple acids move in and out transporters32* (*umamit32*) mutation might have conferred the chlorate resistance of FN2.7R

Assuming that the chlorate resistance phenotype exhibited by the FN2.7R mutant line is independent of its *gai* mutant background and is due to the loss- (rather than gain-) of-function mutation of a single gene, T-DNA insertion mutants were obtained for all of the genes listed in Table 5.1 (except for AT3G42850, since the mutation is synonymous). Preliminary chlorate toxicity assays for these mutants identified *umamit32* (Figure 5.11) as the only mutant that is detectably more resistant to chlorate toxicity compared to WT (Figure 5.12), whilst the other mutants exhibited similar chlorate responses as WT plants (data not shown). This observation suggests that the UMAMIT32 protein, whose biological function is uncharacterised to date (Busov et al., 2004), might somehow regulate plant nitrate metabolism (see discussion below).

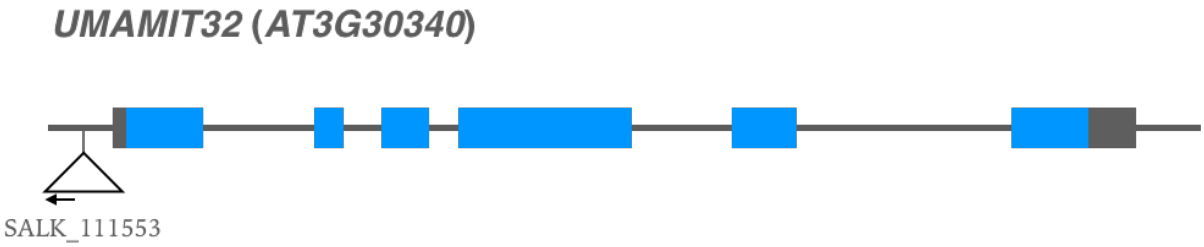


Figure 5.11 Schematic representation of the *UMAMIT32* gene and the site of T-DNA insertion.
The only SALK mutant line available for *UMAMIT32* is SALK_111553, whose T-DNA insertion is located within the promoter region of the gene. 5' and 3' untranslated regions (UTRs) are represented by grey boxes. Exons are represented by blue boxes. Lines connecting exons represent introns whereas lines outside of 5' and 3' UTRs are promoter and intergenic regions. The inverted triangle indicates the site of T-DNA insertion. This diagram is not drawn to scale.

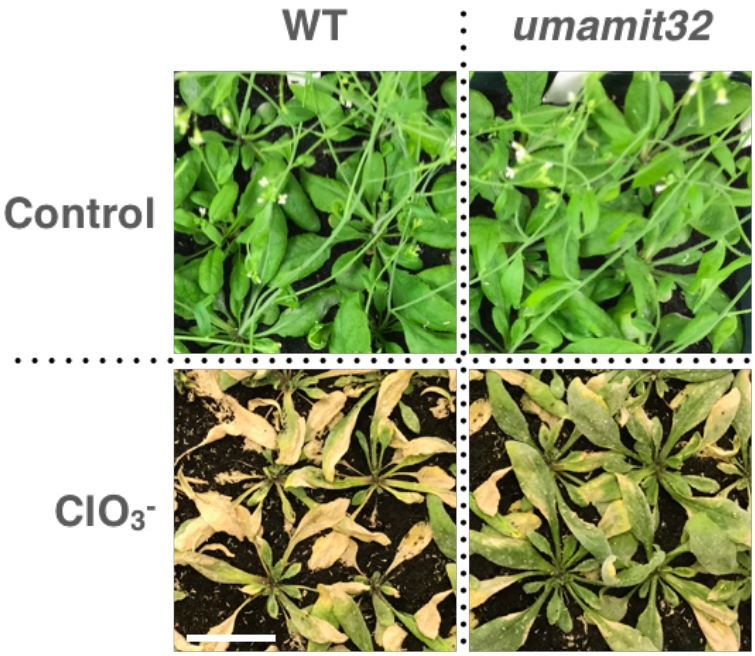


Figure 5.12 Chlorate responses of WT and *umamit32* mutant plants.
Arabidopsis umamit32 mutant plants are more resistant to chlorate toxicity than WT plants. All plants were germinated on agarose before being transplanted to soil and grown at 22–24 °C under 16-h light/8-h dark photoperiod (irradiance 120 µmol of photons/m^2 per second). Four-week old plants were watered with 1.5 mM chlorate to soil saturation, which was repeated every five days (for full details see section 2.4.1). Photos of the plants were taken two weeks after the first chlorate treatment. For plants growing on chlorate (lower panel), inflorescence stems were removed to facilitate the observation of plant chlorate responses. Scale bar = 3 cm.

5.3 Discussion

5.3.1 General comments on mutagenesis and mutant screen

In this study, both EMS- and FN-mutagenized M_2 *gai* populations were screened on chlorate to select for mutants with altered chlorate responses, either more sensitive or more resistant than progenitor *gai* plants, in order to combine the advantages of using these two mutagens. As expected, the EMS and FN treatments induced drastically different spectrums of mutations. Whole-genome sequencing data of the E1.5R and E2.62R mutant lines confirm that EMS mutagenesis results in high mutation densities of almost exclusively G/C to A/T base pair

substitutions (Greene et al., 2003, Martin et al., 2009). As a consequence, in more than one case, additional observable mutant growth and developmental phenotypes were associated with the selected mutants. For example, the backcross of E2.21S with *gai* resulted in the segregation of a wide range of phenotypes (in terms of leaf colour, size and developmental stage), and the fact that the E1.5R mutant plants are severely late flowering. On the contrary, FN induced many fewer mutations consisting of a mixture of SNPs and INDELs per genome, and therefore resulted in much "cleaner" phenotypes. Of the two FN-mutagenized mutants whose genomes were sequenced, FN2.11R and FN2.7R, 25 and 26 homozygous mutations were respectively identified, which falls well within the previously reported eight to 32 mutations induced by 60 Gy of FN irradiation per genome (Belfield et al., 2012). Therefore, in theory, although a mutant exhibiting the target phenotype is more likely to arise among a saturating EMS-mutagenized population, it is much easier to analyse the sequencing data of a FN-mutagenized genome and pinpoint the responsible mutation.

Despite the saturating mutagenesis achieved by the EMS treatment in this study, only two chlorate hypersensitive mutants were isolated from approximately 100,000 EMS-mutagenized M_2 plants. Three main factors are believed to have been responsible for such difficulty in selecting chlorate hypersensitive mutants. Firstly, as mentioned above, mutants exhibiting the strongest sensitivity to chlorate toxicity rarely survive or produce viable seeds, resulting in the loss of the mutant lines. Secondly, the intrinsic individual variation in chlorate response among the M_2 population means that mutants displaying a moderately increased sensitivity to chlorate are often missed. Finally, more than ten mutant lines originally selected for being hypersensitive to chlorate exhibited early leaf chlorosis even on normal soil without chlorate (as an example, see Figure 5.13), suggesting that the mutations might simply cause an enhanced cell apoptosis regardless of the presence of chlorate, and therefore unlikely to specifically affect

plant nitrate metabolism. Nonetheless, three independent hypersensitive mutant lines (E1.7S, FN1.5S and FN2.5S) were identified, among which the E1.7S M_4 plants have been backcrossed once with *gai* plants and displayed expected segregation of the mutant phenotype. It is worth investigating these mutant lines further and determine the mutations responsible for their chlorate hypersensitivity.

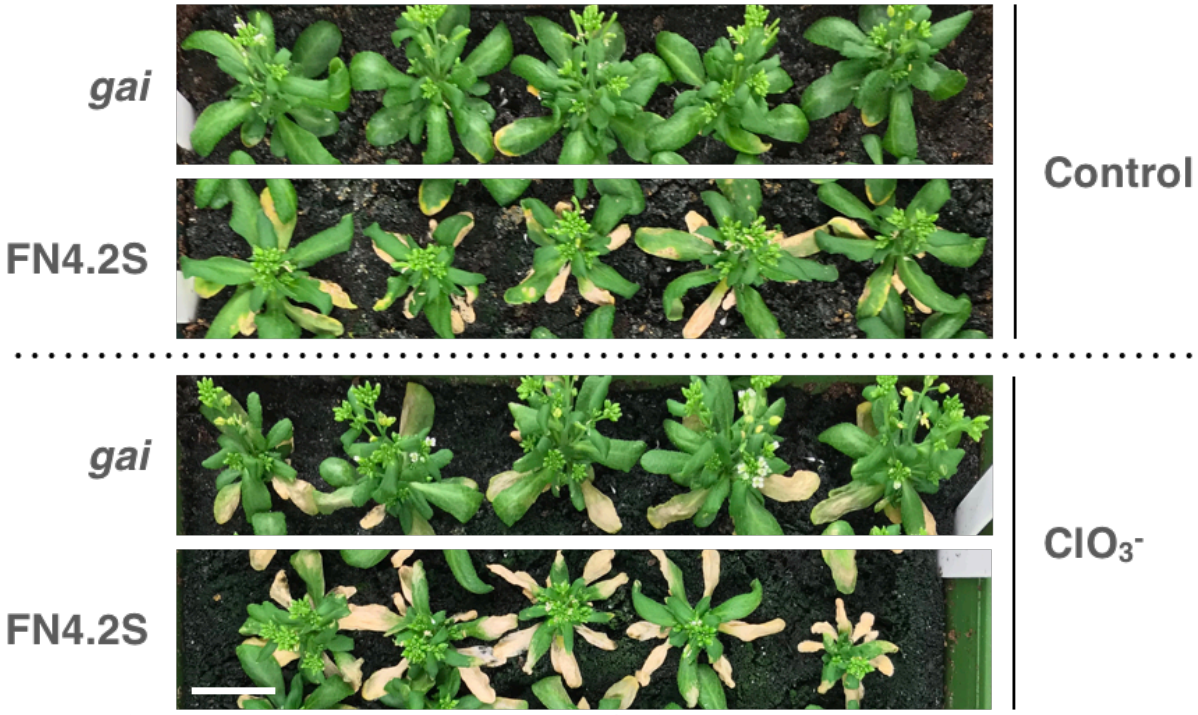


Figure 5.13 An example of a mutant line (FN4.2S) that exhibited early leaf chlorosis both with and without chlorate treatment.
The FN4.2S mutant line was originally selected for being hypersensitive to chlorate than progenitor *gai* plants However, the M_4 generation plants of this mutant line displayed early leaf chlorosis when grown on soil regardless of the presence of chlorate, indicating that this phenotype is not specifically due to chlorate toxicity. All plants were germinated on agarose before being transplanted to soil and grown at 22–24 °C under 16-h light/8-h dark photoperiod (irradiance 120 µmol of photons/m^2 per second). Four-week old plants were watered with 0.5 mM chlorate to soil saturation, which was repeated every five days (for full details see section 2.4.1). Photos of the plants were taken one week after the first chlorate treatment. Scale bar = 3 cm.

5.3.2 Mutations in the *NRT1.1* and *NIA2* genes were identified from the mutants selected for being chlorate resistant

As expected, selection of mutants exhibiting stronger chlorate resistance phenotypes than *gai* yielded mutations in genes previously known to be positive regulators of nitrate metabolism. Specifically, the FN2.11R mutant line was found to harbour a 22 bp deletion in the exon of its *NRT1.1* gene, which encodes a dual-affinity nitrate transporter well-known to confer strong chlorate resistance when mutated (Tsay et al., 1993; also see section 3.2.1). It was concluded in Chapter 3 that *gai*-conferred chlorate resistance is mainly due to reduced shoot nitrate reductase activity rather than nitrate uptake in the root, and that the *gai* mutation actually mildly increases the mRNA abundances of nitrate transporters including *NRT1.1*. Therefore, it is not surprising that the *gai nrt1.1* double mutant is even more resistant to chlorate toxicity than *gai*.

Next, an amino acid substitution (P800 to S) in the major nitrate reductase protein NIA2 is potentially responsible for the chlorate resistance phenotype exhibited by the E2.62R mutant line. P800 locates within the C terminus domain of the protein that binds to NADH, which provides the electron essential for nitrate reduction (Campbell and Kinghorn, 1990). Although both proline and serine are small amino acids commonly positioned at the tight turns of the protein structure, they differ in that proline has a non-polar side chain and is generally non-reactive, whereas serine has a polar side chain that often forms hydrogen bonds with substrates (Barnes, 2007). Therefore, it is reasonable to speculate that this proline to serine substitution has a deleterious effect on nitrate reductase protein function, which in turn reduces nitrate reductase activity to a level even lower than that of *gai* (see section 3.2.6) and thus leading to strong chlorate resistance. However, the sequencing data obtained from a mixture of M_4 plants of this mutant line indicate that this mutation is segregating in the population, although a

segregation of chlorate response was not clearly observed. This phenomenon implies that either a different homozygous mutation is responsible for the mutant phenotype, or that *NIA2* is actually haploinsufficient, meaning that the loss-of-function mutation is dominant relative to the WT allele (Griffiths et al., 2015). To our knowledge, the haploinsufficiency of *NIA2* has not been reported previously. In fact, Wilkinson and Crawford, 1991 showed that the F_1 plants from outcrossing *nia2*/*chl3-5* (*Ler* background) with *Col-0* WT resulted in a 50% decrease in nitrate reductase activity compared to the parental *Col-0* WT plants, but are not detectably more resistant to chlorate than *Col-0* WT. Apart from the apparent difference in the genetic background, it is possible that the harsher chlorate treatment employed in their study (five-day old seedlings supplied with 5 mM nitrate treated with 2 mM chlorate) compared to that in ours (four-week old adult plants growing on nutrient-rich soil treated with 0.5 mM chlorate) masked the effect of a relatively small decrease in nitrate reductase activity on chlorate response. All in all, the questions of whether the P800 to S amino acid substitution of NIA2 is responsible for an enhanced chlorate resistance, and whether the *NIA2* gene is haploinsufficient, require further clarifications.

5.3.3 *UMAMIT32* might be a novel gene involved in plant nitrogen metabolism

The FN2.7R mutant line was originally isolated from the mutant screen for being relatively resistant to chlorate toxicity compared to progenitor *gai* plants. In addition, the FN2.7R mutants also exhibited other visible phenotypes including having pale green leaves, a retarted growth rate, and poor seed quality. The whole-genome sequencing data identified mutations potentially responsible for these additional abberent phenotypes, specifically the mutation of the *LPA1* gene, which is responsible for efficient PSII assembly in the chloroplast and therefore mediates leaf colour and growth regulation (Peng et al., 2018); and the mutation of the

CRU2/*CRB* gene, which plays a role in the seed maturation process (Pang et al., 1988, Fujiwara et al., 2002). However, mutations in genes that are known to be directly involved in nitrate metabolism (such as the nitrate transporter, nitrate reductase and PIF family genes) were not found in the FN2.7R mutant line, indicating that its chlorate resistance phenotype was due to the mutation of a novel gene previously not known to be associated with nitrate metabolism. One promising candidate for that gene is *UMAMIT32*, as preliminary chlorate toxicity assay indicates that a mutant having a T-DNA insertion in the promoter region of this gene exhibited chlorate resistance relative to WT plants. This observation also suggests that *umamit32*-conferred chlorate resistance is independent of the *gai* mutant background, although it might act additively or synergistically with the *gai* mutation.

UMAMIT32 is one of the more than 40 members of the family of *Arabidopsis UMAMIT* genes (divided into six major groups), which is part of the *Medicargo truncatula NODULIN21* (*MtN21*) gene family that encodes nodulins during legume nodulation (Gamas et al., 1996, Ladwig et al., 2012). The MtN21 family is highly conserved in the plant kingdom from mosses, liverworts to higher plants, which is suggestive of their functional importance in plant growth and devlopment, especially in non-nodulating plant species (Ladwig et al., 2012). The MtN21 family in turn belongs to the Plant Drug/Metabolite Transporter (P-DMT) superfamily, the members of which are often poorly characterised functionally (Jack et al., 2001). *Arabidopsis UMAMIT32* was originally identified as one of 38 *Arabidopsis UMAMIT* gene homologous to the *5NG4* gene in loblolly pine, which encodes a protein with ten putative transmembrane domains whose substrate is unknown (Busov et al., 2004). Although the transcript abundance of *5NG4* is found to be highly induced by the phytohormone auxin, it is unlikely to transport auxin given its low sequence similarity to known *Arabidopsis* auxin transporters (Busov et al., 2004). The authors proposed that *5NG4* is involved in the regulation of lateral and/or

adventitious root development because of its specific expression pattern in roots, hypocotyls and juvenille shoot tissue (Busov et al., 2004).

In recent years, several *Arabidopsis UMAMIT* family proteins have been found to be associated with plant nitrogen metabolism, especially with respect to the export of amino acids. Whilst several families of amino acid importers have been identified in *Arabidopsis*, only a very limited amount of amino acid exporters have been reported despite plenty of physiological evidence for the ubiquity of this process throughout the plant (Okumoto and Pilot, 2011, Pratelli and Pilot, 2014). *Arabiodpsis UMAMIT18* (or *SILIQUES ARE RED1* [*SIAR1*]) was found to be expressed in a variety of plant organs including the vasculature, root pericycle and reproductive organs, particularly the chalazal regions of ovules (Ladwig et al., 2012). Functional analysis of the UMAMIT18 protein indicates that it localises on the plasma membrane and is responsible for unloading amino acids from long-distance transport into young siliques. Therefore, the *umamit18* loss-of-function mutant accummulates anthocyanin in their developing siliques as a result of the lack of amino acids, which gives this gene its original name (Ladwig et al., 2012). Similarly, four related UMAMIT proteins (UMAMIT11, UMAMIT14, UMAMIT28 and UMAMIT29) were shown to mediate amino acid transport into developing seeds from the adjacent symplastic regions, with UMAMIT11 and UMAMIT14 regulating phloem unloading whereas UMAMIT28 and UMAMIT29 regulating amino acid export into the seeds (Muller et al., 2015). However, the divergent expression patterns, the differential substrate preferences, and the fact that the loss-of-function mutant of each of these four genes produces a visible phenotype of reduced seed size, suggest that they only share a limited degree of functional redundancy (Muller et al., 2015). More recently, *UMAMIT14* and *UMAMIT18*, which are also expressed in root tissue in addition to reproductive organs, were

discovered to regulate the radial transfer of amino acids from the root pericycle and eventually their secretion into the rhizosphere (Besnard et al., 2016).

Although the functional significance of UMAMIT32 awaits characterisation, like all other UMAMIT proteins, it is predicted to be a transmembrane protein with either nine or ten transmembrane helices, depending on the model used (ARAMEMNON plant membrane protein database, Schwacke et al., 2003). Previous phylogenetic study has placed it within the same class (Class I) as the UMAMIT28 and UMAMIT29 amino acid exporters mentioned above (Ladwig et al., 2012). Moreover, a recent co-expression analysis of *Arabidopsis* nitrate transporters and enzymes involved in cell wall synthesis discovered co-expression of *UMAMIT32* with the high affinity nitrate transporter *NRT2.3* (Landi and Esposito, 2017). These initial lines of evidence imply that *UMAMIT32* might also encode an amino acid transporter that is involved in the regulation of plant nitrogen allocation and homeostasis. Therefore, it could be that the chlorate resistance phenotype exhibited by the *umamit32* mutant is attributable to a localised accumulation of reduced nitrogen metabolite in the root resulted from the deficiency in amino acid re-distribution, exerting a negative feedback regulation on nitrate/chlorate transporter activities. Alternatively, since *UMAMIT32* is expressed in the shoot as well (Arabidopsis eFP Browser, Winter et al., 2007), nitrate/chlorate translocation into the rosette leaves (where the chlorate response was assessed) might be indirectly inhibited in the mutant.

Another potential explanation is that UMAMIT32 is more directly associated with nitrate and/or chlorate transport. Indeed, rather than transporting amino acids like the aforementioned UMAMITs, the earliest studied *Arabidopsis* UMAMIT protein, UMAMIT5 (or WALLS ARE THIN1 [WAT1]) was found to be localised on tonoplast (rather than plasma membrane) and

mediate the export of auxin from the vacuole, thus regulating cellular auxin homeostasis and secondary cell wall development (Ranocha et al., 2010, Ranocha et al., 2013). In addition, the authors also proposed the possibility of members of the UMAMIT family possessing a low substrate specificity and therefore transporting multiple substrates, in a similar fashion to members of the *Arabidopsis* NITRATE TRANSPORTER1/PEPTIDE TRANSPORTER FAMILY (NRT1/NPF) that can transport phytohormones as well as nitrate (Ranocha et al., 2013).

Nevertheless, one critical caveat that is worth addressing is that the nucletotide substitution mutation in the original FN2.7R mutant line is predicted to cause an amino acid substitution (serine to arginine) in the UMAMIT32 protein, which does not necessarily lead to its loss-of-function. The same concern applies to all the other mutations identified from this mutant line that do not result in a premature stop codon. Therefore, with this line being lost, ideally, the exact same mutation should be replicated in the *UMAMIT32* gene (and perhaps the identified mutations in the other genes) in the *gai* mutant background using the CRISPR-Cas9 genome-editing technique, before assessing its chlorate response. Adding another layer of complexity, the T-DNA insertion site of the *umamit32* mutant used in this study is located in the promoter rather than the coding region of the gene. Therefore, it is crucial to measure the mRNA abundance of *UMAMIT32* and confirm that it is either reduced (knock-down mutation) or completely absent (knock-out mutation) in this mutant. In conclusion, notwithstanding the promising chlorate resistance phenotype observed for the *umamit32* mutant, we are still far from fully understanding the regulatory connection between UMAMIT32 and nitrogen metabolism.

5.3.4 Concluding remarks

Chapter 5 outlines the forward genetic screens performed in this study for mutagenized plants in the *gai* mutant background, aiming for the identification of mutants with an altered chlorate response, either more sensitive or more resistant than the progenitor *gai*. Both EMS and FN mutagens were employed to create the M_2 population to maximise the efficiency of the mutant screen. Despite the difficulties with isolation of chlorate hypersensitive mutants (whose nitrate metabolism might be enhanced), three promising independent mutant lines were eventually selected for further analysis and the identification of responsible genes. With respect to the chlorate resistant mutants investigated, two mutants respectively contain a mutation in the nitrate transporter gene *NRT1.1* and the major nitrate reductase gene *NIA2*, both of which are previously known to result in strong chlorate resistance when knocked-out. The identification of these two genes from this mutant screen indirectly validates the experimental setup and procedure. Finally, sequence analyses of the FN2.7R chlorate resistant mutant line produced a list of mutations in genes potentially involved in nitrogen metabolism, among which the T-DNA insertion mutation of *UMAMIT32*, whose function is previously unknown, conferred resistance to chlorate in a preliminary chlorate toxicity assay. Therefore, it is reasonable to speculate that UMAMIT32, like some of the other members of the *Arabidopsis* UMAMIT family that have been reported in recent years, somehow participates in the regulation of systemic or localised nitrogen homeostasis. Depending on confirmation of the role played by *UMAMIT32* in nitrogen metabolism (as outlined above), this gene may become an important target for future biotechnological modifications for the improvement of plant NUE.

CHAPTER 6. Identification of Novel Mutations Conferring Increased Plant Height on *gai* Mutant Plants

6.1 Introduction

In order to ensure survival, plants, as sessile organisms, have evolved extraordinary phenotypic plasticity achieved through the intricate integration of endogenous developmental signals and external environmental cues (Casal et al., 2004). This integration is largely mediated by a variety of phytohormones, which are small plant signalling molecules encompassing a dual function of regulating internal developmental processes as well as adapting to environmental challenges (Daviere and Achard, 2016). As introduced above, GAs are a group of plant hormones that are involved in the regulation of many biological activities including seed germination, stem elongation, juvenile-to-adult phase transition and flower development (Harberd et al., 2009). Historically, genetic screens performed in *Arabidopsis* and rice relying on alteration in plant height, the most readily observable phenotype controlled by GAs, have enabled the identification of the major components of the GA signalling pathway, including GA biosynthetic enzymes, GA receptors, DELLA growth repressors, and the F-box proteins responsible for degrading DELLA proteins (Achard and Genschik, 2009, Gao et al., 2011, Schwechheimer, 2011, Sun, 2011, Wang and Deng, 2011, Hauvermale et al., 2012, Daviere and Achard, 2013). The *Arabidopsis gai* dominant mutant was originally identified because it exhibits a dwarf stature similar to GA-sensitive mutants that are deficient in GA biosynthesis, but *gai* is irresponsive to the GA signal (Koornneef et al., 1985).

Further forward genetic screens using *gai* mutant plants as the starting material for reverted repression of stem elongation have been performed, and yielded two categories of mutations. First, multiple mutagenized *gai* plants with heights indistinguishable from WT were found to contain secondary mutations within the *gai* open reading frame, confirming that *gai* is indeed a gain-of-function mutation and that these additional derivative mutations led to *GAI* loss-of-function (Peng and Harberd, 1993, Peng et al., 1997). One of these mutant alleles, *gai-t6* (Figure 6.1A), which carries a *Ds* insertion that disrupts the *gai* gene, enabled the eventual cloning of *GAI* (Peng et al., 1997).

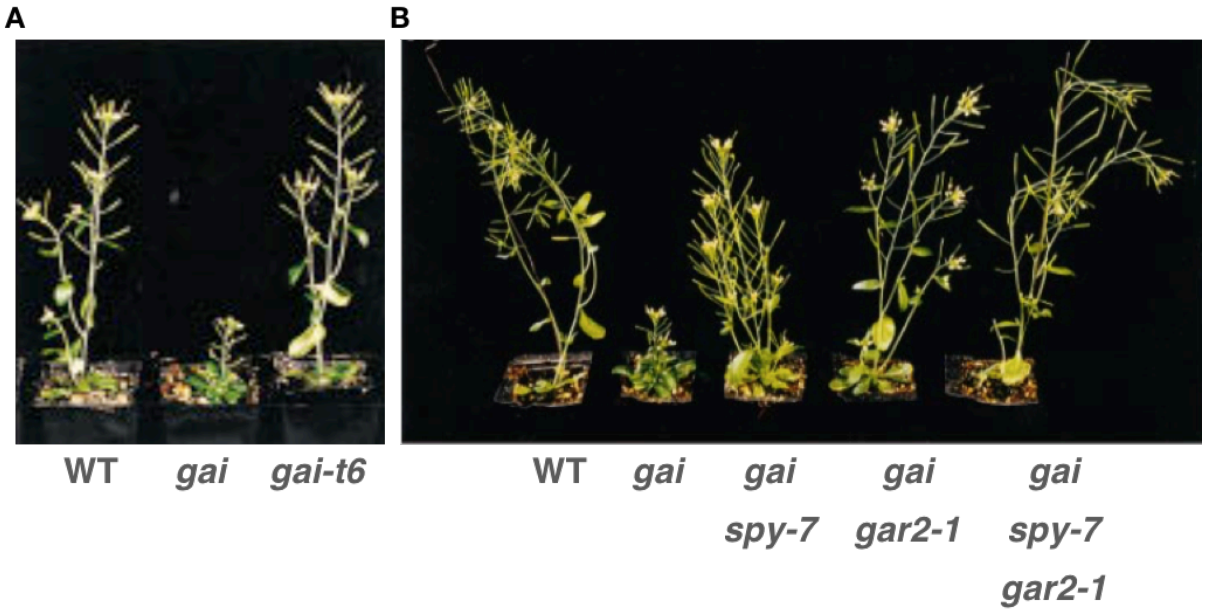


Figure 6.1 Plant heights of WT, *gai* and *gai* plants with additional mutations that lead to a tall phenotype.
(A) Plant heights of WT, *gai* and *gai-t6*. *gai* mutant plants display a dwarf phenotype whilst both WT and *gai-t6* plants are tall. Figure adapted from (Peng et al., 1997). (B) Plant heights of WT, *gai*, *gai spy-7*, *gai gar2-1* and *gai spy-7 gar2-1*. The *spy-7* and *gar2-1* mutations partially suppress the dwarf phenotype conferred by *gai*. Complete suppression of *gai*-mediated inhibition of stem elongation can be achieved by the combined effect of the *spy-7* and *gar2-1* mutations. Figure adapted from (Peng et al., 1999b).

Second, extragenic mutations outside of the *gai* locus have also been identified to either partially or completely suppress *gai*-conferred inhibition of stem elongation. In the *gai* mutant

background, the recessive mutant allele *spindly-7* (*spy-7*, originally named *gai suppressor1-1* [*gas1-1*]) leads to a relatively mild increase in plant height (Figure 6.1B, Carol et al., 1995). Previously, multiple mutant alleles of *SPY* had been isolated from forward screens for resistance to the seed germination inhibition caused by the GA biosynthesis inhibitor paclobutrazol (PAC, Jacobsen and Olszewski, 1993, Carol et al., 1995). When mature, these *spy* mutant plants exhibit a "slender" phenotype somewhat similar to that of WT plants treated with bioactive GA_3 (Jacobsen et al., 1996). Moreover, similar to *spy-7*, when *spy-5* is crossed with *gai*, the homozygous double mutant offspring is twice as tall as *gai* but slightly shorter than WT (Wilson and Somerville, 1995). Taken together, these observations indicate that SPY plays a negative role in the regulation of GA signalling. Nevertheless, it was only recently determined that *SPY* encodes a novel protein O-fucosyltransferase that triggers conformational modification of DELLAs and hence the promotion of their activities (Zentella et al., 2017).

Another extragenic mutation, *gai revertant2-1* (*gar2-1*), was first identified because it partially suppresses the dwarf mutant phenotype conferred by *gai* (Wilson and Somerville, 1995). However, unlike *spy-7*, *gar2-1* is a dominant gain-of-function mutation (Wilson and Somerville, 1995). The WT *GAR2* allele (now known as *SLEEPY1* [*SLY1*]) was later shown to encode an F-box subunit of the SCF^{SLY1} E3 ubiquitin ligase that targets DELLA proteins for ubiquitination, thus promoting their degradation in the proteasome (Dill et al., 2004, Fu et al., 2004, Wang et al., 2009a). Loss-of-function mutant alleles of *SLY1* and the rice orthologous gene *GID2* were first isolated from genetic screens for GA-insensitive dwarf mutant plants (Steber et al., 1998, McGinnis et al., 2003, Sasaki et al., 2003). In contrast, the gain-of-function *gar2-1* (or *sly1-d*) mutation results in an amino acid substitution (E138 to K) at the C terminus of the SLY1 protein, which leads to an enhanced interaction between sly1 and its substrates (Dill et al., 2004, Fu et al., 2004). Consequently, DELLA degradation is promoted, and

inhibition of stem elongation is mitigated, thus explaining why *gai gar2-1* is taller than *gai* (Dill et al., 2004, Fu et al., 2004, Wang et al., 2009a). *gai*-conferred inhibition of plant growth can be almost completely suppressed by the combined effect of both the *spy-7* and *gar2-1* mutations (Figure 6.1B, Peng et al., 1999). Detailed characterisation of the *spy-7* and *gar2-1* mutations indicates that their effects on GA-DELLA signalling are not limited to the regulation of plant height. Instead, it appears that all the conferred effects of the *gai* mutation, including inhibition of seed germination, leaf expansion, pollen tube growth and flowering, as well as elevated leaf chlorophyll content, C-20 oxidase transcripts and GA content, are reverted to various degrees by these two mutations (Peng and Harberd, 1997a, Peng et al., 1999b, Swain et al., 2004). Therefore, SPY and SLY1 are two key components involved in the GA-DELLA signalling pathway.

In this study, whilst selecting for mutant plants with altered chlorate responses among the EMS-mutagenized *Arabidopsis gai* population (see Chapter 5), individuals exhibiting a "tall" phenotype (defined as an increased stem elongation compared to progenitor *gai* plants) were additionally isolated. The reason for this was two-fold. Firstly, novel suppressor mutants of *gai*, either intragenic or extragenic, might provide new insights into the regulatory connection between DELLA proteins and the repression of plant growth, which is still not fully understood. Secondly, the relative chlorate toxicity resistance of these new "tall" mutants might be informative with respect to the linkage between *gai* and nitrate metabolism. For example, any mutations that disrupted the correlation between *gai*-mediated inhibition of plant growth (stem elongation) and chlorate resistance might aid our understanding of the molecular mechanism of the pleiotropic effect of DELLAs on nitrate metabolism.

This chapter outlines the analyses of the tall *gai* mutants selected from the forward genetic screen, and divides them into three categories with respect to the site of the causal mutation: those with a new mutation in *gai*, those with a new mutation in *SLY1*, and those without a detectable new mutation in either of these two genes. Finally, initial characterization of a tall *gai* mutant belonging to the third category, having a height similar to that of WT plants, yet remaining relatively resistant to chlorate toxicity, is described.

6.2 Results

6.2.1 Most tall *gai* mutants contain detectable mutations in *gai*

Previous mutant screens for *gai* suppressor mutations suggest that tall mutants arise relatively frequently among mutagenized *gai* populations, which can be at least partially explained by the fact that random secondary mutations often occur within the *gai* open reading frame, resulting in loss-of-function (Peng and Harberd, 1993, Wilson and Somerville, 1995). It has also been shown that a meristematic cell heterozygous for such a mutation can produce sectors comprising of branches which, when mature, elongate to resemble the phenotype displayed by plants heterozygous for *gai* (and the WT allele, Figure 6.2, Peng and Harberd, 1993, Peng and Harberd, 1997b). Therefore, in this study, selection for tall *gai* mutants was performed at both the M_1 and M_2 generations of the mutagenized *gai* populations. PCR verification was performed on all mutants to confirm the presence of the 51-bp *gai* deletion at the N terminus of the *GAI* gene (similar to that performed in Figure 3.11), thus showing that they are indeed the descendants of mutagenized *gai*, and are not simply WT contaminants.



Figure 6.2 An example of a tall *gai* mutant stem identified within an EMS-mutagenized M_1 *gai* population.
The arrow indicates a visibly elongated inflorescence stem (compared to neighbouring plants). PCR verification confirms that this stem carries the 51-bp *gai* deletion, suggesting that rather than being a WT contaminant, it contains a secondary mutation that confers the tall phenotype. Mutagenized *gai* seeds were germinated directly on normal F2 soil and grown at 22–24 °C under 16-h light/8-h dark photoperiod (irradiance 120 μmol of photons/m^2 per second). Photo of the plants were taken when they were six-week old. Scale bar = 3 cm.

A total of 118 tall mutant individuals was isolated from the M_1 and M_2 generations of the EMS-mutagenized *gai* populations, with heights falling somewhat between that of *gai* and WT control plants (Figure 6.3). These individuals were allowed to self-pollinate, and derived homozygous M_4 populations were investigated further. Sanger sequencing of the *gai* coding region plus an extra approximately 300 bp covering both the promoter and 3' UTR regions was performed for 87 of these mutants. As expected, most of these tall *gai* mutants (69 out of 87, 79%) were found to carry at least one detectable secondary mutation in *gai*, mutations which presumably alter or completely eliminate *gai* function. Among these mutations, approximately 96% (66/69) were G/C to A/T base substitutions, 3% (2/69) were G/C to T/A base substitutions, whilst only a single 1-bp deletion (1%) was detected. These relative frequencies of mutations agree well with the previously established spectrum of EMS-induced mutations (given the

relatively small sample size; Krieg, 1963, Greene et al., 2003, Henry et al., 2014, Addo-Quaye et al., 2018).



Figure 6.3 Examples of M_4 generation tall *gai* mutants identified amongst mutagenized *gai* populations.
Mutants exhibiting an increased plant height relative to the progenitor *gai* (regardless of the extent) were isolated for further analyses. Five such mutants are shown here, compared with WT (right) and a *gai* mutant plant (left). The mutants show varying degrees of tallness. All plants were germinated on agarose before being transplanted to normal F2 soil and grown at 22–24 °C under 16-h light/8-h dark photoperiod (irradiance 120 μmol of photons/m^2 per second). Photo of the plants were taken when they were six-week old. Scale bar = 3 cm.

6.2.2 Intragenic *gai* nonsense and frame shift mutations generally result in complete suppression of *gai*-conferred inhibition of plant growth

Among the 69 tall mutant *gai* plants with intragenic secondary mutations, 30 individuals were found to contain a nonsense mutation, whilst one had a frame shift due to a 1-bp deletion, making up a total of 18 different mutations distributed across *gai* after excluding duplicates with identical mutations (Figure 6.4A). As shown in Figure 6.4B, the deletion and most of the nonsense mutations resulted in complete suppression of *gai*-conferred inhibition of stem elongation, suggesting that they are null mutations. Nevertheless, several of these mutants remained slightly yet significantly shorter than WT, perhaps due to poor seed germination or

seedling establishment caused by mutational damage. Two notable exceptions are mutants with a nonsense mutation at Q47 and Q229 respectively, which exhibited a height intermediate between WT and the *gai* progenitor (Figure 6.4B). Given the high EMS-induced mutation density (see Chapter 5), it is reasonable to speculate that additional mutations in the background of these two mutant lines might have prevented a complete reversion to WT plant height.

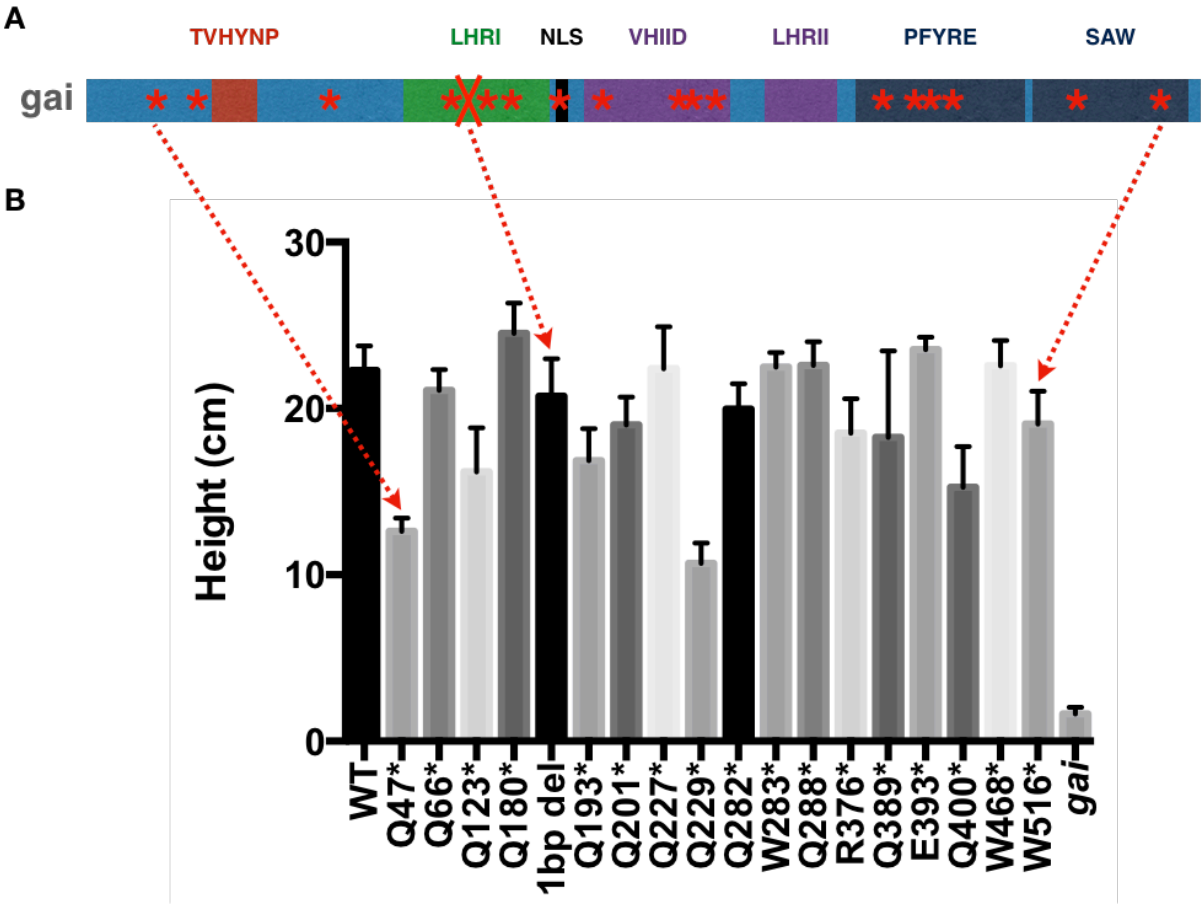


Figure 6.4 Secondary nonsense or deletion mutations in *gai* confer increased plant height. (A) The sites of identified nonsense and deletion mutations with respect to the domain organisation of the mutant gai protein (which lacks the DELLA domain). Asterisks represent the sites of nonsense mutations and the cross represents the site of the 1-bp deletion that results in a frame shift. (B) Heights (inflorescence stem lengths) of M_4 mutant plants at adult stage (six-week old). The sites of the mutated residues are organised on the X axis with regard to their positions along the gai protein. The red dotted lines indicate the sites of the first and last nonsense mutations, as well as the site of the 1-bp deletion. Q47* means that the codon for the 47th amino acid (Q) has been replaced by a premature stop codon. Plants were germinated on agarose before being transplanted to normal F2 soil and grown at 22–24 °C under 16-h light/8-h dark photoperiod (irradiance 120 µmol of photons/m^2 per second). Heights of WT and *gai* are included for comparison. Data are means ± s.d. ($n \geq 10$).

6.2.3 Intragenic missense mutations increase *gai* plant height to various extents

38 out of the 69 tall mutant *gai* plants were found to carry at least one missense mutation, making up a total of 19 distinct amino acid substitution mutations (excluding duplicates with identical mutations), with one line having dual mutations at two different sites (A189 to V and A349 to V, Figure 6.5A). It appears that the distribution of missense mutations causing increased stem elongation is biased towards the C terminal GRAS domain of the gai protein, possibly in accord with previous indications that the N termini of DELLA proteins are primarily responsible for GA signal perception whereas the C termini tend to exert growth repression activities (Hauvermale et al., 2012, Daviere and Achard, 2013, Daviere and Achard, 2016). In contrast to the deletion and nonsense mutations described above (see section 6.2.2), *gai* secondary missense mutations tend to confer partial rather than complete suppression of the dwarf phenotype (Figure 6.5B). Nevertheless, the heights of mutant plants having amino acid substitutions at the end of the PFYRE domain (specifically, S421 to L, S426 to L and E440 to K) are close to those of WT plants (Figure 6.5B), potentially indicating that this region is particularly important for *gai*-mediated inhibition of stem elongation.

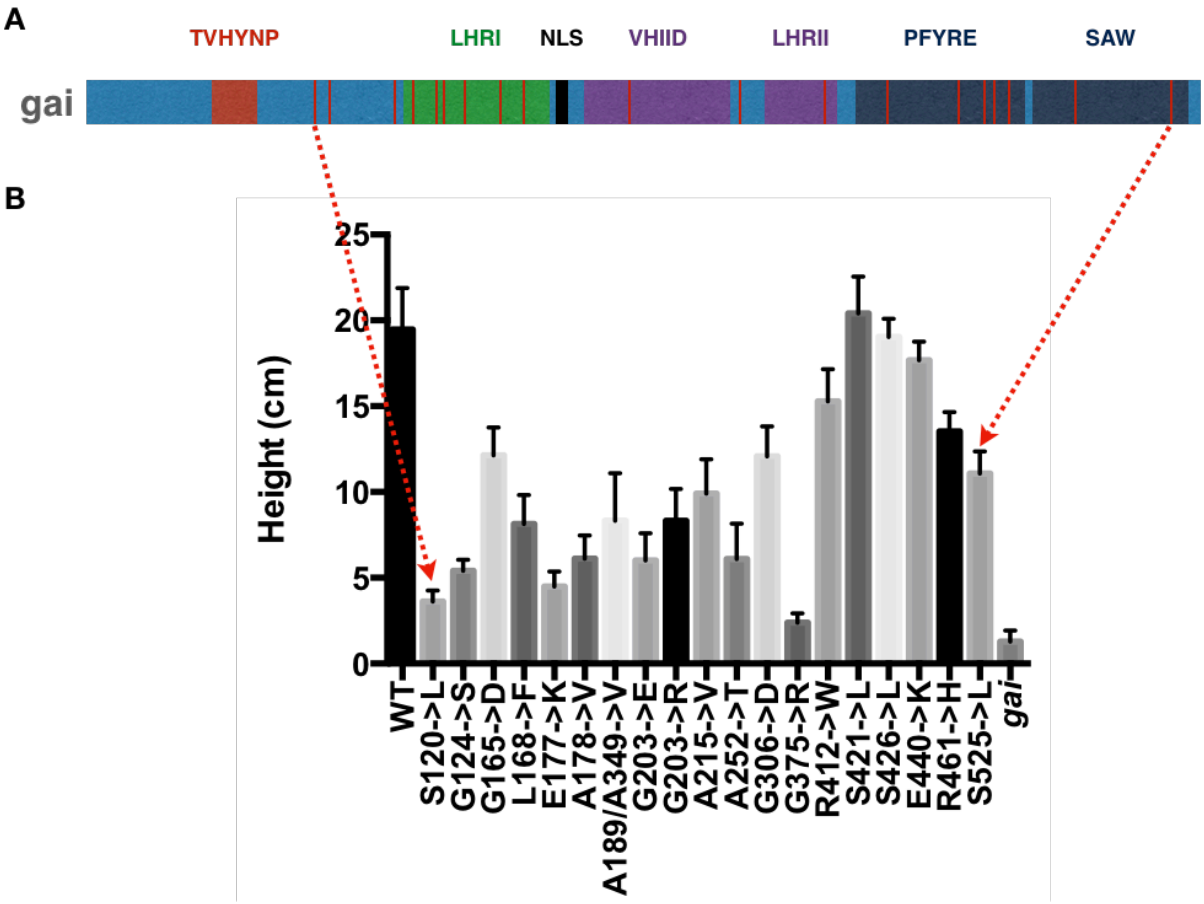


Figure 6.5 Secondary missense mutations in *gai* confer increased plant height.
(A) The sites of identified missense mutations with respect to the domain organisation of the mutant gai protein (which lacks the DELLA domain). Red lines represent the sites of missense mutations. (B) Heights (inflorescence stem lengths) of M_4 mutant plants at adult stage (six-week old). The sites of the mutated residues are organised on the X axis with regard to their positions along the gai protein. The red dotted lines indicate the sites of the first and last amino acid substitutions. S120–>L means that the 120th amino acid (S) has been replaced by an L residue. Plants were germinated on agarose before being transplanted to normal F2 soil and grown at 22–24 °C under 16-h light/8-h dark photoperiod (irradiance 120 µmol of photons/m^2 per second). Heights of WT and *gai* are included for comparison. Data are means ± s.d. ($n \geq 10$).

DELLA proteins are subject to extensive and diverse post-transcriptional modifications which can either promote or repress their activities (Dai and Xue, 2010, Conti et al., 2014, Wang et al., 2014, Zentella et al., 2016, Zentella et al., 2017). For example, SPY-mediated O-fucosylation of *Arabidopsis* RGA has been found to enhance its physical interaction with DELLA-interacting proteins (DIPs) such as BZR1, PIF3 and PIF4, thus antagonising DIP functioning (Zentella et al., 2017). Confirmed and potential RGA O-fucosylation sites have

been identified by liquid chromatography (LC)–electron transfer dissociation (ETD)–MS/MS analysis (Zentella et al., 2017). Based on the sequence homology between RGA and GAI, GAI amino acid S120 is a potential O-fucosylation target that has been mutagenized in one of the tall mutant *gai* plants selected in this study (S120 to L), conferring a slight yet significant increase in plant height (Figure 6.5B). It is therefore possible that this amino acid substitution disrupts SPY-dependent activation of GAI/gai, a hypothesis worthy of further investigation.

6.2.4 Three *sly1* mutations suppress *gai*-conferred inhibition of stem growth and nitrate metabolism

For those tall *gai* mutant plants lacking a detectable secondary mutation in *gai*, Sanger sequencing of the *SLY1* gene was performed, including approximately 300 bp upstream and downstream of the *SLY1* coding region. As mentioned above, a *sly1* gain-of-function mutation resulting in an E138 to K amino acid substitution has been previously shown to partially suppress the dwarf phenotype conferred by *gai* (Dill et al., 2004, Fu et al., 2004). In this present study, not only was the exact same *sly1* mutation (*gar2-1*, Wilson and Somerville, 1995) independently isolated again, two further novel *sly1* mutant alleles (*gar2-2* and *gar2-3* respectively) were also identified as suppressors of *gai*-mediated dwarfism. Unlike the original *gar2-1* mutation, which results in an amino acid substitution within the LSL domain of the SLY1 protein, amino acid substitutions within the GGF domain of SLY1 occur as a result of the *gar2-2* (G84 to D) and *gar2-3* (P114 to L) mutations (Figure 6.6).

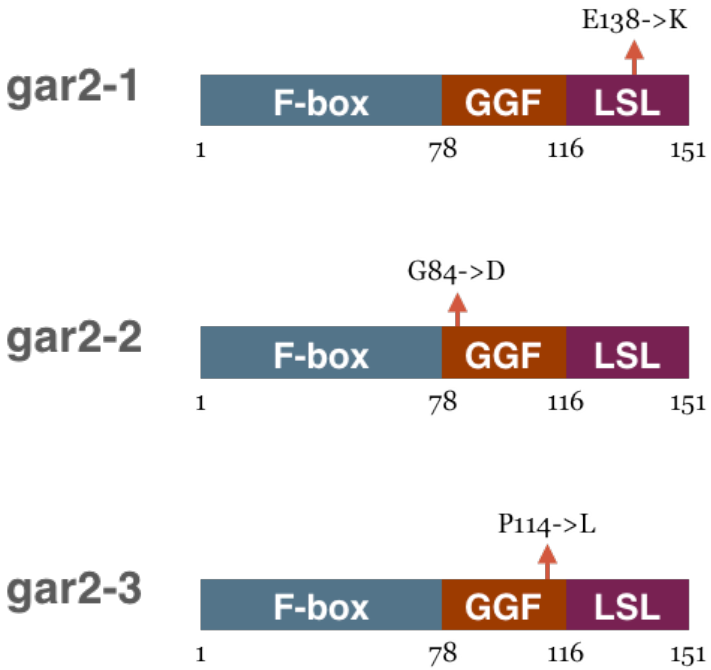


Figure 6.6 Domain organisation of the SLY1/GAR2 protein and positions of amino acid substitutions resulting in suppression of *gai* phenotype.
Schematic representation of the previously defined domain organisation of the SLY1/GAR2 protein (McGinnis et al., 2003). Amino acid substitutions in proteins encoded by the three mutant alleles are labelled at the corresponding sites on the protein. This diagram is not drawn to scale.

Although all three *sly1*/*gar2* mutant alleles confer partially increased stem elongation compared to progenitor *gai* mutant plants, they exhibited significantly different effects on plant growth promotion. Specifically, the extent of suppression of *gai*-mediated dwarfism increases from *gar2-2* to *gar2-1* to *gar2-3*, with the average height of *gar2-3* mutant plants being only slightly less than that of WT plants (Figure 6.7).

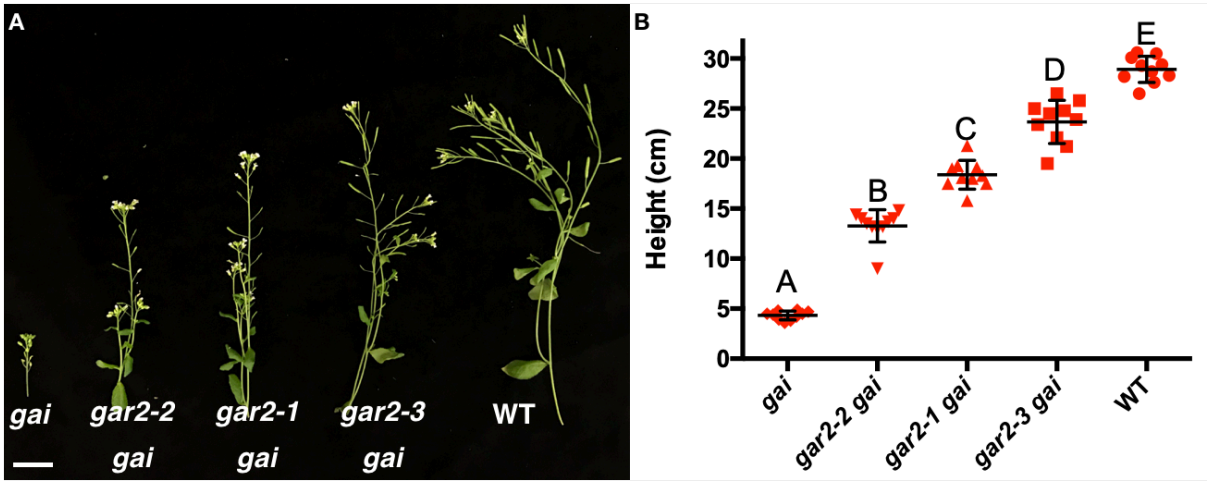


Figure 6.7 Growth phenotypes conferred by the *gar2* mutant alleles.
(A) The *gar2-2*, *gar2-1* and *gar2-3* mutant alleles result in different degrees of suppression of *gai*-mediated dwarfism. All plants were germinated on agarose before being transplanted to normal F2 soil and grown at 22–24 °C under 16-h light/8-h dark photoperiod (irradiance 120 µmol of photons/m^2 per second). Representative homozygous M_4 generation individuals are shown, together with a *gai* and a WT plant for comparison. The photo was taken when the plants were six weeks old. Scale bar = 3 cm. (B) Quantitative measurement of plant heights of WT, the progenitor *gai*, and conferred by the three *sly1*/*gar2* mutations. The lengths of the inflorescence stems of six-week old plants were recorded as a measurement of plant heights. Data are means ± s.d. (n = 10). Statistical analyses were performed with pair-wise student's t-tests. Different uppercase letters depict a P value ≤ 0.0001.

Previous *in vitro* coimmunoprecipitation and yeast two-hybrid assays have shown that the $SLY1^{E138/K}$ protein encoded by the *gar2-1* mutant allele promotes DELLA degradation by enhancing the binding affinity between DELLA and sly1, thus promoting DELLA destruction and increasing plant height (Dill et al., 2004, Fu et al., 2004, Wang et al., 2009a). To determine if the novel *gar2-2* and *gar2-3* mutations suppress *gai* phenotype through a similar mechanism, quantitative yeast two-hybrid protein interaction studies were performed. The DELLA N terminal domain possesses strong self-transactivation activity. This activity can complicate yeast two-hybrid analyses because, when expressed as the bait construct (DELLA-BD), interaction with the prey construct (DIPs-AD) is not required to trigger downstream reporter gene expression (data not shown, Itoh et al., 2002, Dill et al., 2004, Hirano et al., 2012, Yoshida et al., 2014). To circumvent this problem, gai was fused with the activation domain (gai-AD), whilst the SLY1 and sly1 proteins were fused with the binding domain (SLY1/sly1-BD). As

shown in Figure 6.8, no β-galactosidase activity was detected when bait or prey protein partners were expressed alone. As reported previously (Dill et al., 2004, Fu et al., 2004, Hirano et al., 2012), interaction between the gai and WT SLY1 proteins is detectable, despite being of relatively weak strength (Figure 6.8). However, all three mutant sly1 proteins displayed enhanced interaction with gai to various extents, from approximately four-fold (gar2-2) to as much as 75-fold (gar2-3, Figure 6.8). Moreover, the order of increase in the strength of protein interaction corresponds relatively well with that of the increase in adult plant height (Figure 6.7), suggesting that these three mutations in SLY1 result in the suppression of *gai*-dependent dwarfism through different degrees of promotion of their interactions with the gai protein.

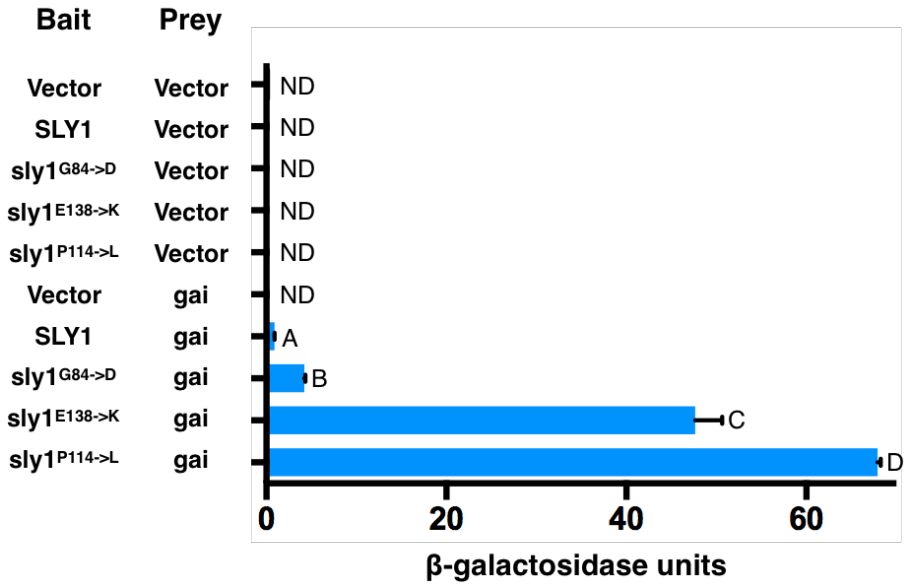


Figure 6.8 Strength of interaction between gai and WT SLY1 or mutant sly1 proteins as measured by quantitative yeast two-hybrid assays.
No protein interaction was detected when bait (SLY1/sly1) or prey (gai) protein partners were expressed alone. The three mutant sly1 proteins exhibited significantly stronger interaction with gai than that between WT SLY1 and gai to various extents. Data are means ± s.d. (n = 3). Statistical analyses were performed with pair-wise student's t-tests. Different uppercase letters depict a P value ≤ 0.0001. ND, not detectable. Chlorophenol red-β-D-galactopyranoside CPRG was chosen as the substrate for the liquid culture β-galactosidase assay (for full details see section 2.10.4).

Peng et al., 1999b demonstrates that in addition to promoting the stem elongation of *gai* mutant plants, the *gar2-1* mutation can also reverse a range of *gai*-dependent phenotypes such as delayed flowering, increased endogenous GA content, and the accumulation of leaf chlorophyll. Accordingly, the possibility that the secondary *gar2-1*, *gar2-2* and *gar2-3* mutations confer increased sensitivity to chlorate toxicity (versus *SLY1 gai* plants) was tested. Figure 6.9 indicates that all three *sly1*/*gar2 gai* mutant lines exhibited a similar chlorate response and are more chlorate sensitive than are progenitor *gai* plants and slightly more resistant than WT plants (Figure 6.9).



Figure 6.9 Chlorate responses of *gai*, WT, and the three *sly1*/*gar gai* mutant plants.
The three *sly1*/*gar2 gai* mutants are more sensitive to chlorate toxicity than *gai* plants and slightly more resistant than WT plants, but not detectably different between themselves. All plants were germinated on agarose before being transplanted to soil and grown at 22–24 °C under 16-h light/8-h dark photoperiod (irradiance 120 µmol of photons/m^2 per second). Four-week old plants were watered with 0.5 mM chlorate to soil saturation, which was repeated every five days (for full details see section 2.4.1). Photos of the plants were taken four weeks after the first chlorate treatment. Inflorescence stems were removed to facilitate the observation of plant chlorate responses. Scale bar = 3 cm.

6.2.5 Initial characterisation of tall mutants lacking detectable mutations in either of *gai* or *SLY1*

Finally, the remaining 15 tall *gai* mutant lines exhibited a wide range of increased plant heights, with some being only slightly taller than *gai* (e.g., W14 and W22), and others almost as tall as WT (e.g., E3.1, Figure 6.10). However, none of these remaining mutant lines carry detectable

mutations in *gai* or *SLY1*. It is of course possible that *gai* or *SLY1* function is altered by mutations outside of the regions sequenced, for example, more than 300 bp upstream of the start codon. Alternatively, the mutations responsible for the tall phenotype might have affected genes other than those already sequenced in this study. Further investigations are required to clarify the causal mutations in these mutant lines.

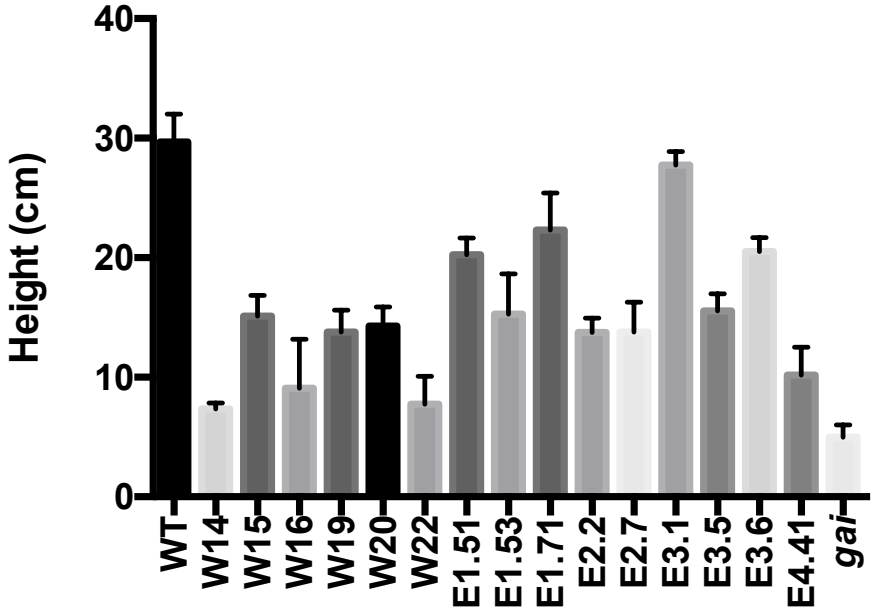


Figure 6.10 Heights of the 15 tall mutant *gai* lines lacking detectable mutations in *gai* or *SLY1*.

In this study, 15 tall mutant *gai* lines were isolated with a variety of plant height (measured at six-week stage) without detectable mutations in *gai* or *SLY1*. This figure shows the heights of homozygous M_4 populations of these tall mutants. The heights of WT and *gai* are included for comparison. All plants were germinated on agarose before being transplanted to normal F2 soil and grown at 22–24 °C under 16-h light/8-h dark photoperiod (irradiance 120 μmol of photons/m^2 per second). The lengths of the inflorescence stems of six-week old plants were recorded as a measurement of plant heights. Data are means ± s.d. (n = 10).

6.2.6 Initial characterisation of a tall *gai* mutant exhibiting a retained chlorate resistance phenotype

Although the tall *gai* mutants described in this chapter were selected on the basis of alteration of plant height, they were growing on chlorate-treated rather than normal soil, enabling a preliminary observation of their chlorate response to be made. Interestingly, when the E3.1 mutant line was first identified on account of its suppression of *gai*-conferred dwarfism, it was noted that it also displayed an apparent chlorate resistance phenotype similar to that of progenitor *gai* plants. Further characterisation was therefore carried out for E3.1 as well as for another tall *gai* mutant, E3.5, a line which was not detectably resistant to chlorate when originally isolated. Both E3.1 and E3.5 plants lack detectable mutations in *gai* or *SLY1* (see section 6.2.5).

As shown in Figure 6.10 and Figure 6.11, both E3.1 and E3.5 plants exhibited a tall phenotype compared to progenitor *gai* plants. The height of the E3.1 mutant line is very similar to that of WT, whilst the E3.5 mutant line is significantly shorter than both E3.1 and WT plants (Figure 6.11). When M_4 homozygotes from these two mutant lines were treated with chlorate, the E3.5 mutant plants displayed an intermediate degree of resistance to chlorate toxicity compared to WT and *gai* plants (Figure 6.12). On the other hand, despite being taller than E3.5, the E3.1 mutant plants appeared to be more resistant to chlorate than both WT and E3.5 plants, and displayed a similar chlorate response as did *gai* plants (Figure 6.2). Thus, unlike in the E3.5 mutant line, the correlation between *gai*-conferred repression of stem elongation and nitrate metabolism is disrupted in the E3.1 mutant line. “Clean-up” backcrossing of E3.1 with *gai* is currently in progress in the hope of eventually identifying the gene responsible for this phenotype through whole-genome sequencing analysis.

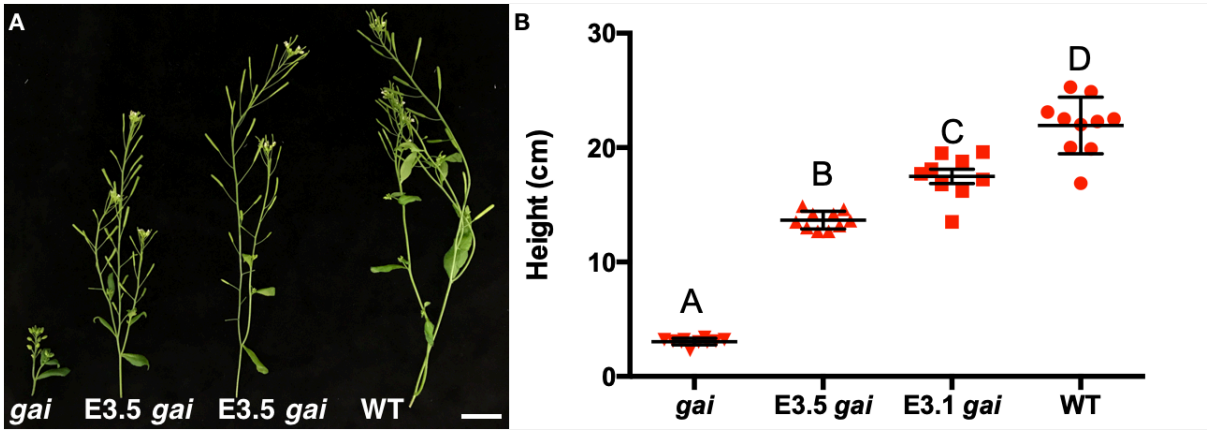


Figure 6.11 Growth phenotypes of E3.5 and E3.1 plants compared to progenitor *gai* and WT plants.

(A) The E3.5 and E3.1 mutant lines exhibited different degrees of suppression of *gai*-mediated dwarfism. All plants were germinated on agarose before being transplanted to normal F2 soil and grown at 22–24 °C under 16-h light/8-h dark photoperiod (irradiance 120 µmol of photons/m^2 per second). Representative homozygous M_4 individuals are shown alongside a *gai* and a WT plant. The photo was taken when the plants were six weeks old. Scale bar = 3 cm. (B) Quantitative measurement of plant heights of WT, progenitor *gai*, and the E3.5 and E3.1 mutant line plants. The lengths of the inflorescence stems of six-week old plants were recorded as a measurement of plant heights. Data are means ± s.d. (n = 10). Statistical analyses were performed with pair-wise student's t-tests. Different uppercase letters depict a P value ≤ 0.001.

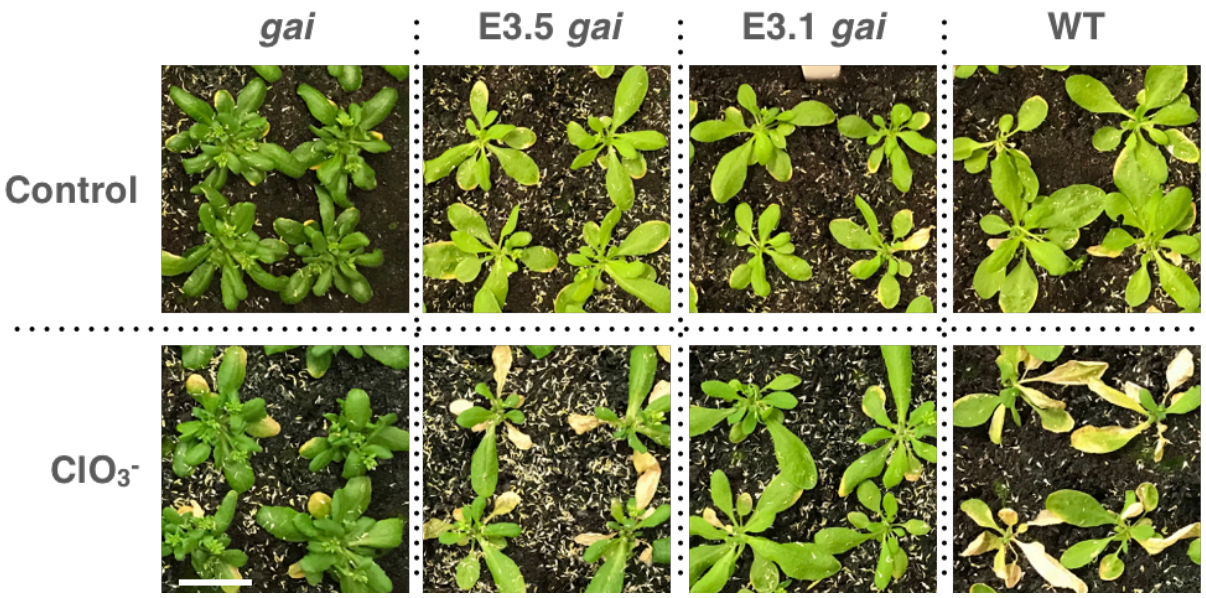


Figure 6.12 Chlorate responses of WT, *gai*, E3.5 and E3.1 mutant plants.
Both E3.5 and E3.1 mutant lines exhibited a tall phenotype relative to progenitor *gai* plants. However, whilst the E3.5 mutant plants are accordingly more sensitive to chlorate toxicity compared to *gai*, the E3.1 mutant plants displayed a similar degree of resistance to chlorate as did *gai* mutant plants, indicating that the correlation between *gai*-dependent inhibition of plant growth and nitrate metabolism is somehow broken in this mutant line. Homozygous M_4 generation plants of the mutant lines are shown in this Figure. All plants were germinated on agarose before being transplanted to soil and grown at 22–24 °C under 16-h light/8-h dark photoperiod (irradiance 120 µmol of photons/m^2 per second). Four-week old plants were watered with 0.5 mM chlorate to soil saturation, which was repeated every five days (for full details see section 2.4.1). Photos of the plants were taken one week after the first chlorate treatment. Inflorescence stems were removed to facilitate the observation of plant chlorate responses. Scale bar = 3 cm.

6.3 Discussion

6.3.1 General comments on the tall mutants with intragenic nonsense or frame shift mutations in *gai*

It has been more than two decades since the first genetic screen for mutations suppressing the dwarf phenotype conferred by the *gai* mutation was carried out (Peng and Harberd, 1993). Thanks to the rapidly developing sequencing technology and the consequent reduction in cost,

high-throughput Sanger sequencing analyses can be performed easily for target genes (i.e. *gai* and *SLY1* in this study) to quickly determine if the causal mutations are intragenic or extragenic. Compared to the number of mutant lines selected for altered chlorate responses (see Chapter 5), many more mutants were isolated for exhibiting an increased plant height among the same EMS-mutagenized *gai* population, suggesting that the suppressors of *gai*-mediated dwarfism arise more frequently. In addition, these tall *gai* mutants reverted the growth repression conferred by *gai* to a range of extents. As reported previously (Peng and Harberd, 1993, Carol et al., 1995, Peng and Harberd, 1997a), most mutants with a height similar to or indistinguishable from that of WT plants (i.e. complete suppression of *gai*-dependent dwarfism) were found to contain intragenic nonsense or frame shift mutations in *gai* that lead to its loss-of-function.

However, it is worth noting that nonsense mutations in DELLA genes are not necessarily equivalent to null mutations. On the contrary, the wheat Green Revolution mutant alleles, *Rht-B1b* and *Rht-D1b*, contain premature stop codons within the N terminal LEQLE domain, and yet confer a dwarf phenotype (Peng et al., 1999a). This seemingly contradictory phenomenon can be explained by the translational reinitiation of the *Rht* gene at the methionine-rich MAMGM motif, which immediately follows the LEQLE domain, and thus producing stabilised DELLA proteins lacking the GA-responsive N termini (Peng et al., 1999a, Van De Velde et al., 2017). It was not known whether mutations of the same property exist in *Arabidopsis* DELLAs. In this study, a nonsense mutation replacing the 47th amino acid (Q) with a premature stop codon was isolated as a suppressor for *gai*-mediated dwarfism. This mutation is located immediately before the LEQLE domain of GAI/gai, and in theory would not affect the dwarf phenotype conferred by the *gai* mutation if translational reinitiation occurs at one of the following methionine residues. Given that the MAMGM domain is unique to

DELLA proteins in monocots, it is possible that translation of the *Arabidopsis gai* gene (and potentially other DELLA genes in dicots) cannot be reinitiated like wheat *Rht* at their N termini.

6.3.2 The tall mutants with missense mutations in *gai* represent a valuable genetic resource for the functional characterisation of DELLA subdomains

As described in Chapter 1 section 1.2.2, DELLA proteins can be roughly divided into two parts, the DELLA-specific N terminal domain and the C terminal GRAS domain (Pysh et al., 1999, Itoh et al., 2005a). From previous genetic screens, it has been found that mutations in the N termini can be gain-of-function mutations that confer a dwarf phenotype (Peng et al., 1997, Dill et al., 2001, Gubler et al., 2002, Asano et al., 2009), whereas mutations in the C termini are usually loss-of-function mutations that lead to a slender phenotype (Silverstone et al., 1998, Ikeda et al., 2001, Bassel et al., 2008, Weston et al., 2008). Therefore, the functions of the N and C termini of DELLA proteins are often associated with GA signal perception and growth repression, respectively (Hauvermale et al., 2012, Daviere and Achard, 2013, Daviere and Achard, 2016). However, accumulating evidence seems to suggest that this functional differentiation is an outdated oversimplification. Two novel amino acid substitution mutations in the C terminal GRAS domains of the DELLA proteins in *Brassica rapa* (BrRGA1, Q328 to R within the VHIID subdomain) and rice (SLR1, G576 to V within the SAW subdomain) have been shown to confer a semi-dwarf and a dwarf phenotype, respectively (Muangprom et al., 2005, Hirano et al., 2010). Detailed characterisation of the effects of these mutations on the encoded mutant proteins indicates that they disrupt the interaction between DELLAs and F-box protein components of SCF ubiquitin ligases, thus resulting in the accumulation of stabilised DELLAs (Muangprom et al., 2005, Hirano et al., 2010). Further alanine scanning experiments with rice SLR1 reveal that all subdomains in the C terminus, with the exception

of the LHRI domain, contribute to stabilising the interaction between SLR1 and the GID2 F-box protein preceding SLR1 degradation (Hirano et al., 2010). Nevertheless, substituting random C terminal amino acids with alanine has only resulted in a slender phenotype, possibly due to the fact that the resultant loss of SLR1 suppressive function generally outweighs the effect of the disrupted SLR1-GID2 interaction (Hirano et al., 2010). On the other hand, the N terminal domains of SLR1, especially TVHYNP, possess a strong transactivation activity that has been shown to be important for SLR1 to exert its suppressive activities (Ikeda et al., 2001, Hirano et al., 2012). Moreover, adding another layer of complexity, the specific functions of the individual DELLA subdomains remain to be fully elucidated (Hirano et al., 2010, Hauvermale et al., 2012).

In this study, 19 individual missense mutations in *gai* were shown to suppress *gai*-mediated inhibition of stem elongation to various extents. Interestingly, all 19 mutations are located within the C terminus GRAS domain, agreeing with the previous findings that despite having a relatively weak transactivation activity compared to the N terminal motifs, the C terminal subdomains are essential for the growth-suppressive activities of DELLAs (Ikeda et al., 2001, Hirano et al., 2012). In an attempt to determine the relative contribution of various C terminal subdomains to the suppressive function of rice SLR1, Hirano et al., 2012 created 14 mutant SLR1 proteins lacking the DELLA domain and fused to VP16 (ΔDELLA-SLR1-VP16, so that they are GA-irresponsive but maintain a strong transactivation activity) with 14 conserved C terminal amino acids being exchanged to alanine, and transformed them into the *slr1* loss-of-function mutant rice. All subdomains in the C terminus (specifically, LHRI, VHIID, LHRII, PFYRE and SAW) were found to be involved in exerting the suppressive activity of SLR1. However, based on the difference in height among these mutant lines, it was concluded that the VHIID and LHRII motifs play a relatively minor role compared to the other three motifs in

mediating SLR1 suppressive activity (Hirano et al., 2012). Accordingly, among the 19 *gai* missense mutants identified in this study, only one contains a mutation in the VHIID domain and one contains a mutation in the LHRII domain, with the latter having a simultaneous mutation in the LHRI domain, which seems to confirm that the VHIID and LHRII motifs have a relatively small effect on DELLA-mediated inhibition of plant growth. On the contrary, whilst the amino acid substitution located at the start of the PFYRE domain resulted in a slight increase in plant height, the three amino acid substitutions located at the end of this motif almost completely reverted *gai*-conferred dwarfism, suggesting that the end of the PFYRE domain might play an important role in inhibiting stem elongation. Interestingly, no known DELLA-DIP interaction requires specifically the PFYRE domain, although the binding between DELLAs and ARABIDOPSIS RESPONSE REGULATOR1 (ARR1) involves the entire GRAS domain except for the LHRI motif to regulate root meristematic growth and seedling de-etiolation (Marin-de la Rosa et al., 2015).

In addition to altering DELLA-DIP interactions, amino acid substitutions in gai might affect post-translational modifications that stabilise DELLAs, and subsequently lead to a reduced repression of plant growth. O-fucosylation of DELLAs by SPY has been shown to induce conformational change of DELLA proteins, and therefore promote their activities (Zentella et al., 2017). Although biochemical evidence for O-fucosylation modification has only been demonstrated for two *Arabidopsis* DELLA proteins, RGA and RGL1 (Zentella et al., 2017), S120 of GAI has been identified in this study as a potential site of O-fucosylation (based on sequence homology between GAI and RGA) that has been substituted by L in one of the tall *gai* mutant lines. It would be interesting to examine in future studies whether this residue can actually be O-fucosylated by SPY, and whether this amino acid substitution results in destabilisation of gai.

Overall, the list of *gai* missense mutations conferring an increase in plant height isolated in this study provides a valuable genetic resource for future investigations of the molecular mechanism of DELLA-mediated repression of plant growth. After all, DIPs and their downstream target genes that are directly involved in regulating stem elongation are far from being fully identified (Hirano et al., 2012). Further experiments, such as yeast two-hybrid screens for these mutant *gai* proteins against a population of known DIPs, should be performed to determine which DELLA-DIP interaction is affected in each case, and how it correlates with the resultant increase in plant height. In addition, it is possible that one or several of the amino acid substitutions identified in this study, depending on which subdomains they are located in, affect stem elongation without having an effect on *gai*-dependent inhibition of nitrate metabolism. Therefore, a chlorate assay for these tall mutants could potentially distinguish specific amino acids that are responsible for growth inhibition from those contributing to repressing nitrate assimilation.

6.3.3 Novel mutant sly1 proteins identified in this study confer an enhanced interaction with gai

In *Arabidopsis* and rice, DELLA proteins are subject to poly-ubiquitination by the $SCF^{SLY1/GID2}$ ubiquitin ligase before their degradation by the 26S proteasome, making it an important pathway for regulating DELLA activities and therefore plant growth (McGinnis et al., 2003, Sasaki et al., 2003, Dill et al., 2004, Fu et al., 2004). The specificity of the $SCF^{SLY1/GID2}$ complex is controlled by the F-box containing SLY1/GID2 protein, which binds to the Skp1 component of the E3 ubiquitin ligase through its N terminal F-box motif (Schulman et al., 2000, Gagne et al., 2002). On the other hand, the C terminus of SLY1/GID2 is responsible for targeting the GRAS domains of DELLA proteins through specific protein-protein interactions

(Kipreos and Pagano, 2000, Vierstra, 2003). Nevertheless, it is not clear to date which SLY1/GID2 C terminal motif(s), GGF, LSL, or both, are required for interacting with DELLAs. In *Arabidopsis*, Fu et al., 2004 showed that the LSL motif of SLY1 is both necessary and sufficient for GAI-SLY1 interaction. In rice, however, it has been shown that the substitution of most conserved amino acids in the GGF and LSL motifs of GID2 to alanine significantly compromises or completely eliminates the SLR1-GID2 interaction (Hirano et al., 2010). Moreover, whilst the truncated GID2 protein containing the intact GGF and LSL domains (E114-P193) is capable of interacting with SLR1, the more truncated form of GID2 lacking a few amino acids in the GGF domain (N123-P193) failed to interact with SLR1 (Hirano et al., 2010). Both of these results demonstrate that the GGF domain of GID2 is essential for recognising SLR1 as the substrate of the E3 ubiquitin ligase complex.

The genetic screen for suppressors of *gai*-mediated growth repression described in this chapter has yielded a *sly1*/*gar2* mutant isolated before, *gar2-1* (Wilson and Somerville, 1995). The resultant amino acid substitution of E137 to K in the LSL motif leads to a stronger interaction between gar2-1 and gai than that between SLY1 and gai, making it the first ever mutation in an F-box protein that enhances its substrate binding capacity (Dill et al., 2004, Fu et al., 2004). In fact, Dill et al., 2004 demonstrates that the strength of interaction between gar2-1 and gai is 3-4 folds higher than that between SLY1 and gai, whereas the strength of interaction between gar2-1 and rga-Δ17 (RGA protein lacking the DELLA motif) is 30-40 folds higher than that between SLY1 and rga-Δ17. Curiously, this research reveals a much more dramatic increase in the strength of gar2-1-gai interaction compared to SLY1-gai (approximately 45 folds), which is probably due to the different quantitative yeast two-hybrid techniques employed in these two studies resulting in a difference in detection sensitivities (Dill et al., 2004).

Furthermore, two novel *sly1*/*gar2* mutations, *gar2-2* and *gar2-3*, were identified from the mutagenized *gai* population for exhibiting an increased stem elongation. Similar to *gar2-1*, these new mutations enhance the physical interaction between gar2 and gai to different extents, and the strength of interaction correlates relatively well with the final height of the mutant plants. Nevertheless, additional experiments, such as quantitative fluorescence lifetime imaging microscopy (FLIM) analysis ought to be performed to confirm that the alteration in sly1/gar2-gai interaction occurs *in vivo*. More importantly, semi-quantitative cell-free degradation assay is currently in progress to verify that these three mutant forms of SLY1 directly promote the degradation of gai, and possibly other DELLA proteins as well. Interestingly, the *gar2-2* and *gar2-3* mutations resulted in amino acid substitutions in the GGF motif of SLY1, which seems to suggest that this motif is also involved in the recognition of SLY1 substrates. Alternatively, the overall 3D structure of the SLY1 protein might be modified in a way that affects its binding with DELLAs. Future protein structural comparisons of WT and the mutant sly1/gar2 proteins should clarify the mechanism of the increased interaction with their substrates.

Finally, chlorate toxicity assay demonstrates that all three *sly1*/*gar2* mutant alleles in the *gai* background confer an increase in chlorate sensitivity compared to *gai*. This observation is in accordance with previous reports that most *gai*-conferred phenotypes investigated, including the inhibition of stem elongation and flowering, are at least partially suppressed in the *gar2-1* mutant (Wilson and Somerville, 1995, Peng et al., 1999b). In fact, it has been hypothesised before that the *gar2-1* mutation might also reduce the abundance of the other four *Arabidopsis* DELLA proteins, and therefore exerting a more global effect on the GA-DELLA signalling pathway of the mutant plant (Fu et al., 2004). Further in-depth characterisation of *gar2-1*, as well as the two new *gar* mutants described in this study, are required to confirm this speculation.

6.3.4 General comments on the tall mutants lacking detectable mutations in *gai* or *SLY1*

With regard to the 15 tall *gai* mutant lines without detectable mutations in *gai* or *SLY1*, it cannot be concluded at this stage that their *gai* or *SLY1* function is not altered given the limited regions of these two genes sequenced. Mutations might occur at sites relatively far away from the start or stop codons of these genes, and are therefore not detected here. Alternatively, these mutant lines might contain mutations in genes not yet examined in this study. Here, three genes that are involved in regulating the GA-DELLA signalling pathway are discussed as being potentially mutated in these lines, although it is entirely possible that the causal mutations reside in other genes. First, given that RGA and GAI redundantly regulate stem elongation (Dill et al., 2001, King et al., 2001), and that *rga* loss-of-function mutant alleles can suppress dwarfism conferred by the *ga1-3* mutation (Silverstone et al., 1997), it is possible that some of these mutant lines that partially recover the height inhibition by *gai* possess a null mutation in *RGA*. Second, as described above, multiple mutant alleles of *spy* can increase plant height to various extents when being crossed into the *gai* mutant background, depending on the strengths of the mutant alleles. More specifically, whilst *spy-4*, one of the strongest known *spy* alleles, is almost fully epistatic to *gai*, *spy-5* and *spy-7*, two weaker *spy* alleles, partially suppress *gai*-conferred growth inhibition (Carol et al., 1995, Wilson and Somerville, 1995, Jacobsen et al., 1996, Peng et al., 1999b). Last but not least, in *Arabidopsis*, *SNEEZY* (*SNE*), the homolog of *SLY1*, is often overlooked as it plays a minor role in regulating DELLA protein abundance compared to *SLY1* (Ariizumi and Steber, 2011, Ariizumi et al., 2011). Nevertheless, it has been shown that the lack of *SLY1* in the *sly1-10* mutant can be partially compensated by overexpressing *SNE* (Fu et al., 2004). Therefore, it is reasonable to speculate that gain-of-function mutant alleles of *SNE*, similar to the three *sly1*/*gar2* mutations identified in this study,

can also result in the suppression of *gai*-conferred phenotypes. Future whole-genome sequencing analyses should reveal the identities of the causal mutations in these mutant lines.

One of the major goals of the mutant screens performed in this research is to genetically uncouple *gai*-conferred inhibition of plant growth and nitrate metabolism (see Chapter 5 for *gai* mutants with altered chlorate responses whilst maintaining a dwarf stature). Intriguingly, one of the 15 tall *gai* mutant lines lacking detectable mutations in *gai* or *SLY1* (E3.1) displayed a chlorate resistance phenotype similar to progenitor *gai* plants. In other words, E3.1 mutant plants retain the relatively poor nitrogen-use efficiency conferred by the *gai* mutation whilst the growth inhibition is relieved. Hence, the causal mutation is likely to be independent of the GA-DELLA signalling pathway. Furthermore, it is probably worth performing a systematic chlorate assay for all of these 15 tall *gai* mutant lines to see if any other mutants exhibit a chlorate response that is disproportional to their heights.

6.3.5 Concluding remarks

Chapter 6 outlines a forward genetic screen of EMS-mutagenized M_1 and M_2 plants in the *gai* mutant background, aiming for the identification of mutants that suppress the *gai*-conferred inhibition of stem elongation. Depending on the natures of the causal mutations, these tall *gai* mutants have been initially divided into three categories. First, mutant lines with secondary intragenic nonsense, frame shift or missense mutations in *gai* provide new insights into the regulatory properties of DELLA proteins, and serve as a valuable genetic resource for the determination of the specific functions of the DELLA subdomains. Second, a previously identified *sly1* mutant, *gar2-1*, and two novel *sly1*/*gar2* mutants were isolated for reverting the inhibition of plant growth as well as nitrate metabolism mediated by the *gai* mutation. Similar

to *gar2-1*, protein interaction analysis suggests that the two new *sly1*/*gar2* mutations probably also promote DELLA degradation through enhancing sly1-DELLA interaction, and therefore antagonising DELLA activities. Finally, for tall *gai* mutants lacking detectable mutations in *gai* or *SLY1*, future whole-genome sequencing analyses will reveal the causal mutations in these mutant lines. One mutant belonging to the third category was found to be as resistant to chlorate toxicity as the progenitor *gai*, indicating that it suppresses *gai*-conferred dwarfism without altering the repression of nitrate metabolism. It would be interesting for further work to be done to identify the mutation responsible for the uncoupling of plant growth and nitrate metabolism regulation in this mutant line.

CHAPTER 7. General Discussion

7.1 Overview

The development and adoption of modern semi-dwarf crop varieties of cereals have led to a striking increase in global crop yields since the first Green Revolution in the 1960s (Trewavas, 2001, Hazell, 2009). The semi-dwarfism of Green Revolution varieties (GRVs) of wheat and rice is conferred by stabilised DELLA proteins, which inhibit plant growth (Peng et al., 1999a, Monna et al., 2002, Sasaki et al., 2002, Spielmeyer et al., 2002). As a result, more energy is diverted to grain filling from stem growth, and the yield-compromising effect of "lodging" (the collapsing of elongated stems) is reduced (Hedden, 2003). However, it was recently discovered that the accumulation of DELLA proteins exerts a negative pleiotropic effect on nitrogen-use efficiency (NUE) in both Green Revolution wheat and rice (Gooding et al., 2012, Li et al., 2018). This project aims to contribute to the understanding of the underlying mechanism of DELLA-mediated inhibition of nitrate metabolism (and therefore NUE), starting with the investigation of the *Arabidopsis thaliana* gain-of-function *gai* mutant as the model system for GRVs.

A nutrient-rich soil-based chlorate (the toxic chemical analogue of nitrate) assay was devised to confirm that, like modern GRV crop species, *Arabidopsis gai* is also deficient in nitrate metabolism. From there onwards, two parallel approaches were taken to proceed with this project. First, step-by-step analyses were carried out in an attempt to understand the regulatory relationship between the GA-DELLA signalling pathway and nitrate metabolism. Then, reverse genetic studies targeting the DELLA-interacting PIF proteins were performed to

determine if they mediate the DELLA-dependent inhibition of nitrate assimilation. Second, attempts were made through forward genetic screens on chlorate using the *gai* mutant as the starting material, in the hope of identifying novel mutations that uncouple *gai*-conferred repression of plant growth and nitrate metabolism. Meanwhile, some progress has been made with respect to the functional characterisation of DELLA subdomains with regard to plant height regulation, as well as the understanding of the DELLA degradation pathway through the interaction with the F-box containing SLY1 protein.

This chapter summarises and discusses the major findings described in this thesis, with a particular focus on the possibility of extending what has been discovered in the plant model organism *Arabidopsis* in this study to crop species. The ultimate goal of this research is to contribute to the development of the next generation GRVs maintaining the yield benefit of semi-dwarfism but with a reduced reliance on external fertiliser application.

7.2 DELLAs Negatively Regulate Plant Nitrate Assimilation

DELLA proteins are master regulators in plants, and the five *Arabidopsis* DELLAs have both shared and distinct roles in regulating almost all aspects of plant growth and development including seed germination, stem elongation, developmental stage transitions and stress responses (Gao et al., 2011). Because of the pleiotropic nature of DELLAs, it is perhaps not surprising that modern semi-dwarf crop varieties with stabilised DELLA proteins exhibit their high-yielding traits at the expense of other undesirable consequences. For example, the semi-dwarf *Rht-B1b* and *RhtD1-b* alleles in wheat confer a reduction in grain size (Miralles et al., 1998), as well as light-insensitive elongation of the coleoptile, a problem particularly

detrimental to early seedling establishment under drought conditions (Chapman et al., 2007). A re-evaluation of *sd1*-mediated lodging-resistance in rice showed that the combined effect of decreased lignin content and culm diameter in *sd1* semi-dwarf rice actually reduces its total biomass and resistance to stem breakage (Okuno et al., 2014). In addition, it has been found that loss-of-function mutations in GA biosynthesis in sorghum result in a dwarf stature with culms susceptible to bending, potentially explaining why DELLA-accumulating mutants have never been artificially selected for during sorghum breeding history (Ordonio et al., 2014). More recently, a negative correlation between wheat NUE and the severity of dwarfing conferred by different *Rht* alleles has been identified (Gooding et al., 2012), indicating a previously uncharacterised regulatory relationship between the GA-DELLA signalling pathway and nitrogen metabolism.

With a particular focus on nitrate as the predominant nitrogen source in most agriculture soils (Crawford and Forde, 2002), it was discovered that the *Arabidopsis* GRV model *gai* mutant is more resistant to chlorate toxicity than WT, indicating that its nitrate metabolism is somehow downregulated. A novel grafting technique was developed in this study to distinguish between the shoot- and/or root-dependency of *gai*-mediated chlorate resistance, and therefore providing insights into the potential explanation for the compromised nitrate metabolism. Grafting experiments imply that the chlorate resistance phenotype conferred by *gai* is largely dependent on the shoot rather than on the root. Enzymatic assays then confirm that shoot nitrate reductase activity is significantly reduced in *gai* compared to WT, whilst no difference in nitrite reductase activity was detected. Similarly, the *ga5* mutant, which is deficient in GA biosynthesis, also exhibited a chlorate resistance phenotype, reduced nitrate reductase activity and unaffected nitrite reductase activity compared to WT, suggesting that the negative effect on nitrate assimilation is due to the accumulation of DELLAs regardless of the underlying mechanism.

Moreover, the same phenotypes were observed in the Green Revolution *sd1 indica* rice used in agriculture, an observation which is consistent with semi-dwarf crop varieties displaying a low NUE.

Despite the above, gene transcript analyses in *Arabidopsis* detected no apparent difference in the mRNA abundances of the two nitrate reductase genes, *NIA1* and *NIA2*, between WT and the *gai* mutant, suggesting that the repression of nitrate reductase activity by *gai* might occur post-translationally. Unexpectedly, the *gai* mutation increases the mRNA abundances of genes encoding the major nitrate transporters, as well as that of mRNA encoding NAR2, the partner protein of the NRT2 nitrate transporters. It is unresolved in this study whether the upregulation of the nitrate transporter genes is a direct effect of stabilised DELLA, or is an indirect consequence of the decreased shoot nitrate reductase activity. What is also unknown is whether this leads to a subsequent increase in nitrate uptake from the media.

During the writing of this thesis, a study was published which reports a global negative effect of accumulating DELLA (SLR1) on NUE in *sd1* mutant rice (Li et al., 2018). Specifically, SLR1 is capable of interacting with GROWTH REGULATORY FACTOR4 (GRF4) competitively with GRF-INTERACTING FACTOR1 (GIF1), which antagonises the positive regulatory role played by the GRF4-GIF1 complex in the transcriptional activation of a range of genes related to nitrogen metabolism, including the major nitrate and ammonium transporters, nitrate reductase, glutamine synthase and NADH-GOGAT (Li et al., 2018). Consequently, the increased GRF4 abundance conferred by the gain-of-function *GRF4*$^{NITROGEN\text{-}MEDIATED\ GROWTH\ RESPONSES2(NGR2)}$ allele in both *sd1* rice and *Rht* wheat leads to an enhanced nitrogen metabolism without affecting the yield benefit of semi-dwarfism, making *GRF4* an important target for biotechnological modifications in the future of crop breeding (Li

et al., 2018). In *Arabidopsis*, nine GRF members have been identified, which are responsible for mediating multiple growth and developmental processes such as organogenesis, leaf size and shape control, flower development, and ovule formation (Kim et al., 2003, Kim and Kende, 2004, Kim and Lee, 2006, Yang et al., 2009). To our knowledge, an interaction between DELLA proteins and GRFs, or the regulation of nitrate metabolism by GRFs, has not yet been demonstrated in *Arabidopsis*. It would be interesting to determine if any of the *Arabidopsis* GRF proteins share similar regulatory properties as rice GRF4. Nevertheless, the inhibitory effect of the rice SLR1 DELLA protein on nitrate metabolism through repressing nitrate reductase activity is in agreement with findings described in this thesis. However, the DELLA (SLR1) accumulation-mediated inhibition of nitrate uptake in rice (Li et al., 2018) appears not to be conserved in the DELLA-accumulating *Arabidopsis gai* or *ga5* mutants, at least as based on the grafting and RT-PCR analyses results presented in this thesis. Further investigations are required to clarify whether the regulation of nitrate uptake by DELLA proteins varies in different plant species.

7.3 PIFs are Promising Targets for Enhancing Future Crop NUE

It has been increasingly recognised that the functional significances of PIF proteins are not restricted to their roles as major mediators of plant light signalling. Instead, PIFs act as central signalling hubs that are embedded in the complex network of various signalling pathways to regulate downstream biological activities including seed germination, shade avoidance responses, thermomorphogenesis, and reproductive organ development, mainly through transcriptional modifications (e.g., Pagnussat et al., 2005, Casson et al., 2009, Franklin et al., 2011, Lee and Thomashow, 2012, Leivar et al., 2012a, Leivar et al., 2012b). In addition, the

regulatory relationship between PIF proteins and nitrate metabolism has been previously explored in one study, which reports that PIF4 upregulates the mRNA abundance of *NRT1.1* while downregulating that of *NIA2*, therefore promoting nitrate uptake while repressing nitrate reductase activity (Jonassen et al., 2009).

DELLAs exert a light-independent inhibitory effect on the activities of PIFs through the combined effect of PIF sequestration from the target promoters and more dramatically, PIF degradation (de Lucas et al., 2008, Feng et al., 2008, Gallego-Bartolome et al., 2010, Li et al., 2016). Hence, PIF-regulated developmental processes, exemplified by the promotion of seedling hypocotyl elongation during skotomorphogenesis, are antagonised by DELLA accumulation (vonArnim and Deng, 1996, Alabadi et al., 2004, Leivar et al., 2008). Given that the DELLA-accumulating *Arabidopsis gai* mutant displayed a repressed nitrate assimilation, various single and multiple *pif* knock-out mutants were investigated in this study to advance the understanding of the roles played by PIFs in nitrate metabolism regulation.

Using the same series of experiments as for the *gai* mutant, strikingly similar phenotypes were observed for the quadruple loss-of-function *pifq* mutant lacking members of the PIF quartet (*pif1 pif3 pif4 pif5*). Specifically, *pifq* mutant plants exhibited strong resistance to chlorate toxicity compared to WT, which is largely shoot- rather than root-dependent. *pifq*-conferred chlorate resistance is likely attributable to the dramatic decrease in shoot nitrate reductase activity relative to that in WT, whereas the nitrite reductase activity is similar in both genotypes. However, unlike *gai*, the *pifq* mutation results in a mild reduction in the mRNA abundance of *NIA2*, the major *Arabidopsis* nitrate reductase gene, while having no obvious effect on the mRNA levels of the other nitrogen-related genes examined in this study. Two previously established PIF-binding motifs were identified in the promoter region of *NIA2*, suggesting the

potential for the direct binding of PIF proteins. Nevertheless, given the disparity between the large effect on nitrate reductase enzymatic activity and the moderate effect on *NIA2* mRNA abundance, it cannot be concluded at this stage that PIF proteins do not additionally affect the post-translational modification of nitrate reductase, possibly downstream of DELLAs (see below).

In an attempt to scrutinise the relative contribution of each PIFq member to the inhibition of nitrate metabolism, investigations were carried out for the single loss-of-function mutants, *pif1*, *pif3*, *pif4* and *pif5*. It was evident that the *pif3* mutation alone is sufficient to inhibit nitrate reductase activity to the same level as *pifq*, and therefore confer the observed chlorate resistance phenotype. Moreover, overexpression of *PIF3* in the *pif3* mutant background can complement *pif3*-mediated repression of nitrate metabolism. On the other hand, the regulatory effect mediated by the other PIFq members, including PIF4, on nitrate assimilation is negligible under our experimental conditions. The apparent contradiction between this study and that conducted by Jonassen et al., 2009 with regard to the regulatory role played by PIF4 in regulating nitrate metabolism might be explained by the different growth conditions and developmental stages of the plants investigated. It has been well-established that light signal inhibits the promotion of seedling hypocotyl elongation mediated by PIF3. However, DELLA proteins antagonise this process through repressing PIF3 activity (Feng et al., 2008, Li et al., 2016). It is therefore reasonable to hypothesise that nitrate metabolism is similarly regulated by the balance of DELLAs and PIF3 levels. Additionally, given its prominent involvement in the phytochrome-mediated light signalling pathway, PIF3 is speculated to be a signalling hub integrating the internal phytohormone GA-DELLA and the external light signals to finetune downstream nitrate reductase activity and therefore nitrate metabolism (Figure 7.1).

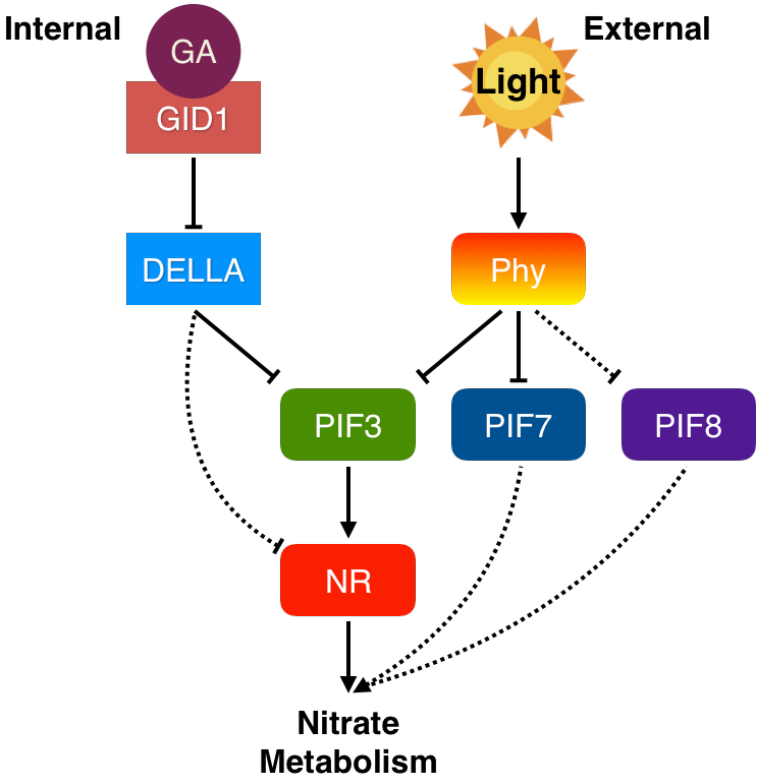


Figure 7.1 The working model of the regulation of nitrate metabolism by the GA-DELLA and PIF signalling pathways.
DELLAs repress nitrate reductase activity and therefore nitrate metabolism possibly through inhibiting PIF3-mediated upregulation of nitrate reductase activity, which is opposed by the presence of GA. PIF3 is also degraded in response to photoactivation of PhyB by light. Therefore, PIF3 integrates the internal GA phytohormone signalling and external light signalling to regulate nitrate metabolism. In addition, PIF7 and PIF8 upregulate nitrate metabolism, but not through the activation of nitrate reductase activity. Dotted lines indicate potential regulatory connections that require further investigation.

Chlorate toxicity assays for the knock-out mutants of PIF members that do not belong to the PIFq family reveal unexpected roles played by PIF7 and PIF8 in promoting nitrate metabolism. Contrary to *pif3*, nitrate reductase activities of the *pif7* and *pif8* mutants are not detectably different from that of WT. Accordingly, the protein-protein interaction between DELLAs and PIF7 or PIF8 is yet to be concretely demonstrated. Therefore, PIF7 and PIF8 might upregulate nitrate metabolism through a distinct mechanism that awaits future elucidation (Figure 7.1).

Compared to the wealth of knowledge about PIF proteins in the model organism *Arabidopsis thaliana*, the molecular identities and functional significances of PIFs in other plants, especially crops, are only recently being explored. Sequence analysis of the rice genome identified six putative PIF-Like (PIL) members, OsPIL11 to OsPIL16, based on the fact that they contain the highly-conserved bHLH domain for DNA binding and the APB (active phytochrome B-binding) motif similar to *Arabidopsis* PIFs (Nakamura et al., 2007). Furthermore, overexpressing five of these OsPILs (OsPIL11 to OsPIL15) in *Arabidopsis* resulted in elongated hypocotyls during photomorphogenesis, suggesting that these OsPILs are likely to share functional similarities with *Arabidopsis* PIFs (Nakamura et al., 2007). However, it was later discovered that the functions of OsPILs are inconsistent when being expressed in different species under different conditions. For example, when overexpressed in tobacco, *OsPIL11* represses seedling growth and promotes cotyledon enlargement under continuous red light (Li et al., 2012b), whereas the overexpression of *OsPIL15* in rice inhibits seedling elongation through antagonising auxin signalling as well as cell wall biogenesis and organisation (Zhou et al., 2014). Detailed characterisation of OsPIL13 has revealed its involvement in promoting rice internode elongation and chlorophyll biosynthesis (Todaka et al., 2012, Sakuraba et al., 2017). However, unlike AtPIFs, OsPIL13 does not physically bind to OsPhyB or interact with the GA-DELLA signalling pathway (Todaka et al., 2012). Finally, OsPIL14 has been shown to interact with OsPhyB (and therefore also known as OsPIF4) and act as the transcriptional repressor for the major stress mediator gene, *DEHYDRATION-RESPONSIVE ELEMENT-BINDING1B* (*OsDREB1B*), indicating that OsPIL14 might be responsible for integrating light and stress signals (Cordeiro et al., 2016).

In another agriculturally important monocot plant, maize (*Zea mays*), the understanding of its seven putative PIF proteins (ZmPIF1 to ZmPIF7) is expanding rapidly (Kumar et al., 2016).

Ectopic expression of *ZmPIF4* and *ZmPIF5* in *Arabidopsis* has demonstrated that they can not only partially complement *pifq*-mediated phenotypes, but also confer exaggerated shade avoidance responses (Shi et al., 2018). Moreover, ZmPIF4 can interact with *Arabidopsis* RGA, which further suggests that PIF functions might be evolutionarily conserved in maize and *Arabidopsis* to a certain extent (Shi et al., 2018). Additionally, both ZmPIF1 and ZmPIF3 have been found to be important mediators of plant stress responses. Transgenic rice plants overexpressing either of these two *PIF* genes are more resistant to drought and salt stresses via the upregulation of genes involved in ABA signalling (Gao et al., 2015, Gao et al., 2018a, Gao et al., 2018b). Furthermore, unlike most other stress-resistance genes that generally reduce productivity when overexpressed, the accumulation of ZmPIF1 and ZmPIF3 has a positive and neutral effect on grain yield, respectively (Gao et al., 2018a, Gao et al., 2018b).

Taken together, priority should first be given to resolving the molecular mechanism of PIF (specifically, PIF3, PIF7 and PIF8)-mediated promotion of nitrate metabolism in the model plant *Arabidopsis*. Given that PIFs are master regulators of multiple biological activities, it is also essential to determine whether increasing PIF abundance would have any undesirable pleiotropic effect such as eliciting constitutive shade avoidance responses due to decreased sensitivity to shade. Next, progress is being made in identifying and characterising PIF family members in crop plants. If the regulatory role played by PIFs in nitrate assimilation is evolutionarily conserved in *Arabidopsis* and crop plants, PIF proteins will become important targets for biotechnological modifications in the future of breeding, especially when some PIF members (especially ZmPIF1) have already been demonstrated to be involved in promoting crop productivity.

7.4 Future Work for the Novel Mutants Identified in This Study

Semi-dwarf GRVs of crops accumulate growth-repressing DELLA proteins, which unfortunately leads to a reduced NUE and therefore the requirement for environmentally-unsustainable levels of fertiliser application (Gooding et al., 2012, Li et al., 2018). This study demonstrates that this negative pleiotropic effect of DELLAs is conserved in *Arabidopsis*, since the dwarf *Arabidopsis gai* mutant is resistant to chlorate toxicity. Next, in an attempt to genetically uncouple *gai*-conferred inhibition of stem elongation and nitrate metabolism, forward genetic screens were performed for EMS- and FN-mutagenized *gai* populations. The resultant mutants can be divided into three major categories. First, three independent mutant lines were isolated for exhibiting a dwarf stature with an increased sensitivity to chlorate toxicity. These mutants are particularly worthy of further investigation as they are likely to have improved nitrate metabolism while maintaining the yield benefit of dwarfism. Ongoing whole-genome sequencing analyses should reveal the responsible mutations, which could potentially provide valuable insights into the molecular mechanism of *gai*-dependent inhibition of nitrate metabolism, as well as new strategies for enhancing NUE. Second, several mutants displayed enhanced chlorate resistance relative to the progenitor *gai*, suggesting that their nitrate metabolism is further repressed by the new mutations. Unsurprisingly, two of these mutations occurred respectively in the low-affinity nitrate transporter gene *NRT1.1* and the major nitrate reductase gene *NIA2*, both previously shown to confer a strong chlorate resistance phenotype when mutated. Meanwhile, whole-genome sequencing analysis of another mutant identified *UMAMIT32* as a candidate gene involved in modulating chlorate response and therefore nitrate metabolism. Five of the more than 40 *Arabidopsis* UMAMIT members have been demonstrated to mediate amino acid transport at specific plant tissues (Ladwig et al., 2012,

Muller et al., 2015, Besnard et al., 2016). Therefore, the *umamit32* mutation might somehow disrupt the transport of amino acids, which indirectly represses nitrate/chlorate uptake and/or assimilation. However, not all known UMAMIT proteins transport amino acids. For example, the substrate of UMAMIT5 is auxin rather than amino acids (Ranocha et al., 2010). Similarly, UMAMIT32 might be more directly involved in the transport of nitrate and/or chlorate. To date, very little is known about the biological functions of UMAMIT family proteins in *Arabidopsis*, let alone in other plants. The findings in this study suggest that it is probably worthy of systematically characterising the functions of UMAMIT family members in both *Arabidopsis* and crops, and determine if modifying their functions has the potential of contributing to promoting nitrogen metabolism and therefore yield. Finally, one mutant exhibiting a tall phenotype while maintaining the relative resistance to chlorate toxicity was isolated, which also breaks the correlation between *gai*-conferred inhibition of stem elongation and nitrate metabolism. The causal mutation awaits identification, which might improve our understanding of DELLA-regulated biological processes.

As discussed above, the negative pleiotropic effects of DELLAs as the master regulators of growth and development, such as the repression of NUE, prevent the maximum yield potentials of modern semi-dwarf crop varieties from being achieved. DELLA proteins function mainly by recruiting downstream DIPs and assembling transcription complexes through their GRAS domains (Locascio et al., 2013). Given that the interactions with different DIPs are mediated by different DELLA GRAS subdomains, it is theoretically possible to induce specific amino acid substitutions that disrupt certain DELLA-mediated processes without affecting others, which provides an additional mean of avoiding the negative pleiotropic effects of DELLAs (Van De Velde et al., 2017). A successful example of this is the barley *sln1m* mutant, which causes an amino acid substitution within the LHRI motif of DELLA that leads to increased

grain size without significantly affecting plant height (Chandler and Harding, 2013). This thesis presents a range of secondary missense mutations in the C terminal GRAS domain of *gai*, which result in different extents of suppression of dwarfism, presumably due to modifications of various DELLA-DIP interactions. Since the regulatory mechanism of DELLA-mediated inhibition of stem elongation remains largely unresolved, these mutants represent a useful genetic resource for identifying the specific amino acids or subdomains essential for particular DELLA-DIP interactions that are involved in the regulation of plant height. This importance extents to cereal crop species, in which only very few DELLA-DIP interactions have been investigated to date (e.g., Nakamura et al., 2013, Yu et al., 2014, Li et al., 2018). Finally, two novel *sly1*/*gar2* mutants, together with the previously identified *gar2-1*, were isolated in this mutant screen for reverting *gai*-conferred dwarfism as well as the deficiency in nitrate metabolism in the *gai* mutant background. Yeast two-hybrid assays indicate that all three *sly1*/*gar2* mutations enhance the interaction between gai and sly1/gar2, potentially promoting subsequent gai degradation, although future protein structural analyses will be required to fully understand the detailed mechanism of such promoted interaction. In conclusion, further characterisation of these tall *gai* mutants will expand our knowledge of the GA-DELLA signalling pathway, which might provide new insights into developing new crop plants with minimised negative pleiotropic effects of stabilised DELLA proteins.

Reference list

ACHARD, P., CHENG, H., DE GRAUWE, L., DECAT, J., SCHOUTTETEN, H., MORITZ, T., VAN DER STRAETEN, D., PENG, J. & HARBERD, N. P. 2006. Integration of plant responses to environmentally activated phytohormonal signals. *Science,* 311**,** 91-94.

ACHARD, P. & GENSCHIK, P. 2009. Releasing the brakes of plant growth: how GAs shutdown DELLA proteins. *Journal of Experimental Botany,* 60**,** 1085-1092.

ACHARD, P., GONG, F., CHEMINANT, S., ALIOUA, M., HEDDEN, P. & GENSCHIK, P. 2008a. The cold-inducible CBF1 factor-dependent signaling pathway modulates the accumulation of the growth-repressing DELLA proteins via its effect on gibberellin metabolism. *The Plant Cell,* 20**,** 2117-2129.

ACHARD, P., GUSTI, A., CHEMINANT, S., ALIOUA, M., DHONDT, S., COPPENS, F., BEEMSTER, G. T. & GENSCHIK, P. 2009. Gibberellin signaling controls cell proliferation rate in Arabidopsis. *Current Biology,* 19**,** 1188-1193.

ACHARD, P., RENOU, J.-P. P., BERTHOMÉ, R., HARBERD, N. P. & GENSCHIK, P. 2008b. Plant DELLAs restrain growth and promote survival of adversity by reducing the levels of reactive oxygen species. *Current Biology,* 18**,** 656-660.

ADDO-QUAYE, C., TUINSTRA, M., CARRARO, N., WEIL, C. & DILKES, B. P. 2018. Whole-genome sequence accuracy is improved by replication in a population of mutagenized sorghum. *G3-Genes Genomes Genetics,* 8**,** 1079-1094.

ALABADI, D., GIL, J., BLAZQUEZ, M. A. & GARCIA-MARTINEZ, J. L. 2004. Gibberellins repress photomorphogenesis in darkness. *Plant Physiology,* 134**,** 1050-1057.

AN, F., ZHANG, X., ZHU, Z., JI, Y., HE, W., JIANG, Z., LI, M. & GUO, H. 2012. Coordinated regulation of apical hook development by gibberellins and ethylene in etiolated Arabidopsis seedlings. *Cell Research,* 22**,** 915-927.

ANDREWS, M. 1986. The partitioning of nitrate assimilation between root and shoot of higher-plants. *Plant Cell and Environment,* 9**,** 511-519.

APPELHAGEN, I., LU, G. H., HUEP, G., SCHMELZER, E., WEISSHAAR, B. & SAGASSER, M. 2011. TRANSPARENT TESTA1 interacts with R2R3-MYB factors and affects early and late steps of flavonoid biosynthesis in the endothelium of Arabidopsis thaliana seeds. *The Plant Journal,* 67**,** 406-419.

ARCHACKI, R., BUSZEWICZ, D., SARNOWSKI, T. J., SARNOWSKA, E., ROLICKA, A. T., TOHGE, T., FERNIE, A. R., JIKUMARU, Y., KOTLINSKI, M., IWANICKA-NOWICKA, R., KALISIAK, K., PATRYN, J., HALIBART-PUZIO, J., KAMIYA, Y., DAVIS, S. J., KOBLOWSKA, M. K. & JERZMANOWSKI, A. 2013. BRAHMA ATPase of the SWI/SNF chromatin remodeling complex acts as a positive regulator of gibberellin-mediated responses in Arabidopsis. *Plos One,* 8, e58588.

ARIIZUMI, T., LAWRENCE, P. K. & STEBER, C. M. 2011. The role of two f-box proteins, SLEEPY1 and SNEEZY, in Arabidopsis gibberellin signaling. *Plant Physiology,* 155**,** 765-775.

ARIIZUMI, T., MURASE, K., SUN, T. P. & STEBER, C. M. 2008. Proteolysis-independent downregulation of DELLA repression in Arabidopsis by the gibberellin receptor GIBBERELLIN INSENSITIVE DWARF1. *The Plant Cell,* 20**,** 2447-2459.

ARIIZUMI, T. & STEBER, C. M. 2011. Mutations in the F-box gene SNEEZY result in decreased Arabidopsis GA signaling. *Plant Signaling & Behavior,* 6**,** 831-833.

ARNAUD, N., GIRIN, T., SOREFAN, K., FUENTES, S., WOOD, T. A., LAWRENSON, T., SABLOWSKI, R. & OSTERGAARD, L. 2010. Gibberellins control fruit patterning in Arabidopsis thaliana. *Genes & Development,* 24**,** 2127-2132.

ASANO, K., HIRANO, K., UEGUCHI-TANAKA, M., ANGELES-SHIM, R. B., KOMURA, T., SATOH, H., KITANO, H., MATSUOKA, M. & ASHIKARI, M. 2009. Isolation and characterization of dominant dwarf mutants, Slr1-d, in rice. *Molecular Genetics and Genomics,* 281**,** 223-231.

ASHIKARI, M., SASAKI, A., UEGUCHI-TANAKA, M., ITOH, H., NISHIMURA, A., DATTA, S., ISHIYAMA, K., SAITO, T., KOBAYASHI, M., KHUSH, G. S., KITANO, H. & MATSUOKA, M. 2002. Loss-of-function of a rice gibberellin biosynthetic gene, GA20 oxidase (GA20ox-2), led to the rice 'green revolution'. *Breeding Science,* 52**,** 143-150.

BACHMANN, M., SHIRAISHI, N., CAMPBELL, W. H., YOO, B. C., HARMON, A. C. & HUBER, S. C. 1996. Identification of Ser-543 as the major regulatory phosphorylation site in spinach leaf nitrate reductase. *The Plant Cell,* 8**,** 505-517.

BAE, G. & CHOI, G. 2008. Decoding of light signals by plant phytochromes and their interacting proteins. *Annual Review of Plant Biology,* 59**,** 281-311.

BAI, M. Y., SHANG, J. X., OH, E., FAN, M., BAI, Y., ZENTELLA, R., SUN, T. P. & WANG, Z. Y. 2012. Brassinosteroid, gibberellin and phytochrome impinge on a common transcription module in Arabidopsis. *Nature Cell Biology,* 14**,** 810-817.

BAILEY, P. C., MARTIN, C., TOLEDO-ORTIZ, G., QUAIL, P. H., HUQ, E., HEIM, M. A., JAKOBY, M., WERBER, M. & WEISSHAAR, B. 2003. Update on the basic helix-loop-helix transcription factor gene family in Arabidopsis thaliana. *The Plant Cell,* 15**,** 2497-2502.

BARNES, M. R. 2007. *Bioinformatics for geneticists: a bioinformatics primer for the analysis of genetic data,* Chichester, England ; Hoboken, NJ, Wiley.

BARTSCH, H., OHSHIMA, H., PIGNATELLI, B. & CALMELS, S. 1992. Endogenously formed N-nitroso compounds and nitrosating agents in human cancer etiology. *Pharmacogenetics,* 2**,** 272-277.

BASSEL, G. W., MULLEN, R. T. & BEWLEY, J. D. 2008. procera is a putative DELLA mutant in tomato (Solanum lycopersicum): effects on the seed and vegetative plant. *Journal of Experimental Botany,* 59**,** 585-593.

BELFIELD, E. J., DING, Z. J., JAMIESON, F. J. C., VISSCHER, A. M., ZHENG, S. J., MITHANI, A. & HARBERD, N. P. 2018. DNA mismatch repair preferentially protects genes from mutation. *Genome Research,* 28**,** 66-74.

BELFIELD, E. J., GAN, X., MITHANI, A., BROWN, C., JIANG, C., FRANKLIN, K., ALVEY, E., WIBOWO, A., JUNG, M., BAILEY, K., KALWANI, S., RAGOUSSIS, J., MOTT, R. & HARBERD, N. P. 2012. Genome-wide analysis of mutations in mutant lineages selected following fast-neutron irradiation mutagenesis of Arabidopsis thaliana. *Genome Research,* 22**,** 1306-1315.

BERNARDO-GARCIA, S., DE LUCAS, M., MARTINEZ, C., ESPINOSA-RUIZ, A., DAVIERE, J. M. & PRAT, S. 2014. BR-dependent phosphorylation modulates PIF4 transcriptional activity and shapes diurnal hypocotyl growth. *Genes & Development,* 28**,** 1681-1694.

BESNARD, J., PRATELLI, R., ZHAO, C. S., SONAWALA, U., COLLAKOVA, E., PILOT, G. & OKUMOTO, S. 2016. UMAMIT14 is an amino acid exporter involved in phloem unloading in Arabidopsis roots. *Journal of Experimental Botany,* 67**,** 6385-6397.

BOSTON, P. F., JACKSON, P., KYNOCH, P. A. M. & THOMPSON, R. J. 1982. Purification, properties, and immunohistochemical localization of human-brain 14-3-3 protein. *Journal of Neurochemistry,* 38**,** 1466-1474.

BOUGUYON, E., BRUN, F., MEYNARD, D., KUBES, M., PERVENT, M., LERAN, S., LACOMBE, B., KROUK, G., GUIDERDONI, E., ZAZIMALOVA, E., HOYEROVA, K., NACRY, P. & GOJON, A. 2015. Multiple mechanisms of nitrate sensing by Arabidopsis nitrate transceptor NRT1.1. *Nature Plants,* 1, 15015.

BOURSIAC, Y., LERAN, S., CORRATGE-FAILLIE, C., GOJON, A., KROUK, G. & LACOMBE, B. 2013. ABA transport and transporters. *Trends in Plant Science,* 18**,** 325-333.

BOUTON, S., LEYDECKER, M. T., MEYER, C. & TRUONG, H. N. 2002. Role of gibberellins and of the RGA and GAI genes in controlling nitrate assimilation in Arabidopsis thaliana. *Plant Physiology and Biochemistry,* 40, 939-947.

BRUGGEMANN, E., HANDWERGER, K., ESSEX, C. & STORZ, G. 1996. Analysis of fast neutron-generated mutants at the Arabidopsis thaliana HY4 locus. *The Plant Journal,* 10**,** 755-760.

BU, Q. Y., ZHU, L., DENNIS, M. D., YU, L., LU, S. E. X., PERSON, M. D., TOBIN, E. M., BROWNING, K. S. & HUQ, E. 2011. Phosphorylation by CK2 enhances the rapid light-induced degradation of phytochrome interacting factor 1 in Arabidopsis. *Journal of Biological Chemistry,* 286, 12066-12074.

BUSOV, V. B., JOHANNES, E., WHETTEN, R. W., SEDEROFF, R. R., SPIKER, S. L., LANZ-GARCIA, C. & GOLDFARB, B. 2004. An auxin-inducible gene from loblolly pine (Pinus taeda L.) is differentially expressed in mature and juvenile-phase shoots and encodes a putative transmembrane protein. *Planta,* 218**,** 916-927.

CAMAÑES, G., PASTOR, V. & CEREZO, M. 2012. A deletion in NRT2. 1 attenuates Pseudomonas syringae-induced hormonal perturbation, resulting in primed plant defenses. *Plant Physiology*, 158, 1054-1066.

CAMPBELL, W. H. 2001. Structure and function of eukaryotic NAD(P)H: nitrate reductase. *Cellular and Molecular Life Sciences,* 58**,** 194-204.

CAMPBELL, W. H. & KINGHORN, K. R. 1990. Functional domains of assimilatory nitrate reductases and nitrite reductases. *Trends in Biochemical Sciences,* 15**,** 315-319.

CAROL, P., PENG, J. & HARBERD, N. P. 1995. Isolation and preliminary characterization of gas1-1, a mutation causing partial suppression of the phenotype conferred by the gibberellin-insensitive (gai) mutation in Arabidopsis thaliana (L.) Heyhn. *Planta,* 197**,** 414-417.

CASAL, J. J., FANKHAUSER, C., COUPLAND, G. & BLAZQUEZ, M. A. 2004. Signalling for developmental plasticity. *Trends in Plant Science,* 9**,** 309-314.

CASEBOW, R., HADLEY, C., UPPAL, R., ADDISU, M., LODDO, S., KOWALSKI, A., GRIFFITHS, S. & GOODING, M. 2016. Reduced Height (Rht) Alleles Affect Wheat Grain Quality. *Plos One,* 11, e0156056.

CASSON, S. A., FRANKLIN, K. A., GRAY, J. E., GRIERSON, C. S., WHITELAM, G. C. & HETHERINGTON, A. M. 2009. Phytochrome B and PIF4 regulate stomatal development in response to light quantity. *Current Biology,* 19**,** 229-234.

CASTAINGS, L., CAMARGO, A., POCHOLLE, D., GAUDON, V., TEXIER, Y., BOUTET-MERCEY, S., TACONNAT, L., RENOU, J. P., DANIEL-VEDELE, F., FERNANDEZ, E., MEYER, C. & KRAPP, A. 2009. The nodule inception-like protein 7 modulates nitrate sensing and metabolism in Arabidopsis. *The Plant Journal,* 57**,** 426-435.

CASTILLON, A., SHEN, H. & HUQ, E. 2007. Phytochrome Interacting Factors: central players in phytochrome-mediated light signaling networks. *Trends in Plant Science,* 12**,** 514-521.
CHAMIZO-AMPUDIA, A., SANZ-LUQUE, E., LLAMAS, A., GALVAN, A. & FERNANDEZ, E. 2017. Nitrate Reductase Regulates Plant Nitric Oxide Homeostasis. *Trends in Plant Science,* 22**,** 163-174.
CHANDLER, P. M. & HARDING, C. A. 2013. 'Overgrowth' mutants in barley and wheat: new alleles and phenotypes of the 'Green Revolution' Della gene. *Journal of Experimental Botany,* 64**,** 1603-1613.
CHANDLER, P. M., MARION-POLL, A., ELLIS, M. & GUBLER, F. 2002. Mutants at the Slender1 locus of barley cv Himalaya. Molecular and physiological characterization. *Plant Physiology,* 129**,** 181-190.
CHAPMAN, S. C., MATHEWS, K. L., TRETHOWAN, R. M. & SINGH, R. P. 2007. Relationships between height and yield in near-isogenic spring wheats that contrast for major reduced height genes. *Euphytica,* 157**,** 391-397.
CHEMINANT, S., WILD, M., BOUVIER, F., PELLETIER, S., RENOU, J.-P. P., ERHARDT, M., HAYES, S., TERRY, M. J., GENSCHIK, P. & ACHARD, P. 2011. DELLAs regulate chlorophyll and carotenoid biosynthesis to prevent photooxidative damage during seedling deetiolation in Arabidopsis. *The Plant Cell,* 23**,** 1849-1860.
CHEN, M., CHORY, J. & FANKHAUSER, C. 2004. Light signal transduction in higher plants. *Annual Review of Genetics,* 38**,** 87-117.
CHEN, M., TAO, Y., LIM, J., SHAW, A. & CHORY, J. 2005. Regulation of phytochrome B nuclear localization through light-dependent unmasking of nuclear-localization signals. *Current Biology,* 15**,** 637-642.
CHEN, X., YAO, Q., GAO, X., JIANG, C., HARBERD, N. P. & FU, X. 2016. Shoot-to-root mobile transcription factor HY5 coordinates plant carbon and nitrogen acquisition. *Current biology,* 26**,** 640-646.
CHENG, C. L., DEWDNEY, J., NAM, H. G., DENBOER, B. G. W. & GOODMAN, H. M. 1988. A new locus (Nia-1) in Arabidopsis thaliana encoding nitrate reductase. *The Embo Journal,* 7**,** 3309-3314.
CHENG, H., QIN, L. J., LEE, S. C., FU, X. D., RICHARDS, D. E., CAO, D. N., LUO, D., HARBERD, N. P. & PENG, J. R. 2004. Gibberellin regulates Arabidopsis floral development via suppression of DELLA protein function. *Development,* 131**,** 1055-1064.
CHI, J. C., ROEPER, J., SCHWARZ, G. & FISCHER-SCHRADER, K. 2015. Dual binding of 14-3-3 protein regulates Arabidopsis nitrate reductase activity. *Journal Biological Inorganic Chemistry,* 20**,** 277-286.
CHOPIN, F., ORSEL, M., DORBE, M. F., CHARDON, F., TRUONG, H. N., MILLER, A. J., KRAPP, A. & DANIEL-VEDELE, F. 2007. The Arabidopsis ATNRT2.7 nitrate transporter controls nitrate content in seeds. *The Plant Cell,* 19**,** 1590-1602.
CIOLFI, A., SESSA, G., SASSI, M., POSSENTI, M., SALVUCCI, S., CARABELLI, M., MORELLI, G. & RUBERTI, I. 2013. Dynamics of the shade-avoidance response in Arabidopsis. *Plant Physiology,* 163**,** 331-353.
CLACK, T., MATHEWS, S. & SHARROCK, R. A. 1994. The phytochrome apoprotein family in Arabidopsis is encoded by 5 genes - the sequences and expression of Phyd and Phye. *Plant Molecular Biology,* 25**,** 413-427.
CONTI, L., NELIS, S., ZHANG, C., WOODCOCK, A., SWARUP, R., GALBIATI, M., TONELLI, C., NAPIER, R., HEDDEN, P., BENNETT, M. & SADANANDOM, A.

2014. Small Ubiquitin-like Modifier protein SUMO enables plants to control growth independently of the phytohormone gibberellin. *Developmental Cell,* 28, 102-110.
COOKSON, S. J., WILLIAMS, L. E. & MILLER, A. J. 2005. Light-dark changes in cytosolic nitrate pools depend on nitrate reductase activity in Arabidopsis leaf cells. *Plant Physiology,* 138**,** 1097-1105.
CORDEIRO, A. M., FIGUEIREDO, D. D., TEPPERMAN, J., BORBA, A. R., LOURENCO, T., ABREU, I. A., OUWERKERK, P. B. F., QUAIL, P. H., OLIVEIRA, M. M. & SAIBO, N. J. M. 2016. Rice phytochrome-interacting factor protein OsPIF14 represses OsDREB1B gene expression through an extended N-box and interacts preferentially with the active form of phytochrome B. *Biochimica et Biophysica Acta-Gene Regulatory Mechanisms,* 1859**,** 393-404.
CORRATGE-FAILLIE, C. & LACOMBE, B. 2017. Substrate (un)specificity of Arabidopsis NRT1/PTR FAMILY (NPF) proteins. *Journal of Experimental Botany,* 68**,** 3107-3113.
COWLING, R. J. & HARBERD, N. P. 1999. Gibberellins control Arabidopsis hypocotyl growth via regulation of cellular elongation. *Journal of Experimental Botany,* 50**,** 1351-1357.
CRAWFORD, N. M. 1995. Nitrate: nutrient and signal for plant growth. *The Plant Cell,* 7**,** 859-868.
CRAWFORD, N. M. & FORDE, B. G. 2002. Molecular and developmental biology of inorganic nitrogen nutrition. *Arabidopsis Book,* 1, e0011.
CRAWFORD, N. M. & GLASS, A. D. M. 1998. Molecular and physiological aspects of nitrate uptake in plants. *Trends in Plant Science,* 3, 389-395.
CREIGHTON, M. T., SANMARTIN, M., KATAYA, A. R. A., AVERKINA, I. O., HEIDARI, B., NEMIE-FEYISSA, D., SANCHEZ-SERRANO, J. J. & LILLO, C. 2017. Light regulation of nitrate reductase by catalytic subunits of protein phosphatase 2A. *Planta,* 246**,** 701-710.
DAI, C. & XUE, H. W. 2010. Rice early flowering1, a CKI, phosphorylates DELLA protein SLR1 to negatively regulate gibberellin signalling. *The Embo Journal,* 29**,** 1916-1927.
DANIEL, H. 2004. Molecular and integrative physiology of intestinal peptide transport. *Annual Review of Physiology,* 66**,** 361-384.
DAVID, L. C., BERQUIN, P., KANNO, Y., SEO, M., DANIEL-VEDELE, F. & FERRARIO-MERY, S. 2016. N availability modulates the role of NPF3.1, a gibberellin transporter, in GA-mediated phenotypes in Arabidopsis. *Planta,* 244**,** 1315-1328.
DAVIERE, J. M. & ACHARD, P. 2013. Gibberellin signaling in plants. *Development,* 140, 1147-1151.
DAVIERE, J. M. & ACHARD, P. 2016. A pivotal role of DELLAs in regulating multiple hormone signals. *Molecular Plant,* 9**,** 10-20.
DE LUCAS, M., DAVIÈRE, J.-M., RODRÍGUEZ-FALCÓN, M., PONTIN, M., IGLESIAS-PEDRAZ, J., LORRAIN, S., FANKHAUSER, C., BLÁZQUEZ, M., TITARENKO, E. & PRAT, S. 2008. A molecular framework for light and gibberellin control of cell elongation. *Nature,* 451**,** 480-484.
DE LUCAS, M. & PRAT, S. 2014. PIFs get BRright: PHYTOCHROME INTERACTING FACTORs as integrators of light and hormonal signals. *New Phytologist,* 202**,** 1126-1141.
DECHORGNAT, J., NGUYEN, C. T., ARMENGAUD, P., JOSSIER, M., DIATLOFF, E., FILLEUR, S. & DANIEL-VEDELE, F. 2010. From the soil to the seeds: the long journey of nitrate in plants. *Journal of Experimental Botany,* 62, 1349-1359.

DENG, M. D., MOUREAUX, T., CHEREL, I., BOUTIN, J. P. & CABOCHE, M. 1991. Effects of nitrogen metabolites on the regulation and circadian expression of tobacco nitrate reductase. *Plant Physiology and Biochemistry,* 29**,** 239-247.

DEVLIN, P. F., YANOVSKY, M. J. & KAY, S. A. 2003. A genomic analysis of the shade avoidance response in Arabidopsis. *Plant Physiology,* 133**,** 1617-1629.

DILL, A., JUNG, H. S. & SUN, T. P. 2001. The DELLA motif is essential for gibberellin-induced degradation of RGA. *Proceedings of National Academy of Sciences of the United States of America,* 98**,** 14162-14167.

DILL, A., THOMAS, S. G., HU, J., STEBER, C. M. & SUN, T. P. 2004. The Arabidopsis F-box protein SLEEPY1 targets gibberellin signaling repressors for gibberellin-induced degradation. *The Plant Cell,* 16**,** 1392-1405.

DONG, J., NI, W. M., YU, R. B., DENG, X. W., CHEN, H. D. & WEI, N. 2017. Light-dependent degradation of PIF3 by SCFEBF1/2 promotes a photomorphogenic response in Arabidopsis. *Current Biology,* 27**,** 2420-2430.

DOSE, M. M., HIRASAWA, M., KLEISSANFRANCISCO, S., LEW, E. L. & KNAFF, D. B. 1997. The ferredoxin-binding site of ferredoxin:nitrite oxidoreductase - Differential chemical modification of the free enzyme and its complex with ferredoxin. *Plant Physiology,* 114**,** 1047-1053.

DOUGLAS, P., MOORHEAD, G., HONG, Y., MORRICE, N. & MACKINTOSH, C. 1998. Purification of a nitrate reductase kinase from Spinacea oleracea leaves, and its identification as a calmodulin-domain protein kinase. *Planta,* 206**,** 435-442.

DU, S., ZHANG, Y., LIN, X., WANG, Y. & TANG, C. 2008. Regulation of nitrate reductase by nitric oxide in Chinese cabbage pakchoi (Brassica chinensis L.). *Plant, Cell & Environment,* 31**,** 195-204.

EDWARDS, K., JOHNSTONE, C. & THOMPSON, C. 1991. A simple and rapid method for the preparation of plant genomic DNA for PCR analysis. *Nucleic Acids Research,* 19**,** 1349.

FAN, X., TANG, Z., TAN, Y., ZHANG, Y., LUO, B., YANG, M., LIAN, X., SHEN, Q., MILLER, A. J. & XU, G. 2016. Overexpression of a pH-sensitive nitrate transporter in rice increases crop yields. *Proceedings of the National Academy of Sciences of the United States of America*, 113, 7118-7123.

FANG, L., HOU, X. L., YEN, L., LEE, C., LIU, L., YAN, X. J. & YU, H. 2011. AtPV42a and AtPV42b redundantly regulate reproductive development in Arabidopsis thaliana. *Plos One,* 6, e19033.

FANG, Z., XIA, K., YANG, X., GROTEMEYER, M., MEIER, S., RENTSCH, D., XU, X. & ZHANG, M. 2013. Altered expression of the PTR/NRT1 homologue OsPTR9 affects nitrogen utilization efficiency, growth and grain yield in rice. *Plant Biotechnology Journal,* 11**,** 446-458.

FANKHAUSER, C. & CHEN, M. 2008. Transposing phytochrome into the nucleus. *Trends in Plant Science,* 13**,** 596-601.

FENG, S., MARTINEZ, C., GUSMAROLI, G., WANG, Y., ZHOU, J., WANG, F., CHEN, L., YU, L., IGLESIAS-PEDRAZ, J. M., KIRCHER, S., SCHÄFER, E., FU, X., FAN, L.-M. & DENG, X. 2008. Coordinated regulation of Arabidopsis thaliana development by light and gibberellins. *Nature,* 451**,** 475-479.

FERNANDEZ, E. & GALVAN, A. 2007. Inorganic nitrogen assimilation in Chlamydomonas. *Journal of Experimental Botany,* 58**,** 2279-2287.

FILLEUR, S., DORBE, M. F., CEREZO, M., ORSEL, M., GRANIER, F., GOJON, A. & DANIEL-VEDELE, F. 2001. An Arabidopsis T-DNA mutant affected in Nrt2 genes is impaired in nitrate uptake. *FEBS Letters,* 489, 220-224.

FORDE, B. G. 2000. Nitrate transporters in plants: structure, function and regulation. *Biochimica et Biophysica Acta,* 1465, 219-235.

FOYER, C. H., VALADIER, M. H., MIGGE, A. & BECKER, T. W. 1998. Drought-induced effects on nitrate reductase activity and mRNA and on the coordination of nitrogen and carbon metabolism in maize leaves. *Plant Physiology,* 117**,** 283-292.

FRANKLIN, K. A., LEE, S. H., PATEL, D., KUMAR, S. V., SPARTZ, A. K., GU, C., YE, S. Q., YU, P., BREEN, G., COHEN, J. D., WIGGE, P. A. & GRAY, W. M. 2011. PHYTOCHROME-INTERACTING FACTOR 4 (PIF4) regulates auxin biosynthesis at high temperature. *Proceedings of the National Academy of Sciences of the United States of America,* 108**,** 20231-20235.

FU, X. D., RICHARDS, D. E., FLECK, B., XIE, D. X., BURTON, N. & HARBERD, N. P. 2004. The Arabidopsis mutant sleepy1(gar2-1) protein promotes plant growth by increasing the affinity of the SCFSLY1 E3 ubiquitin ligase for DELLA protein substrates. *The Plant Cell,* 16**,** 1406-1418.

FUJIWARA, T., NAMBARA, E., YAMAGISHI, K., GOTO, D. B. & NAITO, S. 2002. Storage proteins. *Arabidopsis Book,* 1**,** e0020.

FUKAO, T. & BAILEY-SERRES, J. 2008. Submergence tolerance conferred by Sub1A is mediated by SLR1 and SLRL1 restriction of gibberellin responses in rice. *Proceedings of the National Academy of Sciences of the United States of America,* 105**,** 16814-16819.

FUKAZAWA, J., NAKATA, M., ITO, T., YAMAGUCHI, S. & TAKAHASHI, Y. 2010. The transcription factor RSG regulates negative feedback of NtGA20ox1 encoding GA 20-oxidase. *The Plant Journal,* 62**,** 1035-1045.

GABRIELE, S., RIZZA, A., MARTONE, J., CIRCELLI, P., COSTANTINO, P. & VITTORIOSO, P. 2010. The Dof protein DAG1 mediates PIL5 activity on seed germination by negatively regulating GA biosynthetic gene AtGA3ox1. *The Plant Journal,* 61**,** 312-323.

GAGNE, J. M., DOWNES, B. P., SHIU, S. H., DURSKI, A. M. & VIERSTRA, R. D. 2002. The F-box subunit of the SCF E3 complex is encoded by a diverse superfamily of genes in Arabidopsis. *Proceedings of the National Academy of Sciences of the United States of America,* 99**,** 11519-11524.

GALLEGO-BARTOLOME, J., KAMI, C., FANKHAUSER, C., ALABADI, D. & BLAZQUEZ, M. A. 2011. A hormonal regulatory module that provides flexibility to tropic responses. *Plant Physiology,* 156**,** 1819-1825.

GALLEGO-BARTOLOME, J., MINGUET, E. G., MARIN, J. A., PRAT, S., BLAZQUEZ, M. A. & ALABADI, D. 2010. Transcriptional diversification and functional conservation between DELLA proteins in Arabidopsis. *Molecular Biology and Evolution,* 27**,** 1247-1256.

GAMAS, P., DE CARVALHO-NIEBEL, F., LESCURE, N. & CULLIMORE, J. V. 1996. Use of a subtractive hybridization approach to identify new Medicago truncatula genes induced during root nodule development. *Molecular Plant-Microbe Interactions,* 9**,** 233-242.

GAN, X., STEGLE, O., BEHR, J., STEFFEN, J. G., DREWE, P., HILDEBRAND, K. L., LYNGSOE, R., SCHULTHEISS, S. J., OSBORNE, E. J., SREEDHARAN, V. T., KAHLES, A., BOHNERT, R., JEAN, G., DERWENT, P., KERSEY, P., BELFIELD, E. J., HARBERD, N. P., KEMEN, E., TOOMAJIAN, C., KOVER, P. X., CLARK, R. M., RATSCH, G. & MOTT, R. 2011. Multiple reference genomes and transcriptomes for Arabidopsis thaliana. *Nature,* 477**,** 419-423.

GAO, X. H., XIAO, S. L., YAO, Q. F., WANG, Y. J. & FU, X. D. 2011. An updated GA signaling 'relief of repression' regulatory model. *Molecular Plant,* 4**,** 601-606.

GAO, Y., JIANG, W., DAI, Y., XIAO, N., ZHANG, C. Q., LI, H., LU, Y., WU, M. Q., TAO, X. Y., DENG, D. X. & CHEN, J. M. 2015. A maize phytochrome-interacting factor 3 improves drought and salt stress tolerance in rice. *Plant Molecular Biology,* 87**,** 413-428.

GAO, Y., WU, M. Q., ZHANG, M. J., JIANG, W., LIANG, E. X., ZHANG, D. P., ZHANG, C. Q., XIAO, N. & CHEN, J. M. 2018a. Roles of a maize phytochrome-interacting factors protein ZmPIF3 in regulation of drought stress responses by controlling stomatal closure in transgenic rice without yield penalty. *Plant Molecular Biology,* 97**,** 311-323.

GAO, Y., WU, M. Q., ZHANG, M. J., JIANG, W., REN, X. Y., LIANG, E. X., ZHANG, D. P., ZHANG, C. Q., XIAO, N., LI, Y., DAI, Y. & CHEN, J. M. 2018b. A maize phytochrome-interacting factors protein ZmPIF1 enhances drought tolerance by inducing stomatal closure and improves grain yield in Oryza sativa. *Plant Biotechnology Journal,* 16**,** 1375-1387.

GENOUD, T., SCHWEIZER, F., TSCHEUSCHLER, A., DEBRIEUX, D., CASAL, J. J., SCHAFER, E., HILTBRUNNER, A. & FANKHAUSER, C. 2008. FHY1 mediates nuclear import of the light-activated phytochrome A photoreceptor. *Plos Genetics,* 4, e1000143.

GLASS, A. D. & KOTUR, Z. 2013. A reevaluation of the role of Arabidopsis NRT1.1 in high-affinity nitrate transport. *Plant Physiology,* 163, 1103-1106.

GODFRAY, H. C. J., BEDDINGTON, J. R., CRUTE, I. R., HADDAD, L., LAWRENCE, D., MUIR, J. F., PRETTY, J., ROBINSON, S., THOMAS, S. M. & TOULMIN, C. 2010. Food security: the challenge of feeding 9 billion people. *Science,* 327, 812-818.

GOJON, A., KROUK, G., PERRINE-WALKER, F. & LAUGIER, E. 2011. Nitrate transceptor(s) in plants. *Journal of Experimental Botany,* 62,2299-2308.

GOODING, M. J., ADDISU, M., UPPAL, R. K., SNAPE, J. W. & JONES, H. E. 2012. Effect of wheat dwarfing genes on nitrogen-use efficiency. *Journal of Agricultural Science,* 150, 3-22.

GREENE, E. A., CODOMO, C. A., TAYLOR, N. E., HENIKOFF, J. G., TILL, B. J., REYNOLDS, S. H., ENNS, L. C., BURTNER, C., JOHNSON, J. E., ODDEN, A. R., COMAI, L. & HENIKOFF, S. 2003. Spectrum of chemically induced mutations from a large-scale reverse-genetic screen in arabidopsis. *Genetics,* 164**,** 731-740.

GRIFFITHS, A. J. F., WESSLER, S. R., CARROLL, S. B. & DOEBLEY, J. F. 2015. *Introduction to genetic analysis,* New York, NY, W.H. Freeman & Company, a Macmillan Education imprint.

GRIFFITHS, J., MURASE, K., RIEU, I., ZENTELLA, R., ZHANG, Z. L., POWERS, S. J., GONG, F., PHILLIPS, A. L., HEDDEN, P., SUN, T. P. & THOMAS, S. G. 2007. Genetic characterization and functional analysis of the GID1 gibberellin receptors in Arabidopsis (vol 18, pg 3399, 2006). *The Plant Cell,* 19**,** 726-726.

GUAN, P. 2017. Dancing with Hormones: A Current Perspective of Nitrate Signaling and Regulation in Arabidopsis. *Frontiers in Plant Science,* 8**,** 1697.

GUAN, P. Z., WANG, R. C., NACRY, P., BRETON, G., KAY, S. A., PRUNEDA-PAZ, J. L., DAVANI, A. & CRAWFORD, N. M. 2014. Nitrate foraging by Arabidopsis roots is mediated by the transcription factor TCP20 through the systemic signaling pathway. *Proceedings of the National Academy of Sciences of the United States of America,* 111**,** 15267-15272.

GUBLER, F., CHANDLER, P. M., WHITE, R. G., LLEWELLYN, D. J. & JACOBSEN, J. V. 2002. Gibberellin signaling in barley aleurone cells. Control of SLN1 and GAMYB expression. *Plant Physiology,* 129**,** 191-200.

GUO, F. Q., WANG, R., CHEN, M. & CRAWFORD, N. M. 2001. The Arabidopsis dual-affinity nitrate transporter gene AtNRT1.1 (CHL1) is activated and functions in nascent organ development during vegetative and reproductive growth. *The Plant Cell,* 13, 1761-1777.

GUO, F. Q., YOUNG, J. & CRAWFORD, N. M. 2003. The nitrate transporter AtNRT1.1 (CHL1) functions in stomatal opening and contributes to drought susceptibility in Arabidopsis. *The Plant Cell,* 15, 107-117.

HACHIYA, T. & NOGUCHI, K. 2011. Mutation of NRT1.1 enhances ammonium/low pH-tolerance in Arabiopsis thaliana. *Plant Signaling & Behavior,* 6, 706-708.

HARBERD, N. P., BELFIELD, E. & YASUMURA, Y. 2009. The angiosperm gibberellin-GID1-DELLA growth regulatory mechanism: how an "inhibitor of an inhibitor" enables flexible response to fluctuating environments. *The Plant Cell,* 21, 1328-1339.

HARPER, J. W., ADAMI, G. R., WEI, N., KEYOMARSI, K. & ELLEDGE, S. J. 1993. The p21 Cdk-interacting protein Cip1 is a potent inhibitor of G1 cyclin-dependent kinases. *Cell,* 75**,** 805-816.

HARTWECK, L. M., SCOTT, C. L. & OLSZEWSKI, N. E. 2002. Two O-linked N-acetylglucosamine transferase genes of Arabidopsis thaliana L. Heynh. have overlapping functions necessary for gamete and seed development. *Genetics,* 161**,** 1279-1291.

HAUVERMALE, A. L., ARIIZUMI, T. & STEBER, C. M. 2012. Gibberellin signaling: a theme and variations on DELLA repression. *Plant Physiology,* 160**,** 83-92.

HAYWOOD, V., YU, T. S., HUANG, N. C. & LUCAS, W. J. 2005. Phloem long-distance trafficking of Gibberellic acid-insensitive RNA regulates leaf development. *The Plant Journal,* 42**,** 49-68.

HAZELL, P. B. R. 2009. The Asian green revolution. *International Food Policy Research Institute,* 911.

HEDDEN, P. 2003. The genes of the Green Revolution. *Trends in Genetics,* 19, 5-9.

HEDDEN, P. & PHILLIPS, A. L. 2000. Gibberellin metabolism: new insights revealed by the genes. *Trends in Plant Science,* 5**,** 523-530.

HENRY, I. M., NAGALAKSHMI, U., LIEBERMAN, M. C., NGO, K. J., KRASILEVA, K. V., VASQUEZ-GROSS, H., AKHUNOVA, A., AKHUNOV, E., DUBCOVSKY, J., TAI, T. H. & COMAI, L. 2014. Efficient genome-wide detection and cataloging of EMS-induced mutations using exome capture and next-generation sequencing. *The Plant Cell,* 26**,** 1382-1397.

HERSCH, M., LORRAIN, S., DE WIT, M., TREVISAN, M., LJUNG, K., BERGMANN, S. & FANKHAUSER, C. 2014. Light intensity modulates the regulatory network of the shade avoidance response in Arabidopsis. *Proceedings of the National Academy of Sciences of the United States of America,* 111**,** 6515-6520.

HIRANO, K., ASANO, K., TSUJI, H., KAWAMURA, M., MORI, H., KITANO, H., UEGUCHI-TANAKA, M. & MATSUOKA, M. 2010. Characterization of the molecular mechanism underlying gibberellin perception complex formation in rice. *The Plant Cell,* 22**,** 2680-2696.

HIRANO, K., KOUKETU, E., KATOH, H., AYA, K., UEGUCHI-TANAKA, M. & MATSUOKA, M. 2012. The suppressive function of the rice DELLA protein SLR1 is dependent on its transcriptional activation activity. *The Plant Journal,* 71**,** 443-453.

HO, C.-H., LIN, S.-H., HU, H.-C. & TSAY, Y.-F. 2009. CHL1 functions as a nitrate sensor in plants. *Cell,* 138, 1184-1194.

HOFF, T., TRUONG, H. N. & CABOCHE, M. 1994. The use of mutants and transgenic plants to study nitrate assimilation. *Plant Cell and Environment,* 17**,** 489-506.

HORNITSCHEK, P., KOHNEN, M. V., LORRAIN, S., ROUGEMONT, J., LJUNG, K., LOPEZ-VIDRIERO, I., FRANCO-ZORRILLA, J. M., SOLANO, R., TREVISAN, M., PRADERVAND, S., XENARIOS, I. & FANKHAUSER, C. 2012. Phytochrome interacting factors 4 and 5 control seedling growth in changing light conditions by directly controlling auxin signaling. *The Plant Journal,* 71**,** 699-711.

HORNITSCHEK, P., LORRAIN, S., ZOETE, V., MICHIELIN, O. & FANKHAUSER, C. 2009. Inhibition of the shade avoidance response by formation of non-DNA binding bHLH heterodimers. *The Embo Journal,* 28**,** 3893-3902.

HOU, X. L., LEE, L. Y. C., XIA, K. F., YEN, Y. Y. & YU, H. 2010. DELLAs modulate jasmonate signaling via competitive binding to JAZs. *Developmental Cell,* 19**,** 884-894.

HRUZ, T., LAULE, O., SZABO, G., WESSENDORP, F., BLEULER, S., OERTLE, L., WIDMAYER, P., GRUISSEM, W. & ZIMMERMANN, P. 2008. Genevestigator v3: a reference expression database for the meta-analysis of transcriptomes. *Advances in Bioinformatics,* 2008**,** 420747.

HUANG, L., ZHANG, H., ZHANG, H., DENG, X. W. & WEI, N. 2015. HY5 regulates nitrite reductase 1 (NIR1) and ammonium transporter1;2 (AMT1;2) in Arabidopsis seedlings. *Plant Science,* 238, 330-339.

HUANG, N. C., LIU, K. H., LO, H. J. & TSAY, Y. F. 1999. Cloning and functional characterization of an Arabidopsis nitrate transporter gene that encodes a constitutive component of low-affinity uptake. *The Plant Cell,* 11, 1381-1392.

HUANG, S. S., RAMAN, A. S., REAM, J. E., FUJIWARA, H., CERNY, R. E. & BROWN, S. M. 1998. Overexpression of 20-oxidase confers a gibberellin-overproduction phenotype in Arabidopsis. *Plant Physiology,* 118**,** 773-781.

IKEDA, A., UEGUCHI-TANAKA, M., SONODA, Y., KITANO, H., KOSHIOKA, M., FUTSUHARA, Y., MATSUOKA, M. & YAMAGUCHI, J. 2001. slender rice, a constitutive gibberellin response mutant, is caused by a null mutation of the SLR1 gene, an ortholog of the height-regulating gene GAI/RGA/RHT/D8. *The Plant Cell,* 13**,** 999-1010.

IKEDA, Y., KOIZUMI, N., KUSANO, T. & SANO, H. 2000. Specific binding of a 14-3-3 protein to autophosphorylated WPK4, an SNF1-related wheat protein kinase, and to WPK4-phosphorylated nitrate reductase. (vol 275, pg 31698, 2000). *Journal of Biological Chemistry,* 275**,** 41530-41530.

ITOH, H., SASAKI, A., UEGUCHI-TANAKA, M., ISHIYAMA, K., KOBAYASHI, M., HASEGAWA, Y., MINAMI, E., ASHIKARI, M. & MATSUOKA, M. 2005a. Dissection of the phosphorylation of rice DELLA protein, SLENDER RICE1. *Plant and Cell Physiology,* 46**,** 1392-1399.

ITOH, H., SHIMADA, A., UEGUCHI-TANAKA, M., KAMIYA, N., HASEGAWA, Y., ASHIKARI, M. & MATSUOKA, M. 2005b. Overexpression of a GRAS protein lacking the DELLA domain confers altered gibberellin responses in rice. *The Plant Journal,* 44**,** 669-679.

ITOH, H., UEGUCHI-TANAKA, M., SATO, Y., ASHIKARI, M. & MATSUOKA, M. 2002. The gibberellin signaling pathway is regulated by the appearance and disappearance of SLENDER RICE1 in nuclei. *The Plant Cell,* 14**,** 57-70.

JACK, D. L., YANG, N. M. & SAIER, M. H. 2001. The drug/metabolite transporter superfamily. *European Journal of Biochemistry,* 268**,** 3620-3639.

JACOBSEN, S. E., BINKOWSKI, K. A. & OLSZEWSKI, N. E. 1996. SPINDLY, a tetratricopeptide repeat protein involved in gibberellin signal transduction Arabidopsis. *Proceedings of the National Academy of Sciences of the United States of America,* 93**,** 9292-9296.

JACOBSEN, S. E. & OLSZEWSKI, N. E. 1993. Mutations at the SPINDLY locus of Arabidopsis alter gibberellin signal transduction. *The Plant Cell,* 5**,** 887-896.

JANG, I. C., HENRIQUES, R., SEO, H. S., NAGATANI, A. & CHUA, N. H. 2010. Arabidopsis PHYTOCHROME INTERACTING FACTOR proteins promote phytochrome B polyubiquitination by COP1 E3 ligase in the nucleus. *The Plant Cell,* 22**,** 2370-2383.

JEONG, J. & CHOI, G. 2013. Phytochrome-interacting factors have both shared and distinct biological roles. *Molecules and Cells,* 35**,** 371-380.

JIA, Q., ZHANG, J., WESTCOTT, S., ZHANG, X. Q., BELLGARD, M., LANCE, R. & LI, C. 2009. GA-20 oxidase as a candidate for the semidwarf gene sdw1/denso in barley. *Functional & Integrative Genomics,* 9**,** 255-262.

JIANG, C. F., MITHANI, A., BELFIELD, E. J., MOTT, R., HURST, L. D. & HARBERD, N. P. 2014. Environmentally responsive genome-wide accumulation of de novo Arabidopsis thaliana mutations and epimutations. *Genome Research,* 24**,** 1821-1829.

JIAO, Y. L., LAU, O. S. & DENG, X. W. 2007. Light-regulated transcriptional networks in higher plants. *Nature Reviews Genetics,* 8**,** 217-230.

JOHNSON, E., BRADLEY, M., HARBERD, N. P. & WHITELAM, G. C. 1994. Photoresponses of light-grown phya mutants of Arabidopsis - phytochrome-a is required for the perception of daylength extensions. *Plant Physiology,* 105**,** 141-149.

JONASSEN, E. M., LEA, U. S. & LILLO, C. 2008. HY5 and HYH are positive regulators of nitrate reductase in seedlings and rosette stage plants. *Planta,* 227**,** 559-564.

JONASSEN, E. M., SANDSMARK, B. A. & LILLO, C. 2009. Unique status of NIA2 in nitrate assimilation: NIA2 expression is promoted by HY5/HYH and inhibited by PIF4. *Plant Signaling & Behavior,* 4**,** 1084-1086.

JONES, T. L., TUCKER, D. E. & ORT, D. R. 1998. Chilling delays circadian pattern of sucrose phosphate synthase and nitrate reductase activity in tomato. *Plant Physiology,* 118**,** 149-158.

KAISER, W. M. & HUBER, S. C. 2001. Post-translational regulation of nitrate reductase: mechanism, physiological relevance and environmental triggers. *Journal of Experimental Botany,* 52**,** 1981-1989.

KHANNA, R., SHEN, Y., MARION, C. M., TSUCHISAKA, A., THEOLOGIS, A., SCHAFER, E. & QUAIL, P. H. 2007. The basic helix-loop-helix transcription factor PIF5 acts on ethylene biosynthesis and phytochrome signaling by distinct mechanisms. *The Plant Cell,* 19**,** 3915-3929.

KHUSH, G. S. 2005. What it will take to feed 5.0 billion rice consumers in 2030. *Plant Molecular Biology,* 59, 1-6.

KIBA, T., FERIA-BOURRELLIER, A. B., LAFOUGE, F., LEZHNEVA, L., BOUTET-MERCEY, S., ORSEL, M., BREHAUT, V., MILLER, A., DANIEL-VEDELE, F., SAKAKIBARA, H. & KRAPP, A. 2012. The Arabidopsis nitrate transporter NRT2.4 plays a double role in roots and shoots of nitrogen-starved plants. *The Plant Cell Online,* 24, 245-258.

KIBA, T. & KRAPP, A. 2016. Plant nitrogen acquisition under low availability: regulation of uptake and root architecture. *Plant and Cell Physiology,* 57**,** 707-714.

KIM, D. H., YAMAGUCHI, S., LIM, S., OH, E., PARK, J., HANADA, A., KAMIYA, Y. & CHOI, G. 2008. SOMNUS, a CCCH-type zinc finger protein in Arabidopsis, negatively regulates light-dependent seed germination downstream of PIL5. *The Plant Cell,* 20**,** 1260-1277.

KIM, J., KANG, H., PARK, J., KIM, W., YOO, J., LEE, N., KIM, J., YOON, T. Y. & CHOI, G. 2016. PIF1-interacting transcription factors and their binding sequence elements determine the in vivo targeting sites of PIF1. *The Plant Cell,* 28**,** 1388-1405.

KIM, J. H., CHOI, D. S. & KENDE, H. 2003. The AtGRF family of putative transcription factors is involved in leaf and cotyledon growth in Arabidopsis. *The Plant Journal,* 36**,** 94-104.

KIM, J. H. & KENDE, H. 2004. A transcriptional coactivator, AtGIF1, is involved in regulating leaf growth and morphology in Arabidopsis. *Proceedings of the National Academy of Sciences of the United States of America,* 101**,** 13374-13379.

KIM, J. H. & LEE, B. H. 2006. GROWTH-REGULATING FACTOR4 of Arabidopsis thaliana is required for development of leaves, cotyledons, and shoot apical meristem. *Journal of Plant Biology,* 49**,** 463-468.

KIM, T. W. & WANG, Z. Y. 2010. Brassinosteroid signal transduction from receptor kinases to transcription factors. *Annual Review of Plant Biology, Vol 61,* 61**,** 681-704.

KIM, Y., SCHUMAKER, K. S. & ZHU, J. K. 2006. EMS mutagenesis of Arabidopsis. *Methods in Molecular Biology,* 323**,** 101-103.

KING, K. E., MORITZ, T. & HARBERD, N. P. 2001. Gibberellins are not required for normal stem growth in Arabidopsis thaliana in the absence of GAI and RGA. *Genetics,* 159**,** 767-76.

KIPREOS, E. T. & PAGANO, M. 2000. The F-box protein family. *Genome Biology,* 1, REVIEWS3002.

KOINI, M. A., ALVEY, L., ALLEN, T., TILLEY, C. A., HARBERD, N. P., WHITELAM, G. C. & FRANKLIN, K. A. 2009. High temperature-mediated adaptations in plant architecture require the bHLH transcription factor PIF4. *Current Biology,* 19**,** 408-413.

KONISHI, M. & YANAGISAWA, S. 2013. Arabidopsis NIN-like transcription factors have a central role in nitrate signalling. *Nature Communications,* 4, 1617.

KOORNNEEF, M., ELGERSMA, A., HANHART, C. J., VANLOENENMARTINET, E. P., VANRIJN, L. & ZEEVAART, J. A. D. 1985. A gibberellin insensitive mutant of Arabidopsis thaliana. *Physiologia Plantarum,* 65**,** 33-39.

KOORNNEEF, M. & VANDERVEEN, J. H. 1980. Induction and analysis of gibberellin sensitive mutants in Arabidopsis thaliana (L) Heynh. *Theoretical and Applied Genetics,* 58**,** 257-263.

KORESSAAR, T. & REMM, M. 2007. Enhancements and modifications of primer design program Primer3. *Bioinformatics,* 23**,** 1289-1291.

KOTUR, Z., MACKENZIE, N., RAMESH, S., TYERMAN, S. D., KAISER, B. N. & GLASS, A. D. M. 2012. Nitrate transport capacity of the Arabidopsis thaliana NRT2 family members and their interactions with AtNAR2.1. *New Phytologist,* 194**,** 724-731.

KRAPP, A. 2015. Plant nitrogen assimilation and its regulation: a complex puzzle with missing pieces. *Current Opinion in Plant Biology,* 25, 115-122.

KRAPP, A., BERTHOME, R., ORSEL, M., MERCEY-BOUTET, S., YU, A., CASTAINGS, L., ELFTIEH, S., MAJOR, H., RENOU, J. P. & DANIEL-VEDELE, F. 2011. Arabidopsis roots and shoots show distinct temporal adaptation patterns toward nitrogen starvation. *Plant Physiology,* 157, 1255-1282.

KRAPP, A., DAVID, L. C., CHARDIN, C., GIRIN, T., MARMAGNE, A., LEPRINCE, A. S., CHAILLOU, S., FERRARIO-MERY, S., MEYER, C. & DANIEL-VEDELE, F. 2014. Nitrate transport and signalling in Arabidopsis. *Journal of Experimental Botany,* 65, 789-798.

KRIEG, D. R. 1963. Ethyl Methanesulfonate-Induced Reversion of Bacteriophage T4rii Mutants. *Genetics,* 48**,** 561-580.

KROUK, G., CRAWFORD, N. M., CORUZZI, G. M. & TSAY, Y.-F. F. 2010a. Nitrate signaling: adaptation to fluctuating environments. *Current Opinion in Plant Biology,* 13**,** 266-273.

KROUK, G., LACOMBE, B., BIELACH, A., PERRINE-WALKER, F., MALINSKA, K., MOUNIER, E., HOYEROVA, K., TILLARD, P., LEON, S., LJUNG, K., ZAZIMALOVA, E., BENKOVA, E., NACRY, P. & GOJON, A. 2010b. Nitrate-regulated auxin transport by NRT1.1 defines a mechanism for nutrient sensing in plants. *Developmental Cell,* 18**,** 927-937.

KROUK, G., MIROWSKI, P., LECUN, Y., SHASHA, D. E. & CORUZZI, G. M. 2010c. Predictive network modeling of the high-resolution dynamic plant transcriptome in response to nitrate. *Genome Biology,* 11**,** R123.

KROUK, G., TILLARD, P. & GOJON, A. 2006. Regulation of the high-affinity NO3- uptake system by NRT1.1-mediated NO3- demand signaling in Arabidopsis. *Plant Physiology,* 142**,** 1075-1086.

KUMAR, I., SWAMINATHAN, K., HUDSON, K. & HUDSON, M. E. 2016. Evolutionary divergence of phytochrome protein function in Zea mays PIF3 signaling. *Journal of Experimental Botany,* 67**,** 4231-4240.

KUMAR, S. V., LUCYSHYN, D., JAEGER, K. E., ALOS, E., ALVEY, E., HARBERD, N. P. & WIGGE, P. A. 2012. Transcription factor PIF4 controls the thermosensory activation of flowering. *Nature,* 484**,** 242-245.

LADWIG, F., STAHL, M., LUDEWIG, U., HIRNER, A. A., HAMMES, U. Z., STADLER, R., HARTER, K. & KOCH, W. 2012. Siliques Are Red1 from Arabidopsis acts as a bidirectional amino acid transporter that is crucial for the amino acid homeostasis of siliques. *Plant Physiology,* 158**,** 1643-1655.

LAMBECK, I., CHI, J. C., KRIZOWSKI, S., MUELLER, S., MEHLMER, N., TEIGE, M., FISCHER, K. & SCHWARZ, G. 2010. Kinetic analysis of 14-3-3-inhibited Arabidopsis thaliana nitrate reductase. *Biochemistry,* 49**,** 8177-8186.

LAMBECK, I. C., FISCHER-SCHRADER, K., NIKS, D., ROEPER, J., CHI, J. C., HILLE, R. & SCHWARZ, G. 2012. Molecular mechanism of 14-3-3 Protein-mediated inhibition of plant nitrate reductase. *Journal of Biological Chemistry,* 287**,** 4562-4571.

LANDI, S. & ESPOSITO, S. 2017. Nitrate uptake affects cell wall synthesis and modeling. *Frontiers in Plant Science,* 8, 1376.

LEE, C. M. & THOMASHOW, M. F. 2012. Photoperiodic regulation of the C-repeat binding factor (CBF) cold acclimation pathway and freezing tolerance in Arabidopsis thaliana. *Proceedings of the National Academy of Sciences of the United States of America,* 109**,** 15054-15059.

LEE, D. J. & ZEEVAART, J. A. D. 2005. Molecular cloning of GA 2-oxidase3 from spinach and its ectopic expression in Nicotiana sylvestris. *Plant Physiology,* 138**,** 243-254.

LEE, N. & CHOI, G. 2017. Phytochrome-interacting factor from Arabidopsis to liverwort. *Current Opinion in Plant Biology,* 35**,** 54-60.

LEE, S., CHENG, H., KING, K. E., WANG, W., HE, Y., HUSSAIN, A., LO, J., HARBERD, N. P. & PENG, J. 2002. Gibberellin regulates Arabidopsis seed germination via RGL2, a GAI/RGA-like gene whose expression is up-regulated following imbibition. *Genes & Development,* 16**,** 646-658.

LEGOUIS, J. & PLUCHARD, P. 1996. Genetic variation for nitrogen use efficiency in winter wheat (Triticum aestivum L). *Euphytica,* 92, 221-224.

LEIVAR, P. & MONTE, E. 2014. PIFs: systems integrators in plant development. *The Plant Cell,* 26**,** 56-78.

LEIVAR, P., MONTE, E., AL-SADY, B., CARLE, C., STORER, A., ALONSO, J. M., ECKER, J. R. & QUAIL, P. H. 2008. The Arabidopsis phytochrome-interacting factor PIF7, together with PIF3 and PIF4, regulates responses to prolonged red light by modulating phyB levels. *The Plant Cell,* 20**,** 337-352.

LEIVAR, P., MONTE, E., COHN, M. M. & QUAIL, P. H. 2012a. Phytochrome signaling in green Arabidopsis seedlings: impact assessment of a mutually negative phyB-PIF feedback loop. *Molecular Plant,* 5**,** 734-749.

LEIVAR, P. & QUAIL, P. H. 2011. PIFs: pivotal components in a cellular signaling hub. *Trends in Plant Science,* 16**,** 19-28.

LEIVAR, P., TEPPERMAN, J. M., COHN, M. M., MONTE, E., AL-SADY, B., ERICKSON, E. & QUAIL, P. H. 2012b. Dynamic antagonism between phytochromes and PIF family basic helix-loop-helix factors induces selective reciprocal responses to light and shade in a rapidly responsive transcriptional network in Arabidopsis. *The Plant Cell,* 24**,** 1398-1419.

LEIVAR, P., TEPPERMAN, J. M., MONTE, E., CALDERON, R. H., LIU, T. L. & QUAIL, P. H. 2009. Definition of early transcriptional circuitry involved in light-induced reversal of PIF-imposed repression of photomorphogenesis in young Arabidopsis seedlings. *The Plant Cell,* 21**,** 3535-3553.

LERAN, S., EDEL, K. H., PERVENT, M., HASHIMOTO, K., CORRATGE-FAILLIE, C., OFFENBORN, J. N., TILLARD, P., GOJON, A., KUDLA, J. & LACOMBE, B. 2015. Nitrate sensing and uptake in Arabidopsis are enhanced by ABI2, a phosphatase inactivated by the stress hormone abscisic acid. *Science Signaling,* 8, ra43.

LERAN, S., MUNOS, S., BRACHET, C., TILLARD, P., GOJON, A. & LACOMBE, B. 2013. Arabidopsis NRT1.1 is a bidirectional transporter involved in root-to-shoot nitrate translocation. *Molecular Plant,* 6**,** 1984-1987.

LERAN, S., VARALA, K., BOYER, J. C., CHIURAZZI, M., CRAWFORD, N., DANIEL-VEDELE, F., DAVID, L., DICKSTEIN, R., FERNANDEZ, E., FORDE, B., GASSMANN, W., GEIGER, D., GOJON, A., GONG, J. M., HALKIER, B. A., HARRIS, J. M., HEDRICH, R., LIMAMI, A. M., RENTSCH, D., SEO, M., TSAY, Y. F., ZHANG, M. Y., CORUZZI, G. & LACOMBE, B. 2014. A unified nomenclature of NITRATE TRANSPORTER 1/PEPTIDE TRANSPORTER family members in plants. *Trends in Plant Science,* 19**,** 5-9.

LEZHNEVA, L., KIBA, T., FERIA-BOURRELLIER, A. B., LAFOUGE, F., BOUTET-MERCEY, S., ZOUFAN, P., SAKAKIBARA, H., DANIEL-VEDELE, F. & KRAPP, A. 2014. The Arabidopsis nitrate transporter NRT2.5 plays a role in nitrate acquisition and remobilization in nitrogen-starved plants. *The Plant Journal,* 80**,** 230-241.

LI, C. X., POTUSCHAK, T., COLON-CARMONA, A., GUTIERREZ, R. A. & DOERNER, P. 2005. Arabidopsis TCP20 links regulation of growth and cell division control pathways. *Proceedings of the National Academy of Sciences of the United States of America,* 102**,** 12978-12983.

LI, K., YU, R., FAN, L.-M., WEI, N., CHEN, H. & DENG, X. 2016. DELLA-mediated PIF degradation contributes to coordination of light and gibberellin signalling in Arabidopsis. *Nature Communications,* 7**,** 11868.

LI, L., LJUNG, K., BRETON, G., SCHMITZ, R. J., PRUNEDA-PAZ, J., COWING-ZITRON, C., COLE, B. J., IVANS, L. J., PEDMALE, U. V., JUNG, H. S., ECKER, J. R., KAY, S. A. & CHORY, J. 2012a. Linking photoreceptor excitation to changes in plant architecture. *Genes & Development,* 26**,** 785-790.

LI, L., PENG, W.-F., LIU, Q.-Q., ZHOU, J.-J., LIANG, W.-H. & XIE, X.-Z. 2012b. Expression patterns of OsPIL11, a phytochrome-interacting factor in rice, and preliminary analysis of its roles in light signal transduction. *Rice Science,* 19**,** 263-268.
LI, Q. F., WANG, C. M., JIANG, L., LI, S., SUN, S. S. M. & HE, J. X. 2012c. An interaction between BZR1 and DELLAs mediates direct signaling crosstalk between brassinosteroids and gibberellins in Arabidopsis. *Science Signaling,* 5, ra72.
LI, S., TIAN, Y., WU, K., YE, Y., YU, J., ZHANG, J., LIU, Q., HU, M., LI, H., TONG, Y., HARBERD, N. P. & FU, X. 2018. Modulating plant growth-metabolism coordination for sustainable agriculture. *Nature,* 560**,** 595-600.
LI, W. B., WANG, Y., OKAMOTO, M., CRAWFORD, N. M., SIDDIQI, M. Y. & GLASS, A. D. M. 2007. Dissection of the AtNRT2.1 : AtNRT2.2 inducible high-affinity nitrate transporter gene cluster. *Plant Physiology,* 143, 425-433.
LI, X., SONG, Y. J., CENTURY, K., STRAIGHT, S., RONALD, P., DONG, X. N., LASSNER, M. & ZHANG, Y. L. 2001. A fast neutron deletion mutagenesis-based reverse genetics system for plants. *The Plant Journal,* 27**,** 235-242.
LILLO, C. 1991. Diurnal-variations of corn leaf nitrate reductase - an experimental distinction between transcriptional and posttranscriptional control. *Plant Science,* 73**,** 149-154.
LILLO, C., MEYER, C., LEA, U. S., PROVAN, F. & OLTEDAL, S. 2004. Mechanism and importance of post-translational regulation of nitrate reductase. *Journal of Experimental Botany,* 55**,** 1275-1282.
LILLO, C., MEYER, C. & RUOFF, P. 2001. The nitrate reductase circadian system. The central clock dogma contra multiple oscillatory feedback loops. *Plant Physiology,* 125**,** 1554-1557.
LIN, Y. & CHENG, C. L. 1997. A chlorate-resistant mutant defective in the regulation of nitrate reductase gene expression in arabidopsis defines a new HY locus. *The Plant Cell,* 9, 21-35.
LING, J. J., LI, J., ZHU, D. M. & DENG, X. W. 2017. Noncanonical role of Arabidopsis COP1/SPA complex in repressing BIN2-mediated PIF3 phosphorylation and degradation in darkness. *Proceedings of the National Academy of Sciences of the United States of America,* 114**,** 3539-3544.
LING, Q., HUANG, W. & JARVIS, P. 2011. Use of a SPAD-502 meter to measure leaf chlorophyll concentration in Arabidopsis thaliana. *Photosynthesis Research,* 107**,** 209-214.
LITTLE, D. Y., RAO, H., OLIVA, S., DANIEL-VEDELE, F., KRAPP, A. & MALAMY, J. E. 2005. The putative high-affinity nitrate transporter NRT2.1 represses lateral root initiation in response to nutritional cues. *Proceedings of the National Academy of Sciences of the United States of America,* 102**,** 13693-13698.
LIU, K.-H. H. & TSAY, Y.-F. F. 2003. Switching between the two action modes of the dual-affinity nitrate transporter CHL1 by phosphorylation. *The EMBO Journal,* 22**,** 1005-1013.
LIU, K. H., HUANG, C. Y. & TSAY, Y. F. 1999. CHL1 is a dual-affinity nitrate transporter of arabidopsis involved in multiple phases of nitrate uptake. *The Plant Cell,* 11, 865-874.
LOCASCIO, A., BLAZQUEZ, M. A. & ALABADI, D. 2013. Genomic analysis of DELLA protein activity. *Plant and Cell Physiology,* 54, 1229-1237.
LORRAIN, S., ALLEN, T., DUEK, P. D., WHITELAM, G. C. & FANKHAUSER, C. 2008. Phytochrome-mediated inhibition of shade avoidance involves degradation of growth-promoting bHLH transcription factors. *The Plant Journal,* 53**,** 312-323.

LOZANO-DURAN, R. & ZIPFEL, C. 2015. Trade-off between growth and immunity: role of brassinosteroids. *Trends in Plant Science,* 20**,** 12-19.
LUNTER, G. & GOODSON, M. 2011. Stampy: a statistical algorithm for sensitive and fast mapping of Illumina sequence reads. *Genome Research,* 21**,** 936-939.
LUO, Q., LIAN, H. L., HE, S. B., LI, L., JIA, K. P. & YANG, H. Q. 2014. COP1 and phyB physically interact with PIL1 to regulate its stability and photomorphogenic development in Arabidopsis. *The Plant Cell,* 26**,** 2441-2456.
MACKINTOSH, C. & MEEK, S. E. M. 2001. Regulation of plant NR activity by reversible phosphorylation, 14-3-3 proteins and proteolysis. *Cellular and Molecular Life Sciences,* 58**,** 205-214.
MARCHIVE, C., ROUDIER, F., CASTAINGS, L., BREHAUT, V., BLONDET, E., COLOT, V., MEYER, C. & KRAPP, A. 2013. Nuclear retention of the transcription factor NLP7 orchestrates the early response to nitrate in plants. *Nature Communications,* 4, 1713.
MARIN-DE LA ROSA, N., PFEIFFER, A., HILL, K., LOCASCIO, A., BHALERAO, R. P., MISKOLCZI, P., GRONLUND, A. L., WANCHOO-KOHLI, A., THOMAS, S. G., BENNETT, M. J., LOHMANN, J. U., BLAZQUEZ, M. A. & ALABADI, D. 2015. Genome wide binding site analysis reveals transcriptional coactivation of cytokinin-responsive genes by DELLA proteins. *Plos Genetics,* 11, e1005337.
MARSISCHKY, G. T. & KOLODNER, R. D. 1999. Biochemical characterization of the interaction between the Saccharomyces cerevisiae MSH2-MSH6 complex and mispaired bases in DNA. *Journal of Biological Chemistry,* 274**,** 26668-26682.
MARTIN, B., RAMIRO, M., MARTINEZ-ZAPATER, J. M. & ALONSO-BLANCO, C. 2009. A high-density collection of EMS-induced mutations for TILLING in Landsberg erecta genetic background of Arabidopsis. *BMC Plant Biology,* 9, 147.
MARTIN, G., SOY, J. & MONTE, E. 2016. Genomic analysis reveals contrasting PIFq contribution to diurnal rhythmic gene expression in PIF-induced and -repressed genes. *Frontiers in Plant Science,* 7**,** 962.
MCGINNIS, K. M., THOMAS, S. G., SOULE, J. D., STRADER, L. C., ZALE, J. M., SUN, T. P. & STEBER, C. M. 2003. The Arabidopsis SLEEPY1 gene encodes a putative F-box subunit of an SCF E3 ubiquitin ligase. *The Plant Cell,* 15**,** 1120-1130.
MELNYK, C. W. 2017. Grafting with Arabidopsis thaliana. *Methods in Molecular Biology,* 1497**,** 9-18.
MEREDITH, D. & PRICE, R. A. 2006. Molecular modeling of PepT1- Towards a structure. *Journal of Membrane Biology,* 213**,** 79-88.
MIRALLES, D. J., CALDERINI, D. F., POMAR, K. P. & D'AMBROGIO, A. 1998. Dwarfing genes and cell dimensions in different organs of wheat. *Journal of Experimental Botany,* 49**,** 1119-1127.
MITCHUM, M. G., YAMAGUCHI, S., HANADA, A., KUWAHARA, A., YOSHIOKA, Y., KATO, T., TABATA, S., KAMIYA, Y. & SUN, T. P. 2006. Distinct and overlapping roles of two gibberellin 3-oxidases in Arabidopsis development. *The Plant Journal,* 45**,** 804-818.
MONNA, L., KITAZAWA, N., YOSHINO, R., SUZUKI, J., MASUDA, H., MAEHARA, Y., TANJI, M., SATO, M., NASU, S. & MINOBE, Y. 2002. Positional cloning of rice semidwarfing gene, sd-1: rice "green revolution gene" encodes a mutant enzyme involved in gibberellin synthesis. *DNA Research,* 9**,** 11-17.
MOON, J., ZHU, L., SHEN, H. & HUQ, E. 2008. PIF1 directly and indirectly regulates chlorophyll biosynthesis to optimize the greening process in Arabidopsis. *Proceedings of the National Academy of Sciences of the United States of America,* 105**,** 9433-9438.

MOROT-GAUDRY-TALARMAIN, Y., ROCKEL, P., MOUREAUX, T., QUILLERE, I., LEYDECKER, M. T., KAISER, W. M. & MOROT-GAUDRY, J. F. 2002. Nitrite accumulation and nitric oxide emission in relation to cellular signaling in nitrite reductase antisense tobacco. *Planta,* 215**,** 708-715.

MUANGPROM, A., THOMAS, S. G., SUN, T. P. & OSBORN, T. C. 2005. A novel dwarfing mutation in a green revolution gene from Brassica rapa. *Plant Physiology,* 137**,** 931-938.

MULLER, B., FASTNER, A., KARMANN, J., MANSCH, V., HOFFMANN, T., SCHWAB, W., SUTER-GROTEMEYER, M., RENTSCH, D., TRUERNIT, E., LADWIG, F., BLECKMANN, A., DRESSELHAUS, T. & HAMMES, U. Z. 2015. Amino acid export in developing Arabidopsis seeds depends on UmamiT facilitators. *Current Biology,* 25**,** 3126-3131.

MUNOS, S., CAZETTES, C., FIZAMES, C., GAYMARD, F., TILLARD, P., LEPETIT, M., LEJAY, L. & GOJON, A. 2004. Transcript profiling in the chl1-5 mutant of Arabidopsis reveals a role of the nitrate transporter NRT1.1 in the regulation of another nitrate transporter, NRT2.1. *The Plant Cell,* 16, 2433-2447.

MURASE, K., HIRANO, Y., SUN, T. P. & HAKOSHIMA, T. 2008. Gibberellin-induced DELLA recognition by the gibberellin receptor GID1. *Nature,* 456**,** 459-463.

NAKAGAWA, H. & YAMASHITA, N. 1986. Chlorate reducing activity of spinach nitrate reductase. *Agricultural and Biological Chemistry,* 50**,** 1893-1894.

NAKAJIMA, M., SHIMADA, A., TAKASHI, Y., KIM, Y. C., PARK, S. H., UEGUCHI-TANAKA, M., SUZUKI, H., KATOH, E., IUCHI, S., KOBAYASHI, M., MAEDA, T., MATSUOKA, M. & YAMAGUCHI, I. 2006. Identification and characterization of Arabidopsis gibberellin receptors. *The Plant Journal,* 46**,** 880-889.

NAKAMURA, H., XUE, Y. L., MIYAKAWA, T., HOU, F., QIN, H. M., FUKUI, K., SHI, X., ITO, E., ITO, S., PARK, S. H., MIYAUCHI, Y., ASANO, A., TOTSUKA, N., UEDA, T., TANOKURA, M. & ASAMI, T. 2013. Molecular mechanism of strigolactone perception by DWARF14. *Nature Communications,* 4, 2613.

NAKAMURA, Y., KATO, T., YAMASHINO, T., MURAKAMI, M. & MIZUNO, T. 2007. Characterization of a set of phytochrome-interacting factor-like bHLH proteins in Oryza sativa. *Bioscience Biotechnology and Biochemistry,* 71**,** 1183-1191.

NI, W., XU, S. L., TEPPERMAN, J. M., STANLEY, D. J., MALTBY, D. A., GROSS, J. D., BURLINGAME, A. L., WANG, Z. Y. & QUAIL, P. H. 2014. A mutually assured destruction mechanism attenuates light signaling in Arabidopsis. *Science,* 344**,** 1160-1164.

NI, W. M., XU, S. L., CHALKLEY, R. J., PHAM, T. N. D., GUAN, S. H., MALTBY, D. A., BURLINGAME, A. L., WANG, Z. Y. & QUAIL, P. H. 2013. Multisite light-induced phosphorylation of the transcription factor PIF3 is necessary for both its rapid degradation and concomitant negative feedback modulation of photoreceptor phyB levels in Arabidopsis. *The Plant Cell,* 25**,** 2679-2698.

NI, W. M., XU, S. L., GONZALEZ-GRANDIO, E., CHALKLEY, R. J., HUHMER, A. F. R., BURLINGAME, A. L., WANG, Z. Y. & QUAIL, P. H. 2017. PPKs mediate direct signal transfer from phytochrome photoreceptors to transcription factor PIF3. *Nature Communication,* 8**,** 15236.

NOGUERO, M. & LACOMBE, B. 2016. Transporters involved in root nitrate uptake and sensing by Arabidopsis. *Frontiers in Plant Science,* 7**,** 1391.

NOZUE, K., COVINGTON, M. F., DUEK, P. D., LORRAIN, S., FANKHAUSER, C., HARMER, S. L. & MALOOF, J. N. 2007. Rhythmic growth explained by coincidence between internal and external cues. *Nature,* 448**,** 358-361.

NUSINOW, D. A., HELFER, A., HAMILTON, E. E., KING, J. J., IMAIZUMI, T., SCHULTZ, T. F., FARRE, E. M. & KAY, S. A. 2011. The ELF4-ELF3-LUX complex links the circadian clock to diurnal control of hypocotyl growth. *Nature,* 475**,** 398-402.

OGAWA, M., HANADA, A., YAMAUCHI, Y., KUWAHARA, A., KAMIYA, Y. & YAMAGUCHI, S. 2003. Gibberellin biosynthesis and response during Arabidopsis seed germination. *The Plant Cell,* 15**,** 1591-1604.

OGAWA, M., KUSANO, T., KATSUMI, M. & SANO, H. 2000. Rice gibberellin-insensitive gene homolog, OsGAI encodes a nuclear-localized protein capable of gene activation at transcriptional level. *Gene,* 245**,** 21-29.

OH, E., KANG, H., YAMAGUCHI, S., PARK, J., LEE, D., KAMIYA, Y. & CHOI, G. 2009. Genome-wide analysis of genes targeted by PHYTOCHROME INTERACTING FACTOR 3-LIKE5 during seed germination in Arabidopsis. *The Plant Cell,* 21**,** 403-419.

OH, E., YAMAGUCHI, S., HU, J. H., YUSUKE, J., JUNG, B., PAIK, I., LEE, H. S., SUN, T. P., KAMIYA, Y. & CHOI, G. 2007. PIL5, a phytochrome-interacting bHLH protein, regulates gibberellin responsiveness by binding directly to the GAI and RGA promoters in Arabidopsis seeds. *The Plant Cell,* 19**,** 1192-1208.

OH, E., YAMAGUCHI, S., KAMIYA, Y., BAE, G., CHUNG, W. I. & CHOI, G. 2006. Light activates the degradation of PIL5 protein to promote seed germination through gibberellin in Arabidopsis. *The Plant Journal,* 47**,** 124-139.

OH, E., ZHU, J. Y., BAI, M. Y., ARENHART, R. A., SUN, Y. & WANG, Z. Y. 2014. Cell elongation is regulated through a central circuit of interacting transcription factors in the Arabidopsis hypocotyl. *Elife,* 3, e03031.

OH, E., ZHU, J. Y. & WANG, Z. Y. 2012. Interaction between BZR1 and PIF4 integrates brassinosteroid and environmental responses. *Nature Cell Biology,* 14**,** 802-809.

OKAMOTO, M., VIDMAR, J. J. & GLASS, A. D. M. 2003. Regulation of NRT1 and NRT2 gene families of Arabidopsis thaliana: Responses to nitrate provision. *Plant and Cell Physiology,* 44, 304-317.

OKUMOTO, S. & PILOT, G. 2011. Amino acid export in plants: a missing link in nitrogen cycling. *Molecular Plant,* 4**,** 453-463.

OKUNO, A., HIRANO, K., ASANO, K., TAKASE, W., MASUDA, R., MORINAKA, Y., UEGUCHI-TANAKA, M., KITANO, H. & MATSUOKA, M. 2014. New approach to increasing rice lodging resistance and biomass yield through the use of high gibberellin producing varieties. *Plos One,* 9, e86870.

OLSZEWSKI, N., SUN, T. P. & GUBLER, F. 2002. Gibberellin signaling: biosynthesis, catabolism, and response pathways. *The Plant Cell,* 14**,** S61-S80.

ORDONIO, R. L., ITO, Y., HATAKEYAMA, A., OHMAE-SHINOHARA, K., KASUGA, S., TOKUNAGA, T., MIZUNO, H., KITANO, H., MATSUOKA, M. & SAZUKA, T. 2014. Gibberellin deficiency pleiotropically induces culm bending in sorghum: an insight into sorghum semi-dwarf breeding. *Scientific Reports,* 4, 5287.

ORSEL, M., CHOPIN, F., LELEU, O., SMITH, S. J. & KRAPP, A. 2006. Characterization of a two-component high-affinity nitrate uptake system in Arabidopsis. *Plant Physiology*, 142, 1304-1317.

ORSEL, M., EULENBURG, K., KRAPP, A. & DANIEL-VEDELE, F. 2004. Disruption of the nitrate transporter genes AtNRT2.1 and AtNRT2.2 restricts growth at low external nitrate concentration. *Planta,* 219, 714-721.

ORSEL, M., KRAPP, A. & DANIEL-VEDELE, F. 2002. Analysis of the NRT2 nitrate transporter family in Arabidopsis. Structure and gene expression. *Plant Physiology,* 129, 886-896.

PAGNUSSAT, G. C., YU, H. J., NGO, Q. A., RAJANI, S., MAYALAGU, S., JOHNSON, C. S., CAPRON, A., XIE, L. F., YE, D. & SUNDARESAN, V. 2005. Genetic and molecular identification of genes required for female gametophyte development and function in Arabidopsis. *Development,* 132**,** 603-614.

PAIK, I., KATHARE, P. K., KIM, J. I. & HUQ, E. 2017. Expanding roles of PIFs in signal integration from multiple processes. *Molecular Plant,* 10**,** 1035-1046.

PAIK, I., YANG, S. & CHOI, G. 2012. Phytochrome regulates translation of mRNA in the cytosol. *Proceedings of the National Academy of Sciences of the United States of America,* 109**,** 1335-1340.

PANG, P. P., PRUITT, R. E. & MEYEROWITZ, E. M. 1988. Molecular-cloning, genomic organization, expression and evolution of 12s-seed storage protein genes of Arabidopsis thaliana. *Plant Molecular Biology,* 11**,** 805-820.

PARK, B. S., SONG, J. T. & SEO, H. S. 2011a. Arabidopsis nitrate reductase activity is stimulated by the E3 SUMO ligase AtSIZ1. *Nature Communications,* 2**,** 400.

PARK, E., PARK, J., KIM, J., NAGATANI, A., LAGARIAS, J. C. & CHOI, G. 2012. Phytochrome B inhibits binding of phytochrome-interacting factors to their target promoters. *The Plant Journal,* 72**,** 537-546.

PARK, J., LEE, N., KIM, W., LIM, S. & CHOI, G. 2011b. ABI3 and PIL5 collaboratively activate the expression of SOMNUS by directly binding to its promoter in imbibed Arabidopsis seeds. *The Plant Cell,* 23**,** 1404-1415.

PARKER, J. L. & NEWSTEAD, S. 2014. Molecular basis of nitrate uptake by the plant nitrate transporter NRT1.1. *Nature,* 507, 68-72.

PAWSON, T. & SCOTT, J. D. 1997. Signaling through scaffold, anchoring, and adaptor proteins. *Science,* 278**,** 2075-2080.

PENFIELD, S., JOSSE, E. M. & HALLIDAY, K. J. 2010. A role for an alternative splice variant of PIF6 in the control of Arabidopsis primary seed dormancy. *Plant Molecular Biology,* 73**,** 89-95.

PENG, J. & HARBERD, N. P. 1993. Derivative alleles of the Arabidopsis gibberellin-insensitive (gai) mutation confer a wild-type phenotype. *The Plant Cell,* 5, 351-360.

PENG, J. & HARBERD, N. P. 1997a. Gibberellin deficiency and response mutations suppress the stem elongation phenotype of phytochrome-deficient mutants of Arabidopsis. *Plant Physiology,* 113**,** 1051-1058.

PENG, J. R., CAROL, P., RICHARDS, D. E., KING, K. E., COWLING, R. J., MURPHY, G. P. & HARBERD, N. P. 1997. The Arabidopsis GAI gene defines a signaling pathway that negatively regulates gibberellin responses. *Genes & Development,* 11, 3194-3205.

PENG, J. R. & HARBERD, N. P. 1997b. Transposon-associated somatic gai-loss sectors in Arabidopsis. *Plant Science,* 130**,** 181-188.

PENG, J. R., RICHARDS, D. E., HARTLEY, N. M., MURPHY, G. P., DEVOS, K. M., FLINTHAM, J. E., BEALES, J., FISH, L. J., WORLAND, A. J., PELICA, F., SUDHAKAR, D., CHRISTOU, P., SNAPE, J. W., GALE, M. D. & HARBERD, N. P. 1999a. 'Green revolution' genes encode mutant gibberellin response modulators. *Nature,* 400, 256-261.

PENG, J. R., RICHARDS, D. E., MORITZ, T., CANO-DELGADO, A. & HARBERD, N. P. 1999b. Extragenic suppressors of the Arabidopsis gai mutation alter the dose-response relationship of diverse gibberellin responses. *Plant Physiology,* 119**,** 1199-1207.

PENG, L., MA, J., CHI, W., GUO, J., ZHU, S., LU, Q., LU, C. & ZHANG, L. 2018. LOW PSII ACCUMULATION1 is involved in efficient assembly of photosystem II in Arabidopsis thaliana (vol 18, pg 955, 2006). *The Plant Cell,* 30**,** 245-248.

PFEIFFER, A., SHI, H., TEPPERMAN, J. M., ZHANG, Y. & QUAIL, P. H. 2014. Combinatorial complexity in a transcriptionally centered signaling hub in Arabidopsis. *Molecular Plant,* 7**,** 1598-1618.

PHAM, V. N., KATHARE, P. K. & HUQ, E. 2018. Phytochromes and phytochrome interacting factors. *Plant Physiology,* 176**,** 1025-1038.

PILGRIM, M. L., CASPAR, T., QUAIL, P. H. & MCCLUNG, C. R. 1993. Circadian and light-regulated expression of nitrate reductase in Arabidopsis. *Plant Molecular Biology,* 23**,** 349-364.

PRATELLI, R. & PILOT, G. 2014. Regulation of amino acid metabolic enzymes and transporters in plants. *Journal of Experimental Botany,* 65**,** 5535-5556.

PROVAN, F., AKSLAND, L. M., MEYER, C. & LILLO, C. 2000. Deletion of the nitrate reductase N-terminal domain still allows binding of 14-3-3 proteins but affects their inhibitory properties. *Plant Physiology,* 123**,** 757-764.

PYSH, L. D., WYSOCKA-DILLER, J. W., CAMILLERI, C., BOUCHEZ, D. & BENFEY, P. N. 1999. The GRAS gene family in Arabidopsis: sequence characterization and basic expression analysis of the SCARECROW-LIKE genes. *The Plant Journal,* 18**,** 111-119.

QU, X. Y., ZHAO, Z. & TIAN, Z. X. 2017. ERECTA regulates cell elongation by activating auxin biosynthesis in Arabidopsis thaliana. *Frontiers in Plant Science,* 8, 1688.

QUAIL, P. H., BOYLAN, M. T., PARKS, B. M., SHORT, T. W., XU, Y. & WAGNER, D. 1995. Phytochromes - photosensory perception and signal-transduction. *Science,* 268**,** 675-680.

QUINN, M. H., OLIVERIO, K., YANOVSKY, M. J. & CASAL, J. J. 2002. CP3 is involved in negative regulation of phytochrome A signalling in Arabidopsis. *Planta,* 215**,** 557-564.

QUINT, M., DELKER, C., FRANKLIN, K. A., WIGGE, P. A., HALLIDAY, K. J. & VAN ZANTEN, M. 2016. Molecular and genetic control of plant thermomorphogenesis. *Nature Plants,* 2, 15190.

RADEMACHER, W. 2016. Chemical regulators of gibberellin status and their application in plant production. In *Annual Plant Reviews* (Vol. 49) HEDDEN, P. and THOMAS, S.G., eds In PP. 395-404, John Wiley & Sons

RANATHUNGE, K., EL-KEREAMY, A., GIDDA, S., BI, Y.-M. & ROTHSTEIN, S. J. 2014. AMT1;1 transgenic rice plants with enhanced NH4 + permeability show superior growth and higher yield under optimal and suboptimal NH4 + conditions. *Journal of Experimental Botany,* 65**,** 965-979.

RANOCHA, P., DENANCE, N., VANHOLME, R., FREYDIER, A., MARTINEZ, Y., HOFFMANN, L., KOHLER, L., POUZET, C., RENOU, J. P., SUNDBERG, B., BOERJAN, W. & GOFFNER, D. 2010. Walls are thin 1 (WAT1), an Arabidopsis homolog of Medicago truncatula NODULIN21, is a tonoplast-localized protein required for secondary wall formation in fibers. *The Plant Journal,* 63**,** 469-483.

RANOCHA, P., DIMA, O., NAGY, R., FELTEN, J., CORRATGE-FAILLIE, C., NOVAK, O., MORREEL, K., LACOMBE, B., MARTINEZ, Y., PFRUNDER, S., JIN, X., RENOU, J. P., THIBAUD, J. B., LJUNG, K., FISCHER, U., MARTINOIA, E., BOERJAN, W. & GOFFNER, D. 2013. Arabidopsis WAT1 is a vacuolar auxin transport facilitator required for auxin homoeostasis. *Nature Communications,* 4, 2625.

RAUN, W. R. & JOHNSON, G. V. 1999. Improving nitrogen use efficiency for cereal production. *Agronomy Journal,* 91**,** 357-363.

REED, H. E., SAMMONS, D. J., SMAIL, V. W. & TAYLOR, G. J. 1992. Sensitivity of soft red winter-wheat cultivars to chlorate-induced toxicity. *Journal of Plant Nutrition,* 15**,** 2621-2637.

REED, J. W., NAGATANI, A., ELICH, T. D., FAGAN, M. & CHORY, J. 1994. Phytochrome-A and Phytochrome-B have overlapping but distinct functions in Arabidopsis development. *Plant Physiology,* 104**,** 1139-1149.

REMANS, T., NACRY, P., PERVENT, M., FILLEUR, S., DIATLOFF, E., MOUNIER, E., TILLARD, P., FORDE, B. G. & GOJON, A. 2006a. The Arabidopsis NRT1.1 transporter participates in the signaling pathway triggering root colonization of nitrate-rich patches. *Proceedings of the National Academy of Sciences of the United States of America,* 103, 19206-19211.

REMANS, T., NACRY, P., PERVENT, M., GIRIN, T. & TILLARD, P. 2006b. A central role for the nitrate transporter NRT2. 1 in the integrated morphological and physiological responses of the root system to nitrogen limitation in Arabidopsis. *Plant Physiology*, 140, 909-921.

RICE, W. R. 2014. The synthesis paradigm in genetics. *Genetics,* 196**,** 367-371.

RIEU, I., RUIZ-RIVERO, O., FERNANDEZ-GARCIA, N., GRIFFITHS, J., POWERS, S. J., GONG, F., LINHARTOVA, T., ERIKSSON, S., NILSSON, O., THOMAS, S. G., PHILLIPS, A. L. & HEDDEN, P. 2008. The gibberellin biosynthetic genes AtGA20ox1 and AtGA20ox2 act, partially redundantly, to promote growth and development throughout the Arabidopsis life cycle. *The Plant Journal : for cell and molecular biology,* 53**,** 488-504.

ROBINSON, J. T., THORVALDSDOTTIR, H., WENGER, A. M., ZEHIR, A. & MESIROV, J. P. 2017. Variant review with the integrative genomics viewer. *Cancer Research,* 77**,** e31-e34.

ROBINSON, J. T., THORVALDSDOTTIR, H., WINCKLER, W., GUTTMAN, M., LANDER, E. S., GETZ, G. & MESIROV, J. P. 2011. Integrative genomics viewer. *Nature Biotechnology,* 29**,** 24-26.

RODRIGUEZ, C. M., FREIRE, M. A., CAMILLERI, C. & ROBAGLIA, C. 1998. The Arabidopsis thaliana cDNAs coding for eIF4E and eIF(iso)4E are not functionally equivalent for yeast complementation and are differentially expressed during plant development. *The Plant Journal,* 13**,** 465-473.

RUBIN, G., TOHGE, T., MATSUDA, F., SAITO, K. & SCHEIBLE, W. R. 2009. Members of the LBD family of transcription factors repress anthocyanin synthesis and affect additional nitrogen responses in Arabidopsis. *The Plant Cell,* 21**,** 3567-3584.

RUBIN, G. M. 1990. Flies fron all angles [Review of M. Ashburner, 'Drosophila - a laboratory handbook']. *Nature,* 348**,** 366.

SAGASSER, M., LU, G. H., HAHLBROCK, K. & WEISSHAAR, B. 2002. A. thaliana TRANSPARENT TESTA 1 is involved in seed coat development and defines the WIP subfamily of plant zinc finger proteins. *Genes & Development,* 16**,** 138-149.

SAIJO, Y., ZHU, D. M., LI, J. G., RUBIO, V., ZHOU, Z. Z., SHEN, Y. P., HOECKER, U., WANG, H. Y. & DENG, X. W. 2008. Arabidopsis COP1/SPA1 complex and FHY1/FHY3 associate with distinct phosphorylated forms of phytochrome a in balancing light signaling. *Molecular Cell,* 31**,** 607-613.

SAKAKIBARA, H. 2003. Nitrate-specific and cytokinin-mediated nitrogen signaling pathways in plants. *Journal of Plant Research,* 116**,** 253-257.

SAKAMOTO, T., MIYURA, K., ITOH, H., TATSUMI, T., UEGUCHI-TANAKA, M., ISHIYAMA, K., KOBAYASHI, M., AGRAWAL, G. K., TAKEDA, S., ABE, K., MIYAO, A., HIROCHIKA, H., KITANO, H., AHIKARI, M. & MATSUOKA, M. 2004. An overview of gibberellin metabolism enzyme genes and their related mutants in rice. *Plant Physiology,* 135**,** 1863.

SAKURABA, Y., KIM, E. Y., HAN, S. H., PIAO, W., AN, G., TODAKA, D., YAMAGUCHI-SHINOZAKI, K. & PAEK, N. C. 2017. Rice Phytochrome-Interacting Factor-Like1 (OsPIL1) is involved in the promotion of chlorophyll biosynthesis through feed-forward regulatory loops. *Journal of Experimental Botany,* 68**,** 4103-4114.

SAMBADE, A., PRATAP, A., BUSCHMANN, H., MORRIS, R. J. & LLOYD, C. 2012. The influence of light on microtubule dynamics and alignment in the Arabidopsis hypocotyl. *The Plant Cell,* 24**,** 192-201.

SANZ-LUQUE, E., CHAMIZO-AMPUDIA, A., LLAMAS, A., GALVAN, A. & FERNANDEZ, E. 2015. Understanding nitrate assimilation and its regulation in microalgae. *Frontiers in Plant Science,* 6, 899.

SASAKI, A., ASHIKARI, M., UEGUCHI-TANAKA, M., ITOH, H., NISHIMURA, A., SWAPAN, D., ISHIYAMA, K., SAITO, T., KOBAYASHI, M., KHUSH, G. S., KITANO, H. & MATSUOKA, M. 2002. Green revolution: a mutant gibberellin-synthesis gene in rice. *Nature,* 416**,** 701-702.

SASAKI, A., ITOH, H., GOMI, K., UEGUCHI-TANAKA, M., ISHIYAMA, K., KOBAYASHI, M., JEONG, D. H., AN, G., KITANO, H., ASHIKARI, M. & MATSUOKA, M. 2003. Accumulation of phosphorylated repressor for gibberellin signaling in an F-box mutant. *Science,* 299**,** 1896-1898.

SCHNEIDER, S., BUCHERT, M. & HOVENS, C. M. 1996. An in vitro assay of beta-galactosidase from yeast. *Biotechniques,* 20**,** 960-962.

SCHOMBURG, F. M., BIZZELL, C. M., LEE, D. J., ZEEVAART, J. A. D. & AMASINO, R. M. 2003. Overexpression of a novel class of gibberellin 2-oxidases decreases gibberellin levels and creates dwarf plants. *The Plant Cell,* 15**,** 151-163.

SCHULMAN, B. A., CARRANO, A. C., JEFFREY, P. D., BOWEN, Z., KINNUCAN, E. R. E., FINNIN, M. S., ELLEDGE, S. J., HARPER, J. W., PAGANO, M. & PAVIETICH, N. P. 2000. Insights into SCF ubiquitin ligases from the structure of the Skp1-Skp2 complex. *Nature,* 408**,** 381-386.

SCHWACKE, R., SCHNEIDER, A., VAN DER GRAAFF, E., FISCHER, K., CATONI, E., DESIMONE, M., FROMMER, W. B., FLUGGE, U. I. & KUNZE, R. 2003. ARAMEMNON, a novel database for Arabidopsis integral membrane proteins. *Plant Physiology,* 131**,** 16-26.

SCHWECHHEIMER, C. 2011. Gibberellin signaling in plants - the extended version. *Frontiers in Plant Science,* 2**,** 107.

SHI, Q. B., ZHANG, H. S., SONG, X. Y., JIANG, Y. E., LIANG, R. & LI, G. 2018. Functional characterization of the maize phytochrome-interacting factors PIF4 and PIF5. *Frontiers in Plant Science,* 8, 2273.

SHIKAZONO, N., SUZUKI, C., KITAMURA, S., WATANABE, H., TANO, S. & TANAKA, A. 2005. Analysis of mutations induced by carbon ions in Arabidopsis thaliana. *Journal of Experimental Botany,* 56**,** 587-596.

SHIMADA, A., UEGUCHI-TANAKA, M., NAKATSU, T., NAKAJIMA, M., NAOE, Y., OHMIYA, H., KATO, H. & MATSUOKA, M. 2008. Structural basis for gibberellin recognition by its receptor GID1. *Nature,* 456**,** 520-523.

SHIN, A. Y., HAN, Y. J., BAEK, A., AHN, T., KIM, S. Y., NGUYEN, T. S., SON, M., LEE, K. W., SHEN, Y., SONG, P. S. & KIM, J. I. 2016. Evidence that phytochrome functions as a protein kinase in plant light signalling. *Nature Communications,* 7, 11545.

SHIN, J., KIM, K., KANG, H., ZULFUGAROV, I. S., BAE, G., LEE, C.-H., LEE, D. & CHOI, G. 2009. Phytochromes promote seedling light responses by inhibiting four negatively-acting phytochrome-interacting factors. *Proceedings of the National Academy of Sciences of the United States of America,* 106**,** 7660-7665.

SILVERSTONE, A. L., CIAMPAGLIO, C. N. & SUN, T. 1998. The Arabidopsis RGA gene encodes a transcriptional regulator repressing the gibberellin signal transduction pathway. *The Plant Cell,* 10**,** 155-169.
SILVERSTONE, A. L., MAK, P. Y., MARTINEZ, E. C. & SUN, T. P. 1997. The new RGA locus encodes a negative regulator of gibberellin response in Arabidopsis thaliana. *Genetics,* 146**,** 1087-1099.
SILVERSTONE, A. L., TSENG, T. S., SWAIN, S. M., DILL, A., JEONG, S. Y., OLSZEWSKI, N. E. & SUN, T. P. 2007. Functional analysis of SPINDLY in gibberellin signaling in Arabidopsis. *Plant Physiology,* 143**,** 987-1000.
SINCLAIR, J. 1987. Changes in spinach thylakoid activity due to nitrite ions. *Photosynthesis Research,* 12**,** 255-263.
SOLOMONS, L. & VENNESLA, B. 1972. Nitrate reductase and chlorate toxicity in Chlorella vulgaris Beijerinck. *Plant Physiology,* 50**,** 421-424.
SOY, J., LEIVAR, P., GONZALEZ-SCHAIN, N., SENTANDREU, M., PRAT, S., QUAIL, P. H. & MONTE, E. 2012. Phytochrome-imposed oscillations in PIF3 protein abundance regulate hypocotyl growth under diurnal light/dark conditions in Arabidopsis. *The Plant Journal,* 71**,** 390-401.
SPIELMEYER, W., ELLIS, M. H. & CHANDLER, P. M. 2002. Semidwarf (sd-1), "green revolution" rice, contains a defective gibberellin 20-oxidase gene. *Proceedings of the National Academy of Sciences of the United States of America,* 99**,** 9043-9048.
STEBER, C. M., COONEY, S. E. & MCCOURT, P. 1998. Isolation of the GA-response mutant sly1 as a suppressor of ABI1-1 in Arabidopsis thaliana. *Genetics,* 149**,** 509-521.
STEPHENSON, P. G., FANKHAUSER, C. & TERRY, M. J. 2009. PIF3 is a repressor of chloroplast development. *Proceedings of the National Academy of Sciences of the United States of America,* 106**,** 7654-7659.
STRZALKA, W. & ZIEMIENOWICZ, A. 2011. Proliferating cell nuclear antigen (PCNA): a key factor in DNA replication and cell cycle regulation. *Annals of Botany,* 107**,** 1127-1140.
SUGDEN, C., DONAGHY, P. G., HALFORD, N. G. & HARDIE, D. G. 1999. Two SNF1-Related protein kinases from spinach leaf phosphorylate and inactivate 3-hydroxy-3-methylglutaryl-coenzyme A reductase, nitrate reductase, and sucrose phosphate synthase in vitro. *Plant Physiology,* 120**,** 257-274.
SUGIMURA, T. 2000. Nutrition and dietary carcinogens. *Carcinogenesis,* 21**,** 387-395.
SUGIURA, M., GEORGESCU, M. N. & TAKAHASHI, M. 2007. A nitrite transporter associated with nitrite uptake by higher plant chloroplasts. *Plant and Cell Physiology,* 48**,** 1022-1035.
SUN, J. Q., QI, L. L., LI, Y. N., CHU, J. F. & LI, C. Y. 2012. PIF4-mediated activation of YUCCA8 expression integrates temperature into the auxin pathway in regulating Arabidopsis hypocotyl growth. *Plos Genetics,* 8, e1002594.
SUN, N., WANG, J. J., GAO, Z. X., DONG, J., HE, H., TERZAGHI, W., WEI, N., DENG, X. W. & CHEN, H. D. 2016. Arabidopsis SAURs are critical for differential light regulation of the development of various organs. *Proceedings of the National Academy of Sciences of the United States of America,* 113**,** 6071-6076.
SUN, T. P. 2011. The molecular mechanism and evolution of the GA-GID1-DELLA signaling module in plants. *Current Biology,* 21**,** R338-345.
SUN, T. P., GOODMAN, H. M. & AUSUBEL, F. M. 1992. Cloning the Arabidopsis Ga1 locus by genomic subtraction. *The Plant Cell,* 4**,** 119-128.

SWAIN, S. M., MULLER, A. J. & SINGH, D. P. 2004. The gar2 and rga alleles increase the growth of gibberellin-deficient pollen tubes in Arabidopsis. *Plant Physiology,* 134**,** 694-705.

SWATEK, K. N., GRAHAM, K., AGRAWAL, G. K. & THELEN, J. J. 2011. The 14-3-3 isoforms chi and epsilon differentially bind client proteins from developing Arabidopsis seed. *Journal of Proteome Research,* 10**,** 4076-4087.

TAKAHASHI, M., SASAKI, Y., IDA, S. & MORIKAWA, H. 2001. Nitrite reductase gene enrichment improves assimilation of NO2 in Arabidopsis. *Plant Physiology,* 126**,** 731-741.

TAL, I., ZHANG, Y., JORGENSEN, M. E., PISANTY, O., BARBOSA, I. C. R., ZOURELIDOU, M., REGNAULT, T., CROCOLL, C., OLSEN, C. E., WEINSTAIN, R., SCHWECHHEIMER, C., HALKIER, B. A., NOUR-ELDIN, H. H., ESTELLE, M. & SHANI, E. 2016. The Arabidopsis NPF3 protein is a GA transporter. *Nature Communications,* 7, 11486.

TALON, M., KOORNNEEF, M. & ZEEVAART, J. A. D. 1990a. Accumulation of C19-gibberellins in the gibberellin-insensitive dwarf mutant gai of Arabidopsis thaliana (L) Heynh. *Planta,* 182**,** 501-505.

TALON, M., KOORNNEEF, M. & ZEEVAART, J. A. D. 1990b. Endogenous gibberellins in Arabidopsis thaliana and possible steps blocked in the biosynthetic pathways of the semidwarf ga4 and ga5 mutants. *Proceedings of the National Academy of Sciences of the United States of America,* 87**,** 7983-7987.

TANAKA, K., NAKAMURA, Y., ASAMI, T., YOSHIDA, S., MATSUO, T. & OKAMOTO, S. 2003. Physiological roles of brassinosteroids in early growth of Arabidopsis: Brassinosteroids have a synergistic relationship with gibberellin as well as auxin in light-grown hypocotyl elongation. *Journal of Plant Growth Regulation,* 22**,** 259-271.

TENG, Y. B., CUI, H. Q., WANG, M. Y. & LIU, X. Y. 2017. Nitrate reductase is regulated by CIRCADIAN CLOCK-ASSOCIATED1 in Arabidopsis thaliana. *Plant and Soil,* 416**,** 477-485.

TEPPERMAN, J. M., HUDSON, M. E., KHANNA, R., ZHU, T., CHANG, S. H., WANG, X. & QUAIL, P. H. 2004. Expression profiling of phyB mutant demonstrates substantial contribution of other phytochromes to red-light-regulated gene expression during seedling de-etiolation. *The Plant Journal,* 38**,** 725-739.

THOMAS, S. G., PHILLIPS, A. L. & HEDDEN, P. 1999. Molecular cloning and functional expression of gibberellin 2-oxidases, multifunctional enzymes involved in gibberellin deactivation. *Proceedings of the National Academy of Sciences of the United States of America,* 96**,** 4698-4703.

TILMAN, D., BALZER, C., HILL, J. & BEFORT, B. L. 2011. Global food demand and the sustainable intensification of agriculture. *Proceedings of the National Academy of Sciences of the United States of America,* 108, 20260-20264.

TILMAN, D., CASSMAN, K. G., MATSON, P. A., NAYLOR, R. & POLASKY, S. 2002. Agricultural sustainability and intensive production practices. *Nature,* 418**,** 671-677.

TODAKA, D., NAKASHIMA, K., MARUYAMA, K., KIDOKORO, S., OSAKABE, Y., ITO, Y., MATSUKURA, S., FUJITA, Y., YOSHIWARA, K., OHME-TAKAGI, M., KOJIMA, M., SAKAKIBARA, H., SHINOZAKI, K. & YAMAGUCHI-SHINOZAKI, K. 2012. Rice phytochrome-interacting factor-like protein OsPIL1 functions as a key regulator of internode elongation and induces a morphological response to drought stress. *Proceedings of the National Academy of Sciences of the United States of America,* 109**,** 15947-15952.

TOLEDO-ORTIZ, G., HUQ, E. & QUAIL, P. H. 2003. The Arabidopsis basic/helix-loop-helix transcription factor family. *The Plant Cell,* 15**,** 1749-1770.
TREWAVAS, A. J. 2001. The population/biodiversity paradox. Agricultural efficiency to save wilderness. *Plant Physiology,* 125**,** 174-179.
TRUONG, H.-N., CABOCHE, M. & DANIEL-VEDELE, F. 1997. Sequence and characterization of two Arabidopsis thaliana cDNAs isolated by functional complementation of a yeast gln3 gdh1 mutant. *FEBS Letters,* 410**,** 213-218.
TSAY, Y. F., SCHROEDER, J. I., FELDMANN, K. A. & CRAWFORD, N. M. 1993. The herbicide sensitivity gene CHL1 of Arabidopsis encodes a nitrate-inducible nitrate transporter. *Cell,* 72, 705-713.
TUCKER, D. E., ALLEN, D. J. & ORT, D. R. 2004. Control of nitrate reductase by circadian and diurnal rhythms in tomato. *Planta,* 219**,** 277-285.
TURNBULL, C. G., BOOKER, J. P. & LEYSER, H. M. 2002. Micrografting techniques for testing long-distance signalling in Arabidopsis. *The Plant Journal,* 32, 255-262.
TYLER, L., THOMAS, S. G., HU, J. H., DILL, A., ALONSO, J. M., ECKER, J. R. & SUN, T. P. 2004. DELLA proteins and gibberellin-regulated seed germination and floral development in Arabidopsis. *Plant Physiology,* 135**,** 1008-1019.
UEGUCHI-TANAKA, M., ASHIKARI, M., NAKAJIMA, M., ITOH, H., KATOH, E., KOBAYASHI, M., CHOW, T. Y., HSING, Y. I., KITANO, H., YAMAGUCHI, I. & MATSUOKA, M. 2005. GIBBERELLIN INSENSITIVE DWARF1 encodes a soluble receptor for gibberellin. *Nature,* 437**,** 693-698.
UNTERGASSER, A., CUTCUTACHE, I., KORESSAAR, T., YE, J., FAIRCLOTH, B. C., REMM, M. & ROZEN, S. G. 2012. Primer3-new capabilities and interfaces. *Nucleic Acids Research,* 40, e115.
UPPAL, R. K. & GOODING, M. J. 2013. Gibberellin-responsive and -insensitive dwarfing alleles on wheat performance in contrasting tillage systems. *Field Crops Research,* 141, 55-62.
VAN DE VELDE, K., RUELENS, P., GEUTEN, K., ROHDE, A. & VAN DER STRAETEN, D. 2017. Exploiting DELLA signaling in cereals. *Trends in Plant Science,* 22**,** 880-893.
VAN ZANTEN, M., SNOEK, L. B., PROVENIERS, M. C. G. & PEETERS, A. J. M. 2009. The many functions of ERECTA. *Trends in Plant Science,* 14**,** 214-218.
VARBANOVA, M., YAMAGUCHI, S., YANG, Y., MCKELVEY, K., HANADA, A., BOROCHOV, R., YU, F., JIKUMARU, Y., ROSS, J., CORTES, D., MA, C. J., NOEL, J. P., MANDER, L., SHULAEV, V., KAMIYA, Y., RODERMEL, S., WEISS, D. & PICHERSKY, E. 2007. Methylation of gibberellins by Arabidopsis GAMT1 and GAMT2. *The Plant Cell,* 19**,** 32-45.
VIDAL, A., ABRIL, N. & PUEYO, C. 1995. DNA-Repair by ogt alkyltransferase influences EMS mutational specificity. *Carcinogenesis,* 16**,** 817-821.
VIDAL, E. A., ALVAREZ, J. M., MOYANO, T. C. & GUTIERREZ, R. A. 2015. Transcriptional networks in the nitrate response of Arabidopsis thaliana. *Current Opinion in Plant Biology,* 27**,** 125-132.
VIERSTRA, R. D. 2003. The ubiquitin/26S proteasome pathway, the complex last chapter in the life of many plant proteins. *Trends in Plant Science,* 8**,** 135-142.
VONARNIM, A. & DENG, X. W. 1996. Light control of seedling development. *Annual Review of Plant Physiology and Plant Molecular Biology,* 47**,** 215-243.
WANG, F. & DENG, X. W. 2011. Plant ubiquitin-proteasome pathway and its role in gibberellin signaling. *Cell Research,* 21**,** 1286-1294.

WANG, F., ZHU, D., HUANG, X., LI, S., GONG, Y., YAO, Q., FU, X., FAN, L. M. & DENG, X. W. 2009a. Biochemical insights on degradation of Arabidopsis DELLA proteins gained from a cell-free assay system. *The Plant Cell,* 21**,** 2378-2390.

WANG, F. F., LIAN, H. L., KANG, C. Y. & YANG, H. Q. 2010a. Phytochrome B is involved in mediating red light-induced stomatal opening in Arabidopsis thaliana. *Molecular Plant,* 3**,** 246-259.

WANG, P. C., DU, Y. Y., LI, Y. A., REN, D. T. & SONG, C. P. 2010b. Hydrogen peroxide-mediated activation of map kinase 6 modulates nitric oxide biosynthesis and signal transduction in Arabidopsis. *The Plant Cell,* 22**,** 2981-2998.

WANG, R., LIU, D. & CRAWFORD, N. M. 1998. The Arabidopsis CHL1 protein plays a major role in high-affinity nitrate uptake. *Proceedings of the National Academy of Sciences of the United States of America,* 95, 15134-15139.

WANG, R., XING, X., WANG, Y., TRAN, A. & CRAWFORD, N. M. 2009b. A genetic screen for nitrate regulatory mutants captures the nitrate transporter gene NRT1.1. *Plant Physiology,* 151, 472-478.

WANG, R. C. & CRAWFORD, N. M. 1996. Genetic identification of a gene involved in constitutive, high-affinity nitrate transport in higher plants. *Proceedings of the National Academy of Sciences of the United States of America,* 93, 9297-9301.

WANG, W., HU, B., YUAN, D., LIU, Y., CHE, R., HU, Y., OU, S., LIU, Y., ZHANG, Z., WANG, H., LI, H., JIANG, Z., ZHANG, Z., GAO, X., QIU, Y., MENG, X., LIU, Y., BAI, Y., LIANG, Y., WANG, Y., ZHANG, L., LI, L., SODMERGEN, JING, H., LI, J. & CHU, C. 2018. Expression of the nitrate transporter gene OsNRT1.1A/OsNPF6.3 confers high yield and early maturation in rice. *The Plant Cell,* 30**,** 638-651.

WANG, W., ZHANG, J., QIN, Q., YUE, J., HUANG, B., XU, X., YAN, L. & HOU, S. 2014. The six conserved serine/threonine sites of REPRESSOR OF ga1-3 protein are important for its functionality and stability in gibberellin signaling in Arabidopsis. *Planta,* 240**,** 763-779.

WANG, X. M., FELDMANN, K. A. & SCHOLL, R. L. 1988. A chlorate-hypersensitive, high nitrate chlorate uptake mutant of Arabidopsis thaliana. *Physiologia Plantarum,* 73**,** 305-310.

WANG, X. M., SCHOLL, R. L. & FELDMANN, K. A. 1986. Characterization of a chlorate-hypersensitive, high nitrate reductase Arabidopsis thaliana mutant. *Theoretical and Applied Genetics,* 72**,** 328-336.

WANG, Y. Y., HSU, P. K. & TSAY, Y. F. 2012. Uptake, allocation and signaling of nitrate. *Trends in Plant Science,* 17, 458-467.

WAUGH, R., LEADER, D. J., MCCALLUM, N. & CALDWELL, D. 2006. Harvesting the potential of induced biological diversity. *Trends in Plant Science,* 11**,** 71-79.

WEI, Z. Y., YUAN, T., TARKOWSKA, D., KIM, J., NAM, H. G., NOVAK, O., HE, K., GOU, X. P. & LI, J. 2017. Brassinosteroid biosynthesis is modulated via a transcription factor cascade of COG1, PIF4, and PIF5. *Plant Physiology,* 174**,** 1260-1273.

WESTON, D. E., ELLIOTT, R. C., LESTER, D. R., RAMEAU, C., REID, J. B., MURFET, I. C. & ROSS, J. J. 2008. The pea DELLA proteins LA and CRY are important regulators of gibberellin synthesis and root growth. *Plant Physiology,* 147**,** 199-205.

WILD, M., DAVIERE, J. M., CHEMINANT, S., REGNAULT, T., BAUMBERGER, N., HEINTZ, D., BALTZ, R., GENSCHIK, P. & ACHARD, P. 2012. The Arabidopsis DELLA RGA-LIKE3 is a direct target of MYC2 and modulates jasmonate signaling responses. *The Plant Cell,* 24**,** 3307-3319.

WILHELM, R. 2018. Chemical regulators of gibberellin status and their application in plant production. *In Annual Plant Reviews,* 49**,** 359-404.

WILKINSON, J. Q. & CRAWFORD, N. M. 1991. Identification of the Arabidopsis Chl3 gene as the nitrate reductase structural gene Nia2. *The Plant Cell,* 3, 461-471.
WILKINSON, J. Q. & CRAWFORD, N. M. 1993. Identification and characterization of a chlorate-resistant mutant of Arabidopsis thaliana with mutations in both nitrate reductase structural genes Nia1 and Nia2. *Molecular & General Genetics,* 239**,** 289-297.
WILLIAMS, L. & MILLER, A. 2001. Transporters responsible for the uptake and partitioning of nitrogenous solutes. *Annual Review of Plant Physiology and Plant Molecular Biology,* 52, 659-688.
WILLIGE, B. C., GHOSH, S., NILL, C., ZOURELIDOU, M., DOHMANN, E. M. N., MAIER, A. & SCHWECHHEIMER, C. 2007. The DELLA domain of GA INSENSITIVE mediates the interaction with the GA INSENSITIVE DWARF1A gibberellin receptor of Arabidopsis. *The Plant Cell,* 19**,** 1209-1220.
WILLIGE, B. C., OGISO-TANAKA, E., ZOURELIDOU, M. & SCHWECHHEIMER, C. 2012. WAG2 represses apical hook opening downstream from gibberellin and PHYTOCHROME INTERACTING FACTOR 5. *Development,* 139**,** 4020-4028.
WILSON, R. N., HECKMAN, J. W. & SOMERVILLE, C. R. 1992. Gibberellin is required for flowering in Arabidopsis thaliana under short days. *Plant Physiology,* 100**,** 403-408.
WILSON, R. N. & SOMERVILLE, C. R. 1995. Phenotypic suppression of the gibberellin-insensitive mutant (gai) of Arabidopsis. *Plant Physiology,* 108**,** 495-502.
WINTER, D., VINEGAR, B., NAHAL, H., AMMAR, R., WILSON, G. V. & PROVART, N. J. 2007. An "electronic fluorescent pictograph" browser for exploring and analyzing large-scale biological data sets. *Plos One,* 2, e718.
WIRTH, J., CHOPIN, F., SANTONI, V., VIENNOIS, G., TILLARD, P., KRAPP, A., LEJAY, L., DANIEL-VEDELE, F. & GOJON, A. 2007. Regulation of root nitrate uptake at the NRT2.1 protein level in Arabidopsis thaliana. *Journal of Biological Chemistry,* 282**,** 23541-23552.
XIE, Y. R., LIU, Y., WANG, H., MA, X. J., WANG, B. B., WU, G. X. & WANG, H. Y. 2017. Phytochrome-interacting factors directly suppress MIR156 expression to enhance shade-avoidance syndrome in Arabidopsis. *Nature Communications,* 8, 348.
XIONG, Y. & SHEEN, J. 2015. Novel links in the plant TOR kinase signaling network. *Current Opinion in Plant Biology,* 28**,** 83-91.
XU, H. Y., IWASHIRO, R., LI, T. Z. & HARADA, T. 2013. Long-distance transport of Gibberellic Acid Insensitive mRNA in Nicotiana benthamiana. *BMC Plant Biology,* 13, 165.
XU, X., PAIK, I., ZHU, L. & HUQ, E. 2015. Illuminating progress in phytochrome-mediated light signaling pathways. *Trends in Plant Science,* 20**,** 641-650.
YAMAGUCHI, R., NAKAMURA, M., MOCHIZUKI, N., KAY, S. A. & NAGATANI, A. 1999. Light-dependent translocation of a phytochrome B-GFP fusion protein to the nucleus in transgenic Arabidopsis. *Journal of Cell Biology,* 145**,** 437-445.
YAMAGUCHI, S. 2008. Gibberellin metabolism and its regulation. *Annual review of plant biology,* 59**,** 225-251.
YAMASHINO, T., NOMOTO, Y., LORRAIN, S., MIYACHI, M., ITO, S., NAKAMICHI, N., FANKHAUSER, C. & MIZUNO, T. 2013. Verification at the protein level of the PIF4-mediated external coincidence model for the temperature-adaptive photoperiodic control of plant growth in Arabidopsis thaliana. *Plant Signaling & Behavior,* 8**,** e23390.
YANG, D. L., YAO, J., MEI, C. S., TONG, X. H., ZENG, L. J., LI, Q., XIAO, L. T., SUN, T. P., LI, J. G., DENG, X. W., LEE, C. M., THOMASHOW, M. F., YANG, Y. N., HE, Z. H. & HE, S. Y. 2012. Plant hormone jasmonate prioritizes defense over growth by

interfering with gibberellin signaling cascade. *Proceedings of the National Academy of Sciences of the United States of America,* 109**,** E1192-E1200.

YANG, F. X., LIANG, G., LIU, D. M. & YU, D. Q. 2009. Arabidopsis MiR396 mediates the development of leaves and flowers in transgenic tobacco. *Journal of Plant Biology,* 52**,** 475-481.

YEH, K. C. & LAGARIAS, J. C. 1998. Eukaryotic phytochromes: light-regulated serine/threonine protein kinases with histidine kinase ancestry. *Proceedings of the National Academy of Sciences of the United States of America,* 95**,** 13976-13981.

YOSHIDA, H., HIRANO, K., SATO, T., MITSUDA, N., NOMOTO, M., MAEO, K., KOKETSU, E., MITANI, R., KAWAMURA, M., ISHIGURO, S., TADA, Y., OHME-TAKAGI, M., MATSUOKA, M. & UEGUCHI-TANAKA, M. 2014. DELLA protein functions as a transcriptional activator through the DNA binding of the INDETERMINATE DOMAIN family proteins. *Proceedings of the National Academy of Sciences of the United States of America,* 111, 7861-7866.

YOUN, J. H., KIM, T. W., JOO, S. H., SON, S. H., ROH, J., KIM, S., KIM, T. W. & KIM, S. K. 2018. Function and molecular regulation of DWARF1 as a C-24 reductase in brassinosteroid biosynthesis in Arabidopsis. *Journal of Experimental Botany,* 69**,** 1873-1886.

YU, L.-H., WU, J., TANG, H., YUAN, Y., WANG, S.-M., WANG, Y.-P., ZHU, Q.-S., LI, S.-G. & XIANG, C.-B. 2016. Overexpression of Arabidopsis NLP7 improves plant growth under both nitrogen-limiting and -sufficient conditions by enhancing nitrogen and carbon assimilation. *Scientific Reports,* 6**,** 27795.

YU, N., LUO, D. X., ZHANG, X. W., LIU, J. Z., WANG, W. X., JIN, Y., DONG, W. T., LIU, J. Y., LIU, H., YANG, W. B., ZENG, L. J., LI, Q., HE, Z. H., OLDROYD, G. E. D. & WANG, E. 2014. A DELLA protein complex controls the arbuscular mycorrhizal symbiosis in plants. *Cell Research,* 24**,** 130-133.

YU, S., GALVAO, V. C., ZHANG, Y. C., HORRER, D., ZHANG, T. Q., HAO, Y. H., FENG, Y. Q., WANG, S., SCHMID, M. & WANG, J. W. 2012. Gibberellin regulates the Arabidopsis floral transition through miR156-targeted SQUAMOSA promoter binding-like transcription factors. *The Plant Cell,* 24**,** 3320-32.

ZEEVAART, J. A. D. & TALON, M. 1992. Gibberellin mutants in Arabidopsis thaliana. *Progress in Plant Growth Regulation,* 13**,** 34-42.

ZENTELLA, R., HU, J., HSIEH, W. P., MATSUMOTO, P. A., DAWDY, A., BARNHILL, B., OLDENHOF, H., HARTWECK, L. M., MAITRA, S., THOMAS, S. G., COCKRELL, S., BOYCE, M., SHABANOWITZ, J., HUNT, D. F., OLSZEWSKI, N. E. & SUN, T. P. 2016. O-GlcNAcylation of master growth repressor DELLA by SECRET AGENT modulates multiple signaling pathways in Arabidopsis. *Genes & Development,* 30**,** 164-176.

ZENTELLA, R., SUI, N., BARNHILL, B., HSIEH, W. P., HU, J., SHABANOWITZ, J., BOYCE, M., OLSZEWSKI, N. E., ZHOU, P., HUNT, D. F. & SUN, T. P. 2017. The Arabidopsis O-fucosyltransferase SPINDLY activates nuclear growth repressor DELLA. *Nature Chemical Biology*, 13, 479-485.

ZHANG, B., HOLMLUND, M., LORRAIN, S., NORBERG, M., BAKO, L., FANKHAUSER, C. & NILSSON, O. 2017. BLADE-ON-PETIOLE proteins act in an E3 ubiquitin ligase complex to regulate PHYTOCHROME INTERACTING FACTOR 4 abundance. *Elife,* 6, e26759.

ZHANG, H. M. & FORDE, B. G. 1998. An Arabidopsis MADS box gene that controls nutrient-induced changes in root architecture. *Science,* 279**,** 407-409.

ZHANG, Y., LIU, Z., LIU, R., WANG, L. & BI, Y. 2011. Gibberellins negatively regulate light-induced nitrate reductase activity in Arabidopsis seedlings. *Journal of plant physiology,* 168**,** 2161-2168.

ZHANG, Y., MAYBA, O., PFEIFFER, A., SHI, H., TEPPERMAN, J. M., SPEED, T. P. & QUAIL, P. H. 2013. A quartet of PIF bHLH factors provides a transcriptionally centered signaling hub that regulates seedling morphogenesis through differential expression-patterning of shared target genes in Arabidopsis. *Plos Genetics,* 9**,** e1003244.

ZHENG, Y., GAO, Z. & ZHU, Z. 2016. DELLA-PIF modules: old dogs learn new tricks. *Trends in Plant Science,* 21**,** 813-815.

ZHONG, S., SHI, H., XUE, C., WANG, L., XI, Y., LI, J., QUAIL, P. H., DENG, X. W. & GUO, H. 2012. A molecular framework of light-controlled phytohormone action in Arabidopsis. *Current Biology,* 22**,** 1530-1535.

ZHOU, J., LIU, Q., ZHANG, F., WANG, Y., ZHANG, S., CHENG, H., YAN, L., LI, L., CHEN, F. & XIE, X. 2014. Overexpression of OsPIL15, a phytochrome-interacting factor-like protein gene, represses etiolated seedling growth in rice. *Journal of Integrative Plant Biology,* 56**,** 373-387.

ZHOU, Q. Q., HARE, P. D., YANG, S. W., ZEIDLER, M., HUANG, L. F. & CHUA, N. H. 2005. FHL is required for full phytochrome A signaling and shares overlapping functions with FHY1. *The Plant Journal,* 43**,** 356-370.

ZHU, J. Y., OH, E., WANG, T. & WANG, Z. Y. 2016. TOC1-PIF4 interaction mediates the circadian gating of thermoresponsive growth in Arabidopsis. *Nature Communications,* 7**,** 13692.

ZHU, L., BU, Q. Y., XU, X. S., PAIK, I., HUANG, X., HOECKER, U., DENG, X. W. & HUQ, E. 2015. CUL4 forms an E3 ligase with COP1 and SPA to promote light-induced degradation of PIF1. *Nature Communications,* 6, 7245.

ZHU, Y. Y., NOMURA, T., XU, Y. H., ZHANG, Y. Y., PENG, Y., MAO, B. Z., HANADA, A., ZHOU, H. C., WANG, R. X., LI, P. J., ZHU, X. D., MANDER, L. N., KAMIYA, Y., YAMAGUCHI, S. & HE, Z. H. 2006. ELONGATED UPPERMOST INTERNODE encodes a cytochrome P450 monooxygenase that epoxidizes gibberellins in a novel deactivation reaction in rice. *The Plant Cell,* 18**,** 442-456.

ZHUO, D. G., OKAMOTO, M., VIDMAR, J. J. & GLASS, A. D. M. 1999. Regulation of a putative high-affinity nitrate transporter (Nrt2;1At) in roots of Arabidopsis thaliana. *The Plant Journal,* 17, 563-568.